



# **Development of Coordinated Methodologies for Modeling CO<sub>2</sub>-Containing Systems in Petroleum Industry**

by

**Mohammad Mahdi Ghiasi**

B.Sc., Chemical Engineering

A dissertation submitted in partial fulfillment of the requirements for the degree of Master of Science in Chemical Engineering

Discipline of Chemical Engineering

School of Engineering

University of KwaZulu-Natal

Durban

South Africa

**Supervisor:** Prof. Amir H. Mohammadi

**Co-supervisor:** Prof. Deresh Ramjugernath

**April 2018**



هو الطيف

اسرار ازل را نه تو دانی و نه من

وین حل معما نه تو خوانی و نه من

هست از پس پرده گفتگوی من و تو

چون پرده براقند نه تو مانی و نه من

حکیم عمر خیام

The secrets eternal neither you know nor I  
And answers to the riddle neither you know nor I  
Behind the veil there is much talk about us, why  
When the veil falls, neither you remain nor I.

Omar Khayyam (Translation by Shahriar Shahriari)

*To my mother, who took me to the right way.*

*Thank you for all your unconditional love.*

## **PREFACE**

The research contained in this dissertation was completed by the candidate while based in the Discipline of Chemical Engineering, School of Engineering of Howard College, University of KwaZulu-Natal, Durban, South Africa. The research was financially supported by Prof. Mohammadi.

The contents of this work have not been submitted in any form to another university and, except where the work of others is acknowledged in the text, the results reported are due to investigations by the candidate.

## **ACKNOWLEDGEMENTS**

First and foremost, my sincere thanks goes to whom gave me my beloved family, and an opportunity to live with them. That is He, the All-Knower of the unseen and the seen.

I would like to single out my supervisors at the University of KwaZulu-Natal, Prof. Amir H. Mohammadi and Prof. Deresh Ramjugernath. I am deeply indebted to you for your knowledge, motivation, and enthusiasm.

I would like to extend my appreciation to my friends Mr. Milad Arabloo, from Sharif University of Technology, and Mr. Mohammad Mahmoodi, from TU Wien, for their collaboration in developing the models and preparing the research works.

Durban, February 2018

Mohammad M. Ghiasi

## ABSTRACT

Clathrate hydrates formation in natural gas processing facilities or transportation pipelines may lead to process and/or safety hazards. On the other hand, a number of applications are suggested on the basis of promoting the gas hydrate formation. Some researchers have investigated separation and purification processes through gas hydrate crystallization technology. Some works report that the hydrate formation is applicable to the gas transportation and storage. Gas hydrate concept is also studied as a potential method for CO<sub>2</sub> capture and/or sequestration. Water desalination/sweetening, and refrigeration and air conditioning systems are other proposed uses of hydrates phenomenon. In the realm of food processing and engineering, several studies have been done investigating the application of gas hydrate technology as an alternative to the conventional processes. Accurate knowledge of phase equilibria of clathrate hydrates is crucial for preventing or utilizing the hydrates.

It is believed that energy production or extraction from different fossil fuels is responsible for considerable emissions of CO<sub>2</sub>, as an important greenhouse gas, into the atmosphere. Furthermore, CO<sub>2</sub> removal from the streams of natural gas is important for enhancing the gaseous streams' heating value. Employment of solvent-based processes and technologies for removing the CO<sub>2</sub> is a widely employed approach in practical applications. Amine-based or pure amine solutions are the most common choice to remove the produced CO<sub>2</sub> in numerous carbon capture systems. Further to the above, ionic liquids (ILs) are capable to be utilized to capture CO<sub>2</sub> from industrial streams. Other potential solvent are sodium piperazine (PZ) and glycinate (SG) solutions. Equilibrium absorption of carbon dioxide in the aqueous phase is a key parameter in any solvent-based CO<sub>2</sub> capture process designing.

The captured CO<sub>2</sub>, then, can be injected into the hydrocarbon reservoirs. In addition to the fact that injection of CO<sub>2</sub> into potential sources is one of the most reliable methodologies for enhanced hydrocarbon recovery, utilizing this process in conjunction with the CO<sub>2</sub> capture systems mitigates the greenhouse effects of CO<sub>2</sub>. One of the most significant variables determining the success of CO<sub>2</sub> injection is known to be the minimum miscibility pressure (MMP) of CO<sub>2</sub>-reservoir oil.

This research study concerns implementation of computer-based methodologies called artificial neural networks (ANNs), classification and regression trees (CARTs)/AdaBoost-CART, adaptive neuro-fuzzy inference systems (ANFISs) and least squares support vector machines (LSSVMs) for modeling: (a) phase equilibria of clathrate hydrates in: 1- pure water, 2- aqueous solutions of salts and/or alcohols, and 3- ILs, (b) phase equilibria (equilibrium) of hydrates of methane in ILs; (c) equilibrium absorption of CO<sub>2</sub> in amine-based solutions, ILs, PZ solutions, and SG solutions; and (d) MMP of CO<sub>2</sub>-reservoir oil. To this end, related experimental data have been gathered from the literature.

Performing error analysis, the performance of the developed models in representing/estimating the independent parameter has been assessed. For the studied hydrate systems, the developed ANFIS, LSSVM, ANN and AdaBoost-CART models show the average absolute relative deviation percent (AARD%) of 0.04-1.09, 0.09-1.01, 0.05-0.81, and 0.03-0.07, respectively. In the case of hydrate+ILs, error analysis of the ANFIS, ANN, LSSVM, and CART models showed 0.31, 0.15, 0.08, and 0.10 AARD% of the results from the corresponding experimental values.

Employing the collected experimental data for carbon dioxide (CO<sub>2</sub>) absorption in amine-based solutions, the presented models based on ANFIS, ANN, LSSVM, and AdaBoost-CART methods regenerated the targets with AARD%s between 2.06 and 3.69, 3.92 and 8.73, 4.95 and



6.52, and 0.51 and 2.76, respectively. For the investigated CO<sub>2</sub>+IL systems, the best results were obtained using CART method as the AARD% found to be 0.04. Amongst other developed models, i.e. ANN, ANFIS, and LSSVM, the LSSVM model provided better results (AARD%=17.17). The proposed AdaBoost-CART tool for the CO<sub>2</sub>+water+PZ system reproduced the targets with an AARD% of 0.93. On the other hand, LSSVM, ANN, and ANFIS models showed AARD% values equal to 16.23, 18.69, and 15.99, respectively. Considering the CO<sub>2</sub>+water+SG system, the proposed AdaBoost-CART tool correlated the targets with a low AARD% of 0.89. The developed ANN, ANFIS, and LSSVM showed AARD% of more than 13. For CO<sub>2</sub>-oil MMP, the proposed AdaBoost-CART model (AARD%=0.39) gives better estimations than the developed ANFIS (AARD%=1.63). These findings revealed the reliability and accuracy of the CART/AdaBoost-CART methodology over other intelligent modeling tools including ANN, ANFIS, and LSSVM.



## Declaration

I, Mohammad Mahdi Ghiasi, declare that:

1. The research reported in this thesis, except where otherwise indicated, is my original work.
2. This thesis has not been submitted for any degree or examination at any other university.
3. This thesis does not contain other persons' data, pictures, graphs or other information, unless specifically acknowledged as being sourced from other persons.
4. This thesis does not contain other persons' writing, unless specifically acknowledged as being sourced from other researchers. Where other written sources have been quoted, then:  
(a) their words have been re-written but the general information attributed to them has been referenced; (b) where their exact words have been used, their writing has been placed inside quotation marks, and referenced.
5. Where I have reproduced a publication of which I am an author, co-author or editor, I have indicated in detail which part of the publication was actually written by myself alone and have fully referenced such publications.
6. This thesis does not contain text, graphics or tables copied and pasted from the internet, unless specifically acknowledged, and the source being detailed in the thesis and in the References sections.

*Ghiasi*

\_\_\_\_\_  
Mohammad Mahdi Ghiasi (Candidate)

\_\_\_\_28 March 2018\_\_\_\_

Date

As the candidate's Supervisor I agree/do not agree to the submission of this thesis.

\_\_\_\_\_  
Prof. Amir H. Mohammadi (Supervisor)

\_\_\_\_\_  
Date

\_\_\_\_\_  
Prof. Deresh Ramjugernath (Co-supervisor)

\_\_\_\_\_  
Date



# Table of Contents

Acronyms .....	x
List of Symbols .....	xi
List of Figures .....	xiv
List of Tables .....	xvii
1. Introduction.....	1
1.1. Machine Learning.....	1
1.2. Study Objectives .....	2
2. Literature review .....	5
2.1. Clathrate hydrates.....	5
2.1.1. An overview of gas hydrate .....	5
2.1.2. Methods for predicting hydrate dissociation conditions .....	6
2.1.3. Modeling studies on hydrate+IL systems .....	7
2.2. CO <sub>2</sub> Capture .....	9
2.2.1. Energy and environment .....	9
2.2.2. CO <sub>2</sub> removal: reasons .....	11
2.2.3. CO <sub>2</sub> removal processes.....	12
2.2.4. Modeling studies on CO <sub>2</sub> capture .....	14
2.3. CO <sub>2</sub> -Oil Minimum Miscibility Pressure (MMP) .....	16
2.3.1. CO <sub>2</sub> -Oil MMP .....	16
2.3.2. Determination of MMP .....	17
3. Modeling tools .....	21
3.1. ANN .....	21
3.2. LSSVM.....	22
3.3. ANFIS.....	24
3.4. Decision Tree & Boosting .....	25
4. Experimental data.....	28
4.1 Hydrate+Water/Ice+Salt/ Alcohol Systems.....	28

4.2.	Hydrate+IL Systems .....	30
4.3.	CO <sub>2</sub> +Water+Amine Systems .....	31
4.4.	CO <sub>2</sub> + IL Systems.....	34
4.5.	CO <sub>2</sub> +Water+PZ system .....	36
4.6.	CO <sub>2</sub> +Water+SG System.....	36
4.8.	Data Validation.....	37
5.	Model development .....	39
5.1.	General step.....	39
5.2.	Hydrate+Water/Ice+Salt/ Alcohol Systems.....	39
5.3.	Hydrate+IL Systems .....	46
5.4.	CO <sub>2</sub> +Water+Amine Systems .....	49
5.5.	CO <sub>2</sub> +IL systems .....	52
5.6.	CO <sub>2</sub> +Water+PZ System .....	52
5.7.	CO <sub>2</sub> +Water+SG System.....	56
5.8.	CO <sub>2</sub> -Oil MMP.....	57
6.	Results and discussion.....	61
6.1.	Model assessment criteria .....	61
6.2.	Hydrate+Water/Ice+Salt/ Alcohol systems .....	62
6.3.	Hydrate+IL System .....	77
6.4.	CO <sub>2</sub> +Water+Amine Systems .....	83
6.5.	CO <sub>2</sub> +IL System.....	97
6.6.	CO <sub>2</sub> +Water+PZ System .....	111
6.7.	CO <sub>2</sub> +Water+SG System.....	118
6.8.	CO <sub>2</sub> -Oil MMP.....	123
7.	Conclusions .....	132
8.	Recommendations .....	136
	References .....	137
	Appendix A.....	166
	Appendix B .....	191

## Acronyms

AEPD	2-amino-2-ethyl-1,3-propanediol
AARD%	Average absolute relative deviation percent
AMP	2-amino-2-methyl-1-propanol
AMPD	2-amino-2-methyl-1,3-propanediol
ANFIS	Adaptive network-based fuzzy inference system
ANN	Artificial neural network
ARD%	Average relative deviation percent
BPNN	Back propagation neural network
CART	Classification and regression tree
CSA	Coupled simulating annealing
DEA	Diethanolamine
DEAB	4-(diethylamino)-2-butanol
DEEA	2-(Diethylamino) ethanol
DT	Decision tree
eCSW	Electrolyte cubic square-well
EOR	Enhanced oil recovery
FFNN	Feed-forward neural network
FIS	Fuzzy inference system
FLN	Functional link network
GEP	Gene expression programming
HDT	Hydrate dissociation temperature
ID3	Iterative dichotomiser 3
LDHI	Low dosage hydrate inhibitor
L-H-V	Liquid-hydrate-vapor
LM	Levenberg-Marquardt
LSSVM	Least squares support vector machine
MDEA	Methyldiethanolamine
MEA	Monoethanolamine
MF	Membership functions
MLP	Multi-layer perceptron
MMC	Minimum miscibility concentration
MMP	Minimum miscibility pressure
MOC	Method of characteristics
NG	Natural gas
PR-EOS	Peng and Robinson equation of state
PSO	Particle swarm optimization
PZ	Piperazine

$R^2$	Coefficient of determination
RBA	Rising bubble apparatus
RBF	Radial basis function
RBFN	Radial basis function network
RNN	Recurrent neural network
SAFT	Statistical associating fluid theory
SG	Sodium glycinate
SVM	Support vector machine
TBAB	Tetra-n-butyl ammonium bromide
TEA	Triethanolamine
TEACL	Tetraethyl-ammonium chloride
THF	Tetrahydrofuran
TIPA	Triisopropanolamine
vdWP	van der Waals and Platteeuw
VIT	Vanishing interfacial tension

## List of Symbols

$a, b, c$	Premise parameters that changes the shape of the MF
-----------	---



$A_1, B_1, A_2, B_2$	Linguistic labels
$argmin$	Argument of the minimum
$b$	Intercept of the linear regression in LSSVM
$b_m$	Bias term
$C_{additive}$	Additive(s) concentration in aqueous phase
$e_k$	Regression error for n training objects
$f$	Activation function
$K_{vs}$	Vapor-solid equilibrium constants
MW C5+	Molecular weight of C5+ fraction in crude oil
$n$	Number of data points
$O_{1,i}$	Output of the ith node
$P$	Pressure
$P_c$	Critical pressure
$P_{CO_2}$	Partial pressure of CO <sub>2</sub>
$P_l$	Probability
$p_1, q_1, r_1, p_2, q_2, r_2$	Consequent parameters
$Q_{LSSVM}$	Cost function of LSSVM model
$r_m$	Linear combiner output
$T$	Temperature
$T_c$	Critical temperature
$T_{Hyd}$	Equilibrium methane HDT in IL
$Var(Y_l)$	Response vector for the left daughter node in DT
$Var(Y_r)$	Response vector for the right daughter node in DT
$w_i$	Firing strength of the ith rule
$\bar{w}_i$	Normalized firing strength
$w_{mn}$	Weights
$x$	Input vector of model parameters
$x_n$	Inputs of neuron
$x_s$	Hydrocarbon's mole fraction in the solid (water-free basis)
$y$	Hydrocarbon's mole fraction in the gas (water-free basis); Outputs
$y_m$	Neuron's output signal
$Z_i$	Gas composition
$\alpha$	CO <sub>2</sub> loading capacity of solvent solutions

$\alpha_k$	Lagrange multiplier
$\gamma$	Regularization constant
$\mu_{Ai}$	MF
$\sigma^2$	Kernel bandwidth
$\varphi$	Feature map
$\omega$	Acentric factor of IL

## List of Figures

<b>FIG. 2.1:</b> CLATHRATE HYDRATE STRUCTURES (SLOAN, 1998) .....	5
<b>FIG. 2.2:</b> CONSUMED ENERGY AND THE WORLD TOTAL ENERGY DEMAND (DATA FROM REF. (INTERNATIONAL ENERGY OUTLOOK 2013, 2013)) .....	9
<b>FIG. 2.3:</b> TOTAL CONSUMPTION OF ENERGY BY FUEL TYPE (DATA FROM REF. (INTERNATIONAL ENERGY OUTLOOK 2013, 2013)) .....	10
<b>FIG. 3.1:</b> A TYPICAL MODEL REPRESENTING AN ARTIFICIAL NEURON.....	21
<b>FIG. 3.3:</b> SIMPLIFIED FLOWCHART OF LSSVM MODEL OPTIMIZED BY CSA ALGORITHM.....	23
<b>FIG. 3.4:</b> SCHEMATIC OF THE LSSVM ALGORITHM .....	23
<b>FIG. 3.5:</b> TYPICAL STRUCTURE OF ANFIS FOR A TWO-INPUT AND ONE OUTPUT PROBLEM .....	24
<b>FIG. 3.6:</b> SIMPLIFIED FLOWCHART OF A TYPICAL HYBRID-ANFIS MODEL.....	25
<b>FIG. 5.1:</b> ANFIS STRUCTURE FOR (A) METHANE HYDRATE SYSTEM; (B) ETHANE HYDRATE SYSTEM; (C)PROPANE HYDRATE SYSTEM; (D) I-BUTANE HYDRATE SYSTEM; (E) HYDROGEN SULFIDE HYDRATE SYSTEM; (F) NITROGEN HYDRATE SYSTEM, AND (G) GAS MIXTURE HYDRATE SYSTEM .....	45
<b>FIG. 5.2:</b> STRUCTURE OF THE CREATED ANFIS MODEL FOR METHANE HYDRATE+IL SYSTEMS .....	48
<b>FIG. 5.3:</b> MEMBERSHIP FUNCTIONS FOR THE INDEPENDENT PARAMETERS ( $C_1$ +IL SYSTEM).....	48
<b>FIG. 5.4:</b> ANFIS TOOL FOR ( $CO_2$ +WATER+PZ) SYSTEM.....	54
<b>FIG. 5.5:</b> SCHEMATICS OF THE ADABOOST-CART MODEL FOR $CO_2$ +WATER+PZ SYSTEM.....	55
<b>FIG. 5.6:</b> STRUCTURE OF THE PROPOSED ADABOOST-CART TOOL TO ESTIMATE THE $CO_2$ LOADING CAPACITY OF SG.....	57
<b>FIG. 5.7:</b> STRUCTURE OF THE CREATED ANFIS MODEL FOR $CO_2$ -RESERVOIR OIL MMP PREDICTION .....	59
<b>FIG. 5.8:</b> SCHEMATICS OF THE ADABOOST-CART TOOL TO ESTIMATE THE $CO_2$ -RESERVOIR OIL MMP.....	60
<b>FIG. 6.1:</b> RELATIVE DEVIATIONS OF THE OUTCOMES OF THE DEVELOPED MODELS FOR METHANE HYDRATE SYSTEM; (A) ADABOOST-CART; (B) ANFIS; (C) ANN, AND (D) LSSVM.....	65
<b>FIG. 6.2:</b> RELATIVE DEVIATIONS OF THE OUTCOMES OF THE DEVELOPED MODELS FOR ETHANE HYDRATE SYSTEM; (A) ADABOOST-CART; (B) ANFIS; (C) ANN, AND (D) LSSVM.....	66
<b>FIG. 6.3:</b> RELATIVE DEVIATIONS OF THE OUTCOMES OF THE DEVELOPED MODELS FOR PROPANE HYDRATE SYSTEM; (A) ADABOOST-CART; (B) ANFIS; (C) ANN, AND (D) LSSVM.....	67
<b>FIG. 6.4:</b> RELATIVE DEVIATIONS OF THE OUTCOMES OF THE DEVELOPED MODELS FOR I-BUTANE HYDRATE SYSTEM; (A) ADABOOST-CART; (B) ANFIS; (C) ANN, AND (D) LSSVM.....	68
<b>FIG. 6.5:</b> RELATIVE DEVIATIONS OF THE OUTCOMES OF THE DEVELOPED MODELS FOR HYDROGEN SULFIDE HYDRATE SYSTEM; (A) ADABOOST-CART; (B) ANFIS; (C) ANN, AND (D) LSSVM.....	69
<b>FIG. 6.6:</b> RELATIVE DEVIATIONS OF THE OUTCOMES OF THE DEVELOPED MODELS FOR NITROGEN HYDRATE SYSTEM; (A) ADABOOST-CART; (B) ANFIS; (C) ANN, AND (D) LSSVM.....	70
<b>FIG. 6.7:</b> RELATIVE DEVIATIONS OF THE OUTCOMES OF THE DEVELOPED MODELS FOR GAS MIXTURE HYDRATE SYSTEM; (A) ADABOOST-CART; (B) ANFIS; (C) ANN, AND (D) LSSVM.....	71
<b>FIG. 6.8:</b> PREDICTIONS OF THE PRESENTED (A) LSSVM MODEL, (B) ANFIS MODEL, (C) CART, AND (D) ANN MODELS VS. THE CORRESPONDING EXPERIMENTAL VALUES .....	78

<b>FIG. 6.9:</b> HISTOGRAM OF ERRORS FOR THE PRESENTED (A) LSSVM, (B) ANFIS, (C) CART, AND (D) ANN MODELS .....	80
<b>FIG. 6.10:</b> HISTOGRAM OF RELATIVE ERRORS OF THE PRESENTED ANN MODELS FOR (A) MEA, (B) DEA, AND (C) TEA AMINE SYSTEMS .....	85
<b>FIG. 6.11:</b> HISTOGRAM OF RELATIVE ERRORS OF THE PRESENTED ADABOOST-CART MODELS FOR (A) MEA, (B) DEA, AND (C) TEA AMINE SYSTEMS .....	86
<b>FIG. 6.12:</b> RELATIVE DEVIATIONS OF THE PREDICTED CO <sub>2</sub> LOADING CAPACITY OF AMINES BY THE PROPOSED ANFIS TOOLS FROM TARGETS FOR: (A) MEA, (B) DEA, AND (C) TEA SYSTEMS ..	87
<b>FIG. 6.13:</b> THE DEVELOPED LSSVM MODEL FOR (A) MEA, (B) DEA, AND (C) TEA AQUEOUS SOLUTIONS VS. THE CORRESPONDING EXPERIMENTAL TARGETS .....	88
<b>FIG. 6.14:</b> COMPARING THE PREDICTIVE MATHEMATICAL MODELS IN TERMS OF HIGH ABSOLUTE RELATIVE DEVIATION (%) FOR (A) MEA, (B) DEA, AND (C) TEA AMINE SYSTEMS.....	90
<b>FIG. 6.15:</b> PERFORMANCE OF THE PROPOSED ADABOOST-CART MODEL IN PREDICTING CO <sub>2</sub> SOLUBILITY IN MEA SOLUTION OF CONCENTRATION 0.1836 MOL/L AT T=313.15 K (J.-Y. PARK ET AL., 2002) .....	92
<b>FIG. 6.16:</b> PERFORMANCE OF THE PROPOSED ADABOOST-CART MODEL IN PREDICTING CO <sub>2</sub> SOLUBILITY IN DEA SOLUTION OF CONCENTRATION 0.1831 MOL/L AT T=338.75 K (JANE & LI, 1997).....	94
<b>FIG. 6.18:</b> RELATIVE IMPORTANCE OF EACH INPUT ON THE CO <sub>2</sub> SOLUBILITY IN (A) MEA, (B) DEA, AND (TEA) SOLUTION IN DEVELOPMENT OF THE PROPOSED ADABOOST-CART MODELS .....	97
<b>FIG. 6.19:</b> CALCULATED SOLUBILITY OF CO <sub>2</sub> IN ILS VS. TARGET VALUES .....	98
<b>FIG. 6.20:</b> THE CREATED TREE-BASED MODEL VS. THE PUBLISHED MODELS IN THE LITERATURE (BAGHBAN ET AL., 2017).....	99
<b>FIG. 6.21:</b> THE PUBLISHED LITERATURE MODELS (BAGHBAN ET AL., 2017) VS. THE CREATED CART TOOL IN TERMS OF HIGH ABSOLUTE RD% .....	100
<b>FIGURE 6.22:</b> PREDICTION CART TOOL OF CO <sub>2</sub> SOLUBILITY IN IL WITH P <sub>C</sub> =2.36 MPa, T <sub>C</sub> =585.3 K, AND $\omega$ =0.7685 .....	106
<b>FIG. 6.23:</b> PREDICTION CART TOOL OF CO <sub>2</sub> SOLUBILITY IN IL WITH P <sub>C</sub> =3.48 MPa, T <sub>C</sub> =756.89 K, AND $\omega$ =0.783.....	107
<b>FIG. 6.24:</b> PREDICTION CART TOOL OF CO <sub>2</sub> SOLUBILITY IN IL WITH P <sub>C</sub> =1.8171 MPa, T <sub>C</sub> =1277.68 K, AND $\omega$ =0.5475 .....	108
<b>FIG. 6.25:</b> PREDICTION CART TOOL OF CO <sub>2</sub> SOLUBILITY IN IL WITH P <sub>C</sub> =1.803 MPa, T <sub>C</sub> =1255.7 K, AND $\omega$ =0.5876.....	109
<b>FIG. 6.26:</b> RELATIVE IMPORTANCE OF EACH INPUT IN CREATION OF THE PROPOSED TREE-BASED TOOL FOR PREDICTING THE CO <sub>2</sub> SOLUBILITY IN ILS.....	110
<b>FIG. 6.27:</b> THE EXPERIMENTAL CO <sub>2</sub> SOLUBILITY IN PZ VS. THE OUTPUTS OF THE CREATED (A) ADABOOST-CART, (B) LSSVM, (C) ANN, AND (D) ANFIS TOOLS .....	112
<b>FIG. 6.28:</b> HISTOGRAM OF ERRORS FOR THE CREATED TOOLS .....	113
<b>FIG. 6.29:</b> ADABOOST-CART PREDICTIONS VS. EXPERIMENTAL DATA BY DASH ET AL. (2012) ..	116
<b>FIG. 6.30:</b> ADABOOST-CART PREDICTIONS VS. EXPERIMENTAL DATA BY DERKS ET AL. (2005)	116
<b>FIG. 6.31:</b> ADABOOST-CART PREDICTIONS VS. EXPERIMENTAL DATA BY KAMPS ET AL. (2003)	117
<b>FIG. 6.32:</b> RELATIVE IMPORTANCE OF THE INPUTS IN CREATION OF THE ADABOOST-CART TOOL FOR (CO <sub>2</sub> +WATER+PZ) SYSTEM .....	117

<b>FIG. 6.33:</b> THE EXPERIMENTAL TARGETS VS. THE OUTPUTS OF THE CREATED ADABOOST-CART TOOL .....	118
<b>FIG. 6.34:</b> ERRORS HISTOGRAM FOR THE CREATED ADABOOST-CART TOOL.....	119
<b>FIG. 6.35:</b> ADABOOST-CART TOOL OF CO <sub>2</sub> SOLUBILITY IN SOLUTION OF SG (10 MASS%) .....	122
<b>FIG. 6.36:</b> RELATIVE IMPORTANCE OF THE INPUTS IN THE CREATION OF THE TREE MODEL .....	122
<b>FIG. 6.37:</b> PARITY PLOT COMPARES THE PREDICTIONS OF THE DEVELOPED (A) ADABOOST-CART AND (B) ANFIS MODELS WITH CORRESPONDING EXPERIMENTAL VALUES .....	124
<b>FIG. 6.38:</b> POINT TO POINT COMPARISON BETWEEN THE OUTPUTS OF THE (A) ADABOOST-CART AND (B) ANFIS TOOLS FOR CO <sub>2</sub> -OIL MMP .....	125
<b>FIG. 6.39:</b> HISTOGRAM OF RELATIVE ERRORS OF THE PRESENTED (A) ADABOOST-CART AND (B) ANFIS MODELS .....	126
<b>FIG. A.1:</b> L-H-V EQUILIBRIUM DATA OF CO <sub>2</sub> HYDRATE FORMATION/DISSOCIATION CONDITIONS IN PURE WATER (ADISASMITO ET AL., 1991; BAI ET AL., 2016; BELANDRIA ET AL., 2010; CHA, HA, ET AL., 2016; CHA, KANG, ET AL., 2016; DEATON & FROST, 1946; PANKAJ D. DHOLABHAI ET AL., 1993; PANKAJ D. DHOLABHAI ET AL., 1996; PANKAJ D. DHOLABHAI ET AL., 1997; DJAVIDNIA ET AL., 2013; PETER ENGLEZOS & HALL, 1994; S.-S. FAN & GUO, 1999; ILANI-KASHKOU LI ET AL., 2016; KHAN ET AL., 2016; LARSON, 1955; J.-W. LEE ET AL., 2002; Y.-J. LEE ET AL., 2012; S. LI ET AL., 2010; TATSUO MAEKAWA, 2011, 2014; MATSUI ET AL., 2010; A. H. MOHAMMADI ET AL., 2005; M. MOHAMMADI ET AL., 2016; MOOIJER-VAN DEN HEUVEL ET AL., 2001; NEMA ET AL., 2016; ROBINSON & METHA, 1971; X.-D. SHEN ET AL., 2015; SUN ET AL., 2016; SUZUKI ET AL., 2013; UNRUH & KATZ, 1949; VLAHAKIS ET AL., 1972; M. WANG ET AL., 2016; M. WANG ET AL., 2017; XU & LIANG, 2014; YU ET AL., 2016; ZHA ET AL., 2012) .....	172
<b>FIG. A.2:</b> COMPARING THE EXPERIMENTAL DATA OF CARBONE (CARBONE, 2011) AND CHUN AND LEE (CHUN & LEE, 1999) FOR HYDRATE SYSTEM OF CO <sub>2</sub> +GLUCOSE+WATER .....	177
<b>FIG. A.3:</b> COMPARING THE EXPERIMENTAL DATA OF SMITH ET AL. (SMITH ET AL., 2016) AND CHUN AND LEE (CHUN & LEE, 1999) FOR HYDRATE SYSTEM OF CO <sub>2</sub> +GLUCOSE+WATER .....	178
<b>FIG. A.4:</b> CROSS PLOT OF THE PREDICTED VS. EXPERIMENTAL METHANE HFDT IN SUGAR SOLUTIONS.....	180
<b>FIG. A.5:</b> COMPARISON OF THE MODEL OUTPUTS WITH EXPERIMENTAL DATA (CARBONE, 2011; JIN ET AL., 2017) FOR CH <sub>4</sub> +SUGAR+WATER HYDRATE SYSTEMS .....	182
<b>FIG. A.6:</b> RELATIVE DEVIATIONS OF THE ESTIMATED CARBON DIOXIDE HFDT IN PURE WATER BY THE NEW EMPIRICAL CORRELATION FROM THE EXPERIMENTAL DATA.....	183
<b>FIG. A.7:</b> CROSS PLOT OF THE PREDICTED VS. EXPERIMENTAL CARBON DIOXIDE HFDT IN PURE WATER .....	184
<b>FIG. A.8:</b> CROSS PLOT OF THE PREDICTED VS. EXPERIMENTAL CARBON DIOXIDE HFDT IN SUGAR SOLUTIONS.....	185
<b>FIG. A.10:</b> COMPARISON OF THE MODEL OUTPUTS WITH EXPERIMENTAL DATA (S. LI, SHEN, LIU, FAN, ET AL., 2015; S. LI, SHEN, LIU, & LI, 2015) FOR CO <sub>2</sub> +JUICE HYDRATE SYSTEMS .....	190

## List of Tables

<b>TABLE 2.1:</b> COMPONENTS OF A TYPICAL NG (CHAPOY, 2004) .....	11
<b>TABLE 4.1:</b> ADDITIVES IN C1 HYDRATE SYSTEM .....	28
<b>TABLE 4.2:</b> ADDITIVES IN C2 HYDRATE SYSTEM .....	29
<b>TABLE 4.3:</b> ADDITIVES IN C3 HYDRATE SYSTEM .....	29
<b>TABLE 4.4:</b> ADDITIVES IN N <sub>2</sub> HYDRATE SYSTEM .....	29
<b>TABLE 4.5:</b> ADDITIVES IN H <sub>2</sub> S HYDRATE SYSTEM .....	29
<b>TABLE 4.6:</b> INFORMATION REGARDING THE COLLECTED DATABANK FOR METHANE HYDRATE IN ILS .....	30
<b>TABLE 4.7:</b> COLLECTED DATA FOR WATER+TEA+CO <sub>2</sub> SYSTEM .....	31
<b>TABLE 4.8:</b> COLLECTED DATA FOR WATER+DEA+CO <sub>2</sub> SYSTEM .....	32
<b>TABLE 4.9:</b> COLLECTED DATA FOR WATER+MEA+CO <sub>2</sub> SYSTEM .....	33
<b>TABLE 4.10:</b> INFORMATION ABOUT THE STUDIED ILS .....	34
<b>TABLE 4.11:</b> EQUILIBRIUM SYSTEM OF CO <sub>2</sub> + PZ+WATER .....	36
<b>TABLE 4.12:</b> EQUILIBRIUM INFORMATION FOR CO <sub>2</sub> SOLUBILITY IN SOLUTION OF SG.....	37
<b>TABLE 5.1:</b> TOPOLOGY OF THE PRESENTED ANN MODELS FOR THE STUDIED HYDRATE SYSTEMS .	40
<b>TABLE 5.2:</b> HYPER-PARAMETERS OF THE PRESENTED LSSVM TOOLS FOR HYDRATE SYSTEMS .....	41
<b>TABLE 5.3:</b> INFORMATION OF THE DEVELOPED ANFIS MODELS FOR THE STUDIED HYDRATE SYSTEMS .....	41
<b>TABLE 5.4:</b> SPECIFICATIONS OF THE PRESENTED ADABOOST MODELS FOR THE STUDIED HYDRATE SYSTEMS .....	45
<b>TABLE 5.5:</b> INFORMATION OF THE PROPOSED ANN MODEL FOR HYDRATE+IL SYSTEMS .....	47
<b>TABLE 5.6:</b> THE DEVELOPED ANFIS MODEL TO PREDICT THE C1 HYDRATE DISSOCIATION TEMPERATURE IN ILS.....	47
<b>TABLE 5.7:</b> TOPOLOGY OF THE PRESENTED ANN MODELS FOR THE STUDIED AMINE SYSTEMS.....	50
<b>TABLE 5.8:</b> HYPER-PARAMETERS OF THE PRESENTED LSSVM TOOLS FOR HYDRATE SYSTEMS .....	50
<b>TABLE 5.9:</b> SPECIFICATIONS OF THE CREATED ANFIS TOOL FOR ESTIMATING THE CO <sub>2</sub> LOADING CAPACITY OF MEA, DEA, AND TEA SOLUTIONS .....	50
<b>TABLE 5.10:</b> SPECIFICATIONS OF THE PRESENTED ADABOOST-CART MODELS FOR THE STUDIED HYDRATE SYSTEMS .....	51
<b>TABLE 5.12:</b> INFORMATION FOR THE BEST ANN MODEL DEVELOPED FOR (CO <sub>2</sub> +WATER+PZ) SYSTEM.....	53
<b>TABLE 5.13:</b> SPECIFICATIONS OF THE CREATED ANFIS TOOL FOR THE CO <sub>2</sub> +WATER+PZ SYSTEM	54
<b>TABLE 5.14:</b> SPECIFICATIONS OF THE PRESENTED ANFIS MODEL FOR PREDICTING SOLUBILITY OF CO <sub>2</sub> IN SG .....	56
<b>TABLE 5.15:</b> INDEPENDENT PARAMETERS AND THEIR RANGES FOR DEVELOPING ANFIS AND ADABOOST-CART MODELS .....	58
<b>TABLE 5.16:</b> SPECIFICATIONS OF THE PRESENTED ANFIS MODEL FOR CO <sub>2</sub> -RESERVOIR OIL MMP PREDICTION .....	59
<b>TABLE 6.1:</b> R <sup>2</sup> VALUES OF THE DEVELOPED MODELS FOR PREDICTING THE HDT OF INVESTIGATED HYDRATE SYSTEMS .....	62

<b>TABLE 6.2:</b> ARD% VALUES OF THE DEVELOPED MODELS FOR PREDICTING THE HDT OF INVESTIGATED HYDRATE SYSTEMS .....	63
<b>TABLE 6.3:</b> AARD% VALUES OF THE DEVELOPED MODELS FOR PREDICTING THE HDT OF INVESTIGATED HYDRATE SYSTEMS .....	63
<b>TABLE 6.4:</b> COMPARISON OF THE MODEL’S OUTPUTS WITH THE EXPERIMENTAL DATA BY HAGHIGH ET AL. (HOOMAN HAGHIGH, ANTONIN CHAPOY, ROD BURGESS, & BAHMAN TOHIDI, 2009) FOR METHANE HYDRATE .....	72
<b>TABLE 6.5:</b> COMPARISON OF THE MODEL’S OUTPUTS WITH THE EXPERIMENTAL DATA BY ROSS AND TOCZYLKIN (ROSS & TOCZYLKIN, 1992) FOR ETHANE HYDRATE .....	73
<b>TABLE 6.6:</b> COMPARISON OF THE MODEL’S OUTPUTS WITH THE EXPERIMENTAL DATA BY NG AND ROBINSON (HENG-JOO NG & ROBINSON, 1985) FOR PROPANE HYDRATE .....	74
<b>TABLE 6.7:</b> COMPARISON OF THE MODEL’S OUTPUTS WITH THE EXPERIMENTAL DATA BY HOLDER AND GODBOLE (HOLDER & GODBOLE, 1982) FOR I-BUTANE HYDRATE.....	74
<b>TABLE 6.8:</b> COMPARISON OF THE MODEL’S OUTPUTS WITH THE EXPERIMENTAL DATA BY MOHAMMADI AND RICHON (A. H. MOHAMMADI & RICHON, 2012) FOR HYDROGEN SULFIDE HYDRATE .....	75
<b>TABLE 6.9:</b> COMPARISON OF THE MODEL’S OUTPUTS WITH THE EXPERIMENTAL DATA BY NIXDORF & OELLRICH (NIXDORF & OELLRICH, 1997) FOR NITROGEN HYDRATE .....	76
<b>TABLE 6.10:</b> COMPARISON OF THE MODEL’S OUTPUTS WITH THE EXPERIMENTAL DATA BY KAMARI & OYARHOSSEIN (E. KAMARI & OYARHOSSEIN, 2012) FOR GAS MIXTURE HYDRATE (C1=81.55%, CO <sub>2</sub> =3.31%, N <sub>2</sub> =0.17%, C2=5.37%, I-C4=2.23%, N-C4=0.51%, I-C5=1.00%, N-C5=0.52%, C6=0.45%, C7=0.75%, C8 <sup>+</sup> =0.70%, H <sub>2</sub> S=1.05%, AND C <sub>2</sub> H <sub>4</sub> =2.39%) .....	76
<b>TABLE 6.11:</b> ERROR ANALYSIS RESULTS OF THE PROPOSED LSSVM, CART AND ANFIS TOOLS .	77
<b>TABLE 6.12:</b> OUTPUTS OF THE PRESENTED MODELS VS. CORRESPONDING EXPERIMENTAL VALUES FOR METHANE HYDRATE+[EMIM][NO <sub>3</sub> ]+WATER SYSTEM .....	81
<b>TABLE 6.13:</b> OUTPUTS OF THE PROPOSED MODELS VS. CORRESPONDING EXPERIMENTAL TARGETS FOR METHANE HYDRATE IN SOME ILs (10 WT% SOLUTION).....	82
<b>TABLE 6.14:</b> OVERALL PERFORMANCE OF THE MODELS FOR AMINE SYSTEMS .....	84
<b>TABLE 6.15:</b> ERROR RANGES OF THE MODELS FOR AMINE SYSTEMS .....	90
<b>TABLE 6.16:</b> RESULTS OF THE BUILT ADABOOST MODEL VS. CORRESPONDING TARGETS FOR MEA SOLUTION OF CONCENTRATION 5 MOL/L.....	91
<b>TABLE 6.17:</b> RESULTS OF THE BUILT ADABOOST MODEL VS. CORRESPONDING TARGETS FOR DEA SOLUTION OF CONCENTRATION 3.5 MOL/L (VALLÉE ET AL., 1999).....	93
<b>TABLE 6.18:</b> RESULTS OF THE BUILT ADABOOST MODEL VS. CORRESPONDING TARGETS FOR TEA SOLUTION OF CONCENTRATION 2 MOL/L (CHUNG ET AL., 2010).....	95
<b>TABLE 6.19:</b> ERROR ANALYSIS FOR THE CREATED CART-BASED TOOL.....	98
<b>TABLE 6.20:</b> THE CREATED CART-BASED TOOL VS. THE LITERATURE MODELS (BAGHBAN ET AL., 2017).....	99
<b>TABLE 6.21:</b> RESULTS OF THE CREATED TREE-BASED TOOL WITH HIGH DEVIATION FROM THE TARGETS .....	101
<b>TABLE 6.22:</b> RESULTS OF THE PUBLISHED LSSVM (BAGHBAN ET AL., 2017) WITH HIGH DEVIATION FROM THE TARGETS .....	102

<b>TABLE 6.23:</b> RESULTS OF THE PUBLISHED ANFIS (BAGHBAN ET AL., 2017) WITH HIGH DEVIATION FROM THE TARGETS .....	103
<b>TABLE 6.24:</b> RESULTS OF THE PUBLISHED MLP-ANN (BAGHBAN ET AL., 2017) WITH HIGH DEVIATION FROM THE TARGETS .....	104
<b>TABLE 6.25:</b> RESULTS OF THE PUBLISHED RBF-ANN (BAGHBAN ET AL., 2017) WITH HIGH DEVIATION FROM THE TARGETS .....	105
<b>TABLE 6.26:</b> ERROR ANALYSIS OF THE CREATED TOOLS FOR (CO <sub>2</sub> +WATER+PZ) SYSTEM.....	111
<b>TABLE 6.27:</b> OUTCOMES OF THE CREATED ADABOOST TOOL VS. THE EXPERIMENTAL DATA BY NGUYEN ET AL. (NGUYEN ET AL., 2010) FOR (CO <sub>2</sub> +WATER+PZ).....	114
<b>TABLE 6.28:</b> OUTCOMES OF THE CREATED ADABOOST TOOL VS. THE EXPERIMENTAL DATA BY BISHNOI AND ROCHELLE (S. BISHNOI & ROCHELLE, 2000).....	115
<b>TABLE 6.29:</b> STATISTICAL VARIABLES FOR THE CREATED ADABOOST-CART TOOL.....	118
<b>TABLE 6.30:</b> STATISTICAL VARIABLES FOR OTHER CREATED TOOLS.....	120
<b>TABLE 6.31:</b> RRESULTS OF THE CREATED ADABOOST-CART TOOL VS. SELECTED TARGETS .....	121
<b>TABLE 6.32:</b> ERROR ANALYSIS RESULTS OF THE CREATED ANFIS AND ADABOOST-CART TOOLS .....	123
<b>TABLE 6.33:</b> OVERALL PERFORMANCE OF THE MODELS FOR CO <sub>2</sub> -RESERVOIR OIL MMP PREDICTION .....	128
<b>TABLE 6.34:</b> PREDICTED PURE CO <sub>2</sub> -OIL MMP BY THE PRESENTED ANFIS AND ADABOOST-CART MODELS .....	129
<b>TABLE 6.35:</b> PREDICTED CO <sub>2</sub> -OIL MMP BY THE PRESENTED ANFIS AND ADABOOST-CART MODELS IN COMPARISON WITH THE REPORTED DATA FOR A DRIVE GAS WITH CO <sub>2</sub> =91.75, C <sub>1</sub> =8.05, AND N <sub>2</sub> =0.20 MOL% AS COMPOSITION.....	130
<b>TABLE 3.36:</b> PREDICTED CO <sub>2</sub> -OIL MMP BY THE PRESENTED ANFIS AND ADABOOST-CART MODELS IN COMPARISON WITH THE REPORTED DATA FOR A DRIVE GAS WITH CO <sub>2</sub> =87.38, C <sub>1</sub> =7.67, C <sub>2</sub> -C <sub>5</sub> =4.67, AND N <sub>2</sub> =0.19 MOL% AS COMPOSITION .....	131
<b>TABLE A.1:</b> INFORMATION ABOUT THE INVESTIGATED SUGARS .....	168
<b>TABLE A.2:</b> DETAILS REGARDING THE GATHERED DATA FOR METHANE HYDRATE IN SUGAR AQUEOUS SOLUTIONS.....	170
<b>TABLE A.3</b> GIVES THE TUNED VALUES OF THE MARGULES COEFFICIENT FOR THE METHANE HYDRATE IN THE STUDIED SUGAR AQUEOUS SOLUTIONS. THESE VALUES ARE OBTAINED USING THE LEVENBERG-MARQUARDT OPTIMIZATION ALGORITHM (M. M. GHIASI, 2012; LEVENBERG, 1944; MARQUARDT, 1963). .....	171
<b>TABLE A.3:</b> OBTAINED MARGULES COEFFICIENT FOR METHANE HYDRATE IN VARIOUS SUGAR AQUEOUS SOLUTIONS AT INVESTIGATED DATA .....	171
<b>TABLE A.4:</b> TUNED COEFFICIENTS USED IN EQ. (A.9) TO PREDICT THE CO <sub>2</sub> HFDT IN PURE WATER .....	173
<b>TABLE A.5:</b> TUNED COEFFICIENTS USED IN EQ. (A.12) TO PREDICT THE CO <sub>2</sub> HFDP IN PURE WATER .....	175
<b>TABLE A.6:</b> DETAILS REGARDING THE GATHERED DATA FOR CO <sub>2</sub> HYDRATE IN SUGAR AQUEOUS SOLUTIONS.....	176
<b>TABLE A.7:</b> OBTAINED MARGULES COEFFICIENT FOR CO <sub>2</sub> HYDRATE IN VARIOUS SUGAR AQUEOUS SOLUTIONS AT INVESTIGATED DATA .....	178



<b>TABLE A.8:</b> CONTENTS OF TOMATO/ORANGE JUICE IN THE GATHERED EXPERIMENTAL DATA .....	179
<b>TABLE A.9:</b> ERROR ANALYSIS RESULTS FOR THE SEMI-THEORETICAL METHOD TO PREDICT/REPRESENT CO <sub>2</sub> HFDT EQUILIBRIUM IN SUGAR AQUEOUS SOLUTIONS.....	181
<b>TABLE A.10:</b> ERROR ANALYSIS RESULTS FOR THE SEMI-THEORETICAL METHOD TO PREDICT/REPRESENT CO <sub>2</sub> HFDT EQUILIBRIUM IN SUGAR AQUEOUS SOLUTIONS.....	186
<b>TABLE A.11:</b> CALCULATED VALUES OF WATER ACTIVITY FOR CO <sub>2</sub> +ORANGE/TOMATO JUICE HYDRATE SYSTEMS .....	188

# 1. Introduction

## 1.1. Machine Learning

Until now, numerous studies have been performed on the applications of data mining and machine learning methodologies in chemical engineering. The accuracy of the results from smart models are normally more than the conventional models (like thermodynamic or empirical) which would be an asset for research and engineering activities.

Some of the widely utilized approaches in engineering fields are ANNs, ANFISs, decision trees (DTs) and SVMs. ANN is a potent machine designed on the foundation of human brain's nervous system [1-4] that can be used for various problems [5-8]. Information regarding the ANNs are given in the literature [9-17]. The ANFIS methodology was formulated by Jang [18]. This technique was developed using the concept of ANNs in combination with the fuzzy inference system (FIS) with the aim of overcoming the shortcomings of these two methods [19]. In ANFIS, the input(s)-output(s) connection is defined by employing the Takagi and Sugeno's type fuzzy rules, i.e. "if-then" [20, 21].

The SVM is another powerful strategy presented based on the machine learning foundations [22-29]. As an advantage over methods like ANN and ANFIS, the SVM model has acceptable generalization performance, and fewer adjustable/tunable parameters [26, 30]. Suykens and Vandewalle [22] presented a modified version of the standard SVM called least square SVM (LSSVM) in order to improve/reduce the model complexity.

DTs are sets of procedures that can be employed for the regression problems and/or classification issues [31]. The DT algorithm is a non-parametric methodology [32, 33]. In

regression analysis, the aim of employing the DTs is presenting a tool to estimate and represent a specified target through learning some decision rules that are simple [34]. The required rules are obtained from the inputs, i.e. independent parameters, of the desired databank for modeling. The DT-based procedure is straightforward and simple to understand: in the root node, the introduced data points into the DT is separated into smaller sub-groups employing the first depicted rule. These produced smaller groups are internal nodes. These nodes, i.e. internal nodes, could be split into smaller categories if needed.

## 1.2. Study Objectives

This study concerns applying innovative machine learning methodologies including ANN, ANFIS, LSSVM, and Decision Tree for modeling gas hydrate equilibrium dissociation conditions, solvent-based CO<sub>2</sub> capture processes, and CO<sub>2</sub>-crude oil minimum miscibility pressure systems. To achieve the research goals, extensive experimental databases have been collected from previously published works that are available in open literature.

The selected systems for conducting the modeling on the basis of machine learning approaches, i.e. ANN, ANFIS, LSSVM, and Decision Tree, are:

- 1- Equilibrium dissociation conditions of gas hydrates in: 1- pure water, 2- salt(s) and/or alcohol(s) aqueous solutions;
- 2- Equilibrium dissociation conditions of methane hydrates in ILs;
- 3- CO<sub>2</sub> equilibrium absorption in various amine aqueous solutions including diethanolamine (DEA), monoethanolamine (MEA), and triethanolamine (TEA);
- 4- CO<sub>2</sub> equilibrium absorption in ILs aqueous solution;

- 5- CO<sub>2</sub> equilibrium absorption in piperazine (PZ) aqueous solution;
- 6- CO<sub>2</sub> equilibrium absorption in sodium glycinate (SG) aqueous solution;
- 7- Minimum miscibility pressure (MMP) systems of carbon dioxide-reservoir oil.

After the development of the predictive tools for the aforementioned systems using the collected experimental data bank, an error analysis is performed to evaluate the capability of the presented tools in predicting/representing the target values. To this end, several statistical parameters are utilized. The best obtained model for each system is determined. Some of the developed models in this research were compared to the existing tools in the literature. Due to the unavailability of the codes of the published models in the literature, comparative study was not performed.

The rest of this work is arranged as follows: first of all, a literature review is presented. Later, a detailed background regarding the aforesaid systems is provided in **Chapter 2**. Next, computational algorithms of the machine learning approaches (ANN, ANFIS, LSSVM, and Decision Tree) will be presented in **Chapter 3**. **Chapter 4** gives the information the used data points for hydrate+water/ice+salt(s)/alcohol(s), hydrate+water+ionic liquid, CO<sub>2</sub>+water+amine, CO<sub>2</sub>+water+ionic liquid, CO<sub>2</sub>+water+piperazine, CO<sub>2</sub>+water+sodium glycinate, and the system of CO<sub>2</sub>-oil minimum miscibility pressure. In **Chapter 5**, the employed statistical parameters for evaluation of the developed models will be introduced. Moreover, this chapter gives the obtained results from modeling processes as well as a discussion of the presented models for the application of interest. Finally, **Chapter 6** summarizes the key findings of this study.

Further to the above, in continuation of our previous work [35], the application of the proposed semi-theoretical approach for modeling the equilibrium conditions of CH<sub>4</sub> hydrate in the presence of a salt/alcohol containing solutions is extended to the hydrates of CH<sub>4</sub> and CO<sub>2</sub> in

aqueous solutions of sugars. Moreover, phase equilibria of CO<sub>2</sub> hydrate in tomato and orange juices were modelled using thermodynamic and empirical approaches. To achieve the research goals, the experimental liquid-hydrate-vapor (L-H-V) phase equilibrium data of CH<sub>4</sub>+xylose+water, CH<sub>4</sub>+xylitol+water, CH<sub>4</sub>+glucose+water, CO<sub>2</sub>+sucrose+water, CO<sub>2</sub>+glucose+water, CO<sub>2</sub>+fructose+water, CO<sub>2</sub>+Orange Juice, and CO<sub>2</sub>+Tomato Juice hydrate systems were gathered from the literature. Moreover, a new empirical tool was presented for accurate estimation of the CO<sub>2</sub> hydrate formation/dissociation temperature in pure water. The detailed information and results regarding the modeling have been reported in **Appendix A**.

## 2. Literature review

### 2.1. Clathrate hydrates

#### 2.1.1. An overview of gas hydrate

Clathrate hydrates are formed from gas molecules that are entrapped into cages of water molecules [36]. Three structures are known to exist for hydrates: 1- structure I (sI); 2- structure II (sII); and 3- structure H (sH). **Fig. 2.1** demonstrates the hydrates structures.

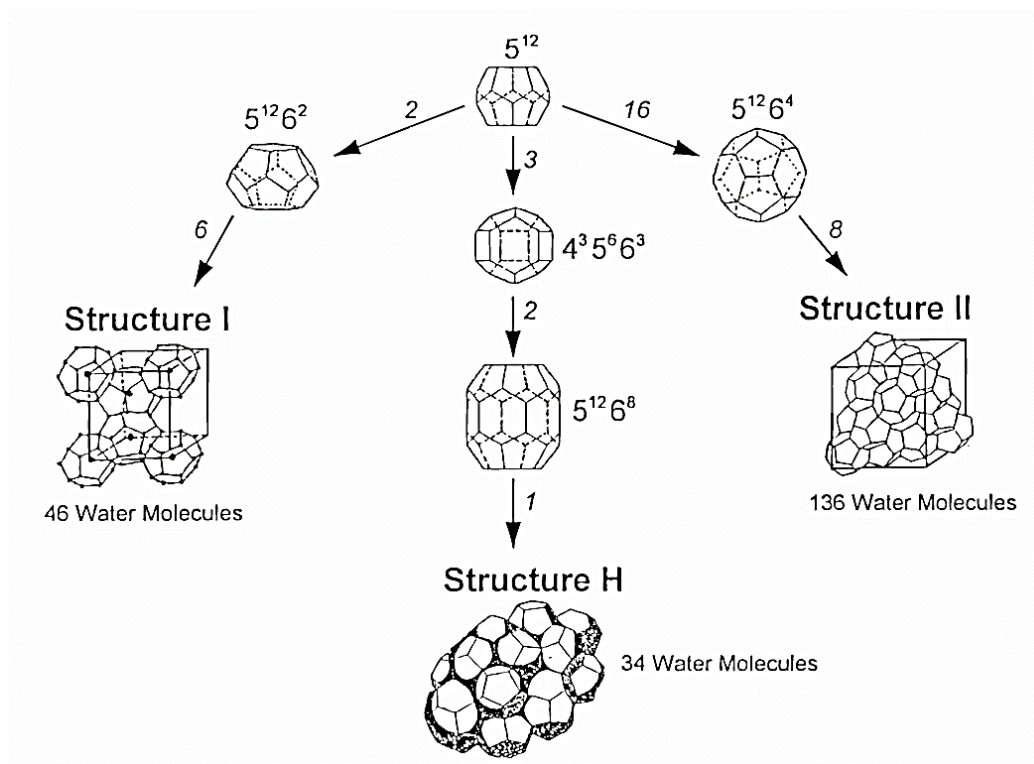


**Fig. 2.1:** Clathrate hydrate structures [36]

Commonly, the sI and sII can form in petroleum industry [37]. Since hydrate formation in petroleum-related pipelines and/or equipment may results in flow assurance concerns, it is important to prevent this occurrence by using proper method(s)/technique(s) [38, 39]. Some

researchers proposed the application of hydrates for desalination of seawater [40, 41]. There are also published works investigated the ability of hydrates as a method for transformation and/or storage of natural gas [42]. Other positive applications of hydrate are separation processes [43], future potential energy sources [44, 45] and CO<sub>2</sub> storage/sequestration [46, 47].

### 2.1.2. Methods for predicting hydrate dissociation conditions

There are various methodologies in the literature for calculation of clathrate hydrates dissociation or formation conditions. Katz and coworkers [48-50] presented a set of vapor-solid equilibrium constants ( $K_{vs}$ ). This approach is developed considering the N<sub>2</sub> a non-hydrate former. The other assumption was that ethane has same  $K_{vs}$  value as n-C<sub>4</sub> has. Nowadays we know that these assumptions are incorrect [51].

Authors like Makogon [52] and Holder et al. [53] presented empirical tools for some pure systems. Katz [54] developed a chart, known as gas gravity graph, for estimating the phase equilibria of sweet natural gas hydrates. Applying this method may results in large errors in some conditions [55]. Another chart method was presented by Baillie and Wichert [56] for sour gases.

In 2013, a semi-theoretical model was proposed by Ghiasi and Mohammadi [57]. This general model, then was specified to be applicable for calculating the hydrate forming conditions of CH<sub>4</sub> in alcohol(s) or salt(s) as thermodynamic inhibitors. The more sophisticated approach is based on statistical thermodynamics [58]. This approach has been modified by several researchers [59] [60] [61] [62] [63]. In addition to these improvements, this theory is applied for estimation of the natural gas hydrate forming conditions in thermodynamic inhibitors [38, 64-69].

Further to the above-mentioned methods, some authors suggested to apply the computational intelligences like ANFS [70], ANN [71] [72] and LSSVM [73] for predicting the hydrate forming or dissociating conditions. In another study [74], the performance of some thermodynamic models is compared to the capabilities of ANN and ANFIS methods in predicting the dissociation pressure of hydrates.

### 2.1.3. Modeling studies on hydrate+IL systems

Using the heterosegmented statistical associating fluid theory (SAFT), Jiang and Adidharma [75] modelled the thermodynamic properties of the imidazolium ILs. Furthermore, they predicted the formation (dissociation) conditions of CH<sub>4</sub> hydrate in imidazolium ILs employing the heterosegmented SAFT in conjunction with the solid solution theory introduced by van der Waals and Platteeuw (vdWP) [58]. In another work, Avula et al. [58] developed a model on the basis of theory of vdWP, Peng and Robinson equation of state (PR-EOS) [76], and the Pitzer–Mayorga–Zavitsas-hydration model for the phase equilibria of methane hydrate in 21 ILs. Keshavarz et al. [77] utilized the vdWP model, PR-EOS, and NRTL model to predict the dissociation conditions of methane hydrate in aqueous solution of 1-butyl-3-methylimidazolium dicyanamide, 1-butyl-3-methylimidazolium tetrafluoroborate and tetraethyl-ammonium chloride. A similar work is done by Tumba et al. [78] for modeling the thermodynamic stability conditions of CH<sub>4</sub> and CO<sub>2</sub> hydrates in tributylmethylphosphonium methylsulfate.

Partoon et al. [79] employed the Maddox et al. [80] tool for non-electrolyte inhibitors for modeling the phase boundary of methane hydrate formation in ILs. Zare et al. [81] employed the electrolyte cubic square-well (eCSW) EOS and the vdWP model to estimate the equilibrium



pressure of methane hydrate dissociation in [BMIM][BF<sub>4</sub>], 1-(2-hydroxyethyl)-3-methylimidazolium tetrafluoroborate ([OH-EMIM][BF<sub>4</sub>]), 1-butyl-3-methylimidazolium methyl sulfate ([BMIM][MeSO<sub>4</sub>]), 1-ethyl-3-methylimidazolium ethyl sulfate ([EMIM][EtSO<sub>4</sub>]), and 1-ethyl-3-methylimidazolium hydrogen sulfate ([EMIM][HSO<sub>4</sub>]). There are far more methods which is not within the scope of this work to mention.

In addition to the thermodynamic modeling, Nazari et al. [82] resolved a five-step mechanism to model the kinetics of formation of the methane hydrate in ILs. In 2016, Rasoolzadeh et al. [83] studied the induction time of methane hydrate formation in three ILs including [BMIM][BF<sub>4</sub>], [BMIM][DCA], and TEACL.

Using the Chen and Gue [84] model and Patel-Teja EOS, Liao et al. [85] modelled the phase equilibria of semi-clathrate hydrate of gas mixtures in tetra-n-butyl ammonium bromide (TBAB) solution. In the case of semi-clathrates of methane and carbon dioxide, Shi and Liang [86] proposed a thermodynamic tool based on the vdWP model, PR-EOS, and e-NRTL activity model for studying the effects of TBAB, TBAC, and TBAF on the stability conditions. In another study, Verrett et al. [87] used the vdWP model, Trebble–Bishnoi EOS, and e-NRTL activity model to investigate the semi-clathrate systems of carbon dioxide and methane in TBAB.

In 2015, Baghban et al. [88] developed predictive mathematical models on the basis of SVM method to predict the dissociation conditions of semi-clathrate hydrates of methane, carbon dioxide, nitrogen, hydrogen, argon, xenon, and hydrogen sulfide in TBAB. In another study, thermodynamic modeling of phase equilibria of semi-clathrate hydrates of the methane, carbon dioxide or nitrogen+ TBAB was presented by Eslamimanesh et al. [89]. A similar work was done by Paricaud [90].

## 2.2. CO<sub>2</sub> Capture

### 2.2.1. Energy and environment

According to a projection by U.S. Information Administration [91], energy consumption of the world will rise in future. **Fig. 2.2** shows the total consumed energy amounts (from 1990 to 2010) as well as the projected world total energy demand in the next decades.

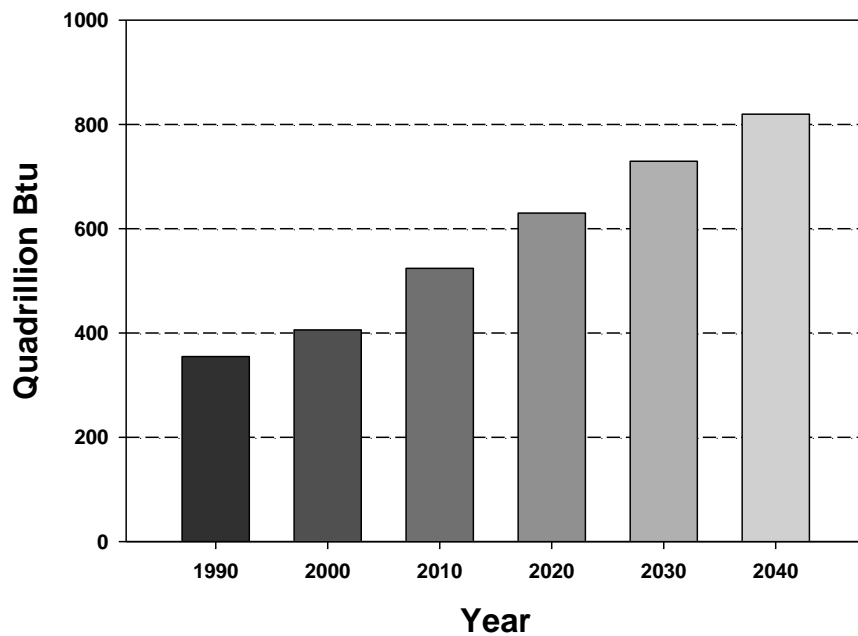


**Fig. 2.2:** Consumed energy and the world total energy demand (data from Ref. [91])

Among the available primary energy sources, i.e. nuclear energy, fossil energy, and renewable energy [92], the fossil fuels play a crucial role in providing the energy demand of world. The outlook for energy by ExxonMobil Corp. [93] suggests that the natural gas (NG) is the fastest-growing fuel through 2040. This finding is in agreement with other studies [91, 94-96]. By fuel

type, **Fig. 2.3** shows the total energy consumption. NG is the cleanest, safest, and most effective fossil fuel [96-98]. This is owing to the fact that NG's CO<sub>2</sub> emission factor is approximately 41% lower than the emission factors of other fossil fuels when combusted [99].

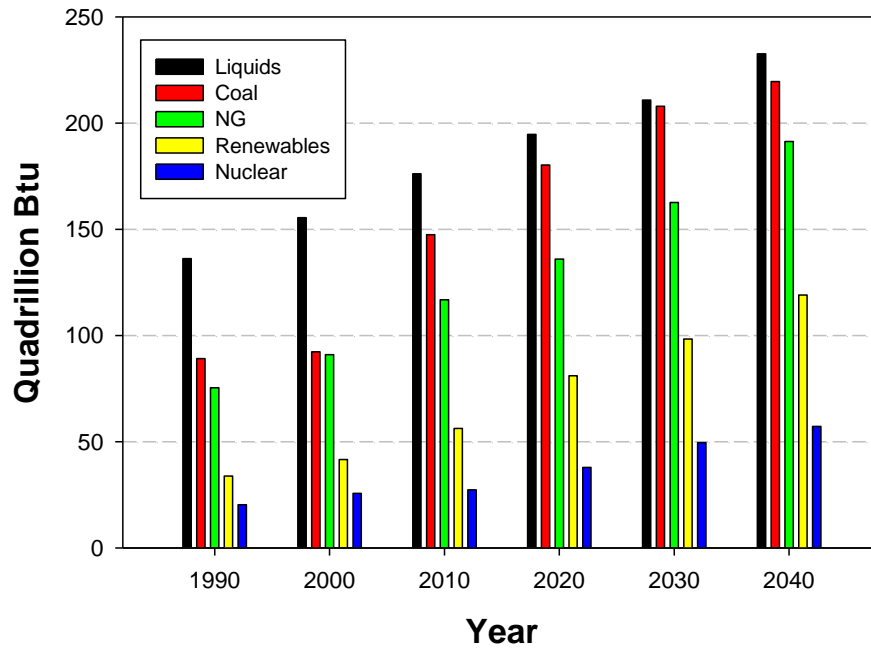


**Fig. 2.3:** Total consumption of energy by fuel type (data from Ref. [91])

As given in **Table 2.1**, the main constituent of a typical NG is CH<sub>4</sub>. Approximately, forty percent of the identified NG reservoirs have CO<sub>2</sub> and H<sub>2</sub>S, known as acid gases [100]. 16 % of these reservoirs are proven to be substantially sour with an acid gas content of more than twenty percent [101, 102].

**Table 2.1:** Components of a typical NG [103]

Hydrocarbons		Non-hydrocarbons	
Component	Concentration, mol%	Component	Concentration, mol%
C1	70-98	N <sub>2</sub>	Trace-15
C2	1-10	CO <sub>2</sub>	Trace-20
C3	Trace-5	H <sub>2</sub> S	Trace-20
C4	Trace-2	He	Up to 5 (not usually)
C5	Trace-1		
C6	Trace-0.5		
C7 and +	Trace		

### 2.2.2. CO<sub>2</sub> removal: reasons

Among the available non-hydrocarbon components in NG, CO<sub>2</sub> is considered as an environment damaging substance. This is owing to the intrinsic properties of CO<sub>2</sub>. For example, dissolving CO<sub>2</sub> in water contributes to producing an acidic solution known as carbonic acid [104, 105]. Consequently, during transportation of NG having CO<sub>2</sub>, corrosion problems occur in the pipelines and other equipment [106-109]. As a result, the operation costs will increase [110].

Further to the above, separation of CO<sub>2</sub> results in progress in transportability of NG and calorific value as well [111]. Moreover, decreasing the volume of NG by capturing the CO<sub>2</sub> reduces the size of the compressor station and also the number of compressors used for transmission of NG. This would be mentioned that existence of CO<sub>2</sub> in gas streams might leads to crystallization of CO<sub>2</sub> within liquefaction processes.

CO<sub>2</sub> is one of the main greenhouse gases. Hence, from environmental point of view, it is of significant importance to limit the CO<sub>2</sub> emissions. Indeed, CO<sub>2</sub> is believed to be the most prominent greenhouse gas [112]. It is responsible for approximately sixty percent of the greenhouse gases effect on the global climate [113, 114]. Generally, maximum allowable concentration of CO<sub>2</sub> in sweet (or sale) gas is 4 ppm [115-118]. For selecting an appropriate process for removal of acid gases, several factors should be considered [108, 116, 119]. A good approach to handle the captured carbon dioxide from NG is acid gas disposal in proper geological sites [120-127].

### 2.2.3. CO<sub>2</sub> removal processes

Several technologies and processes including permeation, cryogenic fractionation, absorption and adsorption can be utilized for CO<sub>2</sub> capture from flue gas or NG streams [128-130]. Furthermore, some hybrid separation approaches are presented in the literature [106, 131-134]. In addition to the main and hybrid methods, acid gas separation can be done employing the hydrate-based process/technology [135-140]. In this method, the H<sub>2</sub>S or CO<sub>2</sub> are separated from crystals of solid clathrate hydrate physically via adsorption.

Cryogenic fractionation includes the compression of the gas stream, and cooling it to low temperature (allowing CO<sub>2</sub> removal by distillation) [141]. As opposed to the available methods for recovering the CO<sub>2</sub>, cryogenic fractionation generates CO<sub>2</sub> at high pressure [142]. This technology is economic just for NGs with high CO<sub>2</sub> content [141, 143]; for example, the Natuna gas field with more than seventy percent CO<sub>2</sub> [144]. Increasing the energy demand contributes to the gas (energy)

production from such fields that were not considered attractive, from economic point of view, until now [145]. A cryogenic-based method is developed for such cases [146].

Permeation process for CO<sub>2</sub> capture is performed using different types of membranes. Unlike N<sub>2</sub>, C<sub>1</sub> and other paraffin hydrocarbons with low permeability coefficients, H<sub>2</sub>S and CO<sub>2</sub> are highly permeable. The membrane removes the issues of utilizing the packed columns. Comprehensive details regarding the permeation process as well as membrane categories are available in the literature [147-154].

Briefly, the adsorption is a physical-chemical method wherein the H<sub>2</sub>S or CO<sub>2</sub> is captured from the gas stream by using different solid adsorbents and/or reaction with some materials on a solid surface [108, 116, 155]. Commonly, the solid technologies are proper only for gases having low to medium quantities of mercaptans or hydrogen sulfide [108, 130]. Acid gas separation utilizing the iron oxide process and molecular sieves are chemical adsorption and physical adsorption, respectively.

Solid methodologies are just suitable to remove small amounts of impurities. However, the absorption processes, both the physical and chemical ones, can be utilized to separate substantial amounts of acid gases. Amongst such available physical solvents as n-methyl-2-pyrrolidone, dimethyl ether of polyethylene glycol and methanol, the main advantage of methanol-base method is its ability to separate the COS. Furthermore, methanol has low selectivity for CO<sub>2</sub> over H<sub>2</sub>S [156]. Among the aforesaid solvents, the n-methyl-2-pyrrolidone has the topmost selectivity for hydrogen sulfide over CO<sub>2</sub> [142]. Since water and hydrocarbons could be solved in these physical solvents, the selectivity of the absorption processes to the acid gases over the hydrocarbons should be reached by controlling the polyglyme distribution of the solvent, water content as well as operating conditions [157].

In the field of CO<sub>2</sub> removal from NG and/or flue gas, the well-known widely employed method, that is commercialized, is chemical absorption process using alkanolamine (or alkanolamine-based) solutions [158-162]. In a respective order, the methyldiethanolamine (MDEA), diethanolamine (DEA) and monoethanolamine (MEA) are tertiary, secondary and primary amines. Triethanolamine (TEA) is another common tertiary amine. [163, 164]. The properties of amine solutions and related information are documented in the literature [108]. Further to these solvents, application of 2-amino-2-methyl-1-propanol (AMP), piperazine (PZ), 4-(diethylamino)-2-butanol (DEAB), 2-(Diethylamino) ethanol (DEEA) and triisopropanolamine (TIPA) to the acid gas removal is also investigated [165-169]. Some published studies investigated the potential of CO<sub>2</sub> separation employing the amines mixtures [170-173]. Mass transfer mechanisms, chemical reaction kinetics and process chemistry of the amine-based absorption methodology is available in the literature [108, 115, 118, 174-180].

Some researchers studied the capability of the sodium glycinate (SG) in CO<sub>2</sub> removal has [181-186]. Based on a research study [184], it is revealed that aqueous solution of SG has a applicable potential to be used as an absorbent for CO<sub>2</sub>. Another potential compound for CO<sub>2</sub> capture is known to be the 1,4-diazacyclohexane (PZ) solutions. Moreover, several hybrid solvents are suggested to unify the concurrent advantages of physical and chemical solvents.

#### 2.2.4. Modeling studies on CO<sub>2</sub> capture

Such thermodynamic-based tools as Deshmukh- Mather model [187], electrolyte NRTL model [188], modified UNIQUAC model [189], and Kent-Eisenberg model [190] are developed to analyse and model the carbon dioxide loading capacity of various solvents at different conditions.

However, these types of approaches have some limitations in terms of the accuracy and range of applicability as well [191]. As an alternative, data mining and machine learning approaches like ANFIS, SVM and ANN can be successfully utilized to represent/predict the targets in a specific process. Published works in the literature affirms that our claim is completely true [71, 72, 192-199]. For amine-based process, Koolivand Salooki et al. [200] presented a neural network tool employing back-propagation (BP) learning algorithm to estimate the reflux amount as well as the outlet down temperature of contactor. Similarly, Saghatoleslami et al. [201] used neural-based genetic algorithm. In a work by Ghiasi and Mohammadi [107], the feasibility and applicability of both standard back-propagation neural network and LSSVM to estimate the optimum circulation rate of MEA in amine treating unit have been evaluated. In 2013 and for amine regenerator tower, a comparison between the abilities of the SVM and ANN in estimating the reflux flow-rate and bottom stream temperature was performed by Adib et al. [202].

In a work by Sipöcz et al. [203], the feed forward ANN was used to model the MEA-based processes (under steady conditions) for removal of CO<sub>2</sub> from the power plant's flue gas. Zhou et al. [204] employed the ANN, sensitivity analysis along with ANFIS for modeling the post combustion process of a amine-based CO<sub>2</sub> capture. Daneshvar et al. [167] proposed a neural network modeling for representing the experimental amounts of CO<sub>2</sub> solubility in TIPA, TIPA+MEA, and MEA aqueous solutions. More studies can be found in the literature [205-207] [208-212].



## **2.3. CO<sub>2</sub>-Oil Minimum Miscibility Pressure (MMP)**

### **2.3.1. CO<sub>2</sub>-Oil MMP**

As a tertiary recovery method, injecting the gases like CO<sub>2</sub> into mature reservoir fields results in increasing the amount of hydrocarbon recovery [213]. Depending on the conditions of the reservoir like composition of the reservoir's oil, pressure, and temperature as well as economic considerations, the type of injection gas could be determined. In addition to carbon dioxide, such gases as hydrocarbon mixtures, flue gases, methane, and nitrogen can be utilized for enhancing the oil recovery from hydrocarbon reservoirs.

Since the 1970s, CO<sub>2</sub> injection into the reservoirs for enhancing the recovery of oil has been recognized as a potential operation [214]. This is generally due to the fact that amongst the available gases that can be employed for injection as a technique for enhanced oil recovery (EOR), utilization of CO<sub>2</sub> has several advantages over other gases. It is well-known that CO<sub>2</sub> emission into the atmosphere is a significant cause of the greenhouse gas effect. As a method of CO<sub>2</sub> utilization, the produced CO<sub>2</sub> from resources like natural gas streams, flue gases, and refinery gases could be injected/sequestered into saline aquifers, gas/oil reservoirs, or coalbeds. As a result, both the economic and environmental goals will be satisfied. Moreover, using CO<sub>2</sub> compared to other gases will cost less and has higher displacement efficiency [215, 216]. The recovery performance of CO<sub>2</sub> injection processes for EOR are examined by several researchers [217-221]. These studies cover both the field scale and laboratory scale investigations.

Considering operational and economic standpoints, production of pure CO<sub>2</sub> gas streams in gas refineries or power plants is not recommended. Commonly, the CO<sub>2</sub> streams from available resources contain amounts of hydrocarbons, nitrogen, and/or hydrogen sulfide. Since the influence

of a drive gas in EOR processes mainly depends on its composition, knowing the accurate composition of an impure CO<sub>2</sub> stream is crucial for designing optimum CO<sub>2</sub>-EOR processes.

Such techniques as immiscible flooding, miscible flooding, near miscible flooding, CO<sub>2</sub> huff-and-puff, and carbonated water flooding are proposed for EOR processes employing CO<sub>2</sub> [222-225]. In terms of the capability for CO<sub>2</sub> sequestration as well as the oil recovery, it is believed that the most effective process is miscible CO<sub>2</sub> flooding [222, 226]. Because of the fact that the efficiency of displacement of the crude oil by CO<sub>2</sub> is highly dependent to pressure, to identify the mutual miscibility between the injected CO<sub>2</sub> and the crude oil, a parameter namely minimum miscibility pressure (MMP) is used.

By definition, MMP is the threshold pressure where flood changes from multiphase flow to single phase flow at reservoir condition. To achieve the highest recovery through CO<sub>2</sub>-EOR miscible process, the hydrocarbon reservoir must be in operation at or above the CO<sub>2</sub>-oil MMP. Hence, MMP plays a vital role in CO<sub>2</sub>-based miscible EOR processes. Inaccurate prediction/calculation of MMP might results in significant problems.

### 2.3.2. Determination of MMP

Experimental, computational, and empirical approaches can be employed for measuring/predicting the MMP. The experimental methods are designed for directly measuring the MMP; in contrast, the computational/empirical approaches are useful for predicting/ calculating the values of MMP.

Several experimental procedures have been proposed to measure the CO<sub>2</sub>-reservoir oil MMP. Slim tube test, rising bubble method, and vanishing interfacial tension (VIT) method are classified as experimental methodologies for MMP determination. For a given reservoir fluid and the injection gas, slim-tube experiments are known to be the standard experimental procedure for MMP or minimum miscibility concentration (MMC) determination [227, 228]. Since the real fluids are used in slim-tube experiments, the reliability of these experiments is generally accepted. In this method, the complex interactions between phase behavior and flow will be captured in a porous medium. It should be noticed that organization of these type of experiments are usually expensive. Furthermore, slim-tube method is slow and time-consuming. Because of this, this approach is not often used for obtaining MMPs in practice.

As an alternative to the slim tube experiments, Christiansen and Hains [229] presented the experiment of rising bubble. This approach is a relatively rapid method for MMP determination. Using rising bubble apparatus (RBA), the gas is introduced via a needle at the tube's bottom; consequently, miscibility development between oil and gas bubble can be observed. Finally, MMP for oil/gas pair could be measured on the basis of the rising gas bubble's shape [229]. Although utilization of RBA is cheap and quick as compared to the slim tube experiments, the rising bubble experiment has major limitations. For example, this method is unreliable in estimating the MMP for a condensing drive [230].

On the basis of measurement of the interfacial tension between the injected gas and the crude oil at a fixed temperature and at various pressures, Rao [231] developed VIT method to determine MMP. Similar to the RBA, VIT is also a visualization technique for defining MMP. In 2006, Ayirala and Rao [232] proposed a modified version of the VIT method. In addition to the aforesaid techniques, mixing cell (multiple-contact) experiment [233] and swelling/extraction test [234] are

other measurement methods.

There are three different frameworks for calculation/prediction of MMP: computational methods that utilize phase behavior computations on the basis of an EOS and computer simulations; empirical correlations on the basis of experimental results; and intelligent/smart models. Generally, three computational methods including analytical calculations, slim-tube compositional simulation, and multi-contact mixing cell are available for the application of interest [233]. In analytical approaches, the method of characteristics (MOC) is employed [235, 236]. MMP prediction by means of methods of mixing cell (cell-to-cell) is based on the repeated contact between oil and gas. In slim tube simulation, one-dimensional flow equation is solved employing the adjusted cubic EOS for the gas and oil [233].

There are several empirical approaches for predicting CO<sub>2</sub>–oil MMP. For example, correlations developed by Alston et al. [237], Emeral and Sarma [238] (corrected by Sebastian et al. [239]), Emeral and Sarma [238] (corrected by Alston et al. [237]), Yelling and Metcalfe [240] (corrected by Sebastian et al. [239]), and Yelling and Metcalfe [240] (corrected by Alston et al. [237]) are empirical models for estimation of the MMP. Li et al. [241] proposed another model in 2012 for MMP prediction. In 2017, Valluri et al. [242] presented a new correlation to predict CO<sub>2</sub>-oil MMP.

In 2013, Shokrollahi et al. [195] employed the method of LSSVM for predicting the MMP of CO<sub>2</sub>-reservoir oil. In another work, Tatar et al. [243] employed radial basis function type ANN to estimate CO<sub>2</sub>-reservoir oil MMP. In 2015, Kamari et al. [244] presented an equation to predict the CO<sub>2</sub>-MMP in live oil systems. This equation is developed on the basis of gene expression programming (GEP). Recently, Karkevandi-Talkhoonchah et al. [245] presented several ANFIS models for prediction of MMP of CO<sub>2</sub>-oil system. They optimized the created ANFIS models

using particle swarm optimization (PSO), back-propagation, ant colony optimization, genetic algorithm, and differential evolution. Based on the results, the ANFIS model optimized with the PSO has the highest accuracy in predicting the target values.

### 3. Modeling tools

#### 3.1. ANN

ANN attains its name from neuron that is a simple processing unit in the human brain. These artificial neurons can be mutually connected in a network such that some signals conveyed between them [1-4]. In 1943, McCulloch and Pitts [10] generated the first “artificial neuron”. **Fig. 3.1** represents a schematic of an artificial neuron. The demonstrated neuron  $m$  in **Fig. 3.1** can be mathematically represented as follows:

$$r_m = \sum_{i=1}^n (w_{mi} x_i + b_m) \dots\dots\dots (3.1)$$

$$y_m = F(r_m) \dots\dots\dots (3.2)$$

in which  $x_1, x_2, \dots, x_n$  indicate the inputs;  $w_{m1}, w_{m2}, \dots, w_{mn}$  are the weights;  $r_m$  shows the linear combiner output;  $b_m$  is the bias term;  $f$  indicates activation function; and  $y_m$  is the neuron’s output signal.

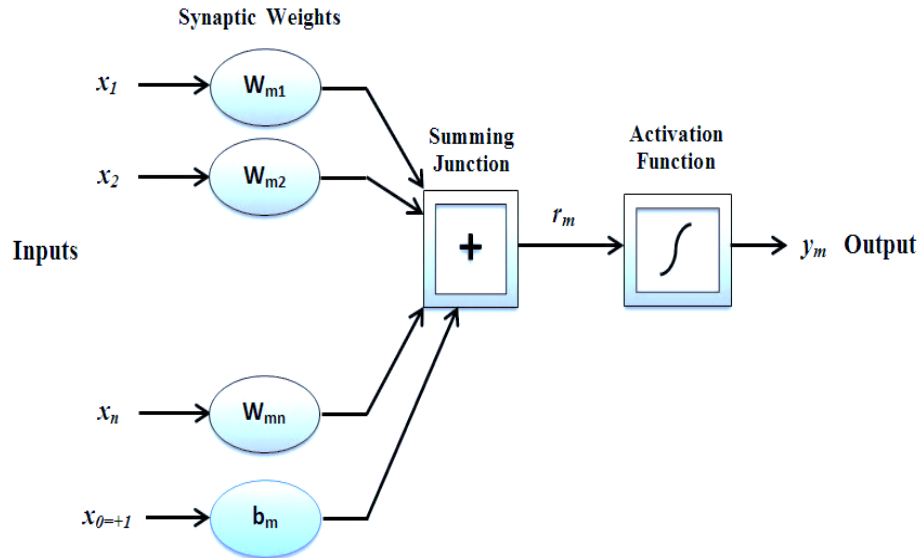


**Fig. 3.1:** A typical model representing an artificial neuron

This study employs the MLPs as the most popular feed-forward networks used in chemical, petroleum and natural gas processes [246, 247]. To train the MLPs and find the synaptic weights, the BP learning algorithm trained by the Levenberg-Marquardt (LM) technique [248-251] was used.

### 3.2. LSSVM

based on statistical learning theory, Vapnik [252-254] developed a supervised learning algorithm namely SVM. After the introduction of SVMs, they became an attractive tools for different analyses [255-264]. Detailed information regarding the SVMs can be found in the literature [252, 254, 265-269]. This work employs the LSSVM algorithm. LSSVM is a reformulation to conventional SVM [266, 270]. Mathematical background of the LSSVM is given in our published works .

In order to obtain the hyper-parameters of the LSSVM algorithm, i.e. regularization constant ( $\gamma$ ) and kernel bandwidth ( $\sigma^2$ ), the optimization algorithm of Coupled Simulating Annealing (CSA) was used [271]. Simplified flowchart of LSSVM model optimized by CSA algorithm is demonstrated in **Fig. 3.3**. **Fig 3.4** shows schematic of the LSSVM algorithm.

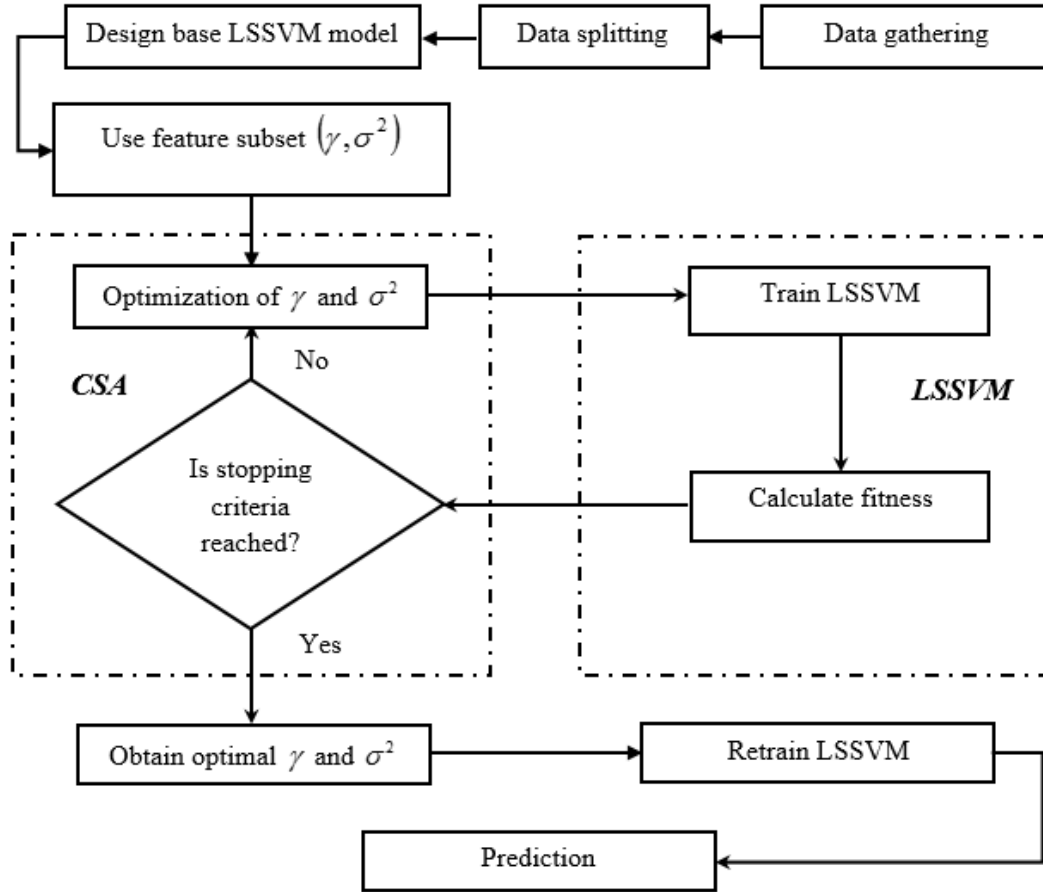


**Fig. 3.3:** Simplified flowchart of LSSVM model optimized by CSA algorithm

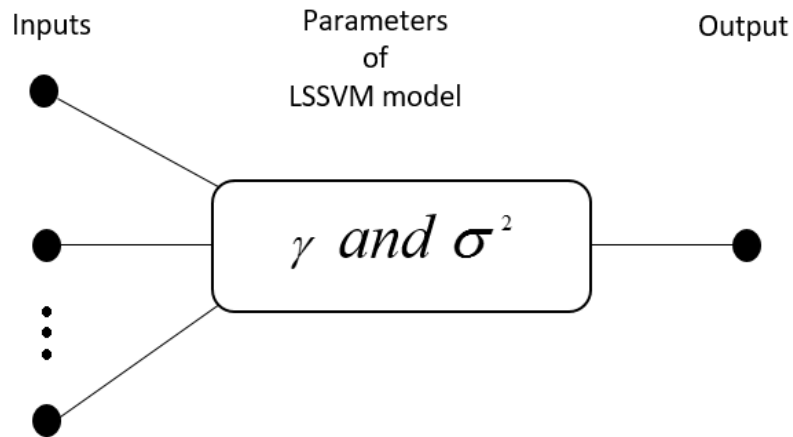


**Fig. 3.4:** Schematic of the LSSVM algorithm



### 3.3. ANFIS

Jang [272] introduced the ANFIS methodology by combining the FIS and ANN algorithms. As depicted in **Fig. 3.5**, the ANFIS has five different layers. In a respective order, the input layer, i.e. layer 0, and the output layer, i.e. layer 5 indicate the inputs and the output. In the hidden layers of this structure, there are different adjustable and fixed nodes. These nodes are functioning as rules and membership functions (MFs) as well.

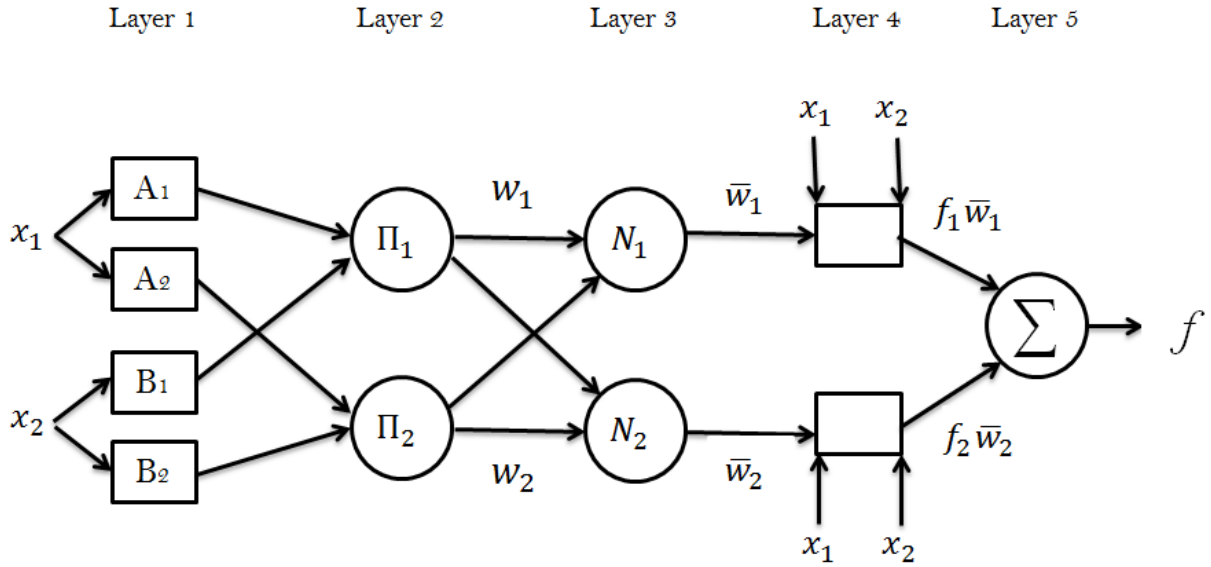


**Fig. 3.5:** Typical structure of ANFIS for a two-input and one output problem

To train the ANFIS model and find the MF parameters, a hybrid learning algorithm was used [272]. The suggested training steps for the Hybrid-ANFIS method is depicted in **Fig.3.6**.

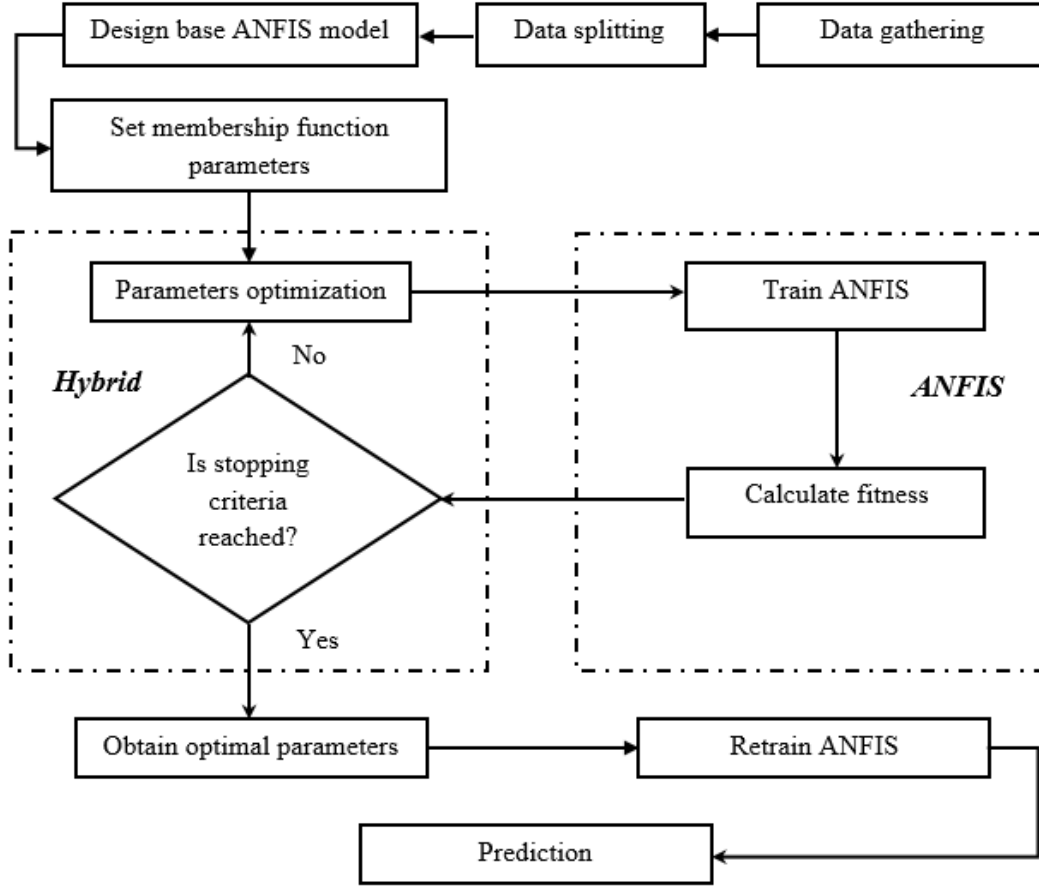


**Fig. 3.6:** Simplified flowchart of a typical Hybrid-ANFIS model

### 3.4. Decision Tree & Boosting

In machine learning, boosting algorithms can be employed for converting weak regressors/classifiers to strong ones [273]. Indeed, boosting algorithm encompasses two or more models to boost the precision of prediction or classification. Among the available boosting algorithms in the literature, the AdaBoost is a widely utilized method. To implement the method of AdaBoost, the information about the functioning of the weak learners is not required in advance [274]. AdaBoost.M1, and AdaBoost.R2, AdaBoost.M2 and AdaBoost.R, are different types of the

AdaBoost method. This work employs the AdaBoost.R2 [275], a boosting method for regression, for developing an ensemble method to predict the target values.

Initially, a weight,  $w_i$ , is assigned to each training data point. For each training sample, the following equation represents the absolute error:

$$e_i = |f_{R2}(x_i) - y_i| \dots\dots\dots (3.3)$$

where  $e_i$ ,  $f_{R2}(x_i)$  and  $y_i$  indicate the absolute error, base regressor prediction, and target, respectively.

To adjust the weights after each boosting iteration, the loss function is used. By considering  $E$  as the maximum value of absolute errors, three different loss functions namely linear, square, and exponential can be calculated according to the following expressions in a respective order:

$$L_i = \frac{e_i}{E} \dots\dots\dots (3.4)$$

$$L_i = \frac{e_i^2}{E^2} \dots\dots\dots (3.5)$$

$$L_i = 1 - \exp\left[-\frac{e_i}{E}\right] \dots\dots\dots (3.6)$$

Finally, the average loss can be calculated as bellows:

$$\bar{L} = \sum L_i p_i \dots\dots\dots (3.7)$$

in which  $p_i$  is the probability that data point  $i$  is in the training set.

In this study, the CART model was selected as the weak learner. In other words, the ensemble method was developed using the AdaBoost algorithm in conjunction with the CART method. CART is a non-parametric learning algorithm of decision trees that generates either regression or classification models. This method was presented by Breiman et al. [\[34\]](#). More information regarding CART method can be found in our previous works [\[276, 277\]](#).

## 4. Experimental data

### 4.1. Hydrate+Water/Ice+Salt/Alcohol Systems

To develop smart tools able to model the dissociation/formation conditions of different clathrate hydrates in pure water or inhibitors, an extensive databank containing more than 3500 experimental data points at (solid/ice/vapor) and (solid/liquid/vapor) equilibrium of several systems were gathered from the open literature published between 1940 and 2013 [36, 38, 49, 66, 67, 94, 278-360].

This assortment contains phase equilibria of several gas mixtures, nitrogen, hydrogen sulfide, methane, ethane, butane and propane in water and solutions of alcohols and/or salts. Detailed information are summarized in **Tables 4.1** to **4.5**.

**Table 4.1:** Additives in C1 hydrate system

Additive	Mean (wt%)	Max (wt%)
NaCl	2.28	22.03
KCl	0.60	15
CaCl <sub>2</sub>	1.20	25.74
MgCl <sub>2</sub>	0.46	15
Methanol	5.48	85
Ethylene glycol	3.30	70
Diethylene glycol	0.67	50
Triethylene glycol	1.18	50
1-propanol	0.61	20
2-propanol	0.60	20

**Table 4.2:** Additives in C2 hydrate system

Additive	Mean (wt%)	Max (wt%)
NaCl	0.51	20
KCl	0.40	10
CaCl <sub>2</sub>	0.47	15
Methanol	5.11	50
Triethylene glycol	1.70	40

**Table 4.3:** Additives in C3 hydrate system

Additive	Mean (wt%)	Max (wt%)
NaCl	2.46	20.03
KCl	1.86	20
CaCl <sub>2</sub>	1.53	15.2
Methanol	2.08	50

**Table 4.4:** Additives in N<sub>2</sub> hydrate system

Additive	Mean (wt%)	Max (wt%)
NaCl	1.76	26.4
KCl	1.49	36
Methanol	12.52	50
Ethylene glycol	0.52	15

**Table 4.5:** Additives in H<sub>2</sub>S hydrate system

Additive	Mean (wt%)	Max (wt%)
NaCl	0.66	20.2
KCl	0.16	15.01
CaCl <sub>2</sub>	0.48	33
MgCl <sub>2</sub>	0.15	10
Methanol	2.80	60
Ethylene glycol	1.23	70

## 4.2. Hydrate+IL Systems

The equilibrium data of methane hydrate dissociation in the presence of 32 ILs are gathered from Ref. [77-79, 81, 361-369]. details regarding the collected database are given in **Table 4.6**.

**Table 4.6:** information regarding the collected databank for methane hydrate in ILs

IL	Temperature range (K)	Pressure range (MPa)	Concentration (wt%)
[3C4C1P][MeSO <sub>4</sub> ]	273.3-287.1	4.09-14.77	26.11, 50.07
[BMIM][Ac]	279.4-286.8	3.49-13.04	10
[BMIM][BF <sub>4</sub> ]	272.9-287.1	2.58-11.50	10,15,20
[BMIM][Br]	285.9-291.6	10.57-20.41	10
[BMIM][Cl]	286.0-291.2	10.67-20.67	10
[BMIM][DCA]	272.5-281.4	2.51-6.26	10
[BMIM][I]	286.2-291.5	10.52-20.45	10
[BMIM][MeSO <sub>4</sub> ]	284.7-287.1	9.39-12.16	10
[EMIM][Ac]	274.5-286.6	3.51-13.08	10
[EMIM][Br]	284.7-290.8	10.10-20.20	10,20
[EMIM][Cl]	272.6-298.0	3.35-35.00	0.1-40.0
[EMIM][ClO <sub>4</sub> ]	275.3-287.6	3.54-13.21	10
[EMIM][EtSO <sub>4</sub> ]	284.6-287.4	8.67-11.65	8,10
[EMIM][HSO <sub>4</sub> ]	281.9-287.2	7.07-11.95	10
[EMIM][I]	276.7-288.0	3.99-14.12	10
[EMIM][NO <sub>3</sub> ]	269.2-289.7	3.08-16.12	1.0-40.0
[EMIM][SCN]	275.2-287.5	3.52-13.15	10
[EMMOR][BF <sub>4</sub> ]	276.9-282.2	3.99-7.06	10
[EMMOR][Br]	277.4-282.2	4.13-6.98	10
[EMPIP][BF <sub>4</sub> ]	272.6-280.8	3.03-6.83	10
[EMPIP][Br]	274.6-282.0	3.13-7.02	10
[MMIM][I]	276.7-288.0	4.00-14.29	10
[N1,1,1,1][Cl]	276.7-288.0	4.66-16.27	10
[N1,1,1,eOH][Cl]	276.7-288.0	4.11-15.01	10
[N2,2,2,2][Cl]	272.1-280.7	2.48-5.99	10
[OH-C2MIM][Cl]	276.6-288.0	4.18-15.31	0.1-10
[OH-EMIM][BF <sub>4</sub> ]	283.4-286.7	9.34-11.50	10, 20
[OH-EMIM][Br]	273.6-285.5	3.60-9.60	5-25
[OH-EMIM][Cl]	271.9-285.0	3.60-9.60	5-25
[OH-EMIM][ClO <sub>4</sub> ]	275.0-287.4	3.45-12.96	10
[OH-EMMIM][Cl]	274.7-287.4	3.51-13.28	10
[PMIM][I]	285.8-291.1	10.54-20.36	10

### 4.3. CO<sub>2</sub>+Water+Amine Systems

The gathered experimental data points comprises equilibrium conditions for absorption of CO<sub>2</sub> in aqueous solutions of MEA, TEA and DEA published in the open literature [370-383]. In a respective order, related information about amine concentration, pressure, CO<sub>2</sub> loading capacity and temperature for TEA, DEA, and MEA systems are summarized in **Tables 4.7** to **4.9**.

**Table 4.7:** Collected data for water+TEA+CO<sub>2</sub> system

Ref.	Temperature, K	CO <sub>2</sub> partial pressure range, kPa	Amine concentration, mol/L	CO <sub>2</sub> loading, (mol CO <sub>2</sub> /mol amine)	NPTS
[383]	313.2, 333.2, 353.2	1.43-153.4	2, 3	0.034-0.534	40
[370]	298.15	1.264-100.27	0.5-5	0.117-0.976	23
<i>Total</i>	<i>298.15-353.2</i>	<i>1.264-153.4</i>	<i>0.5-5</i>	<i>0.034-0.976</i>	<i>63</i>

NPTS indicates number of points.



**Table 4.8:** Collected data for water+DEA+CO<sub>2</sub> system

Ref.	Temperature, K	CO <sub>2</sub> partial pressure, kPa	Amine concentration, mol/L	CO <sub>2</sub> loading, (mol CO <sub>2</sub> /mol amine)	NPTS
[374]	313.15, 333.15, 353.15	13.4965- 286.069	0.32194298, 0.32339248, 0.324846754	0.281-0.817	11
[381]	303, 313, 323	9-104.7	2, 4	0.445-0.786	24
[372]	298.15, 323.15	9.1034- 2013.0344	0.057454573, 0.223622552, 2	0.006-2.012	23
[382]	298.15- 380.57	10.18-7017	2, 2.45, 3.5	0.184-1.273	80
[378]	313.15	10.84-269.3	0.324846754	0.507-0.83	5
[380]	366.48, 394.25	78.15-291.3	0.266020127	0.324-0.421	6
[379]	299.82- 399.82	9.487-6511.27	0.536540558	0.0751-4.7619	194
<i>Total</i>	<i>298.15- 399.82</i>	<i>9-7017</i>	<i>0.057454573-4</i>	<i>0.006-4.7619</i>	<i>343</i>

NPTS indicates number of points.

**Table 4.9:** Collected data for water+MEA+CO<sub>2</sub> system

Ref.	Temperature, K	CO <sub>2</sub> partial pressure, kPa	Amine concentration, mol/L	CO <sub>2</sub> loading, (mol CO <sub>2</sub> /mol amine)	NPTS
[373]	313.15	13.1-2189.1	0.183616859, 0.278962149	0.562-1.068	11
[374]	313.15, 333.15, 353.15	10.6207- 320.1379	0.531093557, 0.533812589, 0.536540558	0.575-0.683	12
[371]	298.15, 373.15	10.1732- 1013.46	5	0.289-851	10
[375]	333.15, 353.15, 373.15	8.2167- 1183.7532	5	0.306-0.646	24
[377]	393.15	9.045-191.9	0.525682276	0.1766-0.4182	18
[376]	313	110-6000	0.536561052	0.65-1.04	6
[378]	313.15	11.85-321.92	0.536540558	0.528-0.705	5
[380]	353.15, 373.15, 393.15	9.877-398.76	0.269189506, 0.270288061, 0.525682276, 0.531093557	0.215-0.473	11
[379]	353.15	8.62-121.8	2.4	0.42-0.58	6
<i>Total</i>	<i>298.15- 393.15</i>	<i>8.2167-6000</i>	<i>0.183616859-5</i>	<i>0.1766-1.068</i>	<i>103</i>

NPTS indicates number of points.

## 4.4. CO<sub>2</sub>+ IL Systems

The gathered collection to model the CO<sub>2</sub> solubility in ILs comprises 5332 equilibrium data sets. Information regarding the investigated ILs in this research as well as the references and the operational conditions of the data points are provided in **Table 4.10**.

**Table 4.10:** Information about the studied ILs

ILs	No.	P range (MPa)	T range (K)	CO <sub>2</sub> solubility (mole fraction)	References
[THTDP][DCA]	105	0.304–90.248	271.11–363.4	0.111–0.843	[384]
[hmim][Tf <sub>2</sub> N]	436	0.0089–45.28	278.12–413.2	0.001–0.8333	[385–394]
[bmim][BF <sub>4</sub> ]	255	0.0097–67.62	278.47–383.15	0.001–0.61	[385, 395–400]
[bmim][Tf <sub>2</sub> N]	447	0.06753–49.99	279.98–453.15	0.01488–0.8041	[401–408]
[bmim][PF <sub>6</sub> ]	406	0.00969–73.5	282.05–295.05	0.0006–0.729	[387, 395, 400, 403, 409–416]
[N4,1,1,1][NTf <sub>2</sub> ]	20	0.03606–20.37	282.94–343.07	0.01424–0.879	[401, 405]
[bmim][Ac]	81	0.0101–75	283.1–353.24	0.063–0.599	[385, 417, 418]
[THTDP][phos]	93	0.163–61.172	283.21–363.39	0.15–0.895	[384]
[emim][Tf <sub>2</sub> N]	345	0.01–43.2	283.43–453.15	0.0001–0.782	[385, 387, 391, 392, 401, 403, 407, 408]
[THTDP][NTf <sub>2</sub> ]	120	0.106–72.185	292.88–363.53	0.169–0.879	[419]
[C <sub>9</sub> mim][PF <sub>6</sub> ]	11	0.86–3.54	293.15–298.15	0.197–0.554	[412]
[C <sub>6</sub> mim][BF <sub>4</sub> ]	161	0.312–86.6	293.18–373.15	0.071–0.703	[387, 394, 420]
m-2-HEAF	80	0.494–52.91	293.21–363.42	0.057–0.534	[421]
[bmim][CH <sub>3</sub> SO <sub>4</sub> ]	54	0.908–9.805	293.2–413.1	0.03185–0.4524	[413]
[P14,6,6,6][Tf <sub>2</sub> N]	98	0.53–22.2	293.35–373.35	0.3606–0.848	[391, 422]
[C <sub>4</sub> mim][DCA]	40	1.018–73.64	293.36–363.25	0.2–0.601	[423]
[C <sub>8</sub> mim][Tf <sub>2</sub> N]	138	0.1123–34.8	297.55–353.15	0.0311–0.8456	[408, 424]
[emim][EtSO <sub>4</sub> ]	40	0.352–9.461	298.04–348.15	0.0174–0.457	[410, 425]
[emim][Ac]	36	0.01–1.9998	298.1–348.2	0.094–0.428	[385, 426]
[emim][TFA]	27	0.01–1.9996	298.1–348.2	0.001–0.282	[426]
[dmim][Tf <sub>2</sub> N]	37	1.439–20.15	298.15–322.2	0.257–0.878	[391, 405, 427]
[HEA]	42	0.116–10.98	298.15–328.15	0.0081–0.4009	[428, 429]
[BHEAA]	18	0.125–1.505	298.15–328.15	0.0089–0.0905	[428]
[HHEMEA]	18	0.124–1.516	298.15–328.15	0.0045–0.0761	[428]
[HEL]	42	0.127–10.09	298.15–328.15	0.0034–0.2442	[428, 429]
[BHEAL]	18	0.121–1.598	298.15–328.15	0.0035–0.0738	[428]
[HHEMEL]	18	0.154–1.535	298.15–328.15	0.0062–0.0776	[428]
[bmim][Tf <sub>2</sub> N]	36	0.0099–1.8997	298.15–343.15	0.002–0.382	[430]
[p(5)mpyr][Tf <sub>2</sub> N]	36	0.0097–1.9002	298.15–343.15	0.002–0.406	[430]

[P4441][Tf <sub>2</sub> N]	36	0.0099–0.8999	298.15–343.15	0.003–0.393	<a href="#">[430]</a>
[emim][BF <sub>4</sub> ]	34	0.251–4.329	298.15–343.2	0.0156–.2406	<a href="#">[387, 431]</a>
[C <sub>6</sub> mim][PF <sub>6</sub> ]	159	0.296–94.6	298.15–373.15	0.058–0.727	<a href="#">[387, 394, 432]</a>
[THTDP][Cl]	70	0.168–24.57	302.55–363.68	0.119–0.8	<a href="#">[419]</a>
[hemim][BF <sub>4</sub> ]	44	0.114–1.194	303.15–353.15	0.004–0.102	<a href="#">[433]</a>
[C <sub>8</sub> mim][PF <sub>6</sub> ]	61	0.1287–10.516	303.15–363.27	0.0231–0.755	<a href="#">[410, 434]</a>
[HMIM][MeSO <sub>4</sub> ]	48	0.3–50.14	303.15–373.15	0.158–0.602	<a href="#">[394]</a>
[C <sub>6</sub> mim][TfO]	134	1.25–100.12	303.15–373.15	0.267–0.816	<a href="#">[394, 435]</a>
[C <sub>2</sub> mim][SCN]	72	1.3–95.34	303.15–373.15	0.169–0.474	<a href="#">[436]</a>
[C <sub>2</sub> mim][N(CN) <sub>2</sub> ]	80	0.88–96.2	303.15–373.15	0.171–0.585	<a href="#">[436]</a>
[C <sub>2</sub> mim][C(CN) <sub>3</sub> ]	80	0.59–88.29	303.15–373.15	0.17–0.703	<a href="#">[436]</a>
[C <sub>3</sub> mpy][Tf <sub>2</sub> N]	56	0.52–47.1	303.15–373.15	0.186–0.787	<a href="#">[437]</a>
[C <sub>5</sub> mpy][Tf <sub>2</sub> N]	64	0.27–55.1	303.15–373.15	0.198–0.785	<a href="#">[437]</a>
[C <sub>7</sub> mpy][Tf <sub>2</sub> N]	64	0.26–72.24	303.15–373.15	0.302–0.853	<a href="#">[437]</a>
[BMP][Tf <sub>2</sub> N]	72	0.68–62.77	303.15–373.15	0.2276–0.8029	<a href="#">[411]</a>
[BMP][MeSO <sub>4</sub> ]	40	3.07–97.3	303.15–373.15	0.2871–0.6049	<a href="#">[411]</a>
[HMP][Tf <sub>2</sub> N]	64	1.06–47.55	303.15–373.15	0.2778–0.8105	<a href="#">[411]</a>
[OMP][Tf <sub>2</sub> N]	72	0.51–35.92	303.15–373.15	0.2409–0.8176	<a href="#">[423]</a>
[BMP][TfO]	64	1.88–70.2	303.15–373.35	0.2583–0.7058	<a href="#">[422]</a>
[C <sub>9</sub> mpy][Tf <sub>2</sub> N]	56	0.26–100.12	303.15–453.15	0.323–96.81	<a href="#">[437]</a>
[THTDP][Br]	47	0.876–12.998	303.19–363.44	0.114–0.694	<a href="#">[384]</a>
[C <sub>2</sub> mim][TfO]	55	0.8–37.8	303.85–344.55	0.1794–0.6268	<a href="#">[435]</a>
[C <sub>4</sub> mim][TfO]	65	0.85–37.5	303.85–344.55	0.2182–0.672	<a href="#">[435]</a>
[C <sub>8</sub> mim][TfO]	65	0.68–34	303.85–344.55	0.2166–0.7414	<a href="#">[435]</a>
[omim][BF <sub>4</sub> ]	121	0.571–85.8	307.79–363.29	0.1005–0.7523	<a href="#">[410, 438]</a>
[emim][PF <sub>6</sub> ]	74	1.49–97.1	308.14–366.03	0.104–0.619	<a href="#">[439]</a>
m-2-HEAA	41	0.84–80.5	312.93–363.61	0.157–0.5	<a href="#">[421]</a>
1-Bromohexane	22	0.537–10.781	313.15–333.15	0.0411–0.9681	<a href="#">[440]</a>
1-Methylimidazole	18	0.99–15.352	313.15–333.15	0.0837–0.9521	<a href="#">[440]</a>
[hmim][Br]	11	3.09–14.891	313.15–333.15	0.132–0.468	<a href="#">[440]</a>
[TDC][DCN]	38	0.01–1.9007	313.15–333.15	0.00175–0.272	<a href="#">[441]</a>
[EMMP][TF <sub>2</sub> N]	39	0.0098–1.9	313.15–333.15	0.00182–0.3165	<a href="#">[441]</a>
[TDC][TF <sub>2</sub> N]	39	0.0097–1.8998	313.15–333.15	0.0023–0.36	<a href="#">[441]</a>
[P6,6,6,14][Cl]	8	8.21–20.71	313.2–323.2	0.714–0.824	<a href="#">[405]</a>
[Pyr4,1][NTf <sub>2</sub> ]	8	8.06–20.38	313.2–323.2	0.65–0.853	<a href="#">[405]</a>
[N1,8,8,8][NTf <sub>2</sub> ]	8	8.08–20.56	313.2–323.2	0.789–0.907	<a href="#">[405]</a>
[bmim][Cl]	45	2.454–36.946	353.15–373.15	0.1306–0.406	<a href="#">[442]</a>

#### 4.5. CO<sub>2</sub>+Water+PZ system

In order to utilize the smart modeling techniques for representing/predicting the solubility of CO<sub>2</sub> in PZ solutions, the required experimental data were collected from the literature [166, 443] [168, 444-446]. Details about the collected databank for the equilibrium system of (CO<sub>2</sub>+PZ+water) are given in **Table 4.11**.

**Table 4.11:** Equilibrium system of CO<sub>2</sub>+ PZ+water

Ref.	No.	T range (K)	C <sub>PZ</sub> (mol/L)	P <sub>CO2</sub> range (kPa)	$\alpha_{\text{CO}_2}$
[443]	17	313.00-343.00	0.600	0.03-40.00	0.160-0.960
[166]	64	287.10-313.10	0.099-1.999	1.93-532.00	0.097-2.680
[168]	315	298.00-328.00	0.200-4.500	0.08-1487.00	0.263-2.956
[444]	58	298.15-343.15	0.200-0.600	0.27-111.37	0.360-1.230
[445]	93	313.13-393.15	1.919-3.912	13.30-9560.00	0.502-1.687
[446]	29	313.15-333.15	1.913-7.708	5.89-15.50	0.260-0.860
<i>Total</i>	<i>577</i>	<i>287.10-393.15</i>	<i>0.099-7.708</i>	<i>0.03-9560.00</i>	<i>0.097-2.956</i>

#### 4.6. CO<sub>2</sub>+Water+SG System

For the system of (CO<sub>2</sub>+sodium glycinate (SG)+water), 197 equilibrium data were collected from the literature. More information about the experimental data points are summarized in **Table 4.12**.

**Table 4.12:** Equilibrium information for CO<sub>2</sub> solubility in solution of SG

Ref.	$T$ , K	$C_{SG}$ , mass%	$P_{CO_2}$ , kPa	$\alpha$ , mol CO <sub>2</sub> / mol SG solution	$n$
[184]	303.15, 313.15, 323.15	10, 20, 30	213.5-5062.5	0.170-1.075	74
[185]	313.15, 323.15, 333.15	5, 10, 15, 20, 25	0.06-773.5	0.0023-1.7490	123

#### 4.7. CO<sub>2</sub>-Reservoir Oil MMP

In order to develop mathematical models for representing/predicting the CO<sub>2</sub>-reservoir oil MMP, previously published experimental data on the parameters affecting the value of CO<sub>2</sub>-reservoir oil MMP have been gathered from literature. The collected data points have been reported by Rathmell et al. [447], Shokir [448], Holm and Josendal [218], Alston et al. [237], Sebastian et al. [239], Eakin and Mitch [449], Harmon and Grigg [450], Emera and Sarma [238], Jacobson [451], Graue and Zana [219], Metcalfe [452], Thakur et al. [453], Gharbi and Elsharkawy [454], Dong et al. [455], Bon et al. [456], and Shokrollahi et al. [195].

#### 4.8. Data Validation

In this work, the mathematical approach of Leverage was employed to assess the gathered datasets for the studied systems. Leverage method comprises of calculation of the differences between target values and model outcomes, i.e. residual, as well as defining a Hat matrix that

includes the predicted values and target values. Information about this technique is given in our published works [\[457, 458\]](#).

Utilizing the Leverage approach, it was found that the gathered databases for hydrate systems, CO<sub>2</sub>+solvent systems, and CO<sub>2</sub>-oil MMP are reliable. Hence, the collected data points were used for both development and performance evaluation of the predictive mathematical models including tree-based, ANN, ANFIS, and LSSVM.

## 5. Model development

### 5.1. General step

The first step in the development of the ANN, LSSVM, DT and ANFIS models is dividing the gathered database into two smaller groups including test dataset and training dataset. For each system, the employed databank was randomly divided into two sub-datasets. The allocated data points for the training are utilized to construct the predictive mathematical model. On the other hand, the test sub-group is employed to assess the performance of the developed models in representing the target values. The utilized softwares for the development of the smart models are Matlab and Python.

### 5.2. Hydrate+Water/Ice+Salt/Alcohol Systems

To develop the predictive tools to estimate the HDT of various systems including propane, methane, ethane, hydrogen sulfide, i-butane and nitrogen in the solutions of alcohol and/or electrolyte or pure water, HDT is considered as a function of concentration(s) of the available additives (salts and/or alcohols) and the system's pressure as well:

$$HDT = f(P, C_{additive}) \dots\dots\dots (5.1)$$

where  $P$  and  $C_{additive}$  indicate pressure and additive(s) concentration in aqueous phase, respectively.

For the desired gas mixtures, another independent parameter was the gas composition:



$$HDT = f(P, Z_i, C_{additive}) \dots\dots\dots (5.2)$$

in which  $Z_i$  is the gas composition.

To construct ANN tools for estimating the HDT of the investigated hydrate systems, the number of hidden neurons was changed from 5 to 15. Subsequently, the performance of the created ANN model was evaluated. **Table 5.1** gives the topology of the best developed ANN model for each system. For all the developed ANN models the transfer function of hyperbolic tangent sigmoid type was used.

**Table 5.1:** Topology of the presented ANN models for the studied hydrate systems

System	Topology
C1	11-9-1
C2	6-8-1
C3	5-10-1
i-C4	1-7-1
H <sub>2</sub> S	5-8-1
N <sub>2</sub>	1-9-1
Gas mix.	23-12-1

The tuned values of the LSSVM hyper-parameters including kernel bandwidth ( $\sigma^2$ ) and regularization constant ( $\gamma$ ) to predict/represent the HDT of H<sub>2</sub>S, C1, C3, C2, N<sub>2</sub>, i-C4 and gas mixture systems are given in **Table 5.2**.

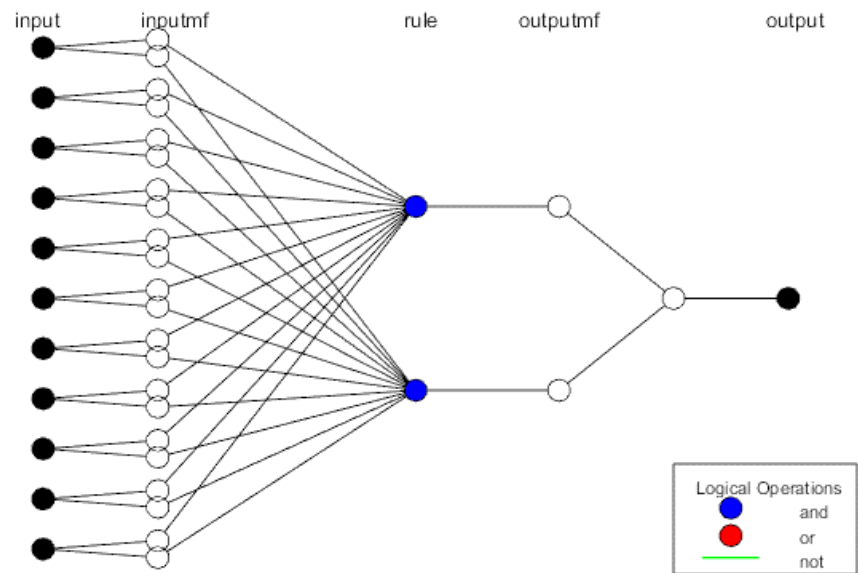
**Table 5.2:** Hyper-parameters of the presented LSSVM tools for hydrate systems

System	$\sigma^2$	$\gamma$
C1	0.142784211937565	644.724445609795
C2	0.004869768861272	185.010666994328
C3	29.75196837406490	106.660364404458
i-C4	0.369711172980082	7437.14229983432
H <sub>2</sub> S	0.008745591455999	47.6432124133609
N <sub>2</sub>	1.385581681162430	39993.4467324536
Gas mix.	0.912513403963931	163.660953927937

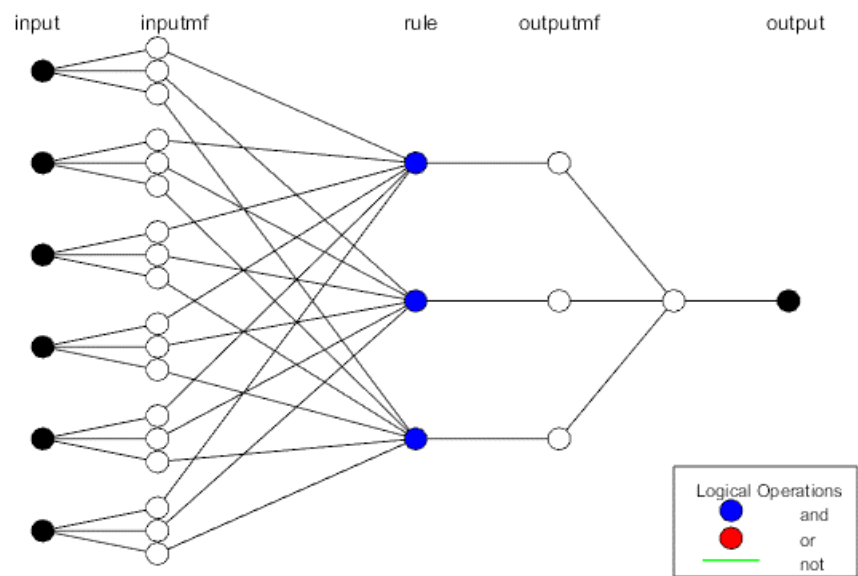
Specifications of the presented ANFIS models are summarized in **Table 5.3**. Structures of the constructed ANFIS models for estimation of the dissociation conditions of C3, N<sub>2</sub>, C1, C2, i-C4, H<sub>2</sub>S and gas mixture are shown in **Fig. 5.1**.

**Table 5.3:** Information of the developed ANFIS models for the studied hydrate systems

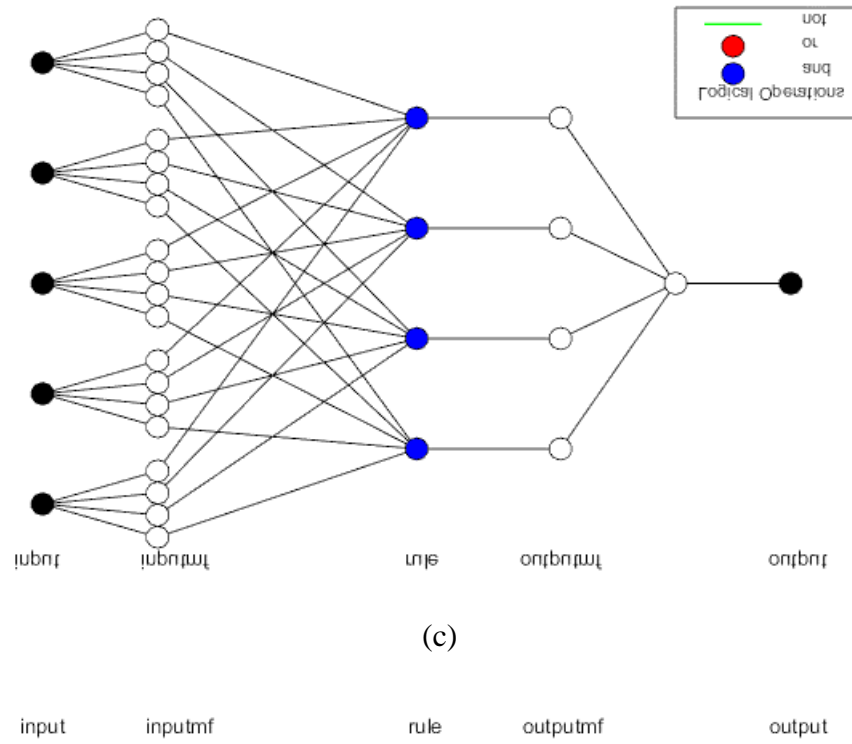
Parameter	System						
	C1	C2	C3	i-C4	H <sub>2</sub> S	N <sub>2</sub>	Gas mix.
Cluster center's range of influence	0.41	0.11	0.21	0.35	0.13	0.18	0.26
No of inputs	11	6	5	1	5	1	23
No of fuzzy rules	2	3	4	2	13	3	4
Max epoch number	700	500	100	200	200	180	200
Initial step size	0.10	0.10	0.10	0.10	0.05	0.05	0.05
Step size decrease rate	0.95	0.95	0.90	0.90	0.90	0.85	0.95
Step size increase rate	1.10	1.05	1.05	1.05	1.05	1.15	1.15



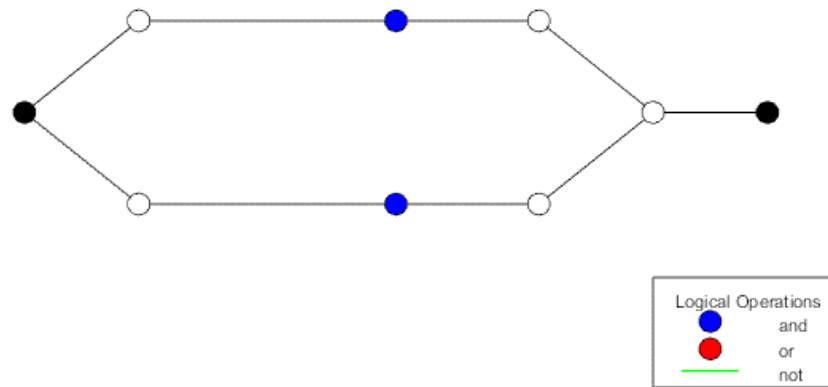
(a)



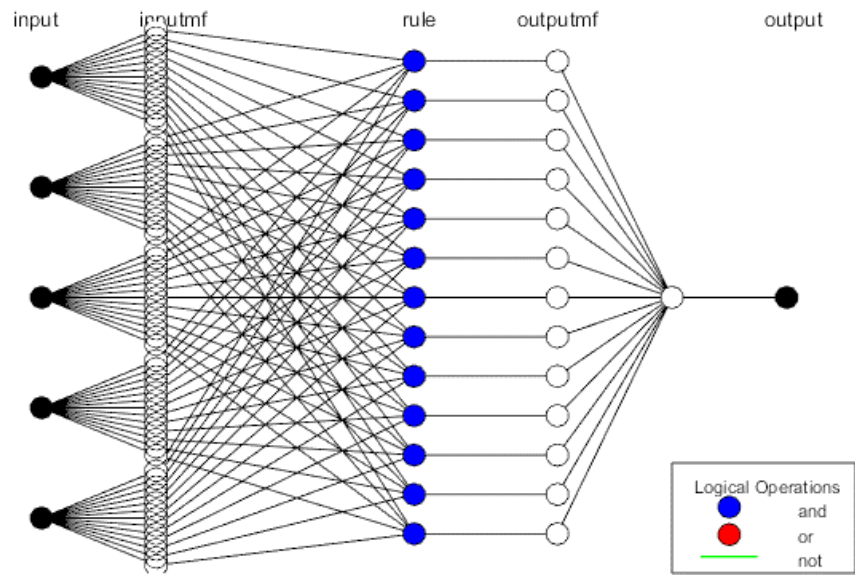
(b)



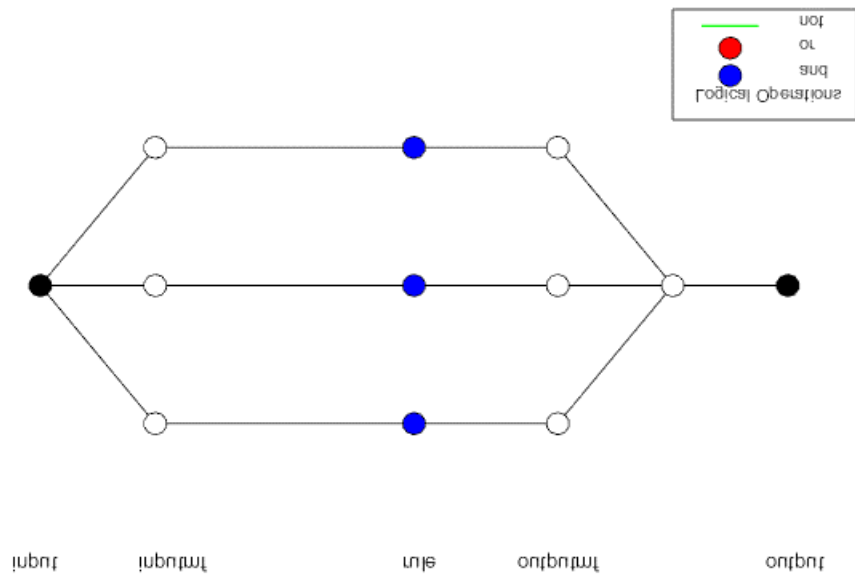
(c)



(d)



(e)



(f)

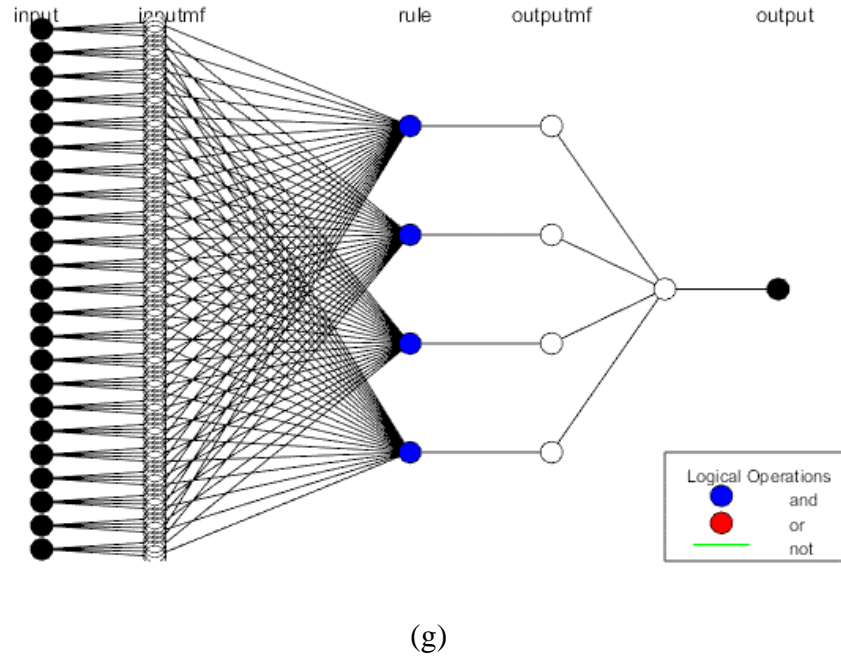


**Fig. 5.1:** ANFIS structure for (a) methane hydrate system; (b) ethane hydrate system; (c)propane hydrate system; (d) i-butane hydrate system; (e) hydrogen sulfide hydrate system; (f) nitrogen hydrate system, and (g) gas mixture hydrate system

Specifications of the presented AdaBoost tools for estimation of the HDT of investigated hydrate systems are summarized in **Table 5.4**. The digraph of the developed AdaBoost-CART model can be found in **Appendix B**.

**Table 5.4:** Specifications of the presented AdaBoost models for the studied hydrate systems

System	Number of Trees	Maximum Depth
C1	7	45
C2	3	40
C3	4	45
i-C4	2	25
H <sub>2</sub> S	6	40
N <sub>2</sub>	2	25
Gas mix.	8	55

### 5.3. Hydrate+IL Systems

With the aim of developing the models, as defined in Eq. (5.3), it is assumed that the equilibrium temperature of methane hydrate dissociation in ILs ( $T_{Hyd}$ , K) is a function of the system's pressure ( $P_{Hyd}$ , MPa), concentration of the aqueous phase ( $C_{IL}$ , wt%), critical temperature of the IL ( $T_c$ , K), and the critical pressure of the IL ( $P_c$ , MPa).

$$T_{Hyd} = f(P_{Hyd}, C_{IL}, P_c, T_c) \dots\dots\dots (5.3)$$

In this work, the critical properties of the investigated ILs are calculated using the group contribution methods presented by Valderrama and Robles [459].

In order to find the optimum ANN model, the number of hidden neurons was changed from 5 to 15. Subsequently, the performance of the created ANN model was evaluated. The network with 10 hidden neurons as well as hyperbolic tangent sigmoid transfer function presents a better performance compared to other structures. The weight and bias values of the best developed ANN model are presented in **Table 5.5**.

The tuned values of the LSSVM hyper-parameters including kernel bandwidth ( $\sigma^2$ ) and regularization constant ( $\gamma$ ) for predicting the dissociation temperature of methane hydrate in the presence of ILs are found to be 1.58390588574261 and 47471.4308399958, respectively. As can be seen, the number of digits of ANN and LSSVM models are different. This is due to the fact that the number of digits of the LSSVM and ANN controlling parameters are generally obtained using sensitivity analysis of the overall errors of the procedure of employed optimization.

Specifications of the developed ANFIS model are summarized in **Table 5.6**. The structure of the constructed ANFIS model for predicting the dissociation conditions of methane hydrate in ILs is shown in **Fig. 5.2**. **Fig. 5.3** illustrates the MFs for the independent parameters including the

system's pressure, concentration of the aqueous phase, critical temperature/pressure of the IL. The vertical axis in **Fig. 5.3** is the degree of membership. This parameter, also known as membership grade, is the output of a MF. The value of it ranges from 0 to 1.

**Table 5.5:** Information of the proposed ANN model for hydrate+IL systems

Hidden layer				Output layer	
Weight matrix				Bias vector	Transposed weight vector
1.3617	-1.8998	-0.0822	0.8246	-2.6571	-0.8618
0.3341	-1.3306	-0.3439	1.8648	-2.1783	-2.2582
-0.37773	0.4412	-1.3430	2.6148	1.3324	1.4962
-2.2096	0.4224	0.7344	2.4015	0.7179	-0.1589
-0.3155	0.2364	-3.6534	0.1131	-4.1347	2.5965
-0.2115	0.2108	-1.0659	1.6358	0.7525	-2.3328
0.8142	0.8558	-3.7081	-0.4779	-1.1096	-0.2216
0.0772	0.1335	-5.2415	-0.0462	-4.5466	-3.0992
0.7812	-0.6621	1.8328	-2.8899	0.4450	-0.3898
-0.2465	0.0235	0.0235	0.3061	4.7785	-4.4022

1.2714

**Table 5.6:** The developed ANFIS model to predict the C1 hydrate dissociation temperature in ILs

Parameter	Description/value
Cluster center's range of influence	0.40
No of inputs	4
No of outputs	1
No of fuzzy rules	6
Max epoch number	700
Initial step size	0.10
Step size decrease rate	0.90
Step size increase rate	1.10



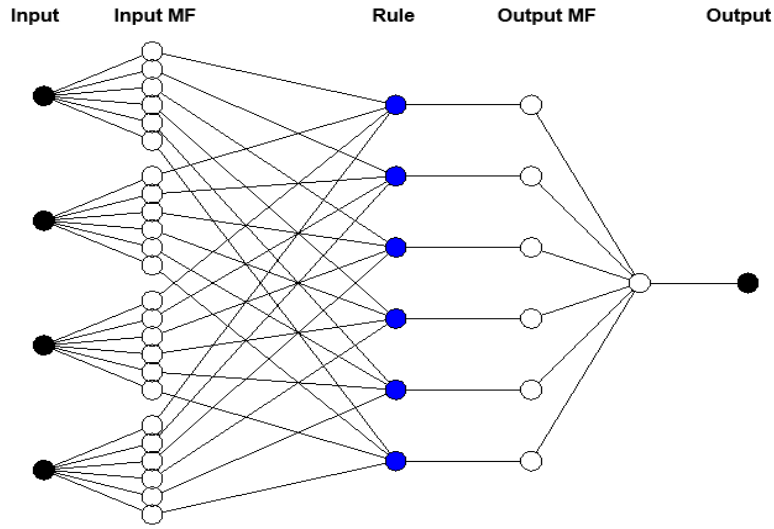


**Fig. 5.2:** Structure of the created ANFIS model for methane hydrate+IL systems

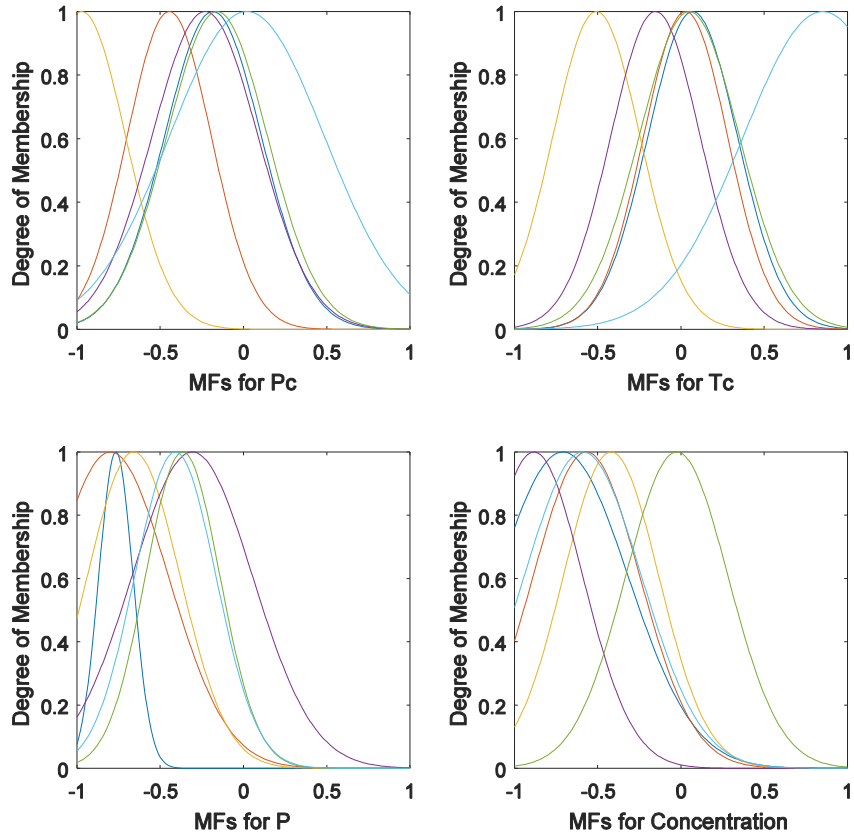


**Fig. 5.3:** Membership functions for the independent parameters ( $C_1$ +IL system)

Using a procedure of trial and error, the tuned value of the maximum depth for the CART model was found to be 13. The initial CART depth was 2 to start the trial and error procedure. The digraph of the developed CART model can be found in **Appendix B**.

#### 5.4. CO<sub>2</sub>+Water+Amine Systems

With the objective of presenting effective models to predict CO<sub>2</sub> loading capacity of amine aqueous solutions,  $\alpha$ , partial pressure of CO<sub>2</sub>,  $P_{CO_2}$ , system's temperature, and concentration of amine in aqueous phase,  $C_{amine}$ , are selected as the independent parameters of modeling.

$$\alpha = f(T, P_{CO_2}, C_{amine}) \dots\dots\dots (5.3)$$

By changing the number of neurons in the hidden layer from 5 to 15, several models were built for predicting the solubility of CO<sub>2</sub> in amine (MEA, DEA, and TEA) aqueous solutions. Subsequently, the performance of the obtained ANN models was evaluated. **Table 5.7** summarizes the topology of the best developed ANN models for each amine system. In this work, the hyperbolic tangent sigmoid transfer function was employed for presenting all the ANN models.

The tuned values of the LSSVM hyper-parameters including kernel bandwidth ( $\sigma^2$ ) and regularization constant ( $\gamma$ ) for prediction/representing the solubility of CO<sub>2</sub> in MEA, DEA, and TEA aqueous solutions are given in **Table 5.8**.

**Table 5.7:** Topology of the presented ANN models for the studied amine systems

System	Topology
CO <sub>2</sub> +MEA+Water	3-11-1
CO <sub>2</sub> +DEA+Water	3-11-1
CO <sub>2</sub> +TEA+Water	3-9-1

**Table 5.8:** Hyper-parameters of the presented LSSVM tools for hydrate systems

System	$\sigma^2$	$\gamma$
CO <sub>2</sub> +MEA+Water	5219.69911188144	13.1865999959447
CO <sub>2</sub> +DEA+Water	500.021537462106	0.42109028447486
CO <sub>2</sub> +TEA+Water	1379192.32247305	4.25519334412296

**Tables 5.9** gives the specifications of the presented ANFIS models for modeling the CO<sub>2</sub> removal with solutions of amine (MEA, DEA, and TEA).

**Table 5.9:** Specifications of the created ANFIS tool for estimating the CO<sub>2</sub> loading capacity of MEA, DEA, and TEA solutions

Parameter	System		
	MEA	DEA	TEA
Cluster center's range of influence	0.3	0.5	0.8
Number of inputs	3	3	3
Number of fuzzy rules	9	8	8
Maximum epoch number	500	1500	500
Initial step size	0.10	0.10	0.10
Step size decrease rate	0.95	0.90	0.90
Step size increase rate	1.05	1.10	1.10

The number of features in AdaBoost-CART methodology is equal to the number of independent variables. Hence, there are three features including  $P_{CO_2}$ ,  $C_{amine}$ , and  $T$ . Next parameter of the AdaBoost-CART method is the maximum depth of CART. This parameter determines the maximum length among the existing paths in a tree that connects a root to a leaf. There is no universal rule to obtain the maximum depth of CART so that the presented tree-based model provides the best outcomes. Furthermore, the optimum number of CART models in the AdaBoost-CART model should be determined.

In this work, a trial and error procedure was used to find the best value for the maximum depth of CART as well as the number of trees in predictive mathematical model. The initial tree depth was 3 for starting the procedure. The obtained results are summarized in **Table 5.10**. The digraph of the developed AdaBoost-CART model can be found in **Appendix B**.

**Table 5.10:** Specifications of the presented AdaBoost-CART models for the studied hydrate systems

System	Number of Trees	Maximum Depth
CO <sub>2</sub> +MEA+Water	3	17
CO <sub>2</sub> +DEA+Water	3	11
CO <sub>2</sub> +TEA+Water	5	16

## 5.5. CO<sub>2</sub>+IL systems

Eq. (5.4) defines the independent variables considered for constructing the CART model for estimation of the solubility of carbon dioxide in ILs.

$$\alpha = f(T, P, T_c, P_c, \omega) \dots\dots\dots (5.4)$$

in which, in respective order,  $P$  and  $T$  are the pressure (MPa) and temperature (K);  $\omega, T_c, P_c$ , indicate the acentric factor of the IL, critical temperature (K), and critical pressure (MPa), respectively. The acentric factor as well as the critical properties for the studied ILs were obtained from Baghban et al. [460].

In this work, using a trial and error procedure, the tuned value of the maximum depth of the CART model found to be 15. To start the trial and error procedure, the initial tree depth was assumed to be 3. The prediction ability of the proposed model will be compared to the capability of the previously published RBF-ANN, LSSVM, MLP-ANN, and ANFIS models by Baghban, Mohammadi and Taleghani [460]. The digraph of the developed CART model can be found in **Appendix B**.

## 5.6. CO<sub>2</sub>+Water+PZ System

For presenting predictive tools, it is considered that the solubility of carbon dioxide in PZ solution is dependent to the concentration of PZ ( $C_{PZ}$ ), CO<sub>2</sub> partial pressure ( $P_{CO_2}$ ) and temperature ( $T$ ). Eq. (5.5) defines the mathematical representation of the independent and dependent parameters:

$$\alpha = f(T, P_{CO_2}, C_{PZ}) \dots\dots\dots (5.5)$$

Considering the ANN methodology, the number of neurons in the hidden layer (or the number of hidden neurons) was adjusted between 5 and 15. Then, the capability of the presented ANN tool in predicting the target values was evaluated employing the mean squared error (MSE) as a cost function. All the created ANN models utilized the transfer function of hyperbolic tangent sigmoid type.

At the end, the obtained topology for the best presented ANN model was 3-9-1. The tuned values for biases and weights of the proposed optimum ANN model with 3-9-1 topology are given in **Table 5.12**.

**Table 5.12:** Information for the best ANN model developed for (CO<sub>2</sub>+water+PZ) system

Hidden layer					Output layer
Weight matrix		Bias vector	Trans. weight vector		Bias
-1.2643	3.4209	-0.0184	-3.6502	-0.5777	-2.3893
2.8040	-0.1054	3.0622	-3.5056	0.0960	
1.3671	1.3623	1.6775	5.3652	0.8594	
2.0448	2.6560	-1.2479	-2.9889	-0.0584	
1.1061	-2.0991	2.8461	0.7045	-0.1810	
-1.5344	1.9070	1.4035	-1.7739	0.1604	
1.6475	-5.6549	0.9918	-8.0949	-4.5166	
1.0310	-4.4735	15.0809	13.4310	-8.4983	
-0.0837	20.6984	0.2548	22.3810	4.9268	

In a respective order, the tuned values of the CSA-LSSVM tool hyper-parameters including regularization constant ( $\gamma$ ) and kernel bandwidth ( $\sigma^2$ ) were computed to be 633.3124026229270 and 0.421303271273034.

Information of the developed ANFIS tool to model the equilibrium solubility of CO<sub>2</sub> in solution of PZ is summarized in **Table 5.13**. **Fig. 5.4** demonstrates the structure of the created ANFIS tool.

**Table 5.13:** Specifications of the created ANFIS tool for the CO<sub>2</sub>+water+PZ system

Parameter	Description/value
Cluster center's range of influence	0.28
No of inputs	3
No of outputs	1
No of fuzzy rules	3
Maximum epoch number	200
Initial step size	0.10
Step size decrease rate	0.90
Step size increase rate	1.10

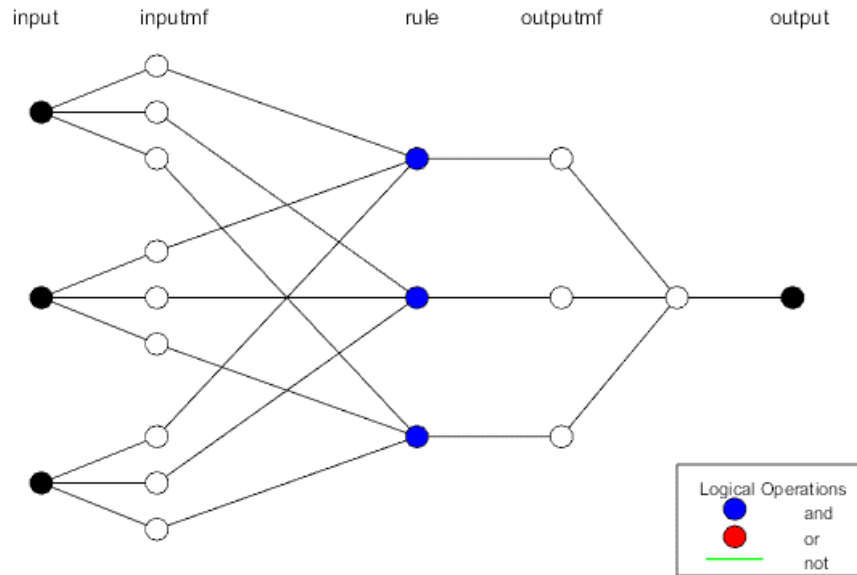


**Fig. 5.4:** ANFIS tool for (CO<sub>2</sub>+water+PZ) system

Employing the trial and error algorithm and changing the CART's number in the AdaBoost-based model, the most accurate AdaBoost-CART tool was found to have 5 DTs. Furthermore, the maximum depth of the CARTs was calculated to be 14. Schematic of the best presented AdaBoost-based model to estimate the carbon dioxide equilibrium absorption in PZ aqueous solution is shown in **Fig. 5.5**. The digraph of the developed CART model can be found in **Appendix B**.

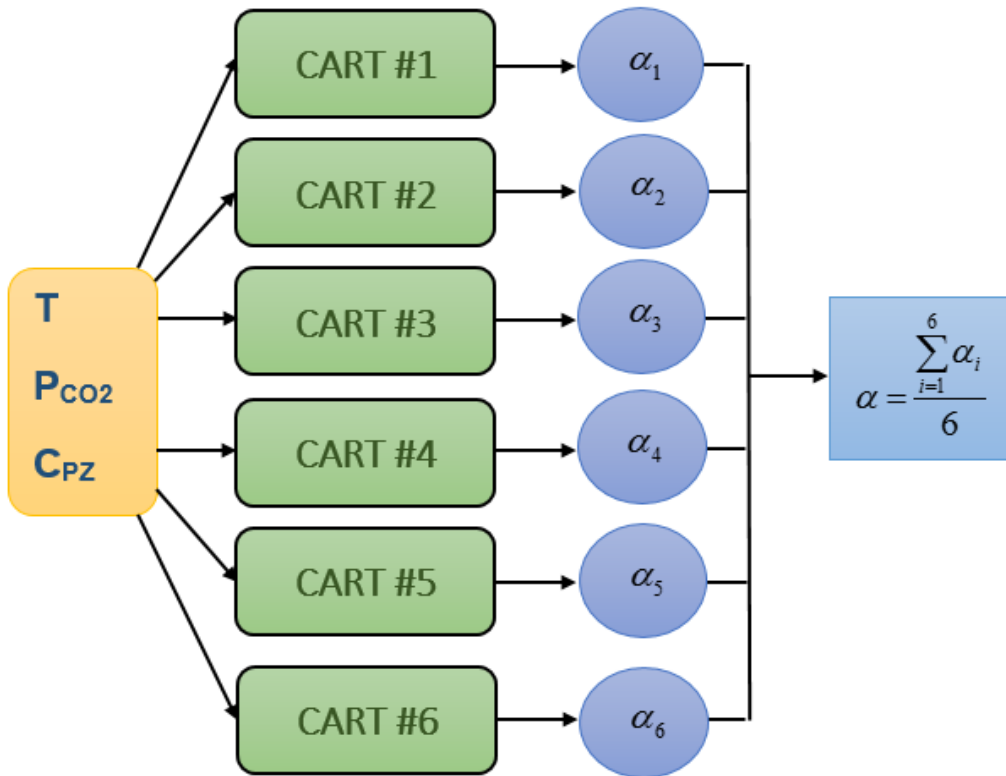


**Fig. 5.5:** Schematics of the AdaBoost-CART model for CO<sub>2</sub>+water+PZ system



## 5.7. CO<sub>2</sub>+Water+SG System

Eq. (5.6) is the mathematical representation of the relation between the dependent and independent variables for the modeling process:

$$\alpha = f(P_{CO_2}, C_{SG}, T) \dots\dots\dots (5.6)$$

where  $C_{SG}$  is the concentration of SG solution

According to the result of the used trial and error procedure, the optimum ANN model has the structure of 3-11-1. The tuned values for the hyper-parameters of LSSVM tool including  $\gamma$  and  $\sigma^2$  are 2391.43658924352 and 20.1719613854336, respectively. **Tables 5.14** gives the details of the proposed ANFIS tool to model the CO<sub>2</sub> removal with SG solution.

**Table 5.14:** Specifications of the presented ANFIS model for predicting solubility of CO<sub>2</sub> in SG

Parameter	Description/value
Cluster center's range of influence	0.63
No of inputs	3
No of outputs	1
No of fuzzy rules	6
Maximum epoch number	700
Initial step size	0.05
Step size decrease rate	1.02
Step size increase rate	1.24

In the case of presenting the AdaBoost-CART tool, a predictive mathematical model with 5 CARTs was found as the optimum structure. The maximum depth of the CART within the

AdaBoost was detected to be 10. The proposed AdaBoost-CART tool is schematically illustrated in **Fig. 5.6**.

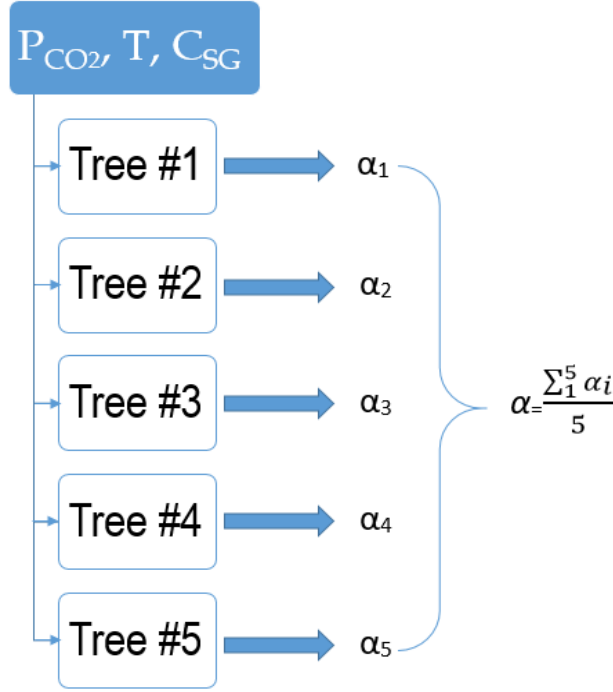


**Fig. 5.6:** Structure of the proposed AdaBoost-CART tool to estimate the CO<sub>2</sub> loading capacity of SG

## 5.8. CO<sub>2</sub>-Oil MMP

In 2013, Tatar et al. [243] developed an ANN model to predict the CO<sub>2</sub>-reservoir oil MMP. In another work, Shokrollahi et al. [30] employed the LSSVM technique for modeling the CO<sub>2</sub>-reservoir oil MMP. In this work, two novel predictive mathematical models are developed on the basis of ANFIS and AdaBoost-CART methodologies.

For building the predictive mathematical models, it is assumed that the CO<sub>2</sub>-reservoir oil MMP is a function of the reservoir temperature, composition of the drive gas, critical temperature

of the drive gas (in average), molecular weight of  $C_{5+}$  fraction in crude oil (MW  $C_{5+}$ ), the ratio of volatile to intermediate components in crude oil. The pure drive gas is  $CO_2$ , and the impure drive gas contains  $CO_2$ ,  $H_2S$ ,  $C1-C5$ , and/or  $N_2$ .  $C1$  and  $N_2$  are the volatile components; and the intermediate components in the crude oil are  $C2-C4$ ,  $H_2S$ , and  $CO_2$ . Finally, nine independent parameters were determined. **Table 5.15** gives the independent parameters and their corresponding ranges. The  $CO_2$ -reservoir oil MMP range is from 6.54 to 34.47 *MPa*, and the average of it is 14.86 *MPa*.

**Table 5.15:** Independent parameters and their ranges for developing ANFIS and AdaBoost-CART models

Parameter	Minimum	Maximum	Average
T (K)	305.35	391.45	341.92
$T_c$ (K)	281.45	338.77	301.95
$CO_2$ (mol%)	40	100	86.56
$H_2S$ (mol%)	0.00	50	5.51
$N_2$ (mol%)	0.00	8.80	0.25
$C1$ (mol%)	0.00	20	4.71
$C2-C5$ (mol%)	0.00	25	2.96
MW of $C_{5+}$	136.47	302.50	188.98
Volatile/Intermediate ratio	0.14	13.61	1.79

**Tables 5.16** summarizes the specifications of the created ANFIS tool for modeling the  $CO_2$ -reservoir oil MMP as a nonlinear function of the aforementioned independent variables. **Fig. 5.7** illustrates the structure of the presented ANFIS model.

**Table 5.16:** Specifications of the presented ANFIS model for CO<sub>2</sub>-reservoir oil MMP prediction

Parameter	Description/value
Cluster center's range of influence	0.52
No of inputs	9
No of outputs	1
No of fuzzy rules	15
Maximum epoch number	200
Initial step size	0.10
Step size decrease rate	0.90
Step size increase rate	1.10

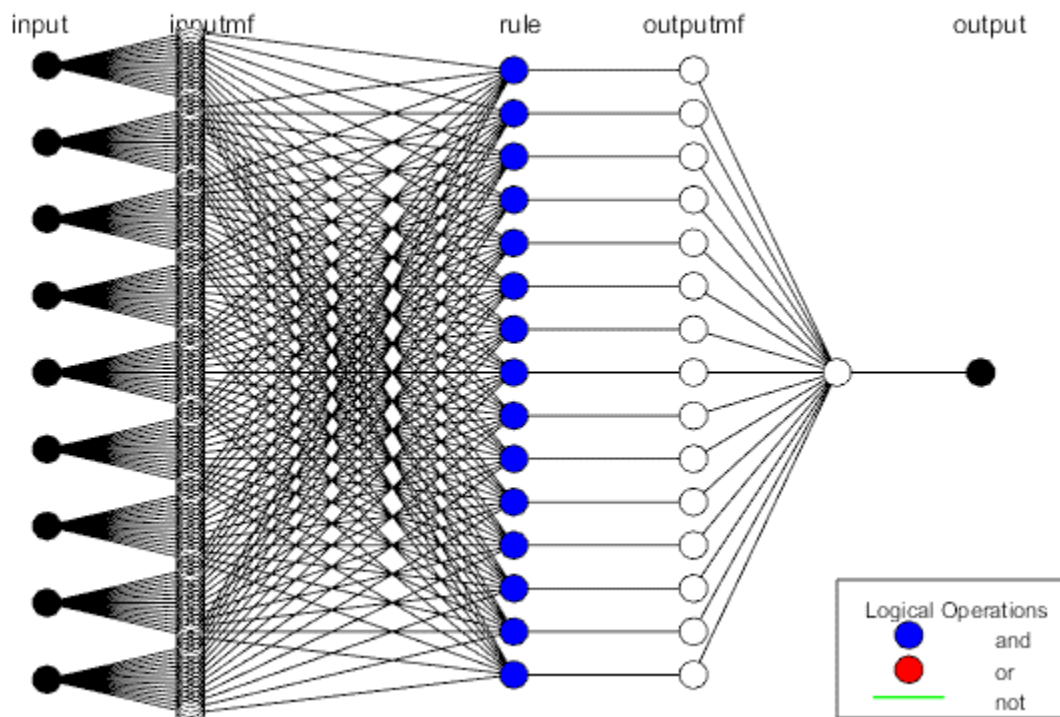


**Fig. 5.7:** Structure of the created ANFIS model for CO<sub>2</sub>-reservoir oil MMP prediction

In the case of development of the CART-based tool for the application of interest, an AdaBoost-CART model with 5 decision trees was obtained as the best model. The maximum depth of each decision tree found to be 13. Schematic of the presented AdaBoost-CART model to predict the CO<sub>2</sub>-reservoir oil MMP is demonstrated in **Fig. 5.8**.

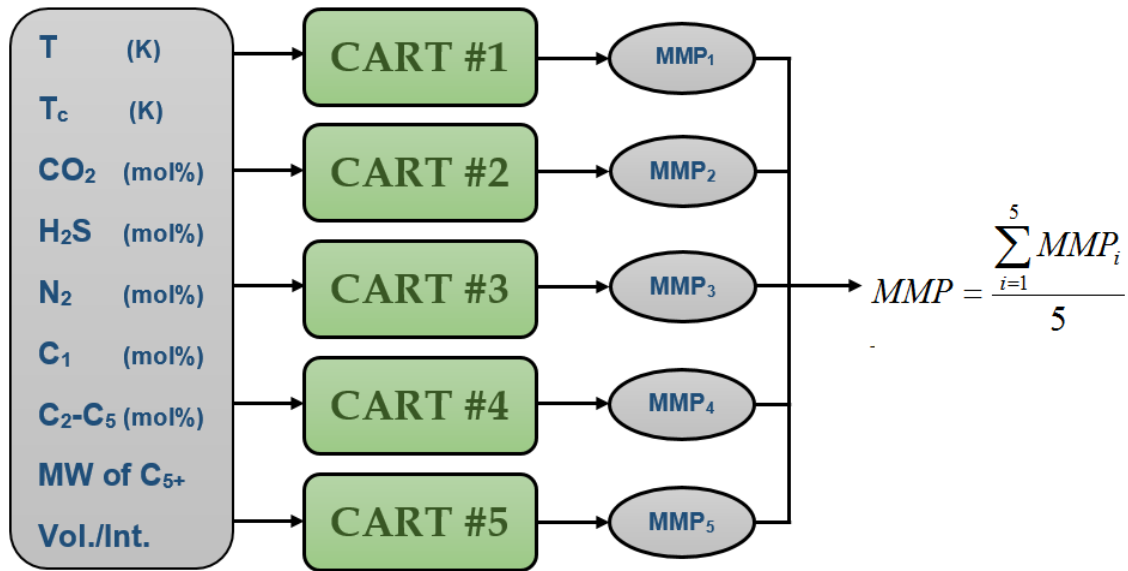


**Fig. 5.8:** Schematics of the AdaBoost-CART tool to estimate the CO<sub>2</sub>-reservoir oil MMP

## 6. Results and discussion

### 6.1. Model assessment criteria

With the aim of assessment of the accuracy of the developed models, statistical variables including average absolute relative deviation percent (AARD%), coefficient of determination ( $R^2$ ) and average relative deviation percent (ARD%) have been utilized. ARD% defines the distribution of errors between negative and positive values. AARD% is a measure of the accuracy of the model.  $R^2$  value mathematically describes the goodness of fit. The higher the  $R^2$  value, the more the data points are fitted to the predictive mathematical model. AARD%, ARD%, and  $R^2$  can be calculated using Eq. (6.1) to (6.3), respectively:

$$AARD\% = \frac{100}{n} \sum_i^n \frac{|pred_i - exp_i|}{exp_i} \dots\dots\dots (6.1)$$

$$ARD\% = \frac{100}{n} \sum_i^n \frac{(pred_i - exp_i)}{exp_i} \dots\dots\dots (6.2)$$

$$R^2 = 1 - \frac{\sum_i (\exp_i - pred_i)^2}{\sum_i (\exp_i - pred_i)^2 + \sum_i (pred_i - \exp\bar{p})^2} \dots\dots\dots (6.3)$$

in which  $exp_i$ ,  $pred_i$ , and  $n$  represent the experimental targets, predictions, and the number of data points, respectively.

Normally,  $R^2$  value ranges between 0 and 1. An  $R^2$  value of 1 indicates that each point on the regression line fits the target. ARD% helps to find out that a predictive mathematical model overestimates or underestimates the target value. If the obtained value for ARD% is negative,

predictions through the applied model are underestimated. Otherwise, the model gives the overestimated estimations. AARD% is a degree of scatter.

## 6.2. Hydrate+Water/Ice+Salt/Alcohol systems

Results of the performance evaluation of the constructed AdaBoost, ANFIS, ANN, and LSSVM models for predicting the equilibrium dissociation temperature of C1, H<sub>2</sub>S, C2, N<sub>2</sub>, C3, i-C4 and gas mixture hydrate systems are summarized in **Tables 6.1** to **6.3**.

**Table 6.1:** R<sup>2</sup> values of the developed models for predicting the HDT of investigated hydrate systems

System	AdaBoost			ANFIS			ANN			LSSVM		
	Train	Test	Overall	Train	Test	Overall	Train	Test	Overall	Train	Test	Overall
C1	0.9996	0.9994	0.9996	0.9759	0.9865	0.9773	0.9483	0.7617	0.9452	0.9957	0.9807	0.9938
C2	0.9977	0.9977	0.9977	0.8890	0.9197	0.8925	0.9208	0.9827	0.9231	0.9633	0.7057	0.9527
C3	0.9988	0.9982	0.9982	0.9700	0.9881	0.9724	0.8851	0.9480	0.8862	0.7459	0.7470	0.7458
i-C4	0.9928	0.9978	0.9967	0.9954	0.9983	0.9950	0.9972	0.9880	0.9970	0.9985	0.9424	0.9984
H <sub>2</sub> S	0.9997	0.9934	0.9994	0.9742	0.9638	0.9739	0.9644	0.9785	0.9649	0.9798	0.8740	0.9680
N <sub>2</sub>	0.9982	0.9993	0.9992	0.9997	0.9998	0.9997	0.9774	0.9940	0.9783	0.9996	0.9992	0.9996
Gas mix.	0.9985	0.9980	0.9980	0.8704	0.8812	0.8711	0.8420	0.8551	0.8526	0.9718	0.9470	0.9699

According to **Table 6.1**, for all the investigated systems, the value of R<sup>2</sup> for the presented AdaBoost models is higher than 0.99. Hence, in terms of the R<sup>2</sup> parameter, the presented AdaBoost models have better performance in predicting/representing the target values. These parameters should be further checked against the thermodynamic model accuracy parameters.

**Table 6.2:** ARD% values of the developed models for predicting the HDT of investigated hydrate systems

System	AdaBoost			ANFIS			ANN			LSSVM		
	Train	Test	Overall	Train	Test	Overall	Train	Test	Overall	Train	Test	Overall
C1	0.00	0.01	0.00	0.01	0.07	0.01	-0.20	-0.11	-0.19	0.00	0.21	0.02
C2	0.01	0.02	0.01	0.03	0.20	0.05	-0.06	0.07	-0.06	0.02	0.34	0.05
C3	-0.01	-0.04	-0.01	0.01	0.30	0.04	0.06	0.01	0.05	0.02	-0.03	0.02
i-C4	0.01	0.23	0.03	0.00	0.11	0.01	-0.01	-0.10	-0.01	0.00	0.06	0.01
H <sub>2</sub> S	-0.06	0.01	0.00	0.01	0.26	0.03	-0.05	0.14	-0.03	0.01	-0.21	-0.01
N <sub>2</sub>	0.00	0.02	0.00	0.00	-0.04	0.00	-0.06	-0.21	-0.08	0.00	0.01	0.00
Gas mix.	0.00	0.00	0.00	0.02	0.02	0.02	0.04	0.22	0.06	0.01	0.02	0.01

According to the obtained values for ARD% that are tabulated in **Table 6.2**, it can be concluded that the errors arising from the presented AdaBoost models for C1, H<sub>2</sub>S, N<sub>2</sub>, and gas mixture hydrate systems as well as the LSSVM model for N<sub>2</sub> hydrate are equally distributed between negative and positive values. On the other hand, since the value of ARD% of the developed ANN model for C1 hydrate is equal to -0.19, this model considerably underestimates the targets. For other developed models, the values of the ARD% parameter are approximately close to zero.

**Table 6.3:** AARD% values of the developed models for predicting the HDT of investigated hydrate systems

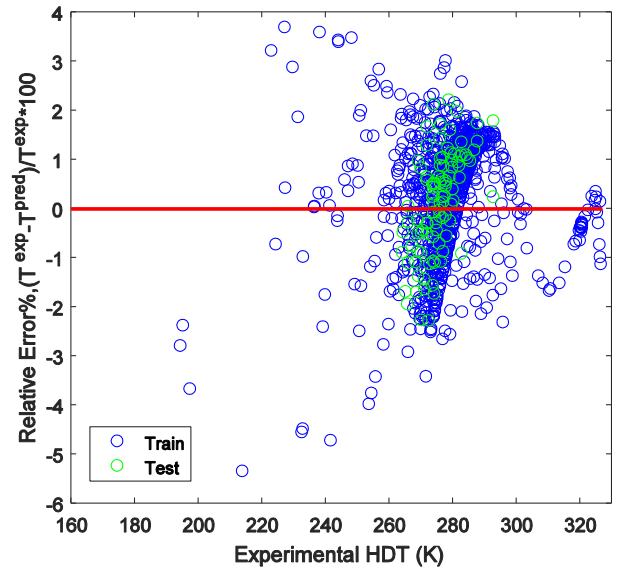
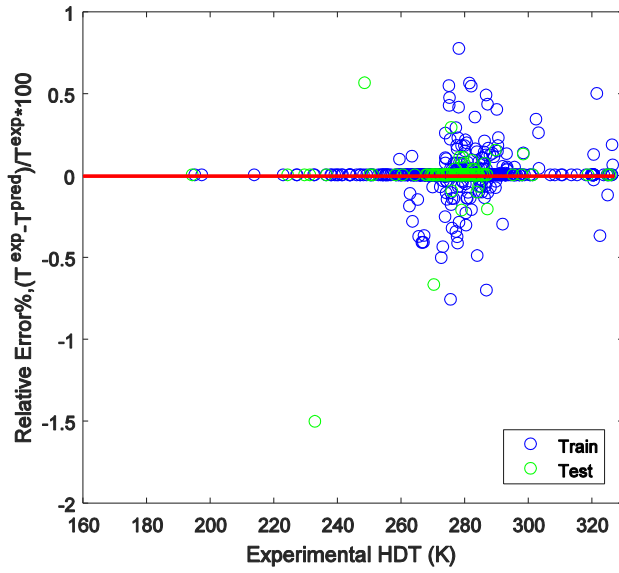
System	AdaBoost			ANFIS			ANN			LSSVM		
	Train	Test	Overall	Train	Test	Overall	Train	Test	Overall	Train	Test	Overall
C1	0.03	0.04	0.03	0.51	0.55	0.51	1.03	0.86	1.01	0.24	0.50	0.27
C2	0.07	0.05	0.07	1.10	1.08	1.09	0.88	0.31	0.83	0.43	1.09	0.49
C3	0.05	0.04	0.05	0.33	0.48	0.35	0.60	0.23	0.56	0.82	0.73	0.81
i-C4	0.03	0.23	0.05	0.13	0.14	0.13	0.08	0.12	0.09	0.06	0.06	0.06
H <sub>2</sub> S	0.02	0.16	0.04	0.51	0.46	0.50	0.64	0.33	0.61	0.38	1.25	0.46
N <sub>2</sub>	0.03	0.09	0.04	0.04	0.05	0.04	0.21	0.21	0.21	0.05	0.06	0.05
Gas mix.	0.03	0.03	0.03	0.91	0.91	0.91	0.92	1.37	0.96	0.31	0.47	0.33



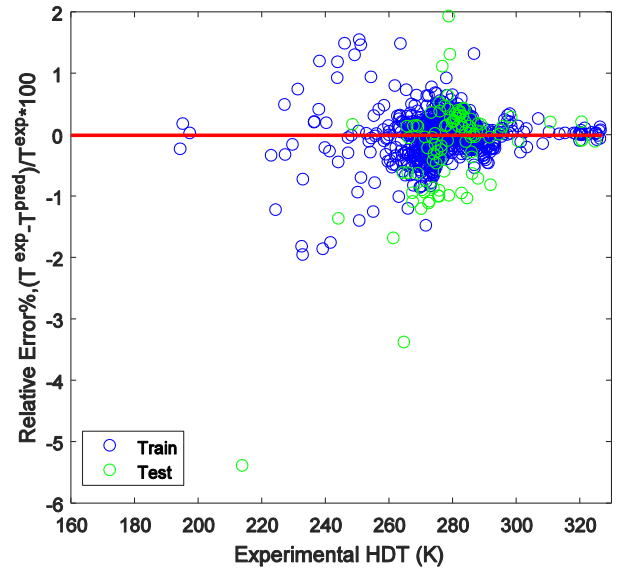
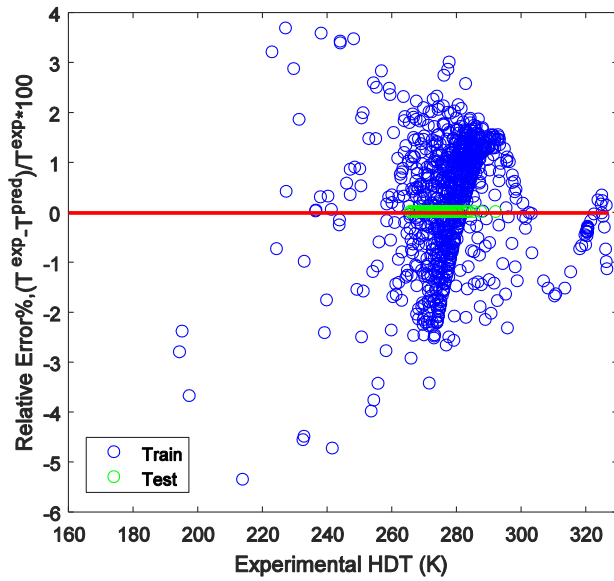
As a degree of scatter, the values of AARD% reveal the excellent performance of the proposed AdaBoost models to predict the dissociation temperature of the investigated hydrates. For all the systems, the presented AdaBoost models represent the target values with AARD%s between 0.03 and 0.07 (**Table 6.3**).

Relative deviations of the outcomes of the developed models for C1, C2, C3, i-C4, H<sub>2</sub>S, N<sub>2</sub>, and gas mixture hydrate systems are demonstrated in **Fig. 6.1** to **6.7**, respectively. As can be seen from **Fig. 6.1**, relative errors of the AdaBoost model for C1 hydrate are distributed between -1.5 and 1. On the other hand, the relative errors of the ANFIS and ANN models range from -6.0 to 4.0; this domain for the LSSVM model is [-6,2].

According to **Fig. 6.2**, the relative deviations of the outputs of the AdaBoost model for C2 hydrate have the values between -2 and 1. For C2 hydrate system, the error ranges of the ANFIS, ANN, and LSSVM models are [-16,4] and [-15,4], and [-14,4], respectively. For all other hydrate systems, except for i-C4 hydrate, the error domains of the developed AdaBoost models are more limited than the error domains of the ANFIS and ANN models. In the case of i-C4 hydrate system, the error range of the AdaBoost model is from -1.2 to 0.6. [-0.5,1], [-0.4,1.0], and [-0.3,0.7] are the ranges for the ANFIS, ANN, and LSSVM models in a respective order.

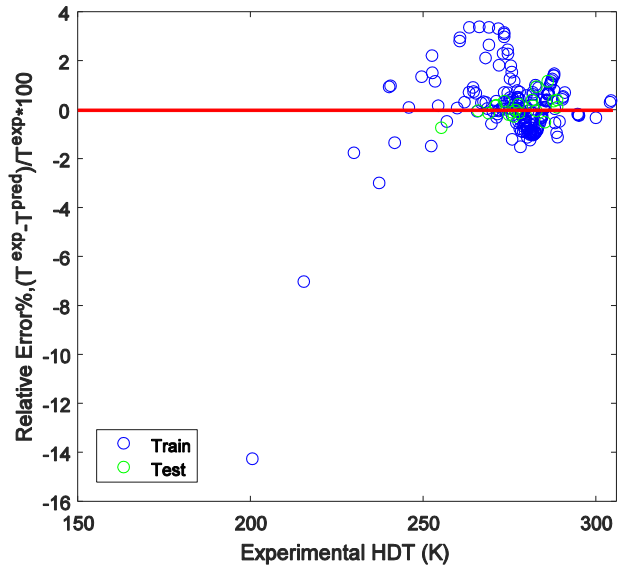
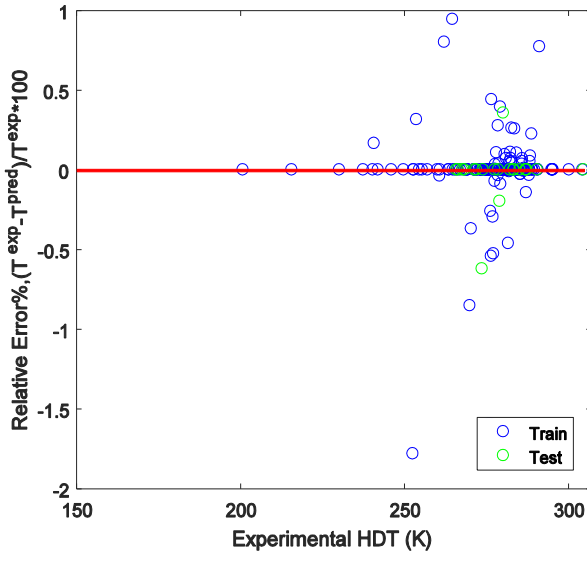


(a), (b)

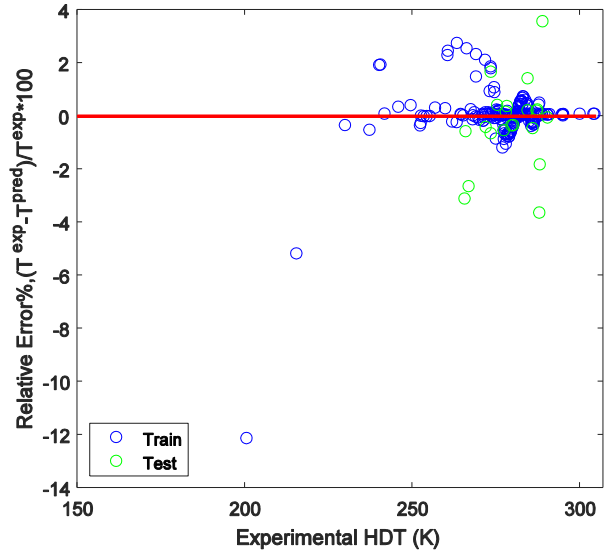
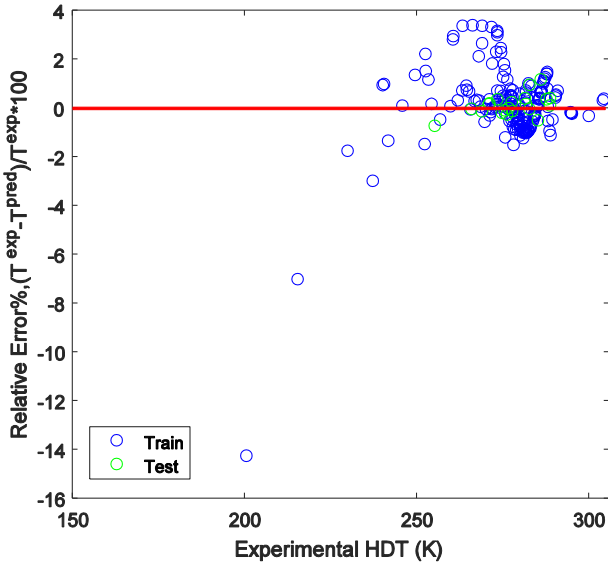


(c), (d)

**Fig. 6.1:** Relative deviations of the outcomes of the developed models for methane hydrate system; (a) AdaBoost-CART; (b) ANFIS; (c) ANN, and (d) LSSVM

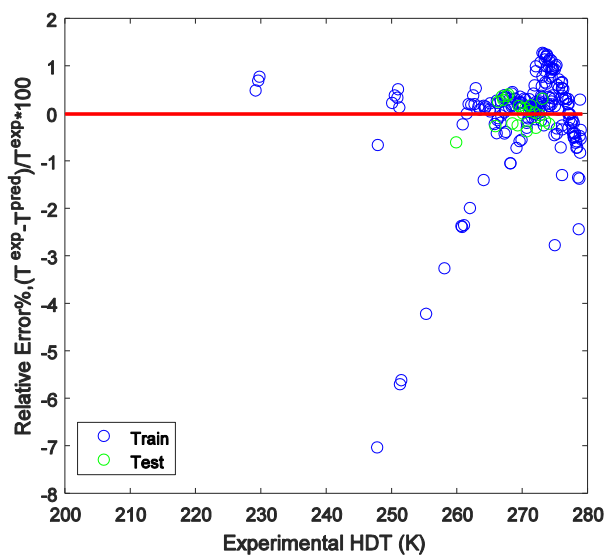
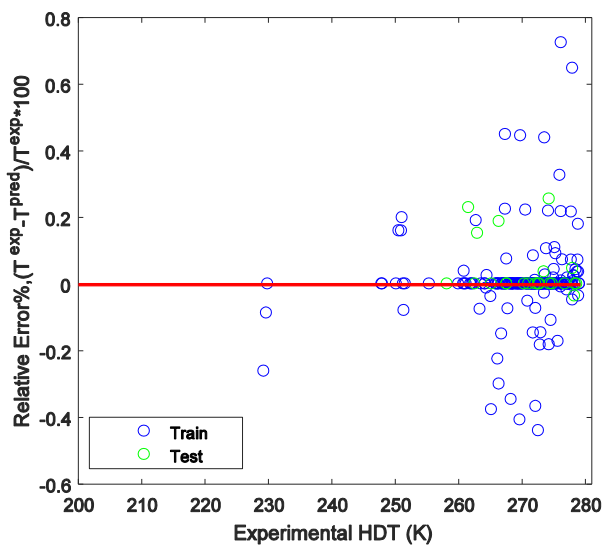


(a), (b)

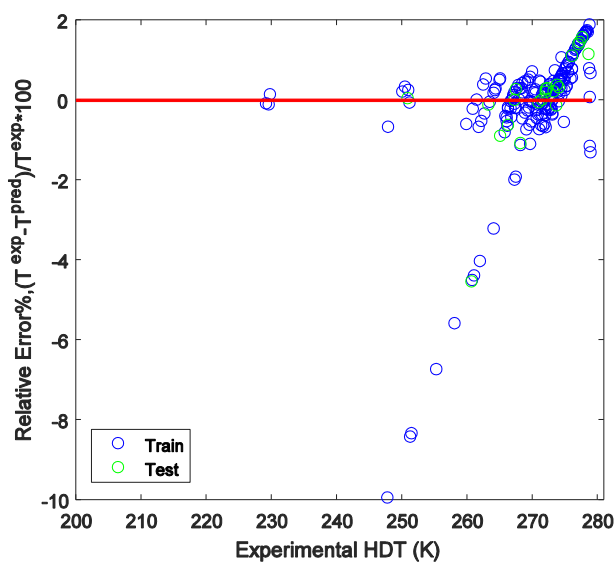
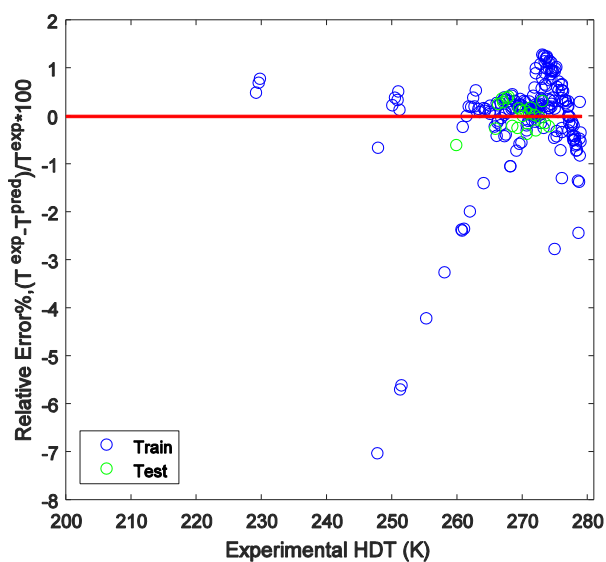


(c), (d)

**Fig. 6.2:** Relative deviations of the outcomes of the developed models for ethane hydrate system;  
(a) AdaBoost-CART; (b) ANFIS; (c) ANN, and (d) LSSVM

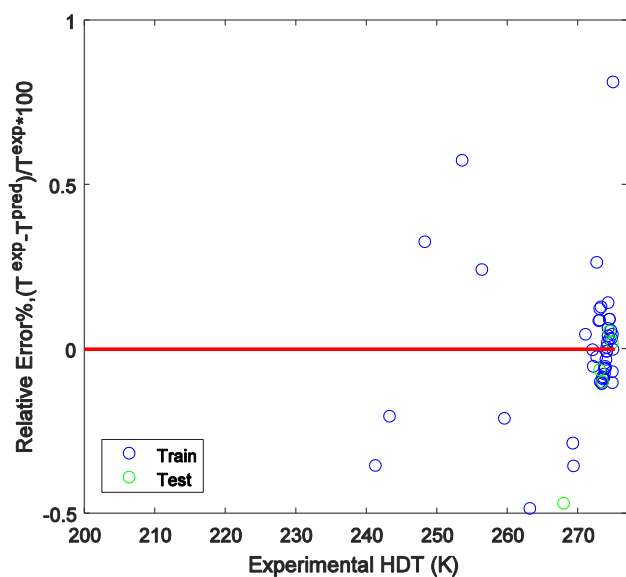
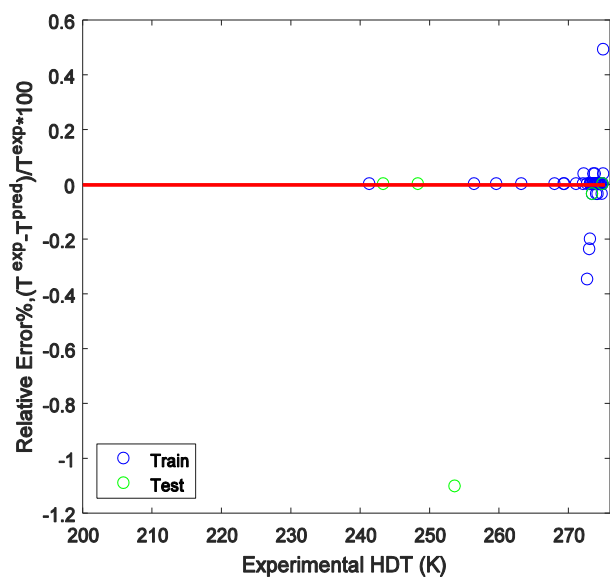


(a), (b)

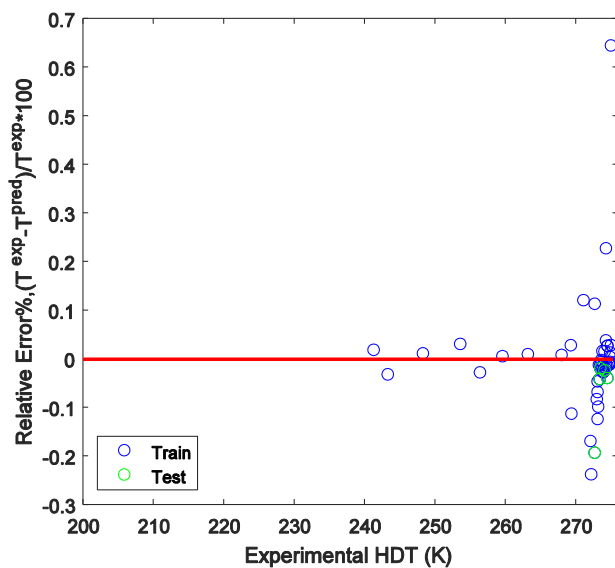
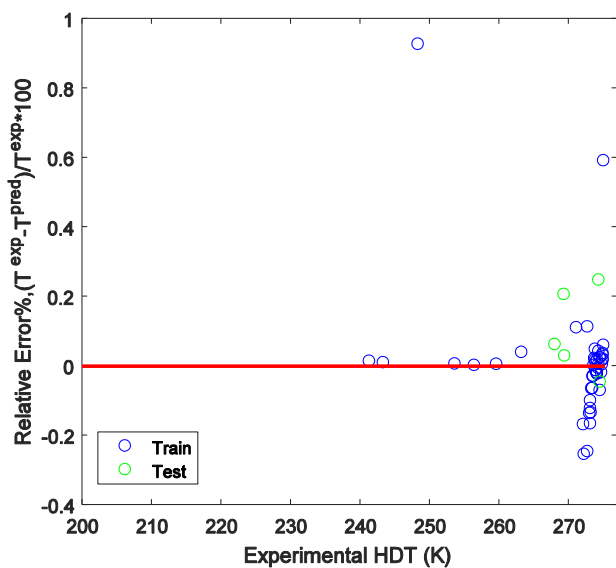


(c), (d)

**Fig. 6.3:** Relative deviations of the outcomes of the developed models for propane hydrate system; (a) AdaBoost-CART; (b) ANFIS; (c) ANN, and (d) LSSVM



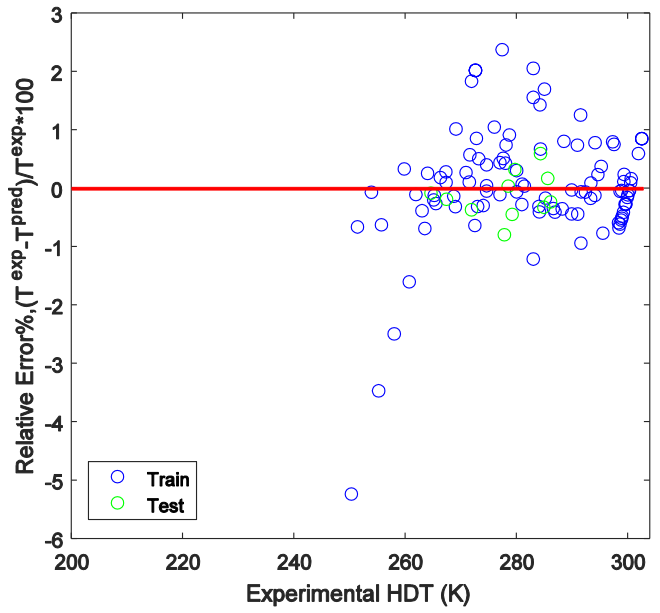
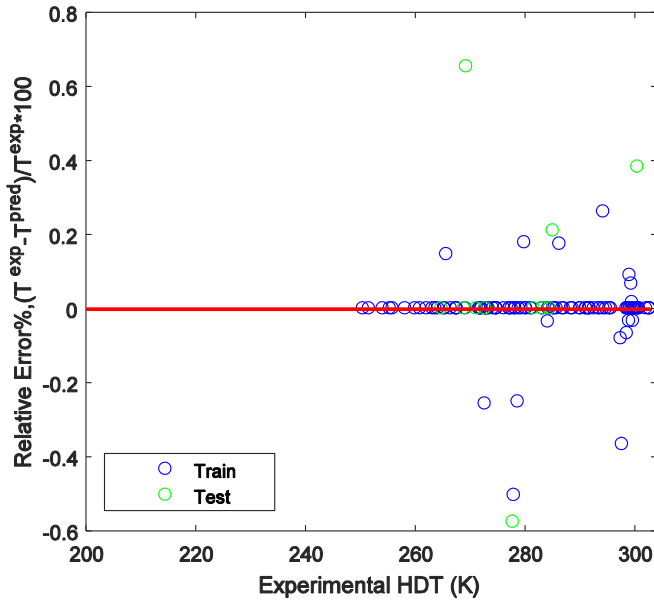
(a), (b)



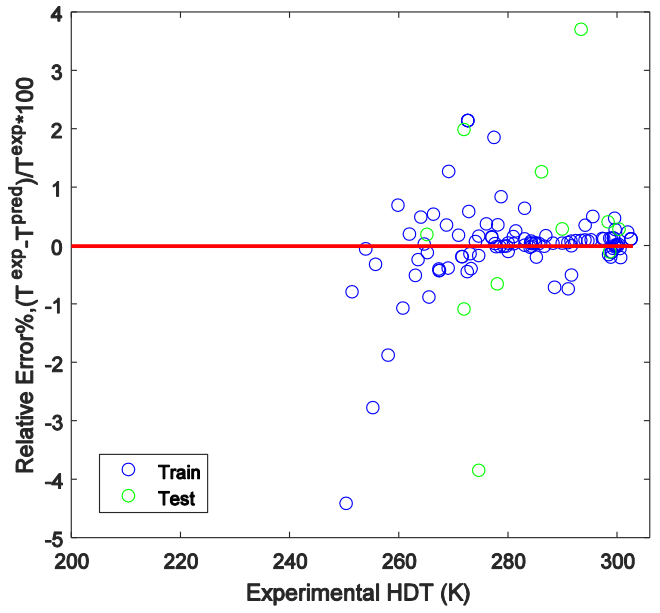
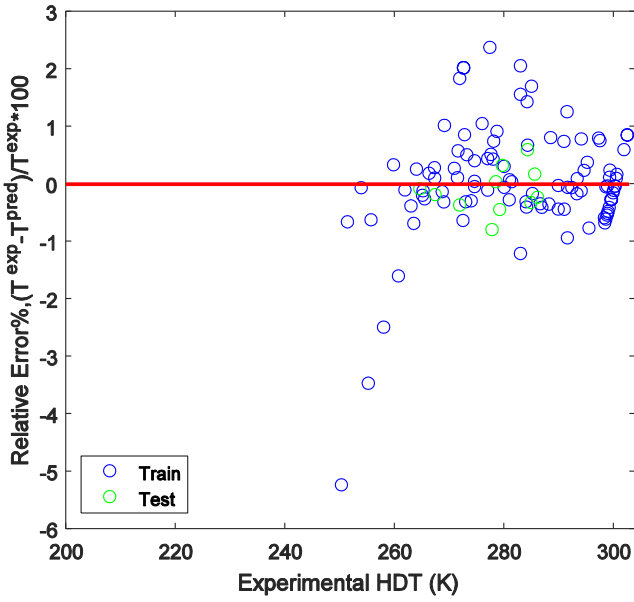
(c), (d)

**Fig. 6.4:** Relative deviations of the outcomes of the developed models for i-butane hydrate system; (a) AdaBoost-CART; (b) ANFIS; (c) ANN, and (d) LSSVM

(a)



(A), (b)



(c), (d)

**Fig. 6.5:** Relative deviations of the outcomes of the developed models for hydrogen sulfide hydrate system; (a) AdaBoost-CART; (b) ANFIS; (c) ANN, and (d) LSSVM

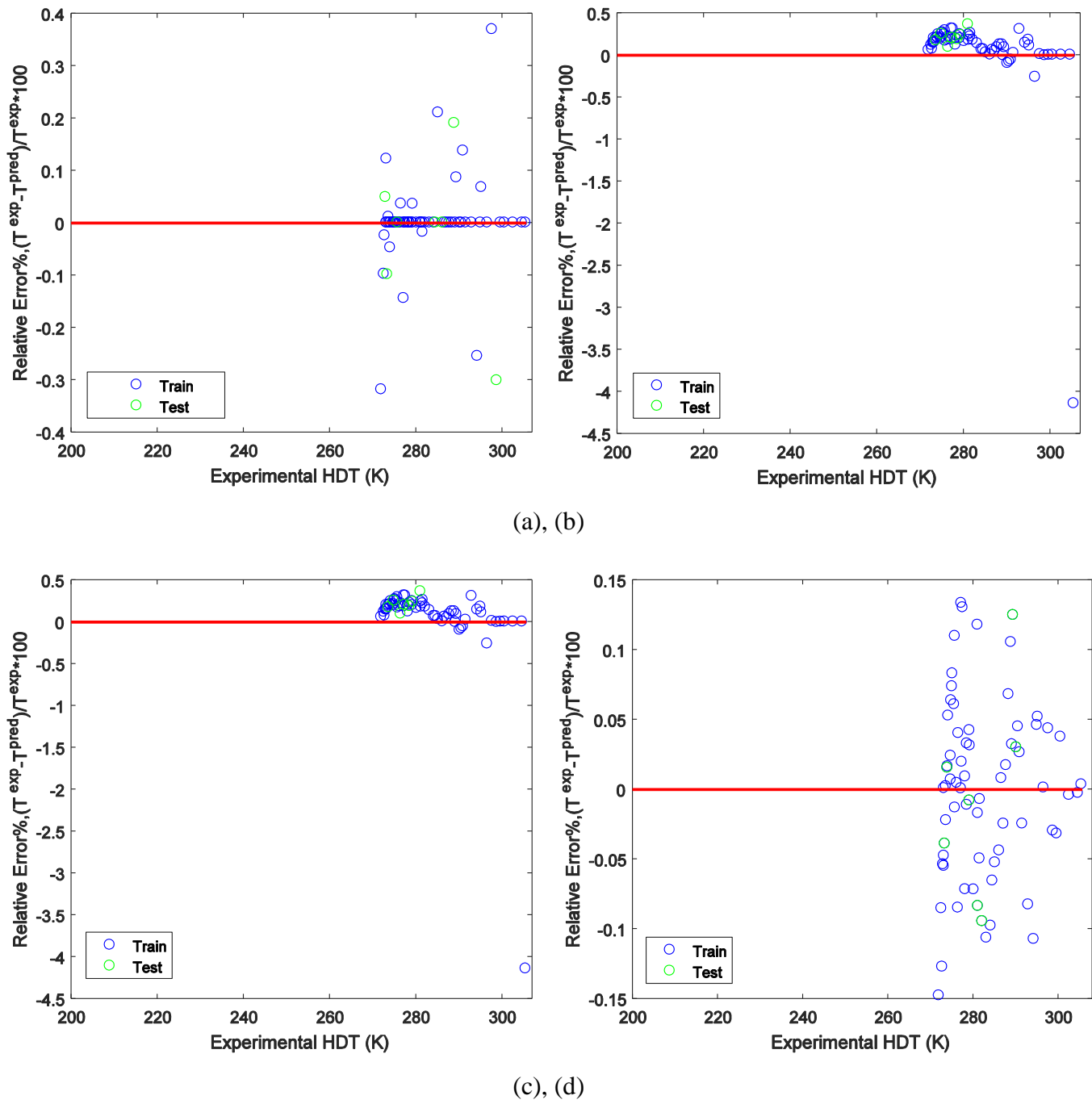


**Fig. 6.6:** Relative deviations of the outcomes of the developed models for nitrogen hydrate system; (a) AdaBoost-CART; (b) ANFIS; (c) ANN, and (d) LSSVM

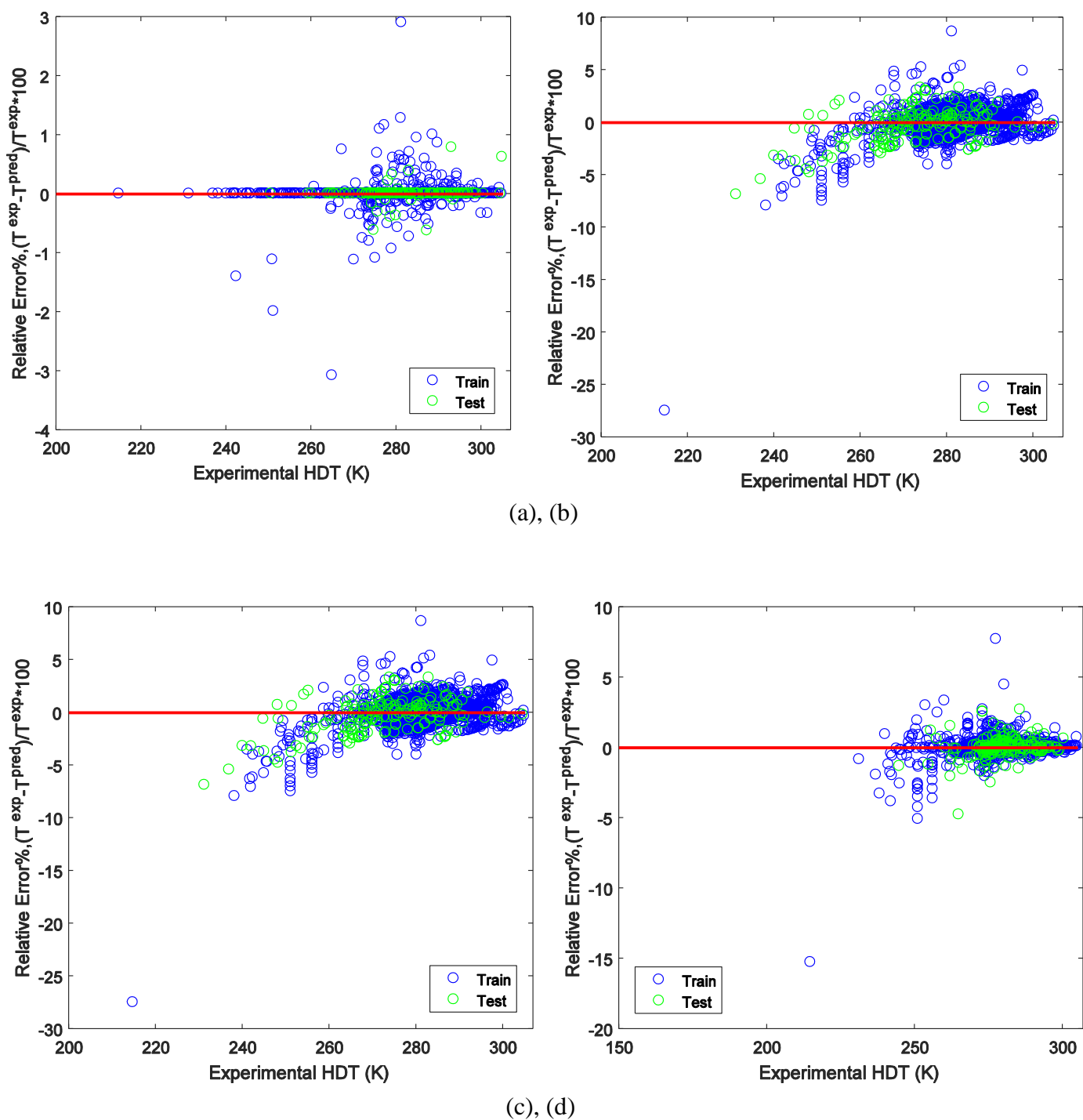


**Fig. 6.7:** Relative deviations of the outcomes of the developed models for gas mixture hydrate system; (a) AdaBoost-CART; (b) ANFIS; (c) ANN, and (d) LSSVM



The ability of the developed AdaBoost tool in predicting the experimental data of Haghighi et al. [294] for methane hydrate+ EG+water system is compared to that of the presented ANFIS and ANN models in **Table 6.4**. As can be observed from **Table 6.4**, using the proposed AdaBoost model, all the reported data are reproduced without error. Employing the ANFIS, ANN, and LSSVM models result in errors from 0.03 to 2.62 K, 0.29 to 4.76 K, and 0.01 to 1.20 K, respectively. Results of the developed smart models in comparison with the experimental data by Ross and Toczykin [338] for ethane hydrate in the aqueous solution of TEG are summarized in **Table 6.5**. Except for two data points, the AdaBoost model regenerated all other targets without error. On the other hand, the ANFIS, ANN, and LSSVM models reproduced the data with the average error of 2.90, 0.93, and 0.04 K, respectively.

**Table 6.4:** Comparison of the model's outputs with the experimental data by Haghighi et al. [294] for methane hydrate

EG, wt%	P, kPa	T, K					Error, K			
		Exp.	AdaBoost	ANFIS	ANN	LSSVM	AdaBoost	ANFIS	ANN	LSSVM
10	6379	279.40	279.40	279.37	278.66	278.20	0.00	0.03	0.74	1.20
	17600	288.25	288.25	288.79	283.49	288.47	0.00	0.54	4.76	0.22
	37448	293.95	293.95	295.63	291.11	293.97	0.00	1.68	2.84	0.02
20	7159	277.75	277.75	276.81	275.79	277.01	0.00	0.94	1.96	0.74
	17779	284.90	284.90	284.68	280.51	285.24	0.00	0.22	4.39	0.34
	29917	289.25	289.25	289.45	285.52	289.39	0.00	0.20	3.73	0.14
30	6862	273.35	273.35	271.73	271.94	272.72	0.00	1.62	1.41	0.63
	18586	281.15	281.15	280.18	277.34	281.44	0.00	0.97	3.81	0.29
	31690	284.80	284.80	285.06	282.91	283.90	0.00	0.26	1.89	0.90
40	5055	264.95	264.95	263.89	266.10	264.86	0.00	1.06	1.15	0.09
	15255	274.10	274.10	272.39	271.02	274.09	0.00	1.71	3.08	0.01
	23166	277.05	277.05	276.90	274.66	277.12	0.00	0.15	2.39	0.07
	31386	279.05	279.05	279.88	278.25	278.67	0.00	0.83	0.80	0.38
50	12621	265.35	265.35	263.19	262.66	264.88	0.00	2.16	2.69	0.47
	21724	269.65	269.65	269.87	267.06	269.91	0.00	0.22	2.59	0.26
	30910	271.55	271.55	274.17	271.26	271.56	0.00	2.62	0.29	0.01

**Table 6.5:** Comparison of the model's outputs with the experimental data by Ross and Toczylkin [338] for ethane hydrate

TEG, wt%	P, <i>kPa</i>	T, K					Error, K			
		Exp.	AdaBoost	ANFIS	ANN	LSSVM	AdaBoost	ANFIS	ANN	LSSVM
40	1970	275.0	275.0	277.01	275.65	275.01	0.00	2.01	0.65	0.01
	2300	275.8	275.8	277.05	276.16	275.80	0.00	1.25	0.36	0.00
	3300	277.9	277.9	277.19	277.36	277.87	0.00	0.71	0.54	0.03
	20770	281.7	283.0	279.61	280.70	281.66	1.30	2.09	1.00	0.04
	33570	283.0	283.0	281.39	283.24	282.95	0.00	1.61	0.24	0.05
20	790	273.7	273.7	281.25	272.84	273.74	0.00	7.55	0.86	0.04
	1290	276.5	278.0	281.32	277.35	276.47	1.50	4.82	0.85	0.03
	1540	278.0	278.0	281.36	278.45	278.01	0.00	3.36	0.45	0.01
	2630	283.0	283.0	281.51	280.43	282.94	0.00	1.49	2.57	0.06
	9720	285.5	285.5	282.49	287.05	285.44	0.00	3.01	1.55	0.06
	28270	288.0	288.0	285.07	287.08	287.93	0.00	2.93	0.92	0.07
	36270	289.0	289.0	286.18	288.80	288.92	0.00	2.82	0.20	0.08
10	1000	277.0	277.0	283.49	277.13	281.94	0.00	6.49	0.13	0.06
	1800	282.0	282.0	283.60	281.65	286.25	0.00	1.60	0.35	0.05
	3720	286.3	286.3	283.87	283.07	288.92	0.00	2.43	3.23	0.08
	23270	289.0	289.0	286.58	287.94	288.72	0.00	2.42	1.06	0.08

**Table 6.6** gives the outputs of the presented models versus the experimental by Ng and Robinson [322] for propane hydrate in the presence of MeOH solution. The maximum error obtained using the AdaBoost model is equal to 0.93 K. The worst predictions of the ANFIS, ANN, and LSSVM models have 2.23, 7.68, and 2.03 K, respectively. **Table 6.7** shows the outcomes of the developed tools in comparison with the experimental data by Holder and Godbole [355] for i-butane hydrate in pure water. For the pressure of 35.1 kPa, the estimation of the AdaBoost model has 2.8 K deviation from the experimental HDT. At other conditions, the results of the AdaBoost tool are better than the outcomes of the ANFIS, ANN, and LSSVM models.

**Table 6.6:** Comparison of the model's outputs with the experimental data by Ng and Robinson [322] for propane hydrate

MeOH, wt%	P, <i>kPa</i>	T, K					Error, K			
		Exp.	AdaBoost	ANFIS	ANN	LSSVM	AdaBoost	ANFIS	ANN	LSSVM
5.00	234	272.12	272.12	272.12	271.77	273.21	0.00	0.00	0.35	1.09
	259	272.58	272.58	272.71	271.99	273.24	0.00	0.13	0.59	0.66
	316	273.28	273.28	273.60	272.50	273.29	0.00	0.32	0.78	0.01
	405	274.18	274.18	274.25	273.27	273.27	0.00	0.07	0.91	0.91
	468	274.79	274.79	274.44	273.79	273.43	0.00	0.35	1.00	1.36
	794	275.02	274.97	274.60	276.33	273.72	0.05	0.42	1.31	1.30
	1720	275.09	274.97	277.16	282.77	274.47	0.12	2.07	7.68	0.62
	6340	274.97	274.97	274.71	274.16	276.54	0.00	0.26	0.81	1.57
10.39	185	268.30	269.23	268.76	271.17	266.94	0.93	0.46	2.87	1.36
	228	269.23	269.23	269.17	271.23	271.26	0.00	0.06	2.00	2.03
	352	271.07	271.07	269.69	271.40	270.11	0.00	1.38	0.33	0.96
	360	270.93	271.07	269.71	271.41	271.29	0.14	1.22	0.48	0.36
	415	271.59	271.59	269.78	271.48	271.31	0.00	1.81	0.11	0.28
	434	271.82	271.59	269.80	271.51	271.31	0.23	2.02	0.31	0.51
	737	272.07	272.07	269.87	271.89	271.38	0.00	2.20	0.18	0.69
	984	272.10	272.07	269.87	272.18	271.43	0.03	2.23	0.08	0.67
	6510	272.08	272.08	269.98	272.45	271.72	0.00	2.10	0.37	0.36

**Table 6.7:** Comparison of the model's outputs with the experimental data by Holder and Godbole [355] for i-butane hydrate

P, kPa	T, K					Error, K			
	Exp.	AdaBoost	ANFIS	ANN	LSSVM	AdaBoost	ANFIS	ANN	LSSVM
17.6	241.4	241.4	242.26	241.37	241.36	0.00	0.86	0.03	0.04
20.2	243.4	243.4	243.90	243.38	243.48	0.00	0.50	0.02	0.08
26.4	248.4	248.4	247.60	246.10	248.38	0.00	0.80	2.30	0.02
35.1	253.7	256.5	252.25	253.69	253.63	2.80	1.45	0.01	0.07
42.8	256.5	256.5	255.89	256.50	256.58	0.00	0.61	0.00	0.08
53.5	259.7	259.7	260.25	259.69	259.69	0.00	0.55	0.01	0.01
66.4	263.3	263.3	264.58	263.20	263.28	0.00	1.28	0.10	0.02
85.5	268.1	268.1	269.37	267.94	268.08	0.00	1.27	0.16	0.02
89.7	269.4	269.4	270.18	268.85	269.33	0.00	0.78	0.55	0.07
91.3	269.5	269.5	270.47	269.43	269.81	0.00	0.97	0.07	0.31

The reported data by Mohammadi and Richon [302] for hydrogen sulfide hydrate in solution of salts and/or alcohol as well as the estimations of the proposed predictive mathematical models are reported in **Table 6.8**. As can be seen, the best results are obtained from the AdaBoost for all the reported thermodynamic conditions. The experimental data by Nixdorf & Oellrich [16] for nitrogen hydrate+water system versus the outputs of the presented AdaBoost, ANFIS, and ANN models are given in **Table 6.9**. At the pressure of 17668.0 kPa, the ANFIS model provides the best estimation. However, the overall performance of the AdaBoost model is better than the ANFIS, ANN, and LSSVM models. **Table 6.10** gives the estimations of the presented models in comparison with the experimental data published by Kamari & Oyarhossein [287] for natural gas hydrate in the presence of pure water. The results prove the ability of the AdaBoost in the prediction of the HDT of the studied hydrate system of natural gas.

**Table 6.8:** Comparison of the model's outputs with the experimental data by Mohammadi and Richon [302] for hydrogen sulfide hydrate

Concentration, wt%				P, <i>kPa</i>	T, K					Error, K			
NaCl	CaCl <sub>2</sub>	MeOH	EG		Exp.	AdaBoost	ANFIS	ANN	LSSVM	AdaBoost	ANFIS	ANN	LSSVM
5	0	0	15	180	272.7	273.4	274.93	274.48	273.96	0.70	2.23	1.78	1.26
				315	278.3	278.3	277.34	276.28	277.35	0.00	0.96	2.02	0.95
				584	284.4	284.4	282.16	280.39	284.22	0.00	2.24	4.01	0.18
				1082	290.1	290.1	291.07	290.23	288.88	0.00	0.97	0.13	1.22
5	0	10	0	189	273.4	273.4	275.16	272.06	274.52	0.00	1.76	1.34	1.12
				288	277.2	277.2	277.76	276.03	276.81	0.00	0.56	1.17	0.39
				456	281.6	281.6	280.61	281.54	280.93	0.00	0.99	0.06	0.67
				777	286.8	286.8	284.69	287.84	286.87	0.00	2.11	1.04	0.07
0	0	30	0	236	267.5	267.5	270.79	266.79	268.61	0.00	3.29	0.71	1.11
				338	271.1	271.1	271.08	270.41	270.65	0.00	0.02	0.69	0.45
				496	274.8	274.8	271.52	274.98	274.39	0.00	3.28	0.18	0.41
0	0	50	0	201	254.1	254.1	253.89	254.31	254.28	0.00	0.21	0.21	0.18
				328	260.0	260.0	258.52	259.18	258.24	0.00	1.48	0.82	1.76
				464	264.2	264.2	262.93	263.57	262.94	0.00	1.27	0.63	1.26

**Table 6.9:** Comparison of the model's outputs with the experimental data by Nixdorf & Oellrich [306] for nitrogen hydrate

P, <i>kPa</i>	T, K					Error, K			
	Exp.	AdaBoost	ANFIS	ANN	LSSVM	AdaBoost	ANFIS	ANN	LSSVM
16935	273.67	273.67	273.61	273.13	273.66	0.00	0.06	0.54	0.40
17668	274.07	274.20	274.00	273.50	274.02	0.13	0.07	0.57	0.23
19521	275.11	275.11	274.96	274.40	274.91	0.00	0.15	0.71	0.35
20748	275.77	275.77	275.55	274.97	275.47	0.00	0.22	0.80	0.15
24092	277.27	277.27	277.02	276.40	276.90	0.00	0.25	0.87	0.00

**Table 6.10:** Comparison of the model's outputs with the experimental data by Kamari & Oyarhossein [287] for gas mixture hydrate (C1=81.55%, CO<sub>2</sub>=3.31%, N<sub>2</sub>=0.17%, C2=5.37%, i-C4=2.23%, n-C4=0.51%, i-C5=1.00%, n-C5=0.52%, C6=0.45%, C7=0.75%, C8<sup>+</sup>=0.70%, H<sub>2</sub>S=1.05%, and C<sub>2</sub>H<sub>4</sub>=2.39%)

P, <i>kPa</i>	T, K					Error, K			
	Exp.	AdaBoost	ANFIS	ANN	LSSVM	AdaBoost	ANFIS	ANN	LSSVM
848.0	274.78	274.78	278.73	281.59	276.41	0.00	3.95	6.81	1.63
1620.2	279.80	279.80	280.53	281.70	278.03	0.00	0.73	1.90	1.77
2275.2	282.03	282.03	282.05	281.80	281.12	0.00	0.02	0.23	0.91
3102.6	284.87	284.87	283.96	281.92	283.61	0.00	0.91	2.95	1.26
4136.8	286.53	286.53	286.26	282.05	286.37	0.00	0.27	4.48	0.16
5308.9	288.18	288.18	288.61	282.20	288.89	0.00	0.43	5.98	0.71

### 6.3. Hydrate+IL System

The summary of the error analysis results, i.e. the obtained values of the ARE%, AARE%, and  $R^2$ %, for the proposed LSSVM, CART and ANFIS tools are given in **Table 6.11**. For all the developed models, the values of  $R^2$  reveal that the dissociation/formation temperature of the C1 hydrate in ILs is predictable from the independent parameters, i.e. pressure of the system, concentration of the aqueous phase, critical temperature of IL, and critical pressure of IL. **Fig. 6.8** depicts the outputs of the presented models versus the corresponding experimental values of methane hydrate dissociation temperature in ILs.

**Table 6.11:** Error analysis results of the proposed LSSVM, CART and ANFIS tools

Model	Dataset	Parameter		
		$R^2$	ARD%	AARD%
LSSVM	Train	0.9911	0.00	0.07
	Test	0.9548	-0.03	0.18
	Total	0.9885	0.00	0.08
ANFIS	Train	0.9724	0.00	0.30
	Test	0.9609	0.12	0.36
	Total	0.9712	0.01	0.31
CART	Train	0.9781	0.00	0.10
	Test	0.9794	0.01	0.10
	Total	0.9785	0.00	0.10
ANN	Train	0.9611	-0.07	0.14
	Test	0.9380	-0.07	0.22
	Total	0.9591	-0.07	0.15

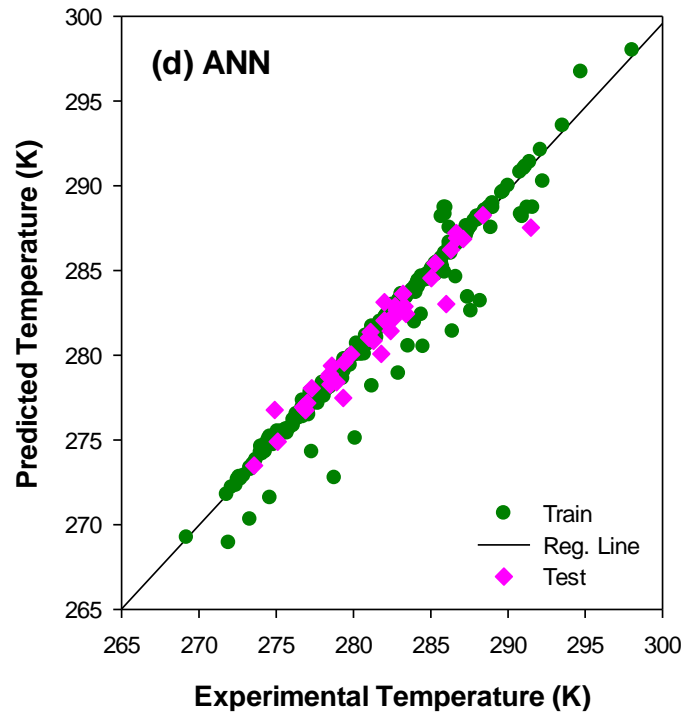
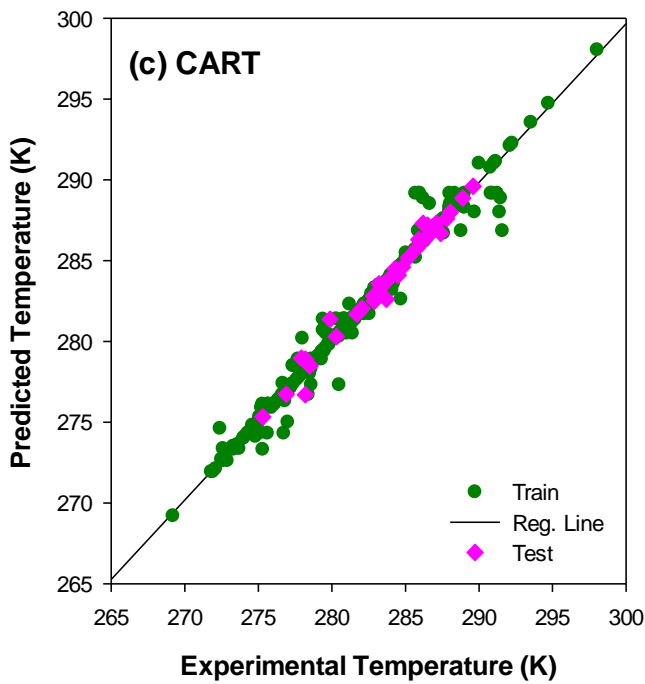
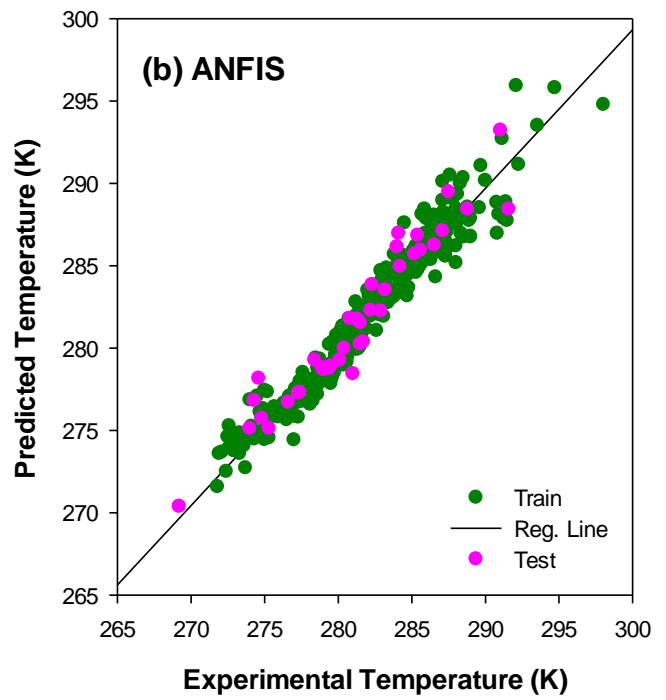
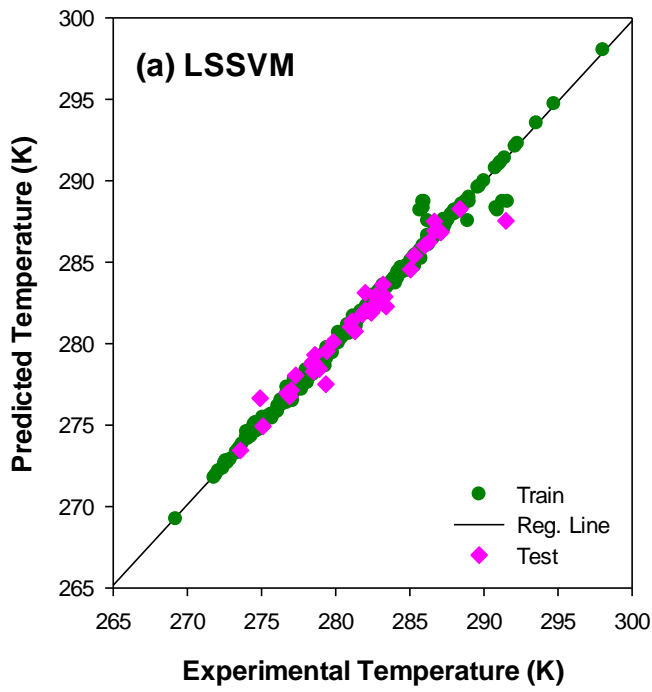


**Fig. 6.8:** Predictions of the presented (a) LSSVM model, (b) ANFIS model, (c) CART, and (d) ANN models vs. the corresponding experimental values

According to **Table 6.11**, the values of ARD% for the presented LSSVM, ANFIS, CART, and ANN models are 0.00, 0.01, 0.00, and -0.07, respectively. Hence, it can be concluded that errors arising from the presented models are equally distributed between negative and positive values. The histograms of the derived relative errors from the presented LSSVM, ANFIS, CART, and ANN models are demonstrated in **Fig. 6.9**.

As can be observed from **Table 6.11**, the calculated values of AARD% for the presented LSSVM, ANFIS, CART, and ANN models are equal to 0.08, 0.31, 0.10, and 0.15, respectively. Hence, all the proposed tools for the application of interest are capable of reproducing the targets with satisfactory precision. However, the LSSVM model with two adjustable hyper-parameter provides better estimations. On the other hand, the weakest results are provided by the ANFIS model.

For the hydrate system of methane+[Emim][NO<sub>3</sub>]+water, **Table 6.12** gives the performance of the presented LSSVM, ANFIS, CART, and ANN models. The concentration of [Emim][NO<sub>3</sub>] in the aqueous phase ranges from 1.0 to 40.0. In **Table 6.13**, for [Pmim][I], [OH-Emmim][Cl], [OH-Emim][ClO<sub>4</sub>], and [N2,2,2,2][Cl] solution of concentration 10 wt%, the predictions obtained from the constructed predictive tools are compared to the corresponding experimental values.



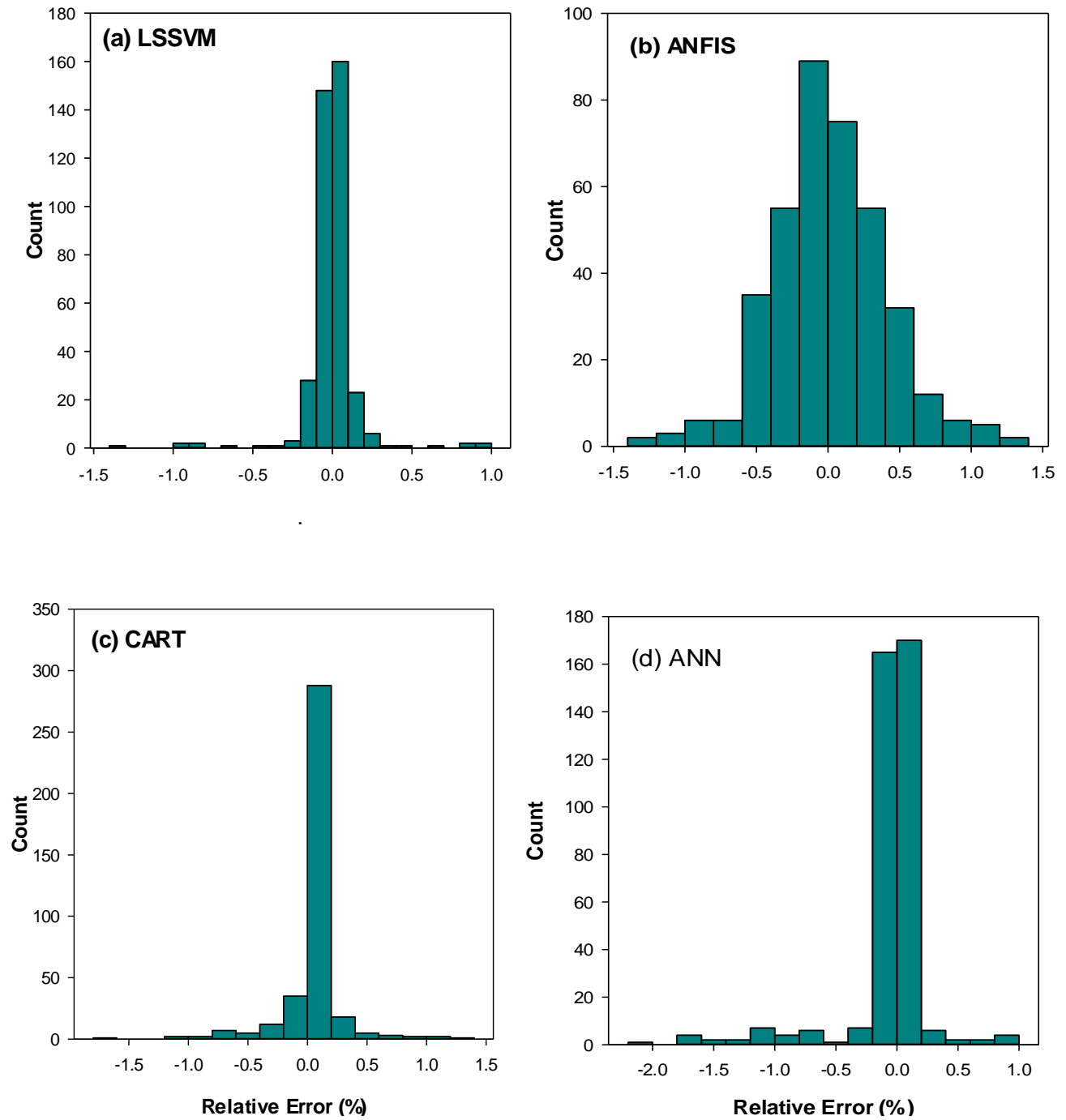


**Fig. 6.9:** Histogram of errors for the presented (a) LSSVM, (b) ANFIS, (c) CART, and (d) ANN models

**Table 6.12:** Outputs of the presented models vs. corresponding experimental values for methane hydrate+[Emim][NO<sub>3</sub>]+water system

wt%	P (MPa)	T (K)		Relative error (%)						
		Exp.	LSSVM	ANFIS	CART	ANN	LSSVM	ANFIS	CART	ANN
1.0	3.54	276.1	276.2	276.0	276.1	276.2	0.02	-0.05	0.00	0.04
	4.98	279.5	279.6	277.8	279.5	279.5	0.02	-0.59	0.00	0.00
	6.55	282.1	282.3	283.1	282.1	282.3	0.08	0.37	0.00	0.07
	8.42	284.5	284.4	287.6	284.1	284.4	-0.04	1.09	-0.14	-0.03
	13.33	288.5	288.6	290.3	288.5	288.6	0.02	0.64	0.00	0.03
2.5	3.57	276.1	275.8	276.2	276.1	275.8	-0.11	0.04	0.00	-0.11
	5.04	279.4	279.3	278.1	279.4	279.3	-0.03	-0.47	0.00	-0.04
	6.41	281.8	281.8	282.5	281.8	281.5	0.00	0.25	0.00	-0.11
	8.29	284.1	284.0	284.2	284.1	284.0	-0.03	0.04	0.00	-0.04
	13.44	288.3	288.2	290.0	288.3	288.2	-0.03	0.59	0.00	-0.03
5.0	3.51	275.7	275.4	276.4	276.1	275.4	-0.11	0.25	0.14	-0.11
	4.75	278.5	278.3	277.4	278.5	278.1	-0.07	-0.39	0.00	-0.14
	6.39	281.4	281.6	281.9	281.4	281.6	0.07	0.18	0.00	0.07
	8.44	284.0	284.1	286.1	284.1	284.0	0.03	0.74	0.03	0.00
	13.20	287.8	287.9	289.0	287.6	287.9	0.03	0.42	-0.07	0.03
5.5	3.08	274.0	274.6	276.8	274.6	274.0	0.22	1.02	0.00	0.22
	4.67	278.3	278.0	277.2	278.0	278.3	-0.11	-0.40	0.00	-0.11
	6.25	281.1	281.4	281.4	281.5	281.1	0.11	0.11	0.00	0.14
	8.21	283.8	283.8	285.7	283.8	283.8	0.00	0.67	0.00	0.00
	12.12	287.1	287.0	288.1	287.0	287.1	-0.03	0.35	0.00	-0.03
	16.12	289.7	289.7	291.1	289.7	288.0	0.00	0.48	-0.58	0.00
10.0	3.05	274.8	275.0	275.8	274.8	274.4	0.07	0.36	0.00	-0.14
	4.91	278.3	278.0	276.8	278.3	278.0	-0.11	-0.54	0.00	-0.11
	6.43	280.8	281.1	280.4	281.4	281.2	0.11	-0.14	0.21	0.14
	8.04	283.2	283.6	283.9	283.6	283.7	0.14	0.25	0.13	0.18
	12.87	286.8	287.2	287.1	286.8	287.2	0.14	0.10	0.00	0.14
20.0	3.53	273.7	273.8	272.7	273.3	273.3	0.04	-0.37	-0.13	-0.13
	4.93	277.0	276.7	274.4	277.0	277.0	-0.11	-0.94	0.00	0.00
	6.05	279.4	279.6	278.3	281.4	281.4	0.07	-0.40	0.70	0.70
	8.18	281.5	281.5	281.5	281.5	281.5	0.00	0.00	0.00	0.00
	12.86	285.3	285.3	286.2	285.3	285.3	0.00	0.32	0.00	0.00
30.0	3.53	271.8	271.8	271.6	271.8	273.8	0.00	-0.07	0.04	0.73
	4.91	275.1	274.9	274.6	274.3	274.2	-0.07	-0.18	-0.29	-0.33
	6.42	277.4	277.5	278.0	278.5	278.1	0.04	0.22	0.38	0.25

	8.20	279.6	279.5	280.3	280.5	280.0	-0.03	0.25	0.32	0.14
	12.88	283.4	283.4	283.6	282.8	285.3	0.00	0.07	-0.21	0.67
40.0	3.41	269.2	269.2	270.4	269.2	269.2	0.00	0.45	0.00	0.00
	4.79	272.4	272.3	272.5	274.6	272.3	-0.04	0.04	0.81	-0.04
	6.35	275.0	275.0	274.4	275.0	275.1	0.00	-0.22	0.00	0.04
	8.11	277.3	277.3	275.8	277.3	274.3	0.00	-0.54	0.00	-1.08
	12.76	281.0	281.0	278.4	281.0	281.0	0.00	-0.93	0.00	0.00

**Table 6.13:** Outputs of the proposed models vs. corresponding experimental targets for methane hydrate in some ILs (10 wt% solution)

IL	P (MPa)	T (K)					Relative error (%)			
		Exp.	LSSVM	ANFIS	CART	ANN	LSSVM	ANFIS	CART	ANN
[Pmim][I]	10.54	285.8	285.2	285.4	285.8	285.2	-0.21	-0.14	0.00	-0.21
	14.68	288.8	288.7	288.6	288.5	288.7	-0.03	-0.07	-0.1	-0.03
	20.36	291.1	291.1	292.7	291.1	291.1	0.00	0.55	0.00	0.00
[OH-Emmim][Cl]	3.51	274.7	274.8	276.1	274.5	274.8	0.04	0.51	-0.07	0.04
	4.91	278.1	277.6	276.9	278.1	277.6	-0.18	-0.43	0.00	-0.18
	6.27	280.5	280.5	280	280.3	280.4	0.00	-0.18	-0.07	-0.03
	8.24	283.2	283	283.5	283.5	283.0	-0.07	0.11	0.11	-0.07
	13.28	287.4	287.3	287.1	287.4	287.3	-0.03	-0.10	0.00	-0.03
[OH-Emim][ClO4]	3.45	275	275	277.4	274.9	275.1	0.00	0.87	-0.04	0.04
	4.94	278.6	278.5	278.3	278.9	278.5	-0.03	-0.11	0.11	-0.03
	6.44	281.3	281.5	280.9	281.3	281.5	0.07	-0.14	0.00	0.07
	8.34	283.5	283.5	283.6	283.5	283.5	0.00	0.04	0.00	0.00
	12.96	287.4	287.4	288.1	286.7	287.4	0.00	0.24	-0.24	0.00
[N2,2,2,2][Cl]	2.48	272.1	272.2	273.7	272.1	272.2	0.04	0.59	0.00	0.04
	3.27	274.9	274.8	275	274.9	274.8	-0.04	0.04	0.00	-0.04
	4.33	277.6	277.6	276.8	278.5	277.6	0.00	-0.29	0.32	0.00
	5.39	279.4	279.7	278.6	279.4	279.8	0.11	-0.29	0.00	0.14
	5.99	280.7	280.7	279.6	280.7	280.1	0.00	-0.39	0.00	-0.21

## 6.4. CO<sub>2</sub>+Water+Amine Systems

The results of presented LSSVM and ANFIS models for prediction of CO<sub>2</sub> solubility in MEA, DEA, and TEA aqueous solutions are compared to the outcomes of the developed ANN and AdaBoost-CART models in **Table 6.14**. Obtained values for the AARD% as a measure of the accuracy of the tools reveal that the proposed AdaBoost-CART models for (H<sub>2</sub>O+TEA+CO<sub>2</sub>), (H<sub>2</sub>O+MEA+CO<sub>2</sub>) and (H<sub>2</sub>O+DEA+CO<sub>2</sub>) systems provide better predictions than other investigated models including ANN, LSSVM, and ANFIS. For all the amine systems, the values of R<sup>2</sup> for the presented AdaBoost-CART models are more than 0.99 indicating that the models perfectly fits the experimental data. As can be seen, employing the ANN models for predicting CO<sub>2</sub> loading capacity of MEA, DEA, and TEA aqueous solutions results in obtaining the worst predictions.

**Fig. 6.10** illustrates the histogram of relative errors in percent for the created ANN models to represent the equilibrium absorption of CO<sub>2</sub> in MEA, DEA, and TEA aqueous solutions. Similarly, **Fig. 6.11** depicts the errors histogram for the presented AdaBoost-CART models. Comparing these figures shows the good precision of the AdaBoost-CART models over the ANN models in estimating the targets. **Fig. 6.12** demonstrates the differences between the predictions of developed ANFIS tools to calculate the CO<sub>2</sub> loading capacity of the studied amines and corresponding experimental targets (in terms of relative error). The regenerated CO<sub>2</sub> loading of amine solutions, i.e. MEA, DEA, and TEA, using the developed LSSVM models are compared to the corresponding experimental data in **Fig. 6.13**.

**Table 6.14:** Overall performance of the models for amine systems

System	Model	Parameter	Value
H <sub>2</sub> O+MEA+CO <sub>2</sub>	LSSVM	$R^2$	0.9803
		ARD%	0.48
		AARD%	4.95
	ANFIS	$R^2$	0.9854
		ARD%	0.56
		AARD%	3.69
	ANN	$R^2$	0.9386
		ARD%	1.67
		AARD%	8.73
H <sub>2</sub> O+DEA+CO <sub>2</sub>	AdaBoost-CART	$R^2$	0.9987
		ARD%	0.15
		AARD%	0.51
	LSSVM	$R^2$	0.9918
		ARD%	-1.15
		AARD%	6.52
	ANFIS	$R^2$	0.9671
		ARD%	-0.11
		AARD%	3.60
H <sub>2</sub> O+TEA+CO <sub>2</sub>	ANN	$R^2$	0.9580
		ARD%	1.31
		AARD%	8.24
	AdaBoost-CART	$R^2$	0.9977
		ARD%	-1.91
		AARD%	2.76
	LSSVM	$R^2$	0.9851
		ARD%	-1.18
		AARD%	6.09
H <sub>2</sub> O+TEA+CO <sub>2</sub>	ANFIS	$R^2$	0.9986
		ARD%	0.03
		AARD%	2.06
	ANN	$R^2$	0.9929
		ARD%	0.58
		AARD%	3.92
	AdaBoost-CART	$R^2$	0.9998
		ARD%	1.14
		AARD%	1.14

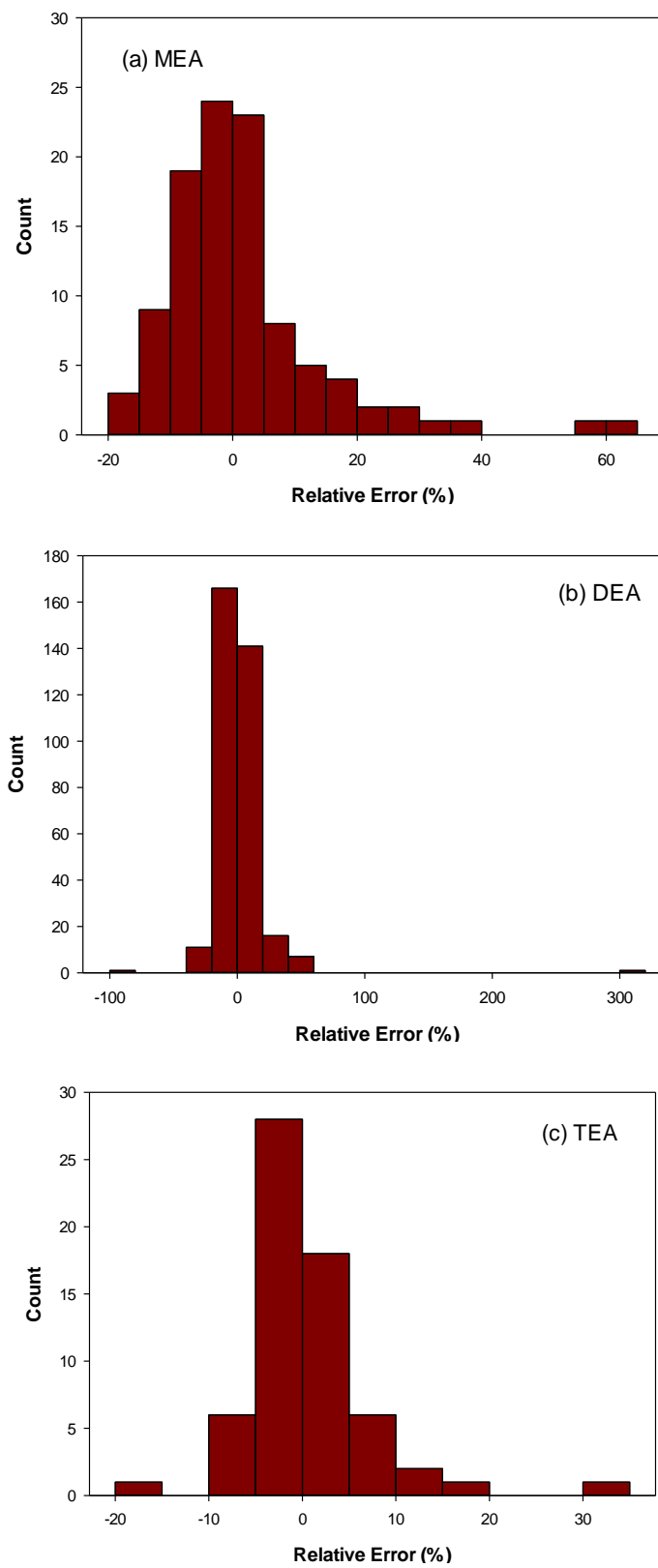


**Fig. 6.10:** Histogram of relative errors of the presented ANN models for (a) MEA, (b) DEA, and (c) TEA amine systems

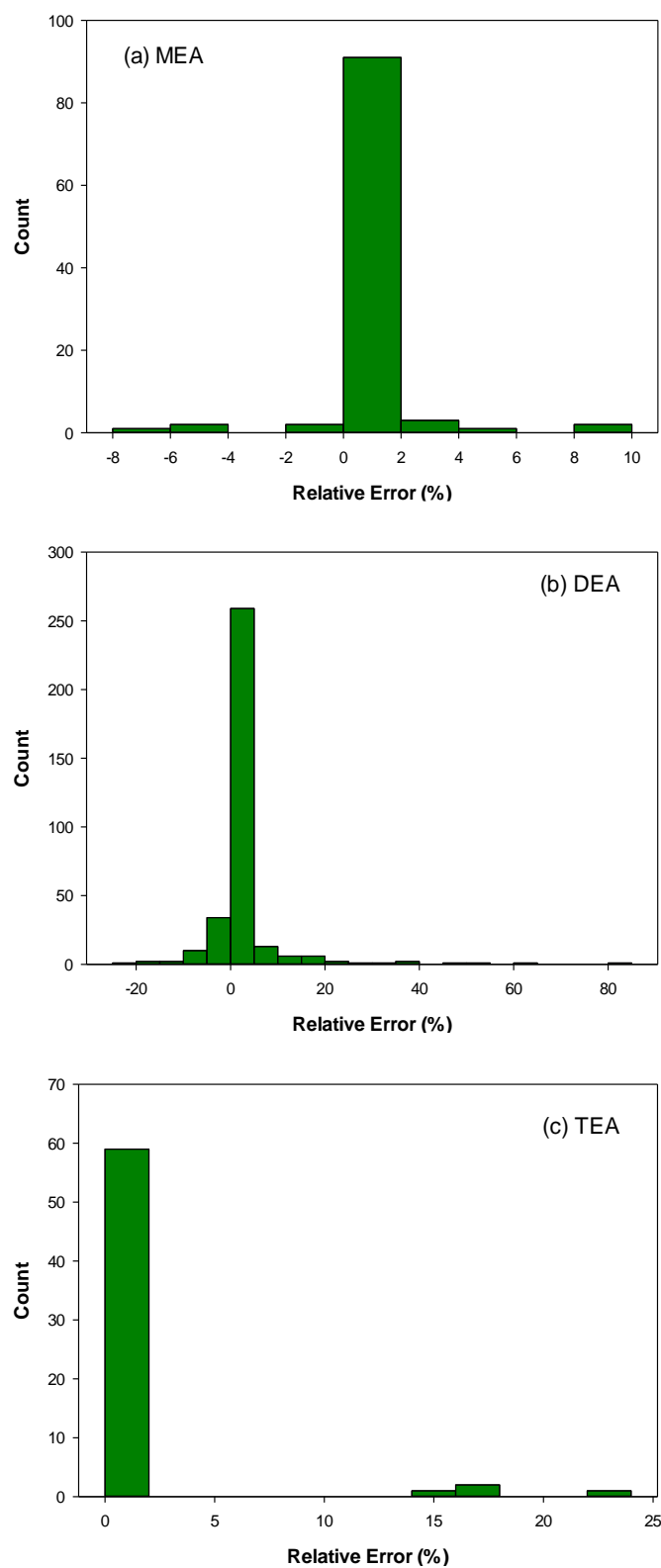


**Fig. 6.11:** Histogram of relative errors of the presented AdaBoost-CART models for (a) MEA, (b) DEA, and (c) TEA amine systems

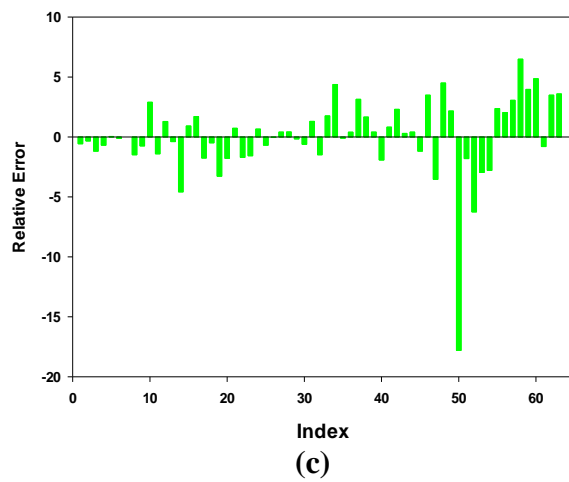
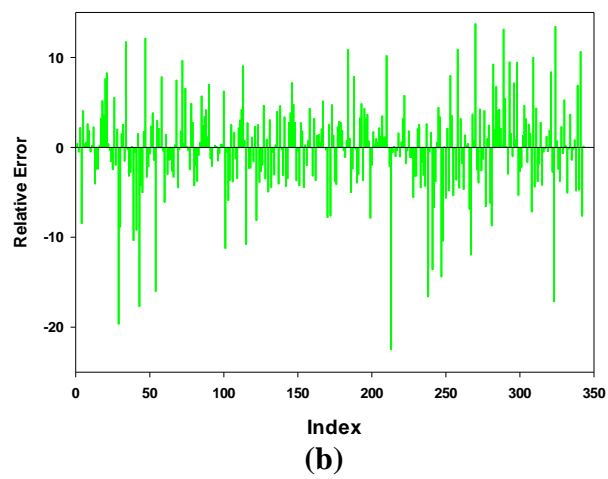
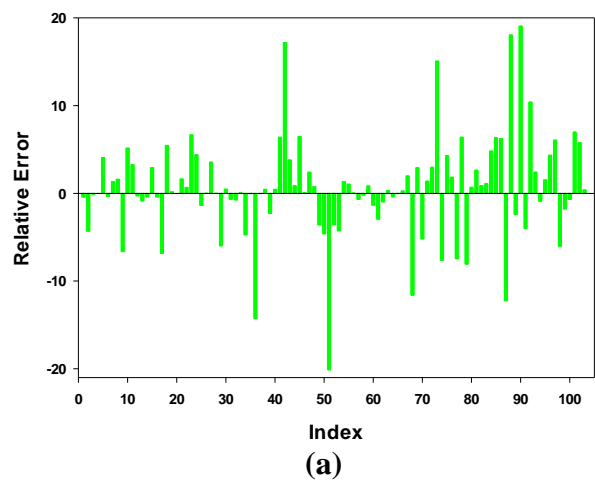
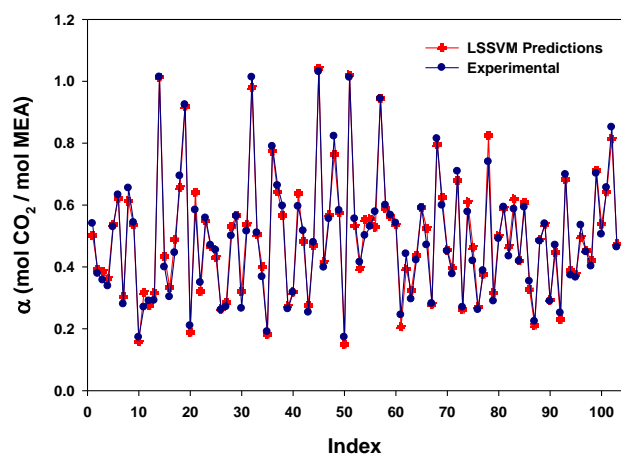
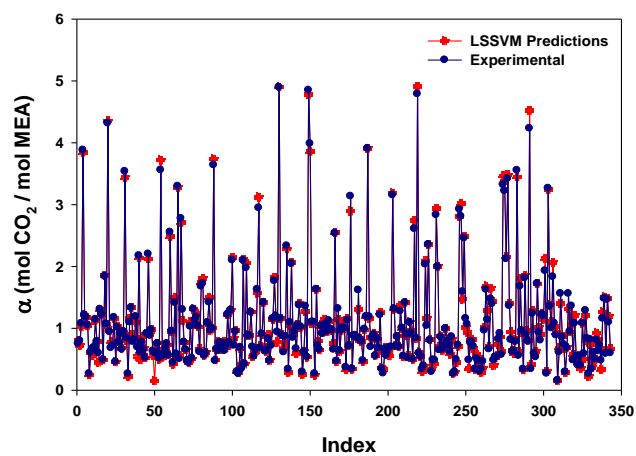


**Fig. 6.12:** Relative deviations of the predicted CO<sub>2</sub> loading capacity of amines by the proposed ANFIS tools from targets for: (a) MEA, (b) DEA, and (c) TEA systems

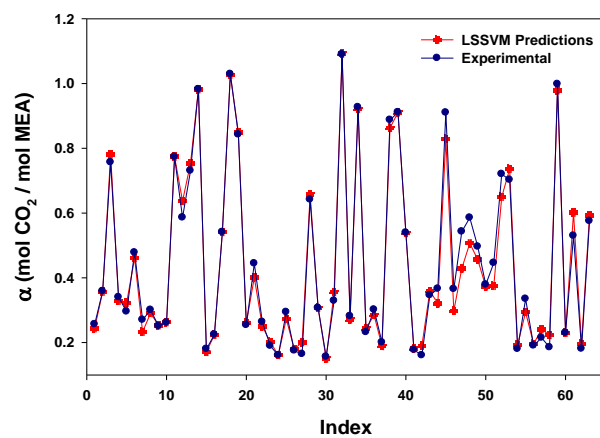




(a)



(b)



(c)

**Fig. 6.13:** The developed LSSVM model for (a) MEA, (b) DEA, and (c) TEA aqueous solutions vs. the corresponding experimental targets

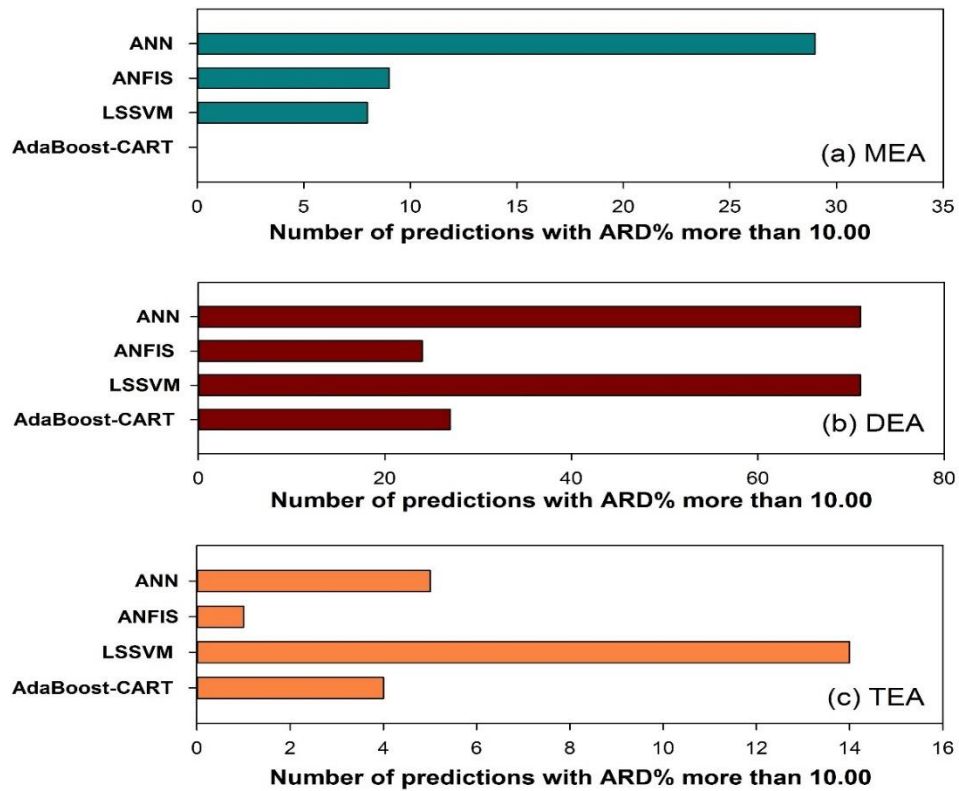
The negative value of ARD% for the developed AdaBoost-CART model for H<sub>2</sub>O+DEA+CO<sub>2</sub> system indicates that the estimations of the model are slightly underestimated. For the presented tree-based models for MEA and TEA systems, the values of ARD% are positive. The values of this parameter for all the developed ANN models are also positive. Hence, the ANN models as well as the tree-based models for MEA and TEA systems give slightly overestimated predictions.

**Table 6.15** summarizes the ranges for the obtained errors (absolute) using the LSSVM and ANFIS models and the proposed ANN and AdaBoost tools as well. For the H<sub>2</sub>O+MEA+CO<sub>2</sub> and H<sub>2</sub>O+DEA+CO<sub>2</sub> systems, maximum errors of the built AdaBoost-CART models are lower than the maximum errors of other models. For H<sub>2</sub>O+TEA+CO<sub>2</sub> system, the ANFIS model has the best error range. Considering the values of maximum error, the ANN models have the weakest performance in representing the target values of the studied amine systems. Graphical comparison of the presented LSSVM, ANFIS, ANN, and AdaBoost-CART models in terms of the number of predictions with absolute relative deviation in percent more than 10.00 is depicted in **Fig. 6.14**.

For MEA solution of 5.00 mol/L, **Table 6.16** gives the outcomes of the proposed AdaBoost-CART model versus corresponding experimental data by Shen and Li [375] (for T=298.15 and T=373.15 K), and Lee et al. [372] (for T=335.15, T=353.15, and T=373.15 K). The estimated CO<sub>2</sub> solubility in 0.1836 mol/L MEA aqueous solution with the developed AdaBoost-CART model is demonstrated in **Fig. 6.15**. The experimental data are reported by Park et al. [373].

**Table 6.15:** Error ranges of the models for amine systems

System	Model	Abs. RD (%)	
		Min	Max
CO <sub>2</sub> +MEA+Water	LSSVM	0.00	18.62
	ANFIS	0.00	25.66
	ANN	0.16	62.35
	AdaBoost-CART	0.00	9.57
CO <sub>2</sub> +DEA+Water	LSSVM	0.01	298.18
	ANFIS	0.00	98.47
	ANN	0.00	317.94
	AdaBoost-CART	0.00	81.24
CO <sub>2</sub> +TEA+Water	LSSVM	0.00	26.48
	ANFIS	0.00	17.80
	ANN	0.00	30.48
	AdaBoost-CART	0.00	22.22

**Fig. 6.14:** Comparing the predictive mathematical models in terms of high absolute relative deviation (%) for (a) MEA, (b) DEA, and (c) TEA amine systems

**Table 6.16:** Results of the built AdaBoost model vs. corresponding targets for MEA solution of concentration 5 mol/L

Ref.	T (K)	P <sub>CO2</sub> (kPa)	$\alpha$ (mol of CO <sub>2</sub> /mol of amine)		Abs. RD%
			Exp.	AdaBoost-CART	
[372]	298.15	10.373	0.555	0.555	0.00
		31.371	0.601	0.601	0.00
		98.629	0.664	0.664	0.00
		322.352	0.739	0.739	0.00
		1013.460	0.851	0.851	0.00
	373.15	10.173	0.289	0.289	0.00
		31.986	0.353	0.353	0.00
		100.563	0.447	0.427	4.47
		316.154	0.501	0.501	0.00
		993.975	0.581	0.581	0.00
[375]	333.15	15.596	0.495	0.495	0.00
		30.768	0.514	0.514	0.00
		59.536	0.526	0.526	0.00
		94.873	0.558	0.565	1.25
		115.201	0.565	0.565	0.00
		439.791	0.592	0.592	0.00
		834.628	0.646	0.646	0.00
	353.15	8.217	0.403	0.403	0.00
		14.430	0.422	0.460	9.00
		24.374	0.446	0.446	0.00
		35.938	0.464	0.464	0.00
		76.629	0.493	0.493	0.00
		115.201	0.515	0.515	0.00
		399.106	0.532	0.532	0.00
	373.15	818.575	0.559	0.559	0.00
		1183.753	0.595	0.595	0.00
		8.710	0.306	0.306	0.00
		20.072	0.347	0.345	0.58
		41.976	0.411	0.411	0.00
		73.710	0.427	0.423	0.94
		100.563	0.423	0.427	0.94
		383.904	0.457	0.457	0.00
		787.400	0.508	0.508	0.00
		1160.997	0.523	0.523	0.00

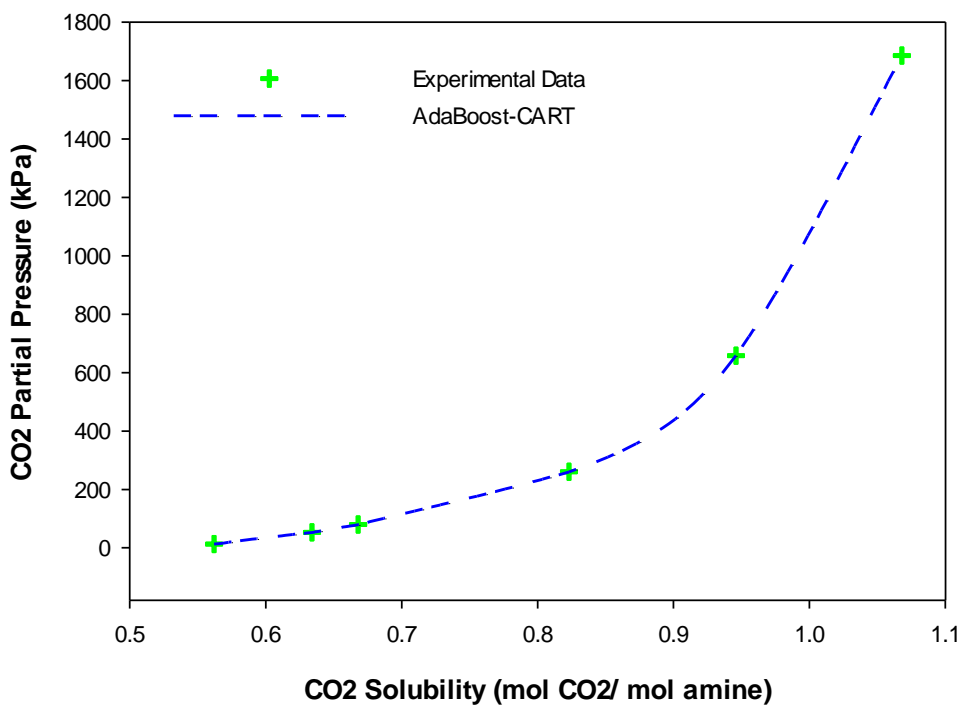


**Fig. 6.15:** Performance of the proposed AdaBoost-CART model in predicting CO<sub>2</sub> solubility in MEA solution of concentration 0.1836 mol/L at T=313.15 K [373]

For the DEA concentration in the aqueous phase at 3.50 mol/L, **Table 6.17** compares the results of the developed AdaBoost-CART model at temperatures between 298.15 and 373.15 K with the experimental data by Vallée et al. [382]. **Fig. 6.16** shows the capability of the presented tree-based tool in reproducing the reported data by Jane and Li [379].

**Table 6.17:** Results of the built AdaBoost model vs. corresponding targets for DEA solution of concentration 3.5 mol/L [382]

T (K)	P <sub>CO2</sub> (kPa)	$\alpha$ (mol of CO <sub>2</sub> /mol of amine)		Abs. RD%
		Exp.	AdaBoost-CART	
298.15	22.19	0.599	0.630	5.17
	70.17	0.693	0.693	0.00
	203.10	0.790	0.790	0.00
	671.31	0.914	0.914	0.00
	2030.90	1.033	1.033	0.00
	6422.30	1.189	1.189	0.00
323.15	21.23	0.468	0.465	0.55
	70.17	0.564	0.564	0.00
	194.29	0.666	0.765	14.82
	701.70	0.782	0.782	0.00
	2030.90	0.922	0.918	0.49
	7017.00	1.081	1.081	0.00
348.15	22.19	0.334	0.334	0.00
	67.13	0.434	0.484	11.52
	221.90	0.540	0.616	14.07
	671.30	0.664	0.664	0.00
	2122.90	0.803	0.803	0.00
	6713.10	0.986	0.986	0.00
373.15	22.19	0.184	0.184	0.00
	70.17	0.295	0.344	16.61
	221.90	0.414	0.414	0.00
	671.30	0.539	0.539	0.00
	2122.90	0.682	0.803	17.74
	6713.10	0.857	0.857	0.00

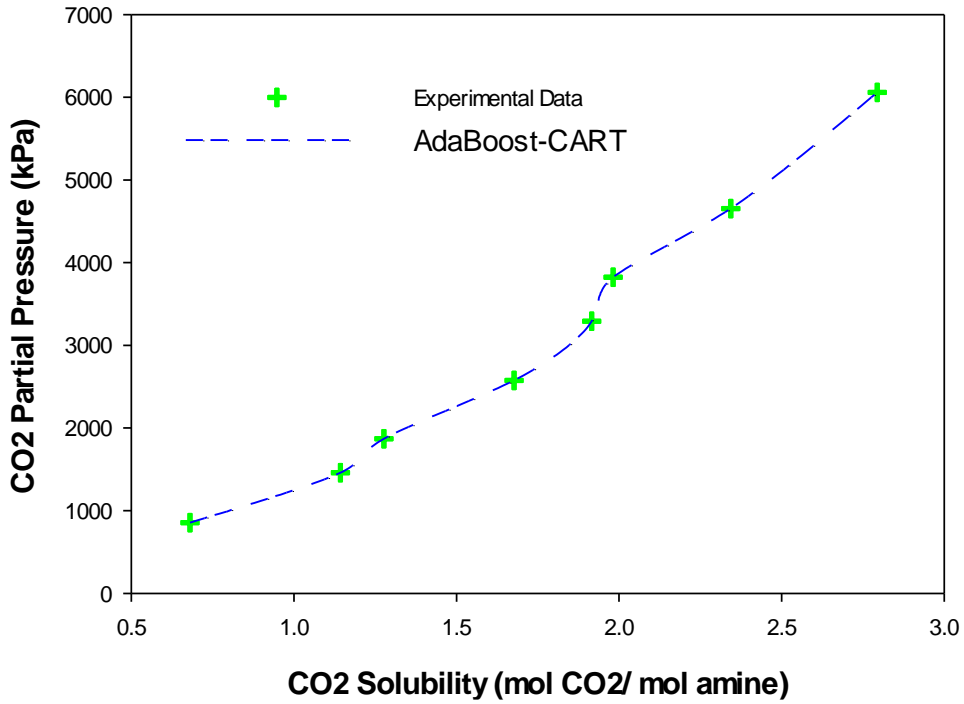


**Fig. 6.16:** Performance of the proposed AdaBoost-CART model in predicting CO<sub>2</sub> solubility in DEA solution of concentration 0.1831 mol/L at T=338.75 K [379]

**Table 6.18** presents a comparison of the developed AdaBoost-CART tool with the real CO<sub>2</sub> loading capacity of TEA solution with a concentration equal to 2.00 mol/L at 313.20-353.20 K temperature range. The capability of the proposed CART-based model in regenerating the reported data by Mason and Dodge [461], for H<sub>2</sub>O+TEA (3.5 mol/L)+CO<sub>2</sub> system is shown in **Fig. 6.17**.

**Table 6.18:** Results of the built AdaBoost model vs. corresponding targets for TEA solution of concentration 2 mol/L [383]

T (K)	P <sub>CO2</sub> (kPa)	$\alpha$ (mol of CO <sub>2</sub> /mol of amine)		Abs. RD%
		Exp.	AdaBoost-CART	
313.2	1.62	0.085	0.085	0.00
	6.56	0.128	0.128	0.00
	9.56	0.169	0.169	0.00
	14.98	0.205	0.205	0.00
	36.27	0.345	0.345	0.00
	92.98	0.534	0.534	0.00
333.2	2.60	0.077	0.077	0.00
	8.58	0.114	0.114	0.00
	32.91	0.207	0.207	0.00
	53.88	0.243	0.243	0.00
	60.17	0.257	0.257	0.00
	90.97	0.340	0.340	0.00
353.2	153.40	0.485	0.485	0.00
	5.42	0.066	0.066	0.00
	8.05	0.080	0.080	0.00
	20.56	0.108	0.108	0.00
	43.01	0.134	0.134	0.00
	98.14	0.178	0.178	0.00
	137.90	0.191	0.191	0.00



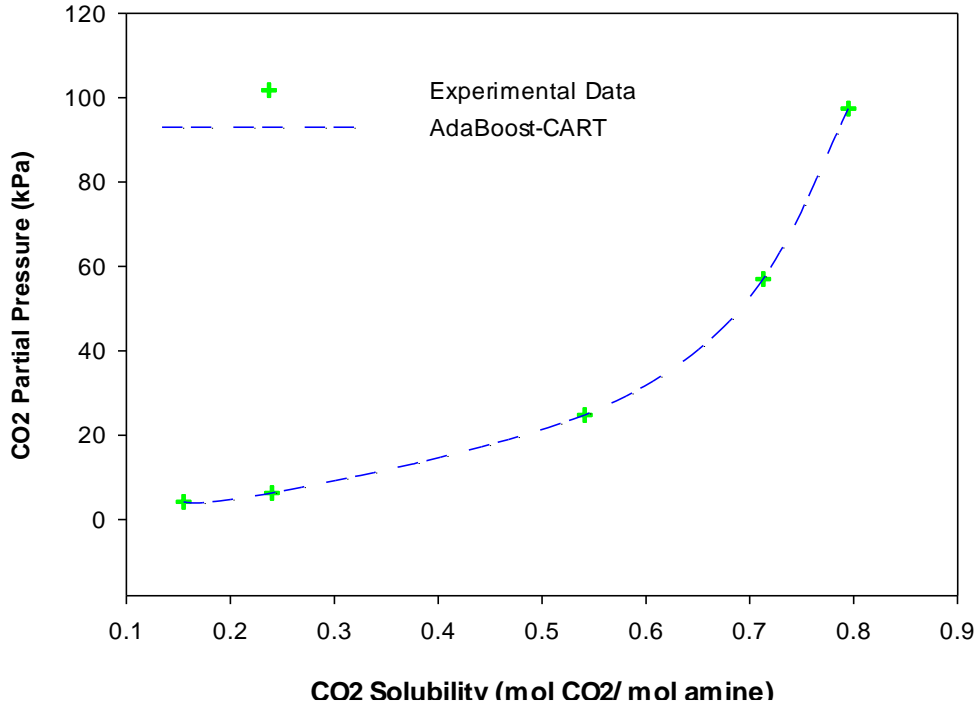


**Fig. 6.17:** Performance of the proposed AdaBoost-CART model in predicting CO<sub>2</sub> solubility in TEA solution of concentration 3.5 mol/L at T=298.15 K [461]

**Fig. 6.18** demonstrates the relative importance of each feature, i.e.  $P_{CO_2}$ ,  $C_{amine}$ , and  $T$ , in the creation of the proposed AdaBoost-CART models for (H<sub>2</sub>O+TEA+CO<sub>2</sub>), (H<sub>2</sub>O+MEA+CO<sub>2</sub>) (H<sub>2</sub>O+DEA+CO<sub>2</sub>) systems. As can be observed from **Fig. 6.18**, in development of the CART-based tools for all the studied systems, the amine concentration in aqueous phase has the lowest importance as compared to other features. On the other hand, CO<sub>2</sub> partial pressure is the most influencing factor in developing the AdaBoost-CART model to predict the solubility of CO<sub>2</sub> in DEA solution. In case of the models for MEA and TEA systems, the temperature is the most effective parameter.

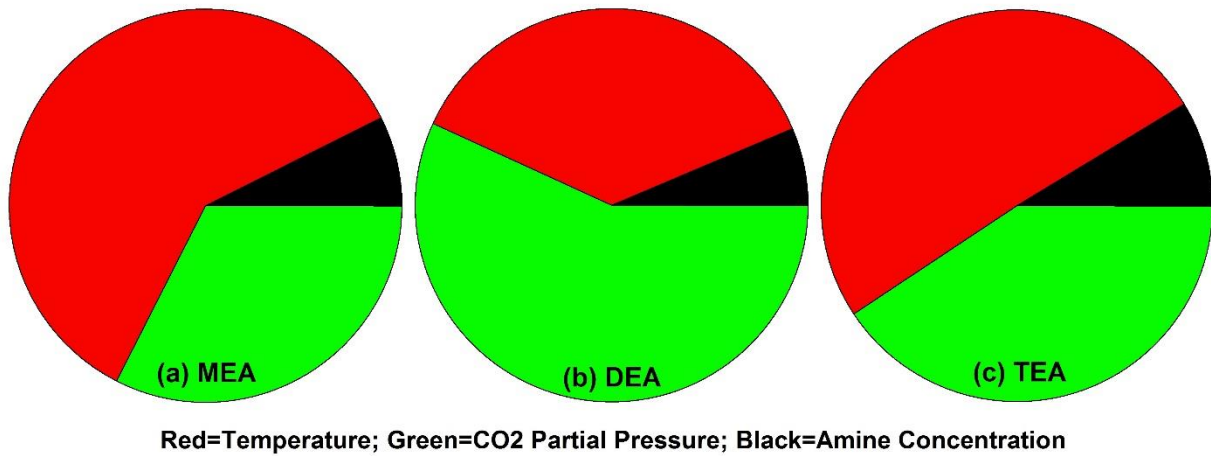


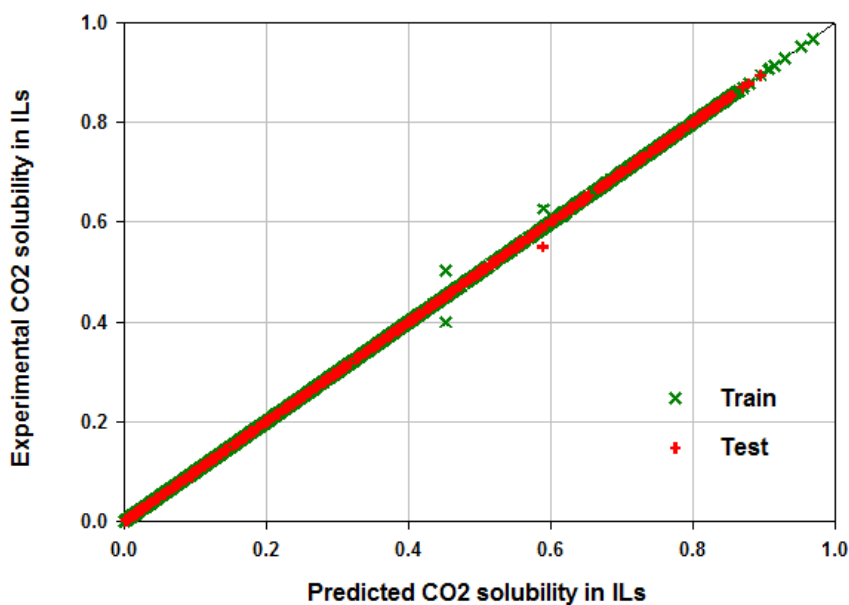
**Fig. 6.18:** Relative importance of each input on the CO<sub>2</sub> solubility in (a) MEA, (b) DEA, and (TEA) solution in development of the proposed AdaBoost-CART models

## 6.5. CO<sub>2</sub>+IL System

Error results of the CART model are given in **Table 6.19**. With accordance to **Table 6.19**, the  $R^2$  between the predictions of the proposed tree-based tool and corresponding target CO<sub>2</sub> solubility in ILs is equal to 1; this reveals that the regression line thoroughly passes through the targets. The  $R^2$  is graphically represented in **Fig. 6.19**. The AARD% calculated for the train data points shows an excellent ability of the CART-based approach via the training (development) phase. Moreover, for the test data points, the AARD% less than 0.05% indicates the vigor of the created model for accurate prediction of the unobserved datasets.

**Table 6.19:** Error analysis for the Created CART-based tool

Dataset	Variable		
	ARD%	$R^2$	AARD%
Train	0.0	1	0.04
Test	0.01	1	0.06

**Fig. 6.19:** Calculated solubility of CO<sub>2</sub> in ILs vs. target values

The accuracy of the calculations of CO<sub>2</sub> solubility in ILs using the created CART and the previously published RBF-ANN, LSSVM, MLP-ANN and ANFIS tools are given in **Table 6.20** and **Fig. 6.20**. As can be observed, among the studied methods by [Baghban, Mohammadi and Taleghani \[460\]](#), the LSSVM tool provides the best outcomes in terms of AARD% and  $R^2$  values. However, comparing the capability of the LSSVM tool with the created CART model indicates that using the CART presents much better calculations as the AARD% and  $R^2$  values are 0.04 and

1, respectively. Since the values of ARD% for all the literature models, i.e. RBF-ANN, LSSVM, MLP-ANN and ANFIS [460], are positive, these tools overestimate the solubility of CO<sub>2</sub> in ILs. Amongst the proposed tools by Baghban, Mohammadi and Taleghani [460], ANFIS presents the weakest estimation capability.

**Table 6.20:** The created CART-based tool vs. the literature models [460]

Tool	Variable		
	ARD%	R <sup>2</sup>	AARD%
CART	0.0	1	0.04
LSSVM	13.60	-7.16	17.17
ANFIS	41.54	0.9185	62.84
MLP-ANN	7.36	0.9726	34.28
RBF-ANN	12.80	0.9821	25.25

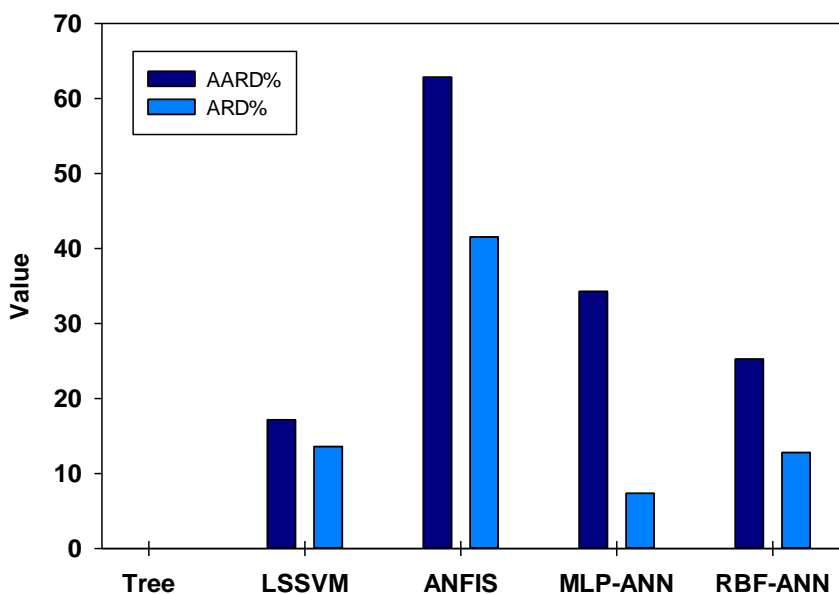


**Fig. 6.20:** The created tree-based model vs. the published models in the literature [460]

**Fig. 6.21** shows the number of estimations by the created tree-based tool and the literature models [460] that resulted in absolute relative deviation percent values more than 25. According to **Fig. 6.21**, just one data is reproduced by the created CART bad absolute RD%. Some of the bad predictions of the created tree and the published models in the literature [460] are given in **Tables 6.21-6.29**. **Table 6.21** indicates that AARD% of the poor outputs of the created tree is less than 6.5%. However, AARD% of bad estimations of the published literature models are more than 1813%, 1494% 5060% and 2432%.

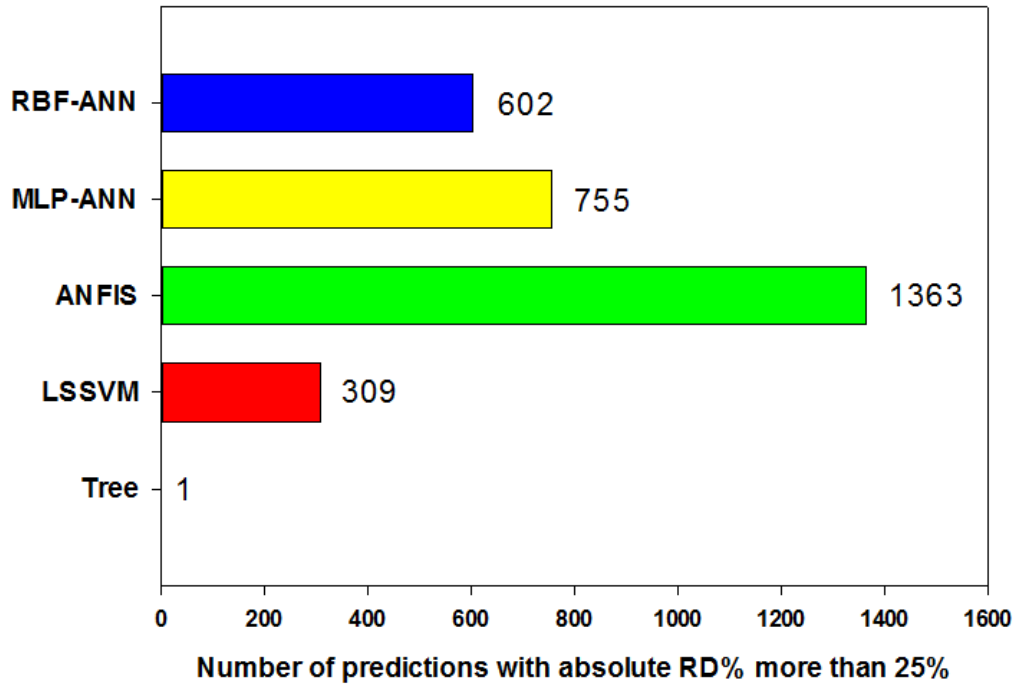


**Fig. 6.21:** The published literature models [460] vs. the created CART tool in terms of high absolute RD%

**Table 6.21:** Results of the created tree-based tool with high deviation from the targets

T, K	P, MPa	Tc	Pc	$\omega$	$\alpha, mol / mol$		RD%
					Exp	Extra Tree	
348.5	0.0485	876.24	2.22	1.327	0.008	0.01	25.00
348.5	0.0485	876.24	2.22	1.327	0.012	0.01	-16.67
343.55	4.495	1225.8	7.95	0.7698	0.4	0.4515	12.87
348.5	0.098	876.24	2.22	1.327	0.017	0.019	11.76
343.55	4.495	1225.8	7.95	0.7698	0.503	0.4515	-10.24
297.4	0.0091	876.24	2.22	1.327	0.007	0.0063	-10.00
348.5	0.098	876.24	2.22	1.327	0.021	0.019	-9.52
313.15	0.0097	1255.7	1.803	0.5876	0.0028	0.003	7.14
314.05	5.15	788.05	3.31	1.225	0.551	0.5891	6.91
314.05	5.15	788.05	3.31	1.225	0.6271	0.5891	-6.06
313.89	0.0386	632.3	2.04	0.8489	0.0054	0.0057	5.55
334.38	0.0435	632.3	2.04	0.8489	0.0054	0.0051	-5.55
324.12	0.0421	632.3	2.04	0.8489	0.0056	0.0053	-5.36
323.15	0.0102	1073.7	1.615	1.0726	0.0019	0.0018	-5.26
297.4	0.0091	876.24	2.22	1.327	0.006	0.0063	5.00
297.4	0.0091	876.24	2.22	1.327	0.006	0.0063	5.00
333.15	0.0101	1255.7	1.803	0.5876	0.0023	0.0024	4.35
344.49	0.0427	632.3	2.04	0.8489	0.0047	0.0049	4.25
334.38	0.0413	632.3	2.04	0.8489	0.0049	0.0051	4.08
323.15	0.0101	1255.7	1.803	0.5876	0.0025	0.0024	-4.00
344.49	0.045	632.3	2.04	0.8489	0.0051	0.0049	-3.92
324.12	0.04	632.3	2.04	0.8489	0.0051	0.0053	3.92
413.1	3.431	1081.6	3.61	0.4111	0.0913	0.0948	3.83
313.89	0.0406	632.3	2.04	0.8489	0.0059	0.0057	-3.39
323.2	0.0828	708.9	1.73	0.7553	0.0124	0.012	-3.22
313.3	0.103	708.9	1.73	0.7553	0.0162	0.0158	-2.47
303.72	0.0772	632.3	2.04	0.8489	0.0127	0.013	2.36
303.72	0.0726	632.3	2.04	0.8489	0.0133	0.013	-2.25
334.15	0.089	632.3	2.04	0.8489	0.0095	0.0097	2.10
313.15	0.348	950.45	33.21	1.666	0.0158	0.0161	1.90

**Table 6.22:** Results of the published LSSVM [460] with high deviation from the targets

T, K	P, MPa	Tc	Pc	$\omega$	$\alpha, mol / mol$		RD%
					Exp	LSSVM	
318	0.0963	788.05	3.31	1.225	0.0001	0.030393	30293.28
322.9	0.0091	876.24	2.22	1.327	0.001	0.031726	3072.55
338	0.098	708.9	1.73	0.7553	0.0006	0.013134	2088.92
282.75	0.01017	632.3	2.04	0.8489	0.002	0.033414	1570.71
322.8	0.0091	876.24	2.22	1.327	0.002	0.031868	1493.41
298	0.0105	708.9	1.73	0.7553	0.001	0.014995	1399.55
298.05	0.01015	708.9	1.73	0.7553	0.001	0.014885	1388.47
298.2	0.01	632.3	2.04	0.8489	0.001	0.010896	989.64
298.15	0.0097	1221.9	1.828	0.2603	0.003	0.032305	976.82
282	0.0089	876.24	2.22	1.327	0.006	0.059445	890.75
298.2	0.01	788.05	3.31	1.225	0.004	0.035366	784.16
298.1	0.01	824.67	28.86	0.6808	0.001	0.008801	780.09
281.9	0.009	876.24	2.22	1.327	0.007	0.059767	753.81
298.15	0.01	1255.8	2.031	0.3193	0.002	0.014736	636.78
298.15	0.01	1255.8	2.031	0.3193	0.002	0.014736	636.78
297.4	0.0091	876.24	2.22	1.327	0.006	0.041903	598.38
297.4	0.0091	876.24	2.22	1.327	0.006	0.041903	598.38
283.05	0.00969	708.9	1.73	0.7553	0.004	0.025309	532.73
283.1	0.0097	708.9	1.73	0.7553	0.004	0.025302	532.55
298.15	0.0099	1155	1.173	0.5207	0.003	0.018405	513.50
297.4	0.0091	876.24	2.22	1.327	0.007	0.041903	498.61
348.5	0.0091	876.24	2.22	1.327	0.004	0.023579	489.47
348.5	0.0091	876.24	2.22	1.327	0.004	0.023579	489.47
297.95	0.00973	632.3	2.04	0.8489	0.002	0.011017	450.83
313.15	0.0097	1255.7	1.803	0.5876	0.00284	0.013331	369.39
313.15	0.0101	1073.7	1.615	1.0726	0.00178	0.007913	344.54
322.9	0.0487	876.24	2.22	1.327	0.009	0.038372	326.36
333.15	0.0101	1255.7	1.803	0.5876	0.0023	0.009586	316.76
333.15	0.0101	1038.7	2.588	0.3334	0.00182	0.007469	310.39
322.9	0.0482	876.24	2.22	1.327	0.01	0.038288	282.88

**Table 6.23:** Results of the published ANFIS [460] with high deviation from the targets

T, K	P, MPa	Tc	Pc	$\omega$	$\alpha, mol / mol$		RD%
					Exp	ANFIS	
318	0.0963	788.05	3.31	1.225	0.0001	0.047109	47008.97
298.1	0.01	824.67	28.86	0.6808	0.001	0.196765	19576.49
298	0.0105	708.9	1.73	0.7553	0.001	0.053345	5234.48
298.05	0.01015	708.9	1.73	0.7553	0.001	0.053176	5217.60
298.15	0.01	1255.8	2.031	0.3193	0.002	0.090346	4417.30
298.15	0.01	1255.8	2.031	0.3193	0.002	0.090346	4417.30
282.75	0.01017	632.3	2.04	0.8489	0.002	0.08212	4006.00
298.2	0.01	632.3	2.04	0.8489	0.001	0.040802	3980.20
343.15	0.0099	1255.8	2.031	0.3193	0.002	0.072611	3530.54
343.15	0.0099	1255.8	2.031	0.3193	0.002	0.072611	3530.54
333.15	0.0101	1255.7	1.803	0.5876	0.0023	0.075709	3191.72
343.15	0.0097	1221.9	1.828	0.2603	0.002	0.063271	3063.56
323.1	0.01	824.67	28.86	0.6808	0.004	0.125239	3030.96
323.15	0.0101	1255.7	1.803	0.5876	0.00254	0.0782	2978.75
298.15	0.0097	1221.9	1.828	0.2603	0.003	0.091873	2962.43
313.15	0.01	1255.8	2.031	0.3193	0.003	0.0853	2743.35
313.15	0.01	1255.8	2.031	0.3193	0.003	0.0853	2743.35
313.15	0.0097	1255.7	1.803	0.5876	0.00284	0.079074	2684.31
323.15	0.01	1038.7	2.588	0.3334	0.00209	0.057706	2661.07
313.15	0.0097	1221.9	1.828	0.2603	0.003	0.080799	2593.29
322.9	0.0091	876.24	2.22	1.327	0.001	0.026472	2547.16
333.15	0.0101	1038.7	2.588	0.3334	0.00182	0.047793	2525.97
283.05	0.00969	708.9	1.73	0.7553	0.004	0.097481	2337.03
283.1	0.0097	708.9	1.73	0.7553	0.004	0.097308	2332.71
313.15	0.0101	1073.7	1.615	1.0726	0.00178	0.041966	2257.64
298.1	0.0498	824.67	28.86	0.6808	0.009	0.197308	2092.31
298.15	0.0099	1155	1.173	0.5207	0.003	0.065271	2075.70
328.15	0.127	821.61	43.54	1.2287	0.0034	0.073509	2062.02
323.15	0.0102	1073.7	1.615	1.0726	0.00187	0.039506	2012.62
348.2	0.0102	708.9	1.73	0.7553	0.001	-0.01896	-1996.21



**Table 6.24:** Results of the published MLP-ANN [460] with high deviation from the targets

T, K	P, MPa	Tc	Pc	$\omega$	$\alpha, mol / mol$		RD%
					Exp	MLP-ANN	
318	0.0963	788.05	3.31	1.225	0.0001	0.010103	10002.97
298.1	0.01	824.67	28.86	0.6808	0.001	0.074585	7358.45
333.15	0.0101	1255.7	1.803	0.5876	0.0023	0.133895	5721.51
323.15	0.0101	1255.7	1.803	0.5876	0.00254	0.127059	4902.32
313.15	0.0097	1255.7	1.803	0.5876	0.00284	0.12388	4261.98
333.15	0.0101	1038.7	2.588	0.3334	0.00182	0.055442	2946.27
323.15	0.01	1038.7	2.588	0.3334	0.00209	0.057863	2668.57
348.15	0.0102	632.3	2.04	0.8489	0.002	-0.04833	-2516.58
298	0.0105	708.9	1.73	0.7553	0.001	0.024982	2398.25
298.05	0.01015	708.9	1.73	0.7553	0.001	0.024849	2384.85
344.49	0.02033	632.3	2.04	0.8489	0.00236	-0.04595	-2047.15
328.15	0.156	853.92	29.28	1.3308	0.0024	-0.04541	-1992.29
328.15	0.158	970.51	28.24	1.6719	0.0027	-0.04723	-1849.11
334.38	0.0197	632.3	2.04	0.8489	0.00243	-0.04197	-1827.22
348.15	0.05013	632.3	2.04	0.8489	0.003	-0.04391	-1563.77
298.15	0.0099	1155	1.173	0.5207	0.003	0.049889	1562.97
324.12	0.01906	632.3	2.04	0.8489	0.00255	-0.03643	-1528.61
338	0.098	708.9	1.73	0.7553	0.0006	0.00962	1503.36
333.15	0.05	1255.7	1.803	0.5876	0.00902	0.139948	1451.53
323.25	0.01015	632.3	2.04	0.8489	0.003	-0.03705	-1335.04
354.2	0.065	632.3	2.04	0.8489	0.004	-0.0444	-1210.01
283.05	0.00969	708.9	1.73	0.7553	0.004	0.051992	1199.79
283.1	0.0097	708.9	1.73	0.7553	0.004	0.051892	1197.30
323.15	0.0501	1255.7	1.803	0.5876	0.01052	0.133765	1171.53
282.75	0.01017	632.3	2.04	0.8489	0.002	0.02511	1155.52
313.89	0.0184	632.3	2.04	0.8489	0.00271	-0.02823	-1141.72
298.15	0.01	1255.8	2.031	0.3193	0.002	0.022679	1033.95
298.15	0.01	1255.8	2.031	0.3193	0.002	0.022679	1033.95
344.49	0.04267	632.3	2.04	0.8489	0.00474	-0.04342	-1015.95
328.15	0.169	950.45	33.21	1.666	0.0035	-0.03154	-1001.11

**Table 6.25:** Results of the published RBF-ANN [460] with high deviation from the targets

T, K	P, MPa	Tc	Pc	$\omega$	$\alpha, mol / mol$		RD%
					Exp	RBF-ANN	
318	0.0963	788.05	3.31	1.225	0.0001	0.014292	14192.04
298.1	0.01	824.67	28.86	0.6808	0.001	-0.00361	-460.91
298	0.0105	708.9	1.73	0.7553	0.001	0.021087	2008.67
298.05	0.01015	708.9	1.73	0.7553	0.001	0.021032	2003.19
298.15	0.01	1255.8	2.031	0.3193	0.002	0.050813	2440.63
298.15	0.01	1255.8	2.031	0.3193	0.002	0.050813	2440.63
282.75	0.01017	632.3	2.04	0.8489	0.002	0.031315	1465.77
298.2	0.01	632.3	2.04	0.8489	0.001	0.00759	659.03
343.15	0.0099	1255.8	2.031	0.3193	0.002	0.010326	416.30
343.15	0.0099	1255.8	2.031	0.3193	0.002	0.010326	416.30
333.15	0.0101	1255.7	1.803	0.5876	0.0023	0.045591	1882.20
343.15	0.0097	1221.9	1.828	0.2603	0.002	-0.0266	-1430.22
323.1	0.01	824.67	28.86	0.6808	0.004	-0.00448	-212.12
323.15	0.0101	1255.7	1.803	0.5876	0.00254	0.04948	1848.02
298.15	0.0097	1221.9	1.828	0.2603	0.003	0.054857	1728.57
313.15	0.01	1255.8	2.031	0.3193	0.003	0.028414	847.12
313.15	0.01	1255.8	2.031	0.3193	0.003	0.028414	847.12
313.15	0.0097	1255.7	1.803	0.5876	0.00284	0.067021	2259.90
323.15	0.01	1038.7	2.588	0.3334	0.00209	0.025532	1121.62
313.15	0.0097	1221.9	1.828	0.2603	0.003	0.028958	865.28
322.9	0.0091	876.24	2.22	1.327	0.001	0.000545	-45.46
333.15	0.0101	1038.7	2.588	0.3334	0.00182	0.028043	1440.81
283.05	0.00969	708.9	1.73	0.7553	0.004	0.025453	536.32
283.1	0.0097	708.9	1.73	0.7553	0.004	0.025335	533.37
313.15	0.0101	1073.7	1.615	1.0726	0.00178	0.005883	230.51
298.1	0.0498	824.67	28.86	0.6808	0.009	0.002013	-77.63
298.15	0.0099	1155	1.173	0.5207	0.003	0.044918	1397.26
328.15	0.127	821.61	43.54	1.2287	0.0034	0.006853	101.56
323.15	0.0102	1073.7	1.615	1.0726	0.00187	2.89E-05	-98.45
348.2	0.0102	708.9	1.73	0.7553	0.001	0.009366	836.56

The created tree-based tool for estimating the CO<sub>2</sub> solubility in different solvents and at various temperatures and pressures are depicted in **Fig. 6.22-25**.

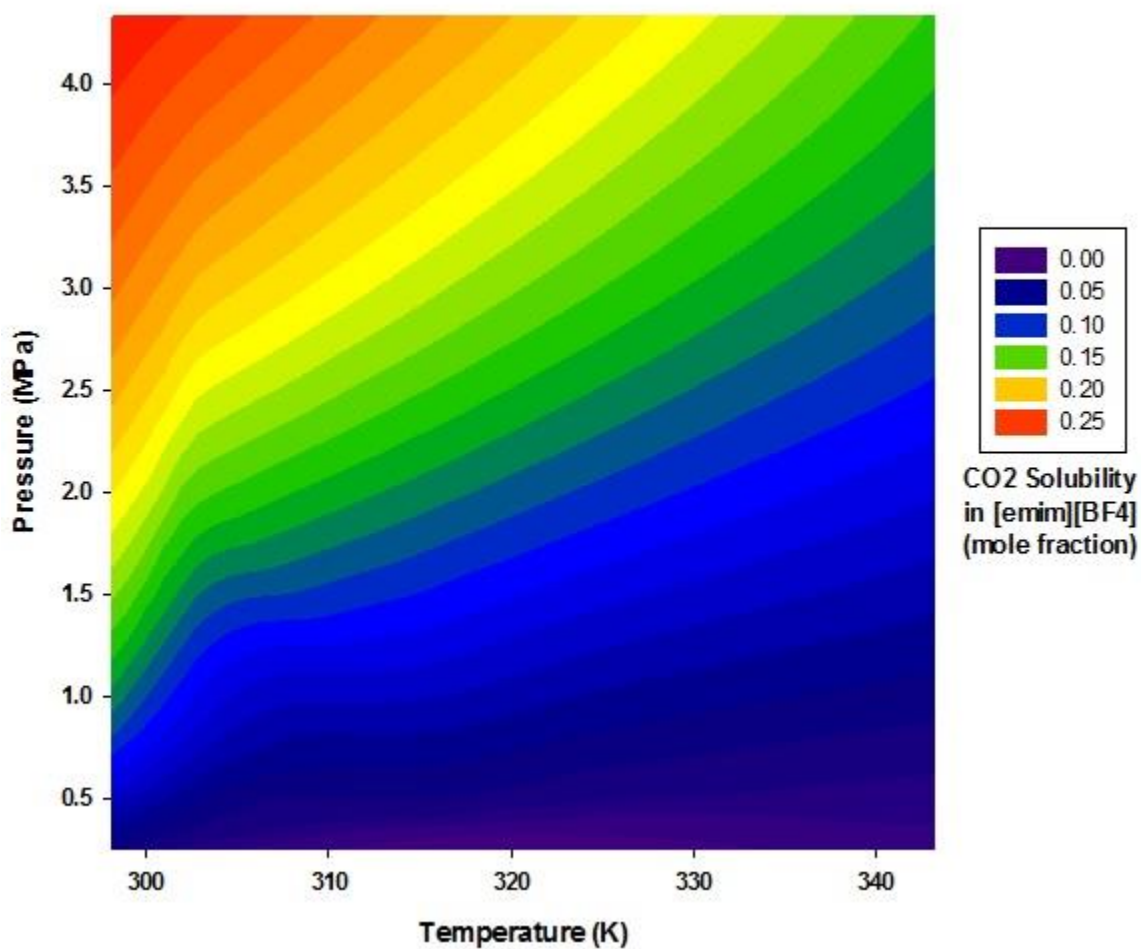


**Figure 6.22:** Prediction CART tool of CO<sub>2</sub> solubility in IL with  $P_C=2.36$  MPa,  $T_C=585.3$  K, and  $\omega=0.7685$

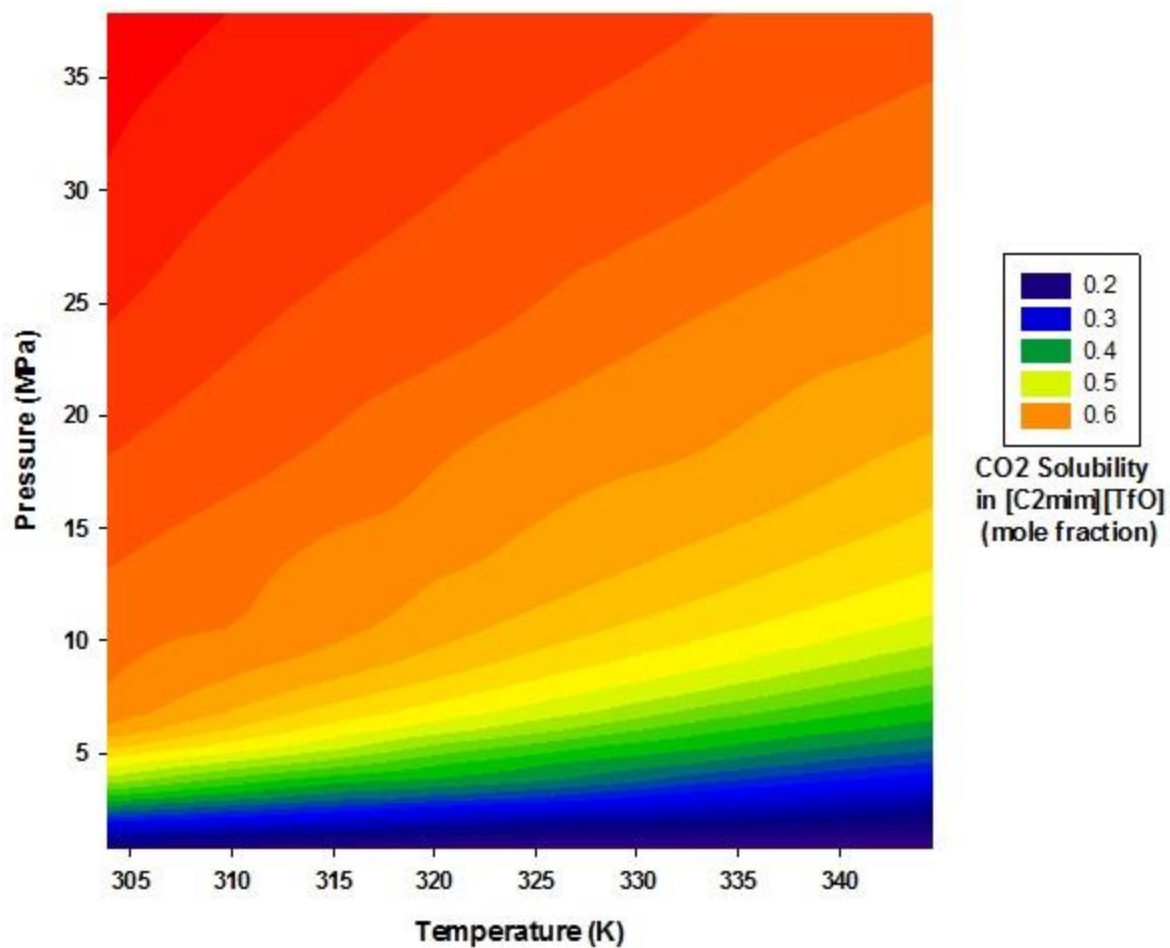


**Fig. 6.23:** Prediction CART tool of CO<sub>2</sub> solubility in IL with  $P_C=3.48$  MPa,  $T_C=756.89$  K, and  $\omega=0.783$

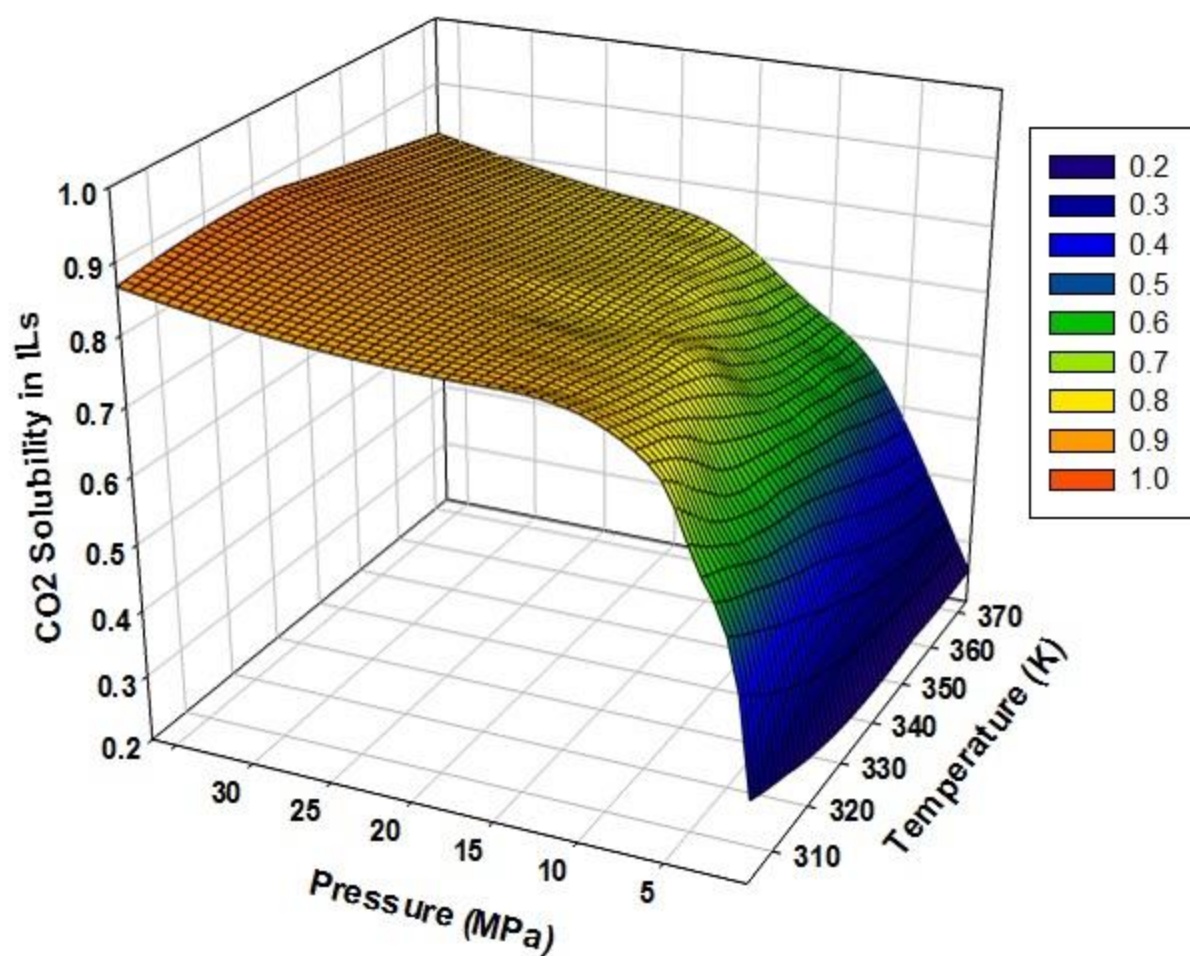


**Fig. 6.24:** Prediction CART tool of CO<sub>2</sub> solubility in IL with  $P_C=1.8171$  MPa,  $T_C=1277.68$  K, and  $\omega=0.5475$

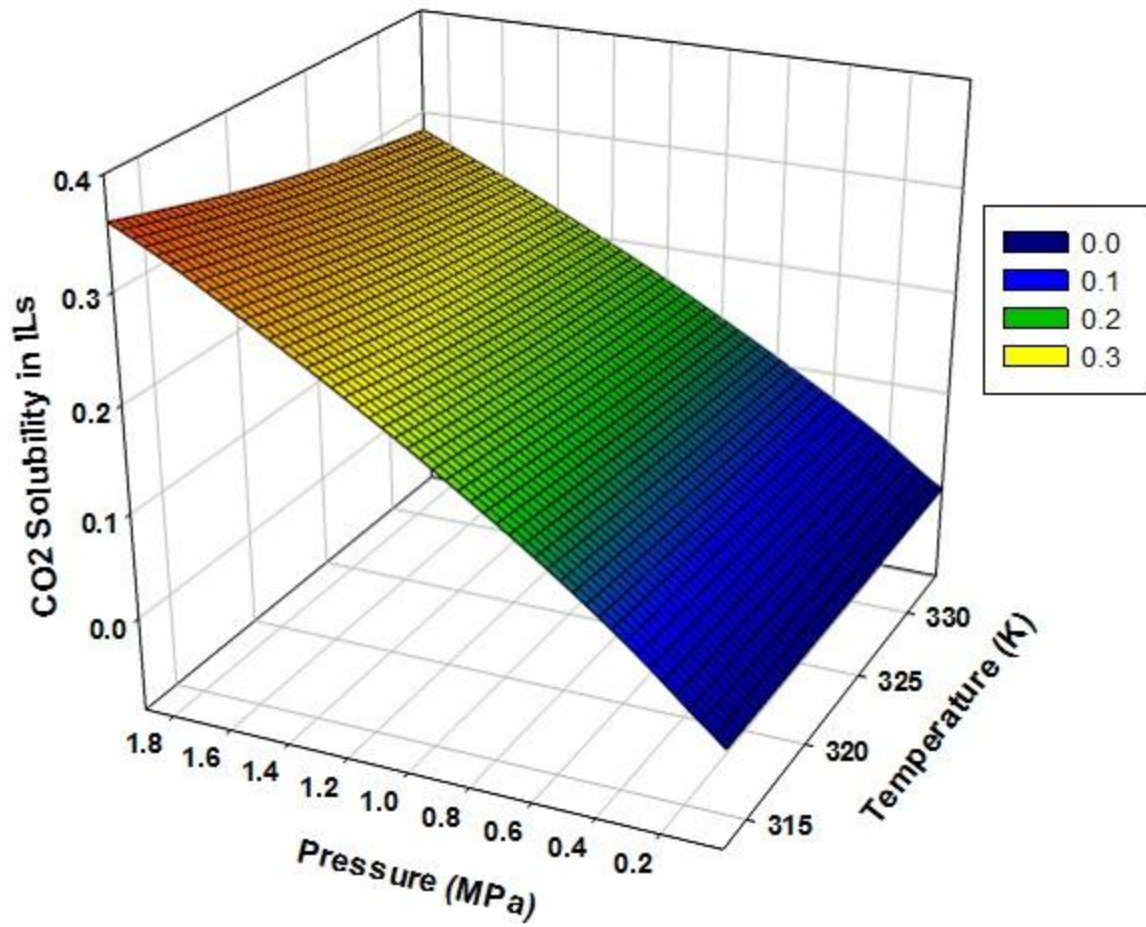


**Fig. 6.25:** Prediction CART tool of CO<sub>2</sub> solubility in IL with  $P_C=1.803$  MPa,  $T_C=1255.7$  K, and  $\omega =0.5876$

The relative importance of each input including pressure, temperature, critical pressure, critical temperature, and acentric factor in the development of the proposed tree-based tool is shown in **Fig. 6.26**. The most important variable that impacts the creation of the presented CART is the system's pressure (73.16%); on the other hand, the critical pressure of the IL has the lowest importance (4.04%). Baghban et al. [460] employed the relevancy factor combined with the

LSSVM tool to determine the effect of the independent variables of the target. In a respective order, pressure and temperature have the highest and lowest impacts.

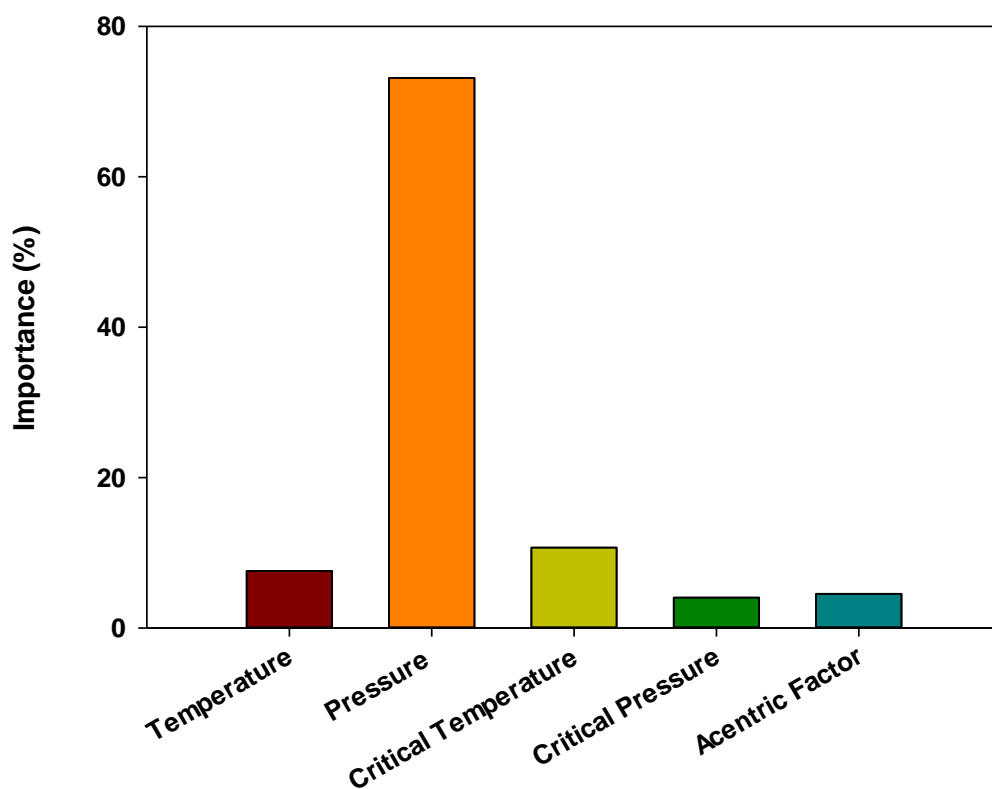


**Fig. 6.26:** Relative importance of each input in creation of the proposed tree-based tool for predicting the CO<sub>2</sub> solubility in ILs



## 6.6. CO<sub>2</sub>+Water+PZ System

**Table 6.26** gives the error analysis information. The *AARD%* of 0.93 proves the robustness of the created AdaBoost-CART tool for (CO<sub>2</sub>+water+PZ) system. Considering the *ARD%*, the developed AdaBoost-CART tool slightly overestimates the targets. As given in **Table 6.26**, there is no satisfactory agreement between the predictions of the LSSVM, ANFIS and ANN tools and the corresponding experimental values.

**Table 6.26:** Error analysis of the created tools for (CO<sub>2</sub>+water+PZ) system

Tool	Dataset	Variable		
		$R^2$	<i>AARD%</i>	<i>ARD%</i>
AdaBoost-CART	Train	0.9970	0.94	0.25
	Test	0.9934	0.83	-0.02
	<i>Total</i>	0.9967	0.93	0.22
LSSVM	Train	0.8840	16.28	6.42
	Test	0.8905	15.84	0.51
	<i>Total</i>	0.8843	16.23	5.82
ANN	Train	0.7858	17.19	6.08
	Test	0.7880	32.16	20.55
	<i>Total</i>	0.7849	18.69	7.53
ANFIS	Train	0.8940	16.06	6.27
	Test	0.8505	15.42	5.23
	<i>Total</i>	0.8890	15.99	6.16

**Fig. 6.27** visualizes the outputs of the developed tools versus the targets (absorption of CO<sub>2</sub> in PZ solution). **Fig. 6.28** is the histogram of the errors for the developed tools. Predictions of the created AdaBoost tool versus the experimental data by Nguyen et al. [446] and Bishnoi and Rochelle [443] are summarized in **Table 6.27** and **Table 6.28**, respectively.



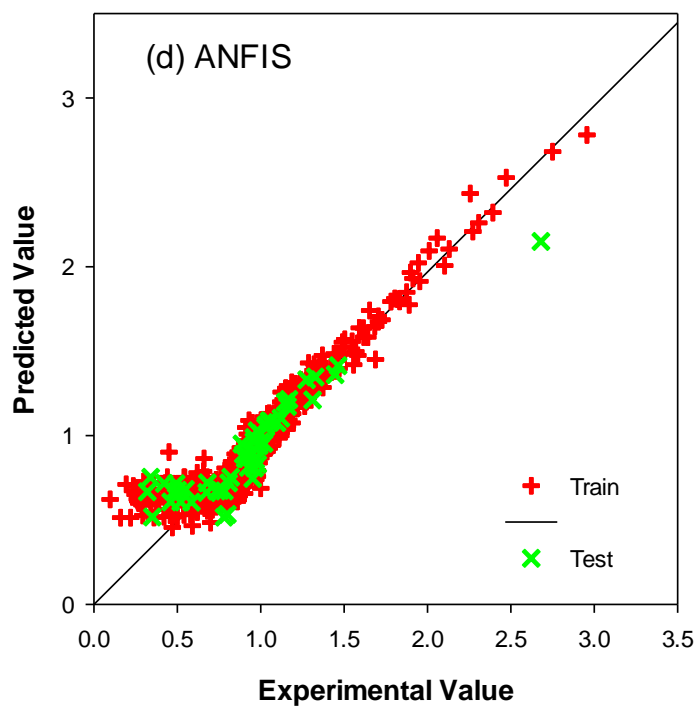
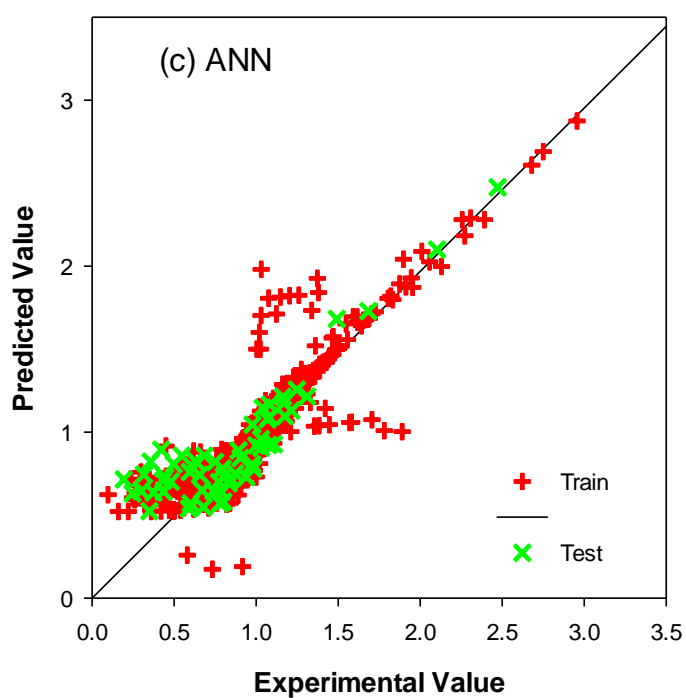
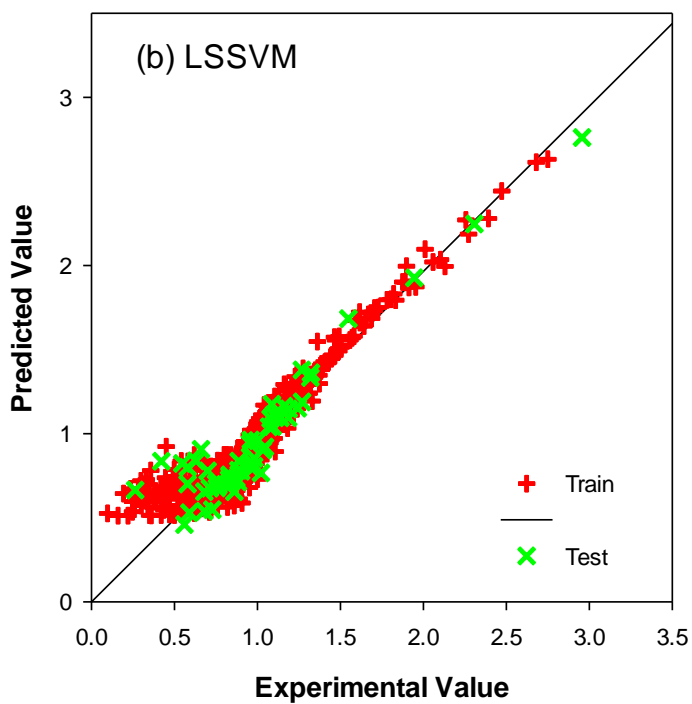
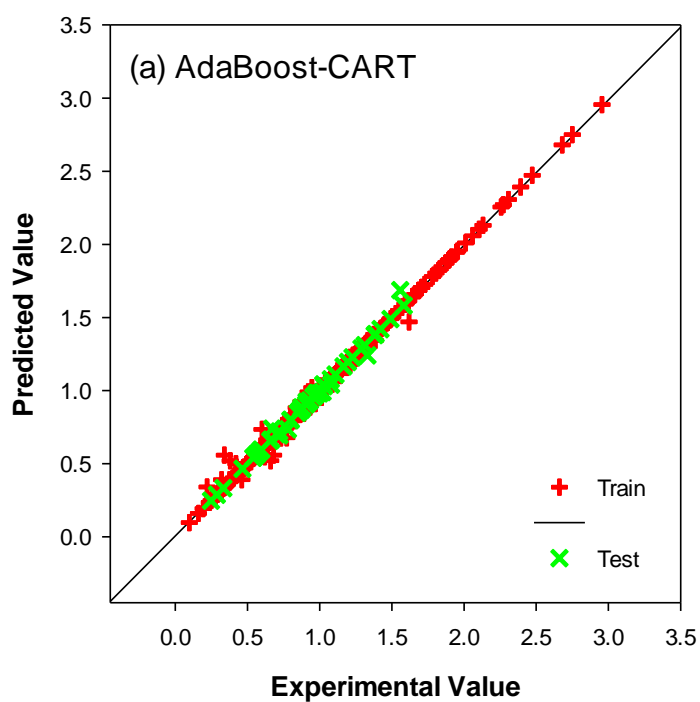


**Fig. 6.27:** The experimental CO<sub>2</sub> solubility in PZ vs. the outputs of the created (a) AdaBoost-CART, (b) LSSVM, (c) ANN, and (d) ANFIS tools

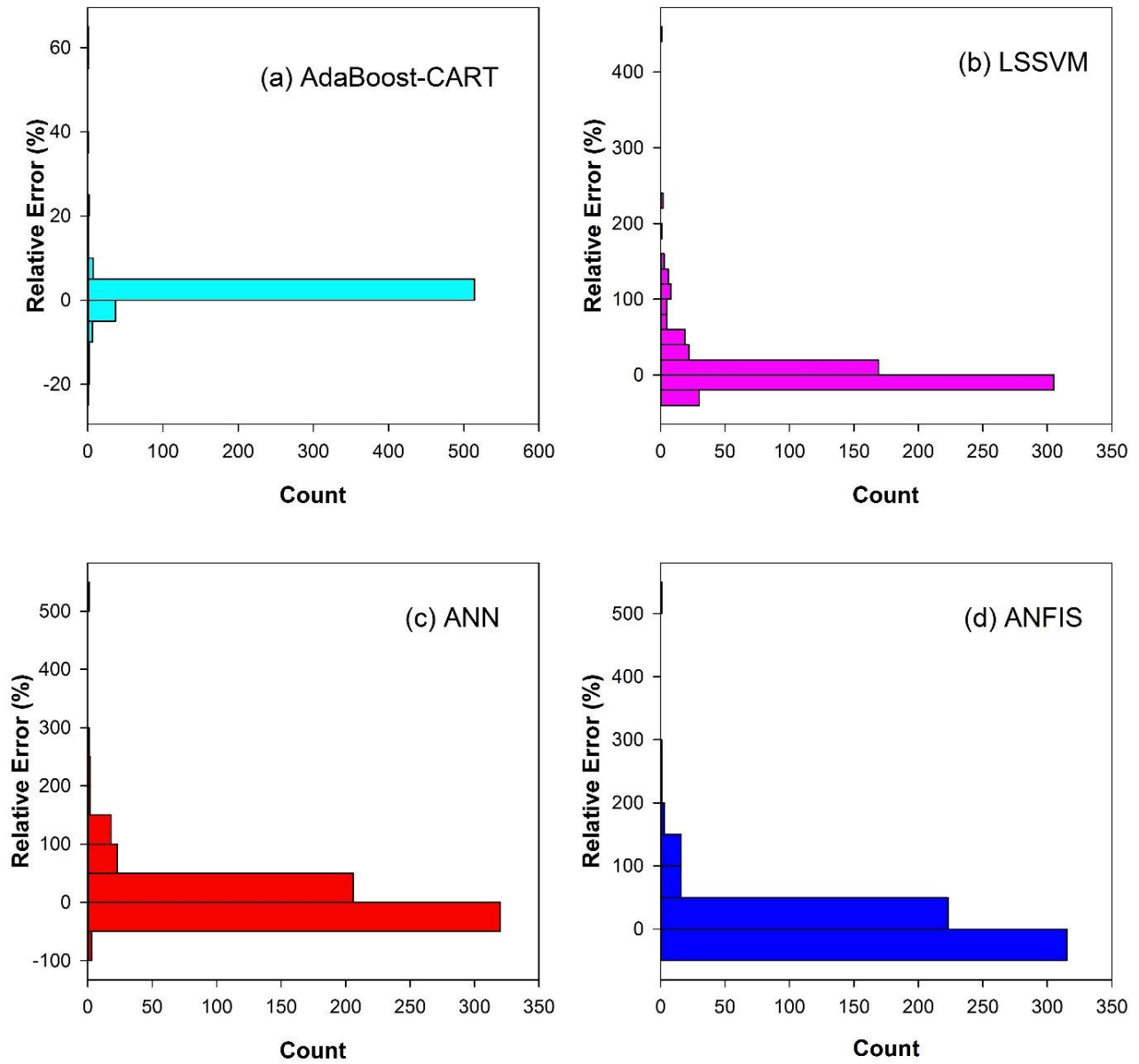


**Fig. 6.28:** Histogram of errors for the created tools

**Table 6.27:** Outcomes of the created AdaBoost tool vs. the experimental data by Nguyen et al. [446] for (CO<sub>2</sub>+water+PZ)

T (K)	P <sub>CO2</sub> (kPa)	$\alpha$ (mol CO <sub>2</sub> /mol PZ)		RE%
		Experimental	AdaBoost-CART	
313.15	7.643	5.89	0.58	0.00
		5.92	0.80	0.00
	4.781	6.83	0.34	64.29
		6.83	0.68	-17.85
		6.86	0.54	0.00
		6.92	0.44	0.00
		6.99	0.82	0.00
		7.07	0.62	0.00
		7.13	0.30	0.00
	1.913	7.18	0.74	0.00
		7.20	0.52	0.00
		7.21	0.46	0.00
		7.51	0.86	0.00
333.15	7.707	15.50	0.80	0.00
	7.708	15.60	0.58	0.00
	4.825	17.30	0.32	21.88
		17.30	0.46	-15.22
		17.40	0.66	0.00
	4.826	17.60	0.60	0.00
		17.60	0.78	-5.77
	1.931	17.90	0.56	0.00
		17.90	0.34	0.00
		18.00	0.26	0.00
		18.10	0.38	36.84
		18.10	0.66	-21.21
		18.20	0.74	0.00
		18.30	0.76	0.00
	4.830	18.50	0.84	0.00
	1.932	18.50	0.82	0.00

**Table 6.28:** Outcomes of the created AdaBoost tool vs. the experimental data by Bishnoi and Rochelle [443]

T (K)	P <sub>CO2</sub> (kPa)	$\alpha$ (mol CO <sub>2</sub> /mol PZ)		RE%
		Experimental	AdaBoost-CART	
313	0.03	0.32	0.32	0.00
	0.04	0.32	0.32	0.00
	0.08	0.47	0.47	0.00
	0.11	0.48	0.47	-2.08
	0.25	0.55	0.55	0.00
	0.45	0.61	0.63	3.28
	0.85	0.72	0.72	0.00
	0.95	0.72	0.72	0.00
	3.00	0.82	0.82	0.00
	40.00	0.96	0.96	0.00
343	0.06	0.16	0.16	0.00
	0.13	0.22	0.22	0.00
	0.45	0.35	0.35	0.00
	0.65	0.42	0.50	19.05
	1.44	0.47	0.47	0.00
	3.43	0.59	0.62	5.08
	7.88	0.72	0.72	0.00

In a respective order, **Figs. 6.29** to **6.31** graphically shows the AdaBoost-CART estimations vs. experimental data reported by Dash et al. [168], Derks et al. [444] and Kamps, Xia and Maurer [445]. The relative importance of the inputs in creation process of the AdaBoost-CART tool for modeling the (CO<sub>2</sub>+water+PZ) equilibrium system is depicted in **Fig. 6.32**.

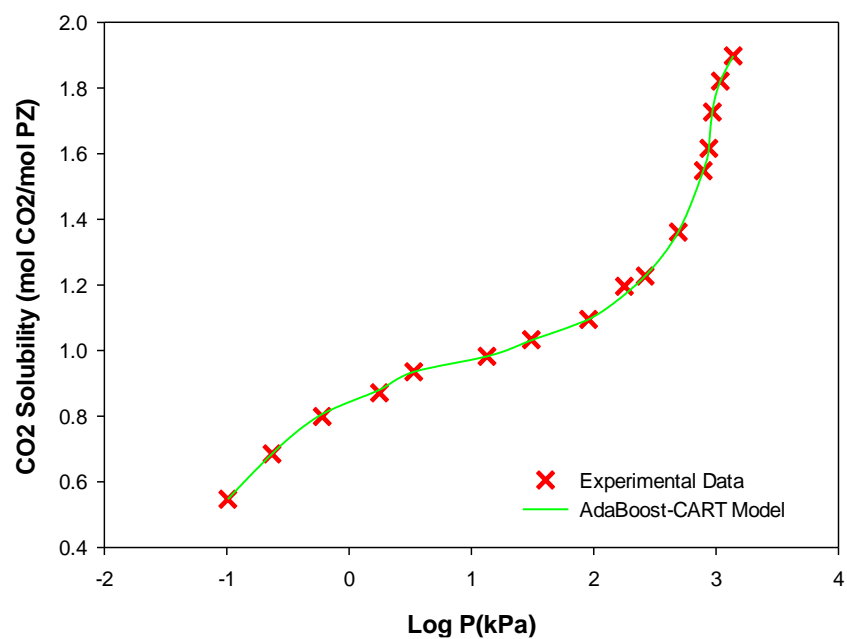


**Fig. 6.29:** AdaBoost-CART predictions vs. experimental data by [Dash, Samanta and Bandyopadhyay \[168\]](#)

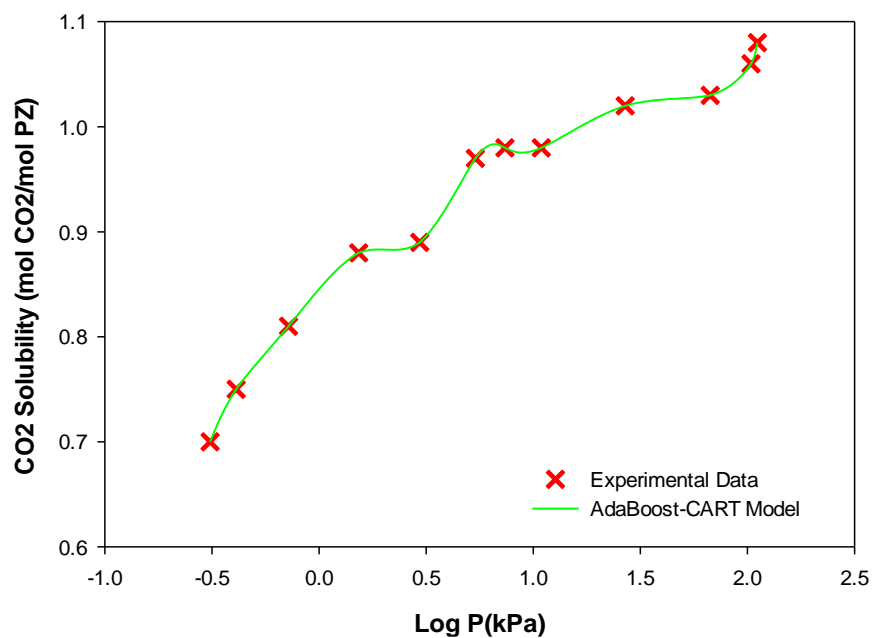


**Fig. 6.30:** AdaBoost-CART predictions vs. experimental data by [Derks, Dijkstra, Hogendoorn and Versteeg \[444\]](#)

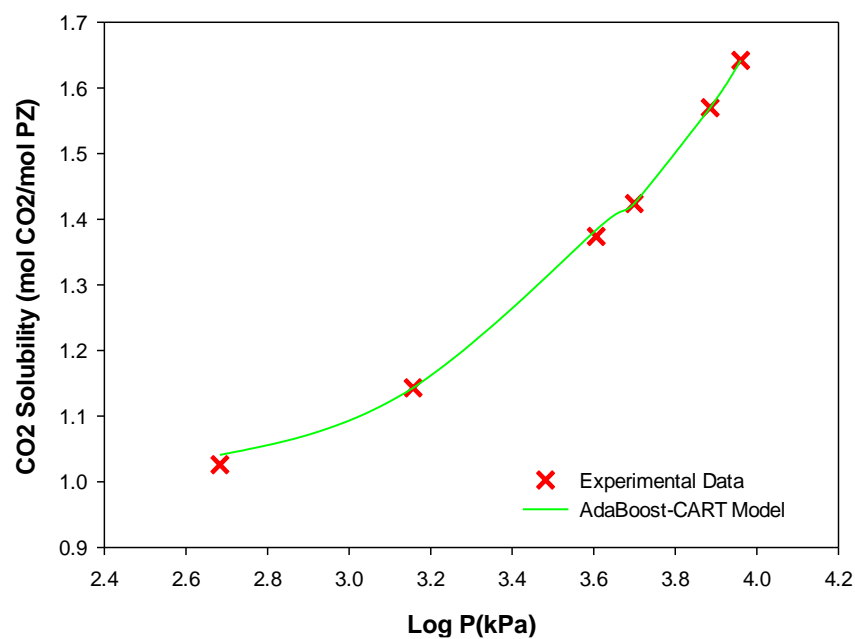


**Fig. 6.31:** AdaBoost-CART predictions vs. experimental data by [Kamps, Xia and Maurer \[445\]](#)

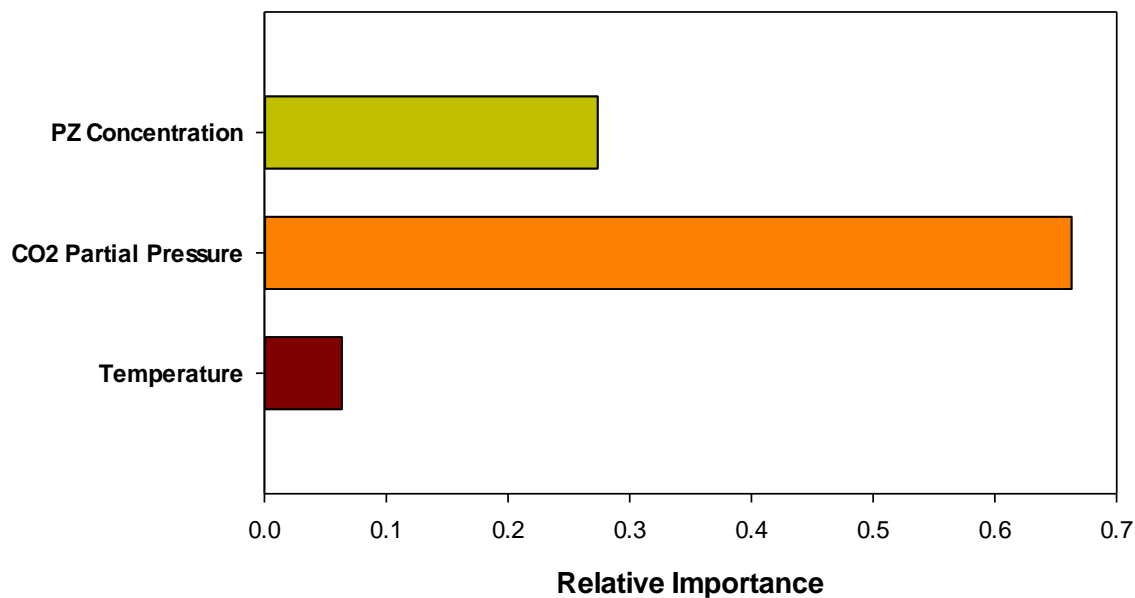


**Fig. 6.32:** Relative importance of the inputs in creation of the AdaBoost-CART tool for (CO<sub>2</sub>+water+PZ) system

## 6.7. CO<sub>2</sub>+Water+SG System

The statistical variables used for error analysis are given in **Table 6.29**. The *AARD%* of 0.89 indicates the excellent performance of the created model. Considering the *ARD%* for all the studied data, the developed AdaBoost-CART tool slightly underestimates the targets. For visualizing the estimations and the targets, **Fig. 6.33** is provided. **Fig. 6.34** depicts the histogram of the errors for the created tree model.

**Table 6.29:** Statistical variables for the created AdaBoost-CART tool

Dataset	Variable	
	<i>AARD%</i>	<i>ARD%</i>
Train	0.76	-0.17
Test	2.04	0.25
<i>Total</i>	0.89	-0.13

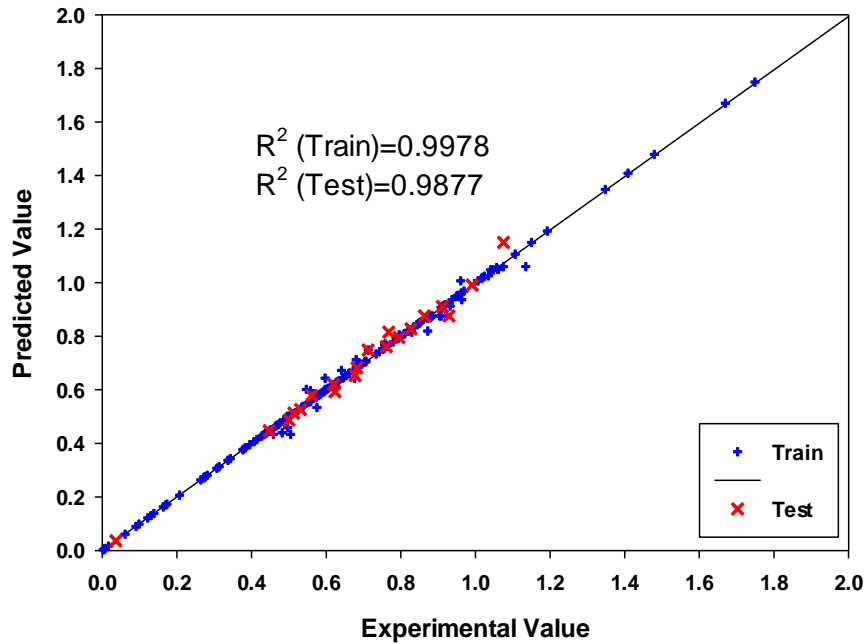


**Fig. 6.33:** The experimental targets vs. the outputs of the created AdaBoost-CART tool

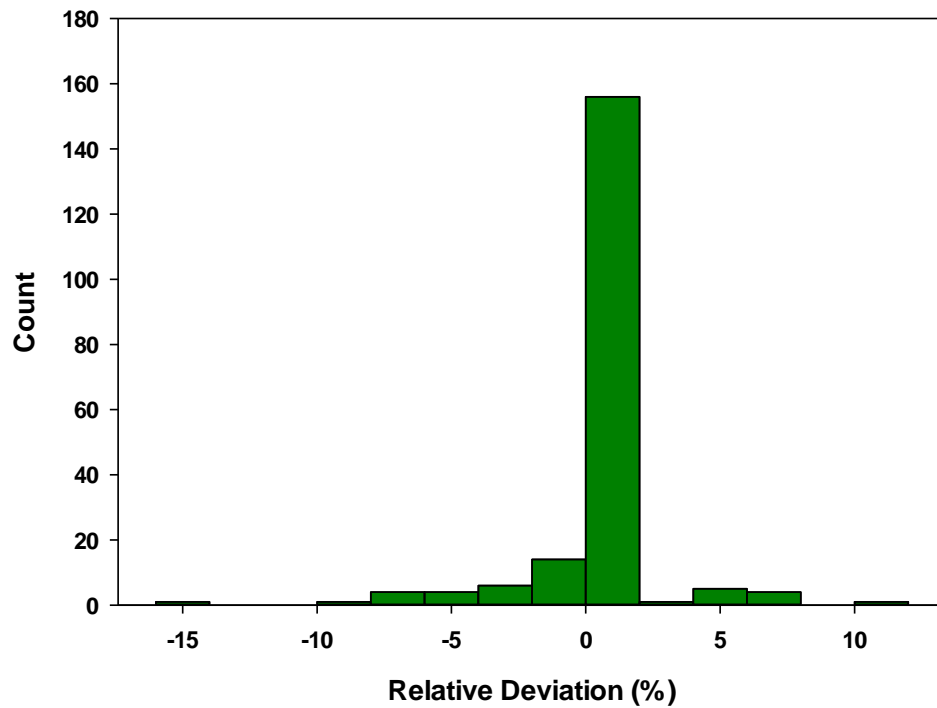


**Fig. 6.34:** Errors histogram for the created AdaBoost-CART tool

The error analysis results for other developed tools are tabulated in **Table 6.30**. With accordance to **Table 6.30**, these tools regenerate the target values with good accuracy. However, it is clear that the AdaBoost-CART methodology provides more robust outcomes than other techniques.



**Table 6.30:** Statistical variables for other created tools

Tool	Dataset	Parameter		
		<i>ARD%</i>	<i>R</i> <sup>2</sup>	<i>AARD%</i>
LSSVM	Train	1.36	0.9070	13.24
	Test	-7.16	0.8808	14.37
	<i>Total</i>	0.49	0.9023	13.36
ANN	Train	4.81	0.8857	18.25
	Test	3.35	0.7078	14.31
	<i>Total</i>	4.66	0.8863	17.85
ANFIS	Train	2.64	0.9259	14.77
	Test	12.21	0.7872	21.15
	<i>Total</i>	3.61	0.9139	15.42

**Table 6.31** compares the outcomes of the created AdaBoost-CART tool in comparison with some target values. For solution of SG with concentration of 10 mass%, **Fig. 6.35** depicts the AdaBoost-CART tool for calculation of the CO<sub>2</sub> solubility in SG.

**Fig. 6.36** illustrates the relative importance of the inputs. As shown in **Fig. 6.36**, the CO<sub>2</sub> partial pressure constitutes the most important variable in the creation of the obtained AdaBoost-CART tool. On the other hand, the system's temperature has the lowest importance on the tree tool development.

**Table 6.31:** Results of the created AdaBoost-CART tool vs. selected targets

$T$ (K)	$C_{SG}$ (mass%)	$P_{CO_2}$ (kPa)	$\alpha$ (mol CO <sub>2</sub> / mol SG solution)		RD %
			Experimental	Predicted	
313.15	5	3.24	0.5718	0.5718	0.00
	10	184.40	1.041	1.0480	0.67
	15	39.84	0.5975	0.6017	0.70
	20	648.60	0.9174	0.9174	0.00
	25	505.74	0.7942	0.7942	0.00
	30	97.80	0.5830	0.5830	0.00
323.15	5	396.09	1.3482	1.3482	0.00
	10	58.10	0.8330	0.8330	0.00
	15	18.38	0.2809	0.2809	0.00
	20	601.39	0.8352	0.8352	0.00
	25	404.89	0.6620	0.6620	0.00
	30	177.90	0.6240	0.6200	-0.64

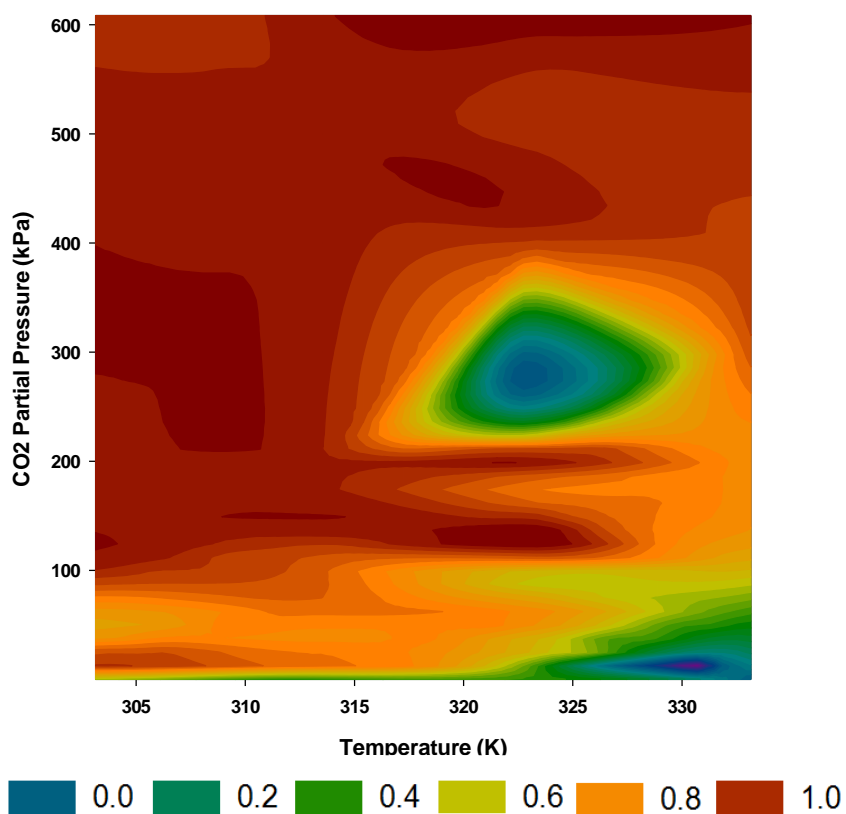


**Fig. 6.35:** AdaBoost-CART tool of CO<sub>2</sub> solubility in solution of SG (10 mass%)

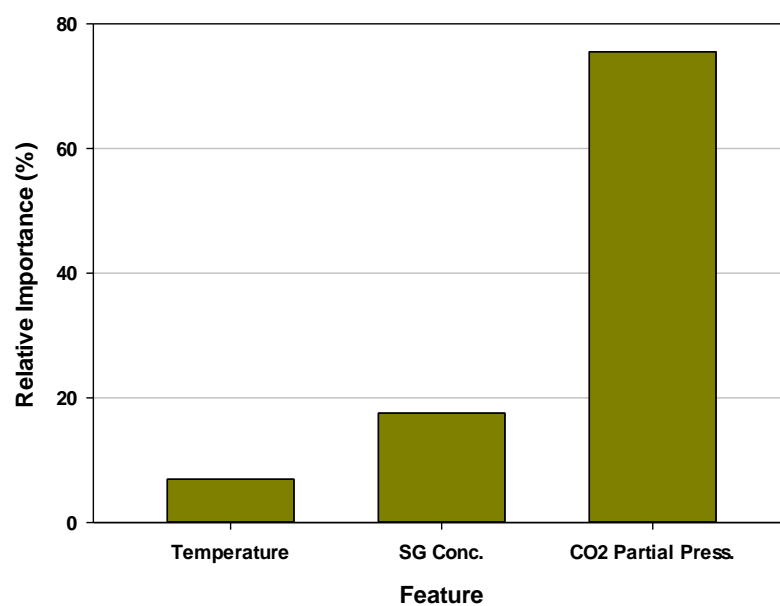


**Fig. 6.36:** Relative importance of the inputs in the creation of the tree model

## 6.8. CO<sub>2</sub>-Oil MMP

Error analysis results for the test and train data sets of the proposed ANFIS and AdaBoost-CART models are given in **Table 6.32**. Both the ANFIS and AdaBoost models provide satisfactory predictions. However, for both train and test datasets, the proposed AdaBoost-CART model gives better estimations than the developed ANFIS. For all the datasets, the obtained values of ARD% are positive. The range of ARD% is from 0.04 to 1.82. Hence, the presented ANFIS and AdaBoost-CART models slightly overestimate the value of CO<sub>2</sub>-reservoir oil MMP.

**Table 6.32:** Error analysis results of the created ANFIS and AdaBoost-CART tools

Model	Status	Parameter	Value
AdsBoost-CART	Train	$R^2$	0.9990
		ARD%	0.16
		AARD%	0.39
	Test	$R^2$	0.9986
		ARD%	0.42
		AARD%	0.42
ANFIS	Train	$R^2$	0.9976
		ARD%	0.04
		AARD%	1.07
	Test	$R^2$	0.9322
		ARD%	1.82
		AARD%	6.90

A comparison between the estimated values of CO<sub>2</sub>-oil MMP and corresponding experimental data is illustrated in **Fig. 6.37** and **6.38**. In **Fig. 6.37**, the cross plot that compares the outputs of the ANFIS and AdaBoost-based models versus experimental CO<sub>2</sub>-oil MMP is shown. In this

figure, the black line ( $45^\circ$  line) is the equality line, where the predictions of the models and the experimental targets are exactly the same. For both the presented ANFIS and AdaBoost-CART models, a tight cloud of points is located about the line of equality, which indicates an excellent association between the predictions of the models and the corresponding targets. For the presented predictive tools, **Fig. 6.38** demonstrates a graphical comparison of the experimental data against the outcomes of the models as point to point analysis. As can be seen, reported CO-oil MMP values are reproduced by the developed models with good accuracy.

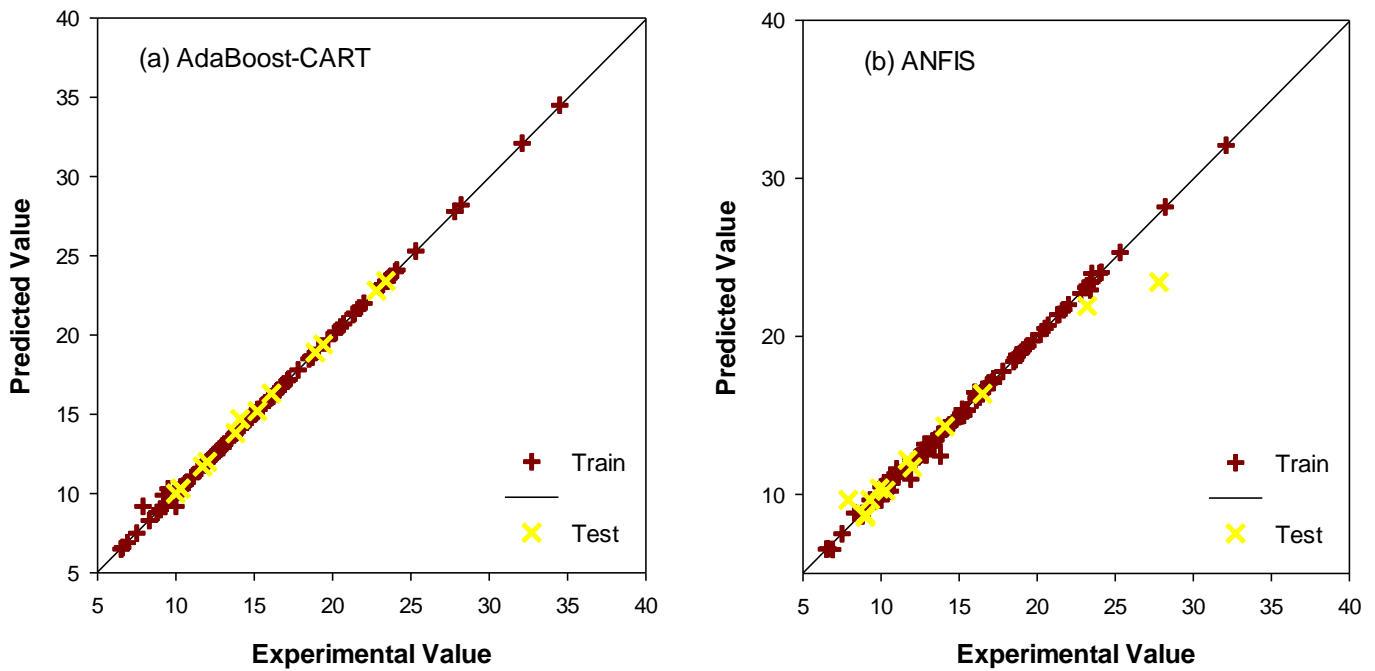


**Fig. 6.37:** Parity plot compares the predictions of the developed (a) AdaBoost-CART and (b) ANFIS models with corresponding experimental values

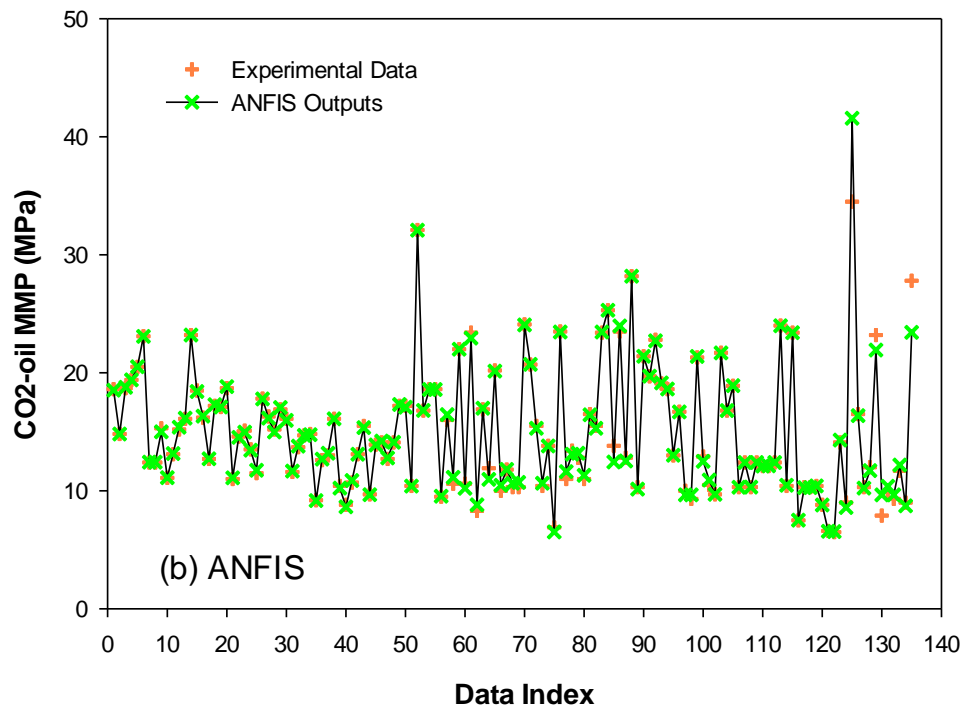
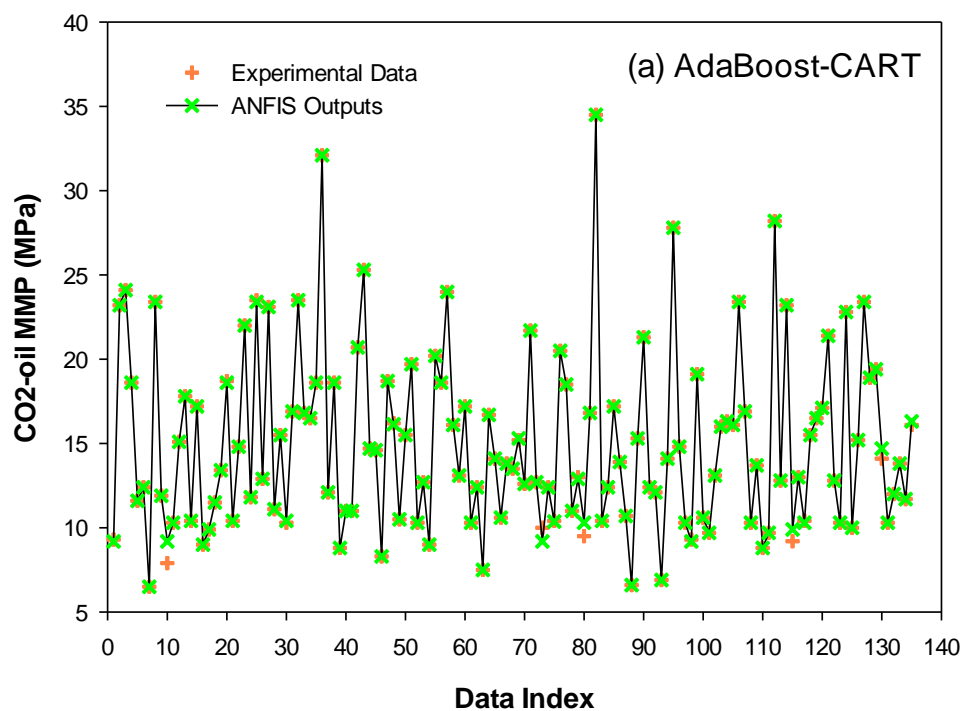


**Fig. 6.38:** Point to point comparison between the outputs of the (a) AdaBoost-CART and (b) ANFIS tools for CO<sub>2</sub>-oil MMP

The histograms of the obtained relative error in percent from the developed ANFIS and AdaBoost-CART models are shown in **Fig. 6.39**. As can be observed from the errors histogram of the AdaBoost-CART tool, most of the experimental data are reproduced with absolute relative errors (REs%) around zero. There is only one prediction with absolute RE% more than 15. In case of the ANFIS model, there are three estimations with absolute RE% more than 15. Further to this, **Fig. 6.39** shows that the proposed AdaBoost-CART model has better range for errors.

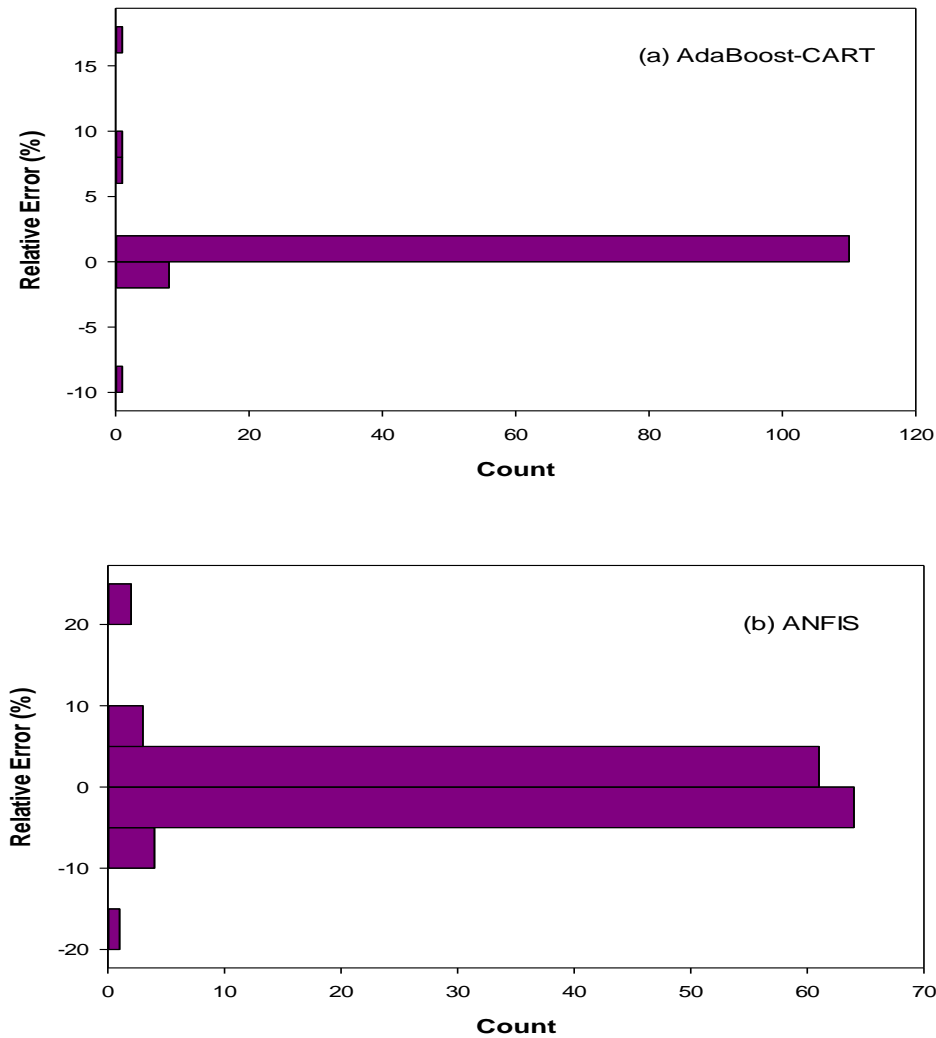


**Fig. 6.39:** Histogram of relative errors of the presented (a) AdaBoost-CART and (b) ANFIS models

The ANN model presented by Tatar et al. [243], LSSVM model developed by Shokrollahi et al. [30], GEP-based model proposed by Kamari et al. [244], and ANFIS-PSO model developed by Karkevandi-Talkhooncheh et al. [245] (for prediction of CO<sub>2</sub>-oil MMP) are selected as basis of comparison. It is proved that the aforesaid ANN, LSSVM, and GEP-based models provide better predictions as compared to the classical approaches including the correlations by Alston et al. [237], Emeral and Sarma [238] (corrected by Sebastian et al. [239]), Emeral and Sarma [238] (corrected by Alston et al. [237]), Yelling and Metcalfe [240] (corrected by Sebastian et al. [239]), and Yelling and Metcalfe [240] (corrected by Alston et al. [237]).

The calculated values of statistical variables ( $R^2$ , ARD%, and AARD%) for the developed ANFIS and AdaBoost-CART models as well as the ANN, LSSVM, GEP-based, and ANFIS-PSO models are summarized in **Table 6.33**. According to the tabulated results in **Table 6.33**, both the presented ANFIS and AdaBoost-CART models provide better predictions as compared to the previously published ANN, LSSVM, GEP-based, and ANFIS-PSO models. Moreover, no model can rival the built AdaBoost-CART model for accuracy. Among the existing intelligent models in the literature, the ANN model presented by Tatar et al. [243] provides better results than other models including LSSVM [195], GEP-based [244], and ANFIS-PSO [245] models.

The estimated pure CO<sub>2</sub>-reservoir oil MMP by the presented ANFIS and AdaBoost-CART models versus the corresponding reported data are given in **Table 6.34**. As can be seen from this table, most of the targets are predicted by the AdaBoost-CART model without error. The RE%s of the ANFIS model are between -15.83 and 20.58.



**Table 6.33:** Overall performance of the models for CO<sub>2</sub>-reservoir oil MMP prediction

Model	Parameter	Value
AdaBoost-CART	$R^2$	0.9990
	ARD%	0.19
	AARD%	0.40
ANFIS	$R^2$	0.9794
	ARD%	0.21
	AARD%	1.63
ANN [243]	$R^2$	0.9905
	ARD%	0.50
	AARD%	2.26
LSSVM [195]	$R^2$	0.9030
	ARD%	***
	AARD%	9.60
GEP [244]	$R^2$	0.8284
	ARD%	-1.65
	AARD%	10.47
ANFIS-PSO [245]	$R^2$	***
	ARD%	-1.36
	AARD%	7.53

**Table 6.34:** Predicted pure CO<sub>2</sub>-oil MMP by the presented ANFIS and AdaBoost-CART models

T (K)	MWC <sub>5+</sub>	Vol./Int.	CO <sub>2</sub> -reservoir oil MMP			Relative error (%)	
			Reported	ANFIS	AdaBoost-CART	ANFIS	AdaBoost-CART
305.35	187.77	0.74	6.9	6.5	6.9	-5.88	0.00
307.55	212.56	1.56	10.0	10.5	10.0	5.00	0.00
310.93	235.56	2.58	16.5	16.4	16.5	-0.61	0.00
312.59	199.70	1.28	13.8	12.4	13.8	-10.14	0.00
313.71	187.80	0.74	8.3	8.8	8.3	6.02	0.00
315.93	196.10	0.82	10.6	10.2	10.6	-3.77	0.00
315.93	204.10	0.81	10.3	10.6	10.3	2.91	0.00
315.93	204.10	0.82	10.3	10.7	10.4	3.88	0.97
315.95	204.10	0.81	10.4	10.6	10.4	1.92	0.00
322.04	187.27	1.50	11.0	11.6	11.0	5.45	0.00
322.05	205.10	0.55	10.6	11.1	10.6	4.72	0.00
327.55	168.39	1.01	11.8	11.8	11.8	0.00	0.00
327.59	185.83	0.14	9.5	9.5	10.3	0.00	8.42
327.59	171.20	0.93	11.0	11.3	11.0	2.73	0.00
327.59	235.56	0.15	12.8	12.5	12.8	-2.34	0.00
327.59	185.83	0.60	10.3	10.1	10.3	-1.94	0.00
327.59	185.83	0.67	10.3	10.2	10.3	-0.97	0.00
330.35	187.77	0.74	11.9	11.0	11.9	-7.56	0.00
330.35	182.60	9.16	13.8	13.8	13.8	0.00	0.00
330.93	202.61	0.42	11.7	12.2	11.7	4.27	0.00
332.15	205.00	0.48	12.8	13.2	12.8	3.12	0.00
338.71	187.27	1.50	13.4	13.1	13.4	-2.24	0.00
340.95	203.81	1.35	16.9	17.0	16.9	0.59	0.00
344.25	221.00	5.90	23.5	23.5	23.5	0.00	0.00
344.25	207.90	0.32	15.5	15.3	15.5	-1.29	0.00
344.26	207.90	0.32	15.5	15.3	15.5	-1.29	0.00
344.26	221.00	5.90	23.4	23.5	23.4	0.43	0.00
349.85	217.67	7.67	20.7	20.7	20.7	0.00	0.00
353.15	240.70	6.20	27.8	23.4	27.8	-15.83	0.00
354.25	198.40	0.59	16.0	16.5	16.0	3.13	0.00
355.35	261.64	0.33	21.4	21.4	21.4	0.00	0.00
358.71	247.80	2.43	34.5	41.6	34.5	20.58	0.00
375.37	205.00	5.21	28.2	28.2	28.2	0.00	0.00
377.55	153.96	1.77	22.0	22.0	22.0	0.00	0.00
383.15	180.60	0.91	20.2	20.1	20.2	-0.50	0.00
385.37	213.50	1.16	24.1	24.1	24.1	0.00	0.00
388.75	261.64	0.33	25.3	25.3	25.3	0.00	0.00
390.37	169.20	1.18	23.4	22.9	23.4	-2.14	0.00
391.45	171.10	1.20	23.5	24.0	23.4	2.13	-0.43

For a drive gas with the carbon dioxide, methane, and nitrogen concentrations equal to 91.75, 8.05, and 0.20 mol%, **Table 6.35** gives the experimental CO<sub>2</sub>-oil MMP and the predictions of the ANFIS and AdaBoost-CART models as well. The AdaBoost-CART model exactly regenerated all the reported targets except for the data with a temperature of 333.15 K, MWC<sub>5+</sub> of 165.59, and Vol./Int. of 4.62. For another impure derive gas (CO<sub>2</sub>=87.38, C<sub>1</sub>=7.67, C<sub>2</sub>-C<sub>5</sub>=4.67, and N<sub>2</sub>=0.19 mol%), the outputs of the developed predictive mathematical models are compared to the experimental data in **Table 6.36**. CO<sub>2</sub>-reservoir oil MMPs represented/predicted by the AdaBoost-CART model are in substantial agreement with the experimental/target values. ANFIS model estimates the target with RE%s between -2.27 and 1.87.

**Table 6.35:** Predicted CO<sub>2</sub>-oil MMP by the presented ANFIS and AdaBoost-CART models in comparison with the reported data for a drive gas with CO<sub>2</sub>=91.75, C<sub>1</sub>=8.05, and N<sub>2</sub>=0.20 mol% as composition

T (K)	MWC <sub>5+</sub>	Vol./Int.	CO <sub>2</sub> -reservoir oil MMP			Relative error (%)	
			Reported	ANFIS	AdaBoost-CART	ANFIS	AdaBoost-CART
333.15	165.59	4.62	16.2	16.3	16.1	0.62	-0.41
	138.50	0.51	11.0	11.1	11.0	0.91	0.00
	136.47	0.63	15.1	15.0	15.1	-0.66	0.00
353.15	165.59	4.62	17.2	17.3	17.2	0.58	0.00
	138.50	0.51	12.7	12.7	12.7	0.00	0.00
	136.47	0.63	17.1	17.1	17.1	0.00	0.00
373.15	165.59	4.62	18.5	18.4	18.5	-0.54	0.00
	138.50	0.51	14.6	14.5	14.6	-0.68	0.00
	136.47	0.63	18.7	18.8	18.7	0.53	0.00

**Table 3.36:** Predicted CO<sub>2</sub>-oil MMP by the presented ANFIS and AdaBoost-CART models in comparison with the reported data for a drive gas with CO<sub>2</sub>=87.38, C<sub>1</sub>=7.67, C<sub>2</sub>-C<sub>5</sub>=4.67, and N<sub>2</sub>=0.19 mol% as composition

T (K)	MWC <sub>5+</sub>	Vol./Int.	CO <sub>2</sub> -reservoir oil MMP			Relative error (%)	
			Reported	ANFIS	AdaBoost-CART	ANFIS	AdaBoost-CART
333.15	136.47	0.63	12.7	12.7	12.8	0.79	0.00
	138.50	0.51	8.8	8.8	8.6	-2.27	0.00
	165.59	4.62	12.0	12.0	11.7	-2.00	0.00
353.15	165.59	4.62	13.1	13.1	13.1	0.00	0.00
	138.50	0.51	9.7	9.7	9.7	0.00	0.00
	136.47	0.63	14.1	14.7	14.2	0.71	4.26
373.15	138.50	0.51	10.7	10.7	10.9	1.87	0.00
	136.47	0.63	15.5	15.5	15.3	-1.29	0.00
	165.59	4.62	13.9	13.9	13.9	0.00	0.00

## 7. Conclusions

In this research study, several machine learning and data mining approaches including LSSVM, CART/AdaBoost-CART ANN and ANFIS were utilized for modeling the equilibrium conditions of the following systems: hydrate+water/ice+salt(s)/alcohol(s), hydrate+IL, CO<sub>2</sub>+water+amine, CO<sub>2</sub>+IL, CO<sub>2</sub>+water+PZ, CO<sub>2</sub>+water+SG, and CO<sub>2</sub>-reservoir oil MMP. Further to the above, a semi-empirical/theoretical methodology was extended to the phase equilibria of hydrates of methane (C1) and carbon dioxide (CO<sub>2</sub>) in aqueous solutions of sugars. Moreover, phase equilibria of carbon dioxide hydrate in tomato and orange juices were modelled using thermodynamic and empirical approaches. Detained information were provided in **Appendix A**.

To perform the modeling using the aforementioned methodologies, extensive databases were gathered from the literature. The collected databanks cover wide ranges of dependent and independent parameters of the investigated systems. In brief, a total number of 3510, 384, 509, 5368, 597, 197, and 135 experimental data points were collected for gas hydrates in pure water or aqueous solution of salt(s) and/or alcohol(s), methane hydrate in the presence of IL, CO<sub>2</sub> loading capacity of solution of amines (MEA, DEA, or TEA), CO<sub>2</sub> loading capacity of ILs, CO<sub>2</sub> loading capacity of PZ solution, CO<sub>2</sub> loading capacity of SG solution, and CO<sub>2</sub>-oil MMP, respectively.

For each system, the employed databank was randomly divided into two sub-datasets namely test and training datasets. All the models were developed employing the training data. The allocated data points for the test were used to evaluate the capability of the developed model in predicting the target values. Statistical variables including AARD%, R<sup>2</sup> and ARD% were selected as the criteria for evaluating the accuracy of the created LSSVM, ANN, ANFIS, and CART/AdaBoost-CART models.

The summary of obtained results from error analysis for the developed LSSVM, ANN, ANFIS, and CART/AdaBoost-CART models to model/represent the equilibrium conditions of the investigated systems is as follows:

- A. Considering the error analysis results, all the developed LSSVM, ANN, ANFIS, and AdaBoost-CART models for methane, hydrogen sulfide, ethane, nitrogen, propane, i-butane, and gas mixture hydrates in pure water or aqueous solutions of thermodynamic additives/inhibitors provide satisfactory predictions when predicting the HDT. However, the most accurate estimations were obtained from the developed AdaBoost-CART models. All the proposed AdaBoost-CART models for hydrate systems of ethane, methane, propane, hydrogen sulfide, i-butane, gas mixture and nitrogen reproduced the experimental data with AARD% values equal to 0.03, 0.07, 0.05, 0.05, 0.04, 0.04, and 0.03, respectively. Furthermore, all the tree-based models indicated  $R^2$  value of greater than 0.99. Except for the developed ANN model for methane hydrate system, with ARD% value of -0.19, the ARD%s for all the predictive mathematical models are close to zero. Hence, the errors are almost equally distributed between positive and negative values.
- B. Error analysis indicated AARD% values equal to 0.08, 0.31, 0.10, and 0.15 for the presented LSSVM, ANFIS, CART, and ANN models to predict methane hydrate dissociation in the presence of IL. Hence, all the models provide satisfactory results. However, the LSSVM model gives the best predictions. Since the value of AARD% for test dataset of the CART tool is lower than that of the LSSVM model, it can be concluded that the performance of the CART model in estimation of the unseen data is better than the LSSVM model. For all the presented models, ARD% was close to zero.

- C. Comparing the results of the created LSSVM, ANFIS, AdaBoost-CART, and ANN models revealed that for all the amine systems including (H<sub>2</sub>O+TEA+CO<sub>2</sub>), (H<sub>2</sub>O+MEA+CO<sub>2</sub>) and (H<sub>2</sub>O+DEA+CO<sub>2</sub>) the proposed AdaBoost models reproduce the targets with lowest AARD% (0.51, 2.76, and 1.14, respectively) and highest R<sup>2</sup> (0.9987, 0.9977, and 0.9929, respectively). Among other developed models, i.e. ANFIS, ANN, and LSSVM models, the ANFIS models provided the best estimations. On the other hand, the weakest results were obtained using the ANN model.
- D. For CO<sub>2</sub>+IL system, a predictive tool was presented on the basis of CART methodology. The presented AdaBoost-CART model then was compared with the created LSSVM, RBF-ANN, ANFIS, and MLP-ANN models by Baghban et al. [460] in predicting the solubility of CO<sub>2</sub> in ILs. Error analysis indicated that the CART model that was proposed for the prediction of CO<sub>2</sub> loading capacity of various ILs has an AARD%=0.04 and a R<sup>2</sup>=1. On the other hand, the LSSVM, RBF-ANN, ANFIS, MLP-ANN models developed by Baghban et al. [460] have an overall AARD% of 17.17, 62.84, 34.28, and 25.25, respectively. Hence, employing the available intelligent models in the literature results in considerable deviation in calculation of CO<sub>2</sub> solubility in ILs. ARD%s equal to 13.60, 41.54, 7.36, and 12.80 reveals that these models overestimate the target values. In case of the proposed CART model, error analysis indicated an ARD% =0.00 which shows equally distributed deviations between positive and negative values.
- E. The AARD%s for the created ANFIS, AdaBoost-CART, LSSVM and AAN tools for equilibrium system of (CO<sub>2</sub>+water+PZ) were calculated to be 15.99, 0.93, 16.23 and

18.69, respectively. Moreover, the previously mentioned tools have an overall  $R^2$  of 0.8890, 0.9967, 0.8843 and 0.7849, respectively. Considering the statistical parameters as criteria for model assessment, it can be concluded that utilization of the ANN, LSSVM and ANFIS tools for prediction of CO<sub>2</sub> solubility in PZ results in drastic errors. Hence, it is recommended to use the AdaBoost-based model for calculating/estimating CO<sub>2</sub> loading capacity of PZ solution.

- F. Similar to the CO<sub>2</sub>+water+PZ system, the performance of the ANN, LSSVM, and ANFIS tools in modeling the equilibrium absorption of CO<sub>2</sub> in SG solution found to be unsatisfactory. This is due to the fact that the obtained AARD%s for the developed ANN, LSSVM, and ANFIS models are equal to 14.31, 13.36, and 15.42, respectively. As opposed to these methods, it was found that the AdaBoost-CART methodology can be successfully utilized for the application of interest. With an AARD% value of 0.89, the proposed tree-based model, i.e. AdaBoost-CART model, is a reliable and accurate predictive tool.
- G. With the aim of modeling CO<sub>2</sub>-reservoir oil MMP, Hybrid-ANFIS and AdaBoost-CART methodologies were employed. The performance of the developed tools in the predicting the MMP of CO<sub>2</sub>-oil, then, was compared to the ability of the previously published ANN, LSSVM, GEP-based, and PSO-ANFIS models in the estimation of CO<sub>2</sub>-oil MMP. With accordance to the error analysis results, both the Hybrid-ANFIS and AdaBoost-CART models developed in this study provide better estimations than the available models in the literature. The overall AARD% of the ANN model developed by Tatar et al. [243], LSSVM model developed by Shokrollahi et al. [195], GEP-based model developed by Kamari et al. [244], and PSO-ANFIS model developed



by et al. [245], are 2.26, 9.60, 10.47, and 7.53, respectively. The total AARD% for the Hybrid-ANFIS and AdaBoost-CART modes presented in the current work were 0.40 and 1.63, respectively, which indicate accuracy and robustness of the employed methods for CO<sub>2</sub>-oil MMP prediction. However, the proposed AdaBoost-CART model is more accurate and reliable for the estimation of CO<sub>2</sub>-oil MMP. This model indicated an  $R^2=0.9990$ .

The presented models in this study pave the way for a more accurate, reliable, and fast estimations of the targets.

## 8. Recommendations

Among the investigated methodologies for developing coordinated models to estimate/represent the target values, the CART/AdaBoost-CART method showed great performance and capability. Hence:

- 1- Considering the robustness of the CART/AdaBoost-CART technique in modeling the studied equilibrium systems, it is recommended to utilize the developed models on the basis of this technique in development of engineering software dealing with problems like PVT, CO<sub>2</sub> capture, and hydrate calculations.
- 2- In near future where adequate data is available, new models with wider application ranges can be developed.
- 3- It is recommended to assess the ability of CART/AdaBoost-CART method in modeling other processes in chemical, natural gas, and petroleum engineering.

## References

- [1] M.T. Hagan, H.B. Dcmuth, M. Beale, Neural Network Design, PWS Publishing Company, USA, 1996.
- [2] J.A. Freeman, D.M. Skapura, Neural Networks: Algorithms, Applications, and Programming Techniques, Addison-Wesley Publishing Company, USA, 1991.
- [3] A. Chouai, S. Laugier, D. Richon, Modeling of thermodynamic properties using neural networks: Application to refrigerants, Fluid Phase Equilibria, 199 (2002) 53-62.
- [4] L. Piazza, G. Scalabrin, P. Marchi, D. Richon, Enhancement of the extended corresponding states techniques for thermodynamic modeling. I. Pure fluids, International Journal of Refrigeration, 29 (2006) 1182-1194.
- [5] N.K. Bose, P. Liang, Neural Network Fundamentals with Graphs, Algorithms, and Applications, McGraw-Hill, USA, 1996.
- [6] S.S. Haykin, Neural Networks: A Comprehensive Foundation, Prentice Hall International, 1999.
- [7] C.G. Looney, Pattern Recognition Using Neural Networks, Theories and Algorithms for Engineers and Scientists, Oxford University Press, USA, 1997.
- [8] N.K. Kasabov, Foundations of Neural Networks, Fuzzy Systems, and Knowledge Engineering, MIT Press, 1996.
- [9] D.O. Hebb, The organization of behavior: A neuropsychological theory, John Wiley and Sons, Inc., USA, 1949.
- [10] W. McCulloch, W. Pitts, A logical calculus of the ideas immanent in nervous activity, The bulletin of mathematical biophysics, 5 (1943) 115-133.
- [11] B.G. Farley, W. Clark, Simulation of self-organizing systems by digital computer, IRE Transactions on Information Theory 4(1954) 76-84.
- [12] N. Rochester, J. Holland, L. Haibt, W. Duda, Tests on a cell assembly theory of the action of the brain, using a large digital computer, Information Theory, IRE Transactions on, 2 (1956) 80-93.
- [13] F. Rosenblatt, The Perceptron: A Probabilistic Model For Information Storage And Organization In The Brain, Psychological Review 65 (1958) 386-408.
- [14] M. Minsky, S. Papert, Perceptrons: An Introduction to Computational Geometry, MIT Press, Cambridge, MA, 1969.
- [15] D.E. Rumelhart, J.L. McClelland, S.D.P.R.G. University of California, Parallel Distributed Processing: Foundations, MIT Press, 1986.
- [16] K.L. Priddy, P.E. Keller, Artificial Neural Networks: An Introduction, Society of Photo Optical, 2005.
- [17] Advances in Neural Networks – ISNN 2012, Springer Berlin Heidelberg, 2012.
- [18] J.-S. Jang, ANFIS: adaptive-network-based fuzzy inference system, Systems, Man and Cybernetics, IEEE Transactions on, 23 (1993) 665-685.
- [19] E. Heidari, S. Ghoreishi, Prediction of supercritical extraction recovery of EGCG using hybrid of Adaptive Neuro-Fuzzy Inference System and mathematical model, The Journal of Supercritical Fluids, 82 (2013) 158-167.
- [20] E.H. Mamdani, S. Assilian, An experiment in linguistic synthesis with a fuzzy logic controller, International journal of man-machine studies, 7 (1975) 1-13.
- [21] T. Takagi, M. Sugeno, Fuzzy identification of systems and its applications to modeling and control, Systems, Man and Cybernetics, IEEE Transactions on, (1985) 116-132.

- [22] J.A.K. Suykens, J. Vandewalle, Least Squares Support Vector Machine Classifiers, *Neural Processing Letters*, 9 (1999) 293-300.
- [23] C. Cortes, V. Vapnik, Support-vector networks, *Machine Learning*, 20 (1995) 273-297.
- [24] V. Vapnik, *The Nature of Statistical Learning Theory*, Springer, 2000.
- [25] A. Baylar, D. Hanbay, M. Batan, Application of least square support vector machines in the prediction of aeration performance of plunging overfall jets from weirs, *Expert Systems with Applications*, 36 (2009) 8368-8374.
- [26] S. Rafiee-Taghanaki, M. Arabloo, A. Chamkalani, M. Amani, M.H. Zargari, M.R. Adelzadeh, Implementation of SVM framework to estimate PVT properties of reservoir oil, *Fluid Phase Equilibria*, 346 (2013) 25-32.
- [27] E.D. Übeyli, Least squares support vector machine employing model-based methods coefficients for analysis of EEG signals, *Expert Systems with Applications*, 37 (2010) 233-239.
- [28] S.R. Amendolia, G. Cossu, M.L. Ganadu, B. Golosio, G.L. Masala, G.M. Mura, A comparative study of K-Nearest Neighbour, Support Vector Machine and Multi-Layer Perceptron for Thalassemia screening, *Chemometrics and Intelligent Laboratory Systems*, 69 (2003) 13-20.
- [29] T.-S. Chen, J. Chen, Y.-C. Lin, Y.-C. Tsai, Y.-H. Kao, K. Wu, A Novel Knowledge Protection Technique Base on Support Vector Machine Model for Anti-classification, in: M. Zhu (Ed.) *Electrical Engineering and Control*, Springer Berlin Heidelberg, 2011, pp. 517-524.
- [30] A. Shokrollahi, M. Arabloo, F. Gharagheizi, A.H. Mohammadi, Intelligent model for prediction of CO<sub>2</sub> – Reservoir oil minimum miscibility pressure, *Fuel*, 112 (2013) 375-384.
- [31] J.R. Quinlan, *Induction of decision trees*, *Machine Learning*, 1 (1986) 81-106.
- [32] R. Weber, Fuzzy ID3: a class of methods for automatic knowledge acquisition, in: *proceedings of the 2nd International Conference on Fuzzy Logic and Neural Networks*, Iizuka, Japan, 1992, pp. 265-268.
- [33] M. Umamo, H. Okamoto, I. Hatono, H. Tamura, F. Kawachi, S. Umedz, J. Kinoshita, Fuzzy Decision Trees by Fuzzy ID3 algorithm and its Applications to Diagnosis System, in: *proceedings of the third IEEE Conference on Fuzzy Systems*, Orlando, 1994, pp. 2113-2118.
- [34] L. Breiman, J. Friedman, C.J. Stone, R.A. Olshen, *Classification and Regression Trees*, Taylor & Francis, 1984.
- [35] M.M. Ghiasi, A.H. Mohammadi, Determination of Methane-Hydrate Phase Equilibrium in the Presence of Electrolytes or Organic Inhibitors by using a Semi-Theoretical Framework, *Energy Technology*, 1 (2013) 519-529.
- [36] E.D. Sloan, *Clathrate Hydrates of Natural Gases*, 2nd ed., Marcel Dekker, Inc., USA, 1998.
- [37] J. Carroll, *Natural Gas Hydrate, A Guide for Engineers*, 2nd ed., Gulf Professional Publishing, USA, 2009.
- [38] H. Najibi, A. Chapoy, H. Haghighi, B. Tohidi, Experimental determination and prediction of methane hydrate stability in alcohols and electrolyte solutions, *Fluid Phase Equilibria*, 275 (2009) 127-131.
- [39] A. Bahadori, H.B. Vuthaluru, S. Mokhtab, M.O. Tade, Predicting hydrate forming pressure of pure alkanes in the presence of inhibitors, *Journal of Natural Gas Chemistry*, 17 (2008) 249-255.
- [40] W.G. Knox, M. Hess, G.E. Jones, H.B. Smith, The Hydrate Process, *Chemical Engineering Progress*, 57 (1961) 66-71.
- [41] J. Javanmardi, M. Moshfeghian, Energy consumption and economic evaluation of water desalination by hydrate phenomenon, *Applied Thermal Engineering*, 23 (2003) 845-857.

- [42] Y.H. Jeon, N.J. Kim, W.G. Chun, S.H. Lim, C.B. Kim, B.K. Hur, A study of the kinetics characteristics of natural gas hydrate, *Journal of Industrial and Engineering Chemistry*, 12 (2006) 733-738.
- [43] B. Zhang, Q. Wu, Thermodynamic Promotion of Tetrahydrofuran on Methane Separation from Low-Concentration Coal Mine Methane Based on Hydrate, *Energy & Fuels*, 24 (2010) 2530-2535.
- [44] S. Fan, Y. Zhang, G. Tian, D. Liang, D. Li, Natural Gas Hydrate Dissociation by Presence of Ethylene Glycol, *Energy & Fuels*, 20 (2005) 324-326.
- [45] P. Englezos, Clathrate hydrates, *Industrial & Engineering Chemistry Research*, 32 (1993) 1251-1274.
- [46] P. Linga, R. Kumar, P. Englezos, The clathrate hydrate process for post and pre-combustion capture of carbon dioxide, *Journal of Hazardous Materials*, 149 (2007) 625-629.
- [47] H.N. Duc, F. Chauvy, J.M. Herri, CO<sub>2</sub> capture by hydrate crystallization – A potential solution for gas emission of steelmaking industry, *Energy Conversion and Management*, 48 (2007) 1313-1322.
- [48] W.I. Wilcox, D.B. Carson, D.L. Katz, Natural Gas Hydrates, *Industrial & Engineering Chemistry*, 33 (1941) 662-665.
- [49] C.H. Unruh, D.L. Katz, Gas Hydrates of Carbon Dioxide-Methane Mixture, *Trans AIME*, 186 (1949) 83-86.
- [50] L.J. Noaker, D.L. Katz, Gas Hydrates of Hydrogen Sulphide-Methane Mixtures, *Trans AIME*, 201 (1954) 237-239.
- [51] J.M. Campbell, *Gas Conditioning and Processing*, 7th ed., Campbell Petroleum Series, USA, 1992.
- [52] Y.F. Makogon, *Hydrates of Natural gas*, Penn Well Publishing, USA, 1981.
- [53] G.D. Holder, S.P. Zetts, N. Pradham, Phase behavior in systems containing clathrate hydrates, *Reviews in Chemical Engineering*, 5 (1988) 1-70.
- [54] D.L. Katz, Prediction of conditions for hydrate formation in natural gases, *Trans AIME*, 160 (1945) 140-149.
- [55] Y. Seo, H. Lee, A New Hydrate-Based Recovery Process for Removing Chlorinated Hydrocarbons from Aqueous Solutions, *Environmental Science & Technology*, 35 (2001) 3386-3390.
- [56] C. Baillie, E. Wichert, Chart gives hydrate formation temperature for natural gas, *Oil and Gas Journal*, 85 (1987) 37-39.
- [57] M.M. Ghiasi, A. Bahadori, S. Zendehboudi, Estimation of triethylene glycol (TEG) purity in natural gas dehydration units using fuzzy neural network, *Journal of Natural Gas Science and Engineering*, 17 (2014) 26-32.
- [58] J.H. van der Waals, J.C. Platteeuw, Clathrate solutions, *Advances in Chemical Physics*, 2 (1959) 1-57.
- [59] W.R. Parrish, J.M. Prausnitz, Dissociation pressures of gas hydrates formed by gas mixtures, *Industrial & Engineering Chemistry Process Design and Development*, 11 (1972) 26-34.
- [60] I. Nagata, R. Kobayashi, Predictions of dissociation pressures of mixed gas hydrates from data for hydrates of pure gases with water, *Industrial and Engineering Chemistry Fundamentals*, 5 (1966) 466-469.
- [61] H.J. Ng, D.B. Robinson, The measurement and prediction of hydrate formation in liquid hydrocarbon–water system, *Industrial and Engineering Chemistry Fundamentals*, 15 (1976) 293-298.

- [62] V.T. John, K.D. Papadopoulos, G.D. Holder, A generalized model for predicting equilibrium conditions for gas hydrates, *AIChE Journal*, 31 (1985) 252-259.
- [63] P.B. Dharmawardhana, W.R. Parrish, E.D. Sloan, Experimental thermodynamic parameters for the prediction of natural gas hydrate dissociation conditions, *Industrial and Engineering Chemistry Fundamentals*, 19 (1980) 410-414.
- [64] H. Tavasoli, F. Feyzi, M.R. Dehghani, F. Alavi, Prediction of gas hydrate formation condition in the presence of thermodynamic inhibitors with the Elliott–Suresh–Donohue Equation of State, *Journal of Petroleum Science and Engineering*, 77 (2011) 93-103.
- [65] K. Nasrifar, M. Moshfeghian, A model for prediction of gas hydrate formation conditions in aqueous solutions containing electrolytes and/or alcohol, *Journal of Chemical Thermodynamics*, 33 (2001) 999-1014.
- [66] M. Kharrat, D. Dalmazzone, Experimental determination of stability conditions of methane hydrate in aqueous calcium chloride solutions using high pressure differential scanning calorimetry, *Journal of Chemical Thermodynamics*, 35 (2003) 1489-1505.
- [67] R. Masoudi, B. Tohidi, R. Anderson, R.W. Burgass, J. Yang, Experimental measurement and thermodynamic modelling of clathrate hydrate equilibria and salt solubility in aqueous ethylene glycol and electrolyte solutions, *Fluid Phase Equilibria*, 219 (2004) 157-163.
- [68] R. Masoudi, B. Tohidi, A. Danesh, A.C. Todd, A new approach in modelling phase equilibria and gas solubility in electrolyte solutions and its applications to gas hydrates, *Fluid Phase Equilibria*, 215 (2004) 163-174.
- [69] J. Javanmardi, M. Moshfeghian, A new approach for prediction of gas hydrate formation conditions in aqueous electrolyte solutions, *Fluid Phase Equilibria*, 168 (2000) 135-148.
- [70] B. ZareNezhad, A. Aminian, Accurate prediction of sour gas hydrate equilibrium dissociation conditions by using an adaptive neuro fuzzy inference system, *Energy Conversion and Management*, 57 (2012) 143-147.
- [71] A. Elgibaly, A. Elkamel, A new correlation for predicting hydrate formation conditions for various gas mixtures and inhibitors, *Fluid Phase Equilibria*, 152 (1998) 23-42.
- [72] G. Zahedi, Z. Karami, H. Yaghoobi, Prediction of hydrate formation temperature by both statistical models and artificial neural network approaches, *Energy Conversion and Management*, 50 (2009).
- [73] A. Eslamimanesh, F. Gharagheizi, M. Illbeigi, A.H. Mohammadia, A. Fazlali, D. Richona, Phase equilibrium modeling of clathrate hydrates of methane, carbon dioxide, nitrogen, and hydrogen + water soluble organic promoters using Support Vector Machine algorithm, *Fluid Phase Equilibria*, 316 (2012) 34-45.
- [74] N. Zeinali, M. Saber, A. Ameri, Comparative Analysis of Hydrate Formation Pressure Applying Cubic Equations of State (EoS), Artificial Neural Network (ANN) and Adaptive Neuro-Fuzzy Inference System (ANFIS), *International Journal of Thermodynamics*, 15 (2012) 91-101.
- [75] H. Jiang, H. Adidharma, Thermodynamic modeling of aqueous ionic liquid solutions and prediction of methane hydrate dissociation conditions in the presence of ionic liquid, *Chemical Engineering Science*, 102 (2013) 24-31.
- [76] D.-Y. Peng, D.B. Robinson, A New Two-Constant Equation of State, *Industrial & Engineering Chemistry Fundamentals*, 15 (1976) 59-64.
- [77] L. Keshavarz, J. Javanmardi, A. Eslamimanesh, A.H. Mohammadi, Experimental measurement and thermodynamic modeling of methane hydrate dissociation conditions in the presence of aqueous solution of ionic liquid, *Fluid Phase Equilibria*, 354 (2013) 312-318.
- [78] K. Tumba, P. Reddy, P. Naidoo, D. Ramjugernath, A. Eslamimanesh, A.H. Mohammadi, D. Richon, Phase Equilibria of Methane and Carbon Dioxide Clathrate Hydrates in the Presence of

Aqueous Solutions of Tributylmethylphosphonium Methylsulfate Ionic Liquid, *Journal of Chemical & Engineering Data*, 56 (2011) 3620-3629.

[79] B. Partoon, N.M.S. Wong, K.M. Sabil, K. Nasrifar, M.R. Ahmad, A study on thermodynamics effect of [EMIM]-Cl and [OH-C2MIM]-Cl on methane hydrate equilibrium line, *Fluid Phase Equilibria*, 337 (2013) 26-31.

[80] R.N. Maddox, M. Moshfeghian, C.H. Tu, A. Shariat, A.J. Flying, Predicting Hydrate Temperature at High Inhibitor Concentration, in: *Proceeding of Laurence Reid Gas Conditioning Conference*, 1991.

[81] M. Zare, A. Haghtalab, A.N. Ahmadi, K. Nazari, Experiment and thermodynamic modeling of methane hydrate equilibria in the presence of aqueous imidazolium-based ionic liquid solutions using electrolyte cubic square well equation of state, *Fluid Phase Equilibria*, 341 (2013) 61-69.

[82] K. Nazari, A.N. Ahmadi, M.R. Moradi, V. Sahraei, V. Taghikhani, C.A. Ghobti, thermodynamic study of methane hydrate formation in the presence of [BMIM][BF<sub>4</sub>] and [BMIM][MS] ionic liquids, in: *7th International Conference on Gas Hydrates (ICGH 2011)*, Edinburgh, Scotland, U.K., 2011.

[83] A. Rasoolzadeh, J. Javanmardi, A. Eslamimanesh, A.H. Mohammadi, Experimental study and modeling of methane hydrate formation induction time in the presence of ionic liquids, *Journal of Molecular Liquids*, 221 (2016) 149-155.

[84] G.-J. Chen, T.-M. Guo, Thermodynamic modeling of hydrate formation based on new concepts, *Fluid Phase Equilibria*, 122 (1996) 43-65.

[85] Z. Liao, X. Guo, Y. Zhao, Y. Wang, Q. Sun, A. Liu, C. Sun, G. Chen, Experimental and Modeling Study on Phase Equilibria of Semiclathrate Hydrates of Tetra-n-butyl Ammonium Bromide + CH<sub>4</sub>, CO<sub>2</sub>, N<sub>2</sub>, or Gas Mixtures, *Industrial & Engineering Chemistry Research*, 52 (2013) 18440-18446.

[86] L.-l. Shi, D.-q. Liang, Thermodynamic model of phase equilibria of tetrabutyl ammonium halide (fluoride, chloride, or bromide) plus methane or carbon dioxide semiclathrate hydrates, *Fluid Phase Equilibria*, 386 (2015) 149-154.

[87] J. Verrett, J.-S. Renault-Crispo, P. Servio, Phase equilibria, solubility and modeling study of CO<sub>2</sub>/CH<sub>4</sub>+tetra-n-butylammonium bromide aqueous semi-clathrate systems, *Fluid Phase Equilibria*, 388 (2015) 160-168.

[88] A. Baghban, M.A. Ahmadi, B. Pouladi, B. Amanna, Phase equilibrium modeling of semi-clathrate hydrates of seven commonly gases in the presence of TBAB ionic liquid promoter based on a low parameter connectionist technique, *The Journal of Supercritical Fluids*, 101 (2015) 184-192.

[89] A. Eslamimanesh, A.H. Mohammadi, D. Richon, Thermodynamic modeling of phase equilibria of semi-clathrate hydrates of CO<sub>2</sub>, CH<sub>4</sub>, or N<sub>2</sub>+tetra-n-butylammonium bromide aqueous solution, *Chemical Engineering Science*, 81 (2012) 319-328.

[90] P. Paricaud, Modeling the Dissociation Conditions of Salt Hydrates and Gas Semiclathrate Hydrates: Application to Lithium Bromide, Hydrogen Iodide, and Tetra-n-butylammonium Bromide + Carbon Dioxide Systems, *The Journal of Physical Chemistry B*, 115 (2011) 288-299.

[91] International energy outlook 2013, in, U.S. Energy Information Administration, Washington, DC 20585, 2013.

[92] U.S.D.o. Energy, <http://energy.gov/science-innovation/energy-sources>, in.

[93] The Outlook for Energy: A View to 2040, in, ExxonMobil Corp., <http://exxonmobil.com/energyoutlook>, 2014.

[94] A.J. Kidnay, W.R. Parrish, D.G. McCartney, *Fundamentals of Natural Gas Processing*, Taylor & Francis Group, Boca Raton, 2011.

- [95] L.O. Nord, R. Anantharaman, O. Bolland, Design and off-design analyses of a pre-combustion CO<sub>2</sub> capture process in a natural gas combined cycle power plant, *International Journal of Greenhouse Gas Control*, 3 (2009) 385-392.
- [96] J.G. Speight, *Natural Gas: A Basic Handbook*, Gulf Publishing Company, Houston, USA, 2007.
- [97] K. Schoots, R. Rivera-Tinoco, G. Verbong, B. van der Zwaan, Historical variation in the capital costs of natural gas, carbon dioxide and hydrogen pipelines and implications for future infrastructure, *International Journal of Greenhouse Gas Control*, 5 (2011) 1614-1623.
- [98] Y. Xiao, B.T. Low, S.S. Hosseini, T.S. Chung, D.R. Paul, The strategies of molecular architecture and modification of polyimide-based membranes for CO<sub>2</sub> removal from natural gas—A review, *Progress in Polymer Science*, 34 (2009) 561-580.
- [99] N. Armaroli, V. Balzani, *Energy for a Sustainable World From the Oil Age to a Sun-Powered Future*, WILEY-VCH Verlag GmbH & Co. , KGaA, Weinheim, 2011.
- [100] H.P. van Kemenade, J.J.H. Brouwers, S.J.M. de Rijke, Comparing the Volume and Energy Consumption of Sour-Gas Cleaning by Condensed Rotational Separation and Amine Treatments, *Energy Technology*, 1 (2013) 392-394.
- [101] F. Lallemand, G. Perdu, C. Maretto, C. Weiss, J. Magne-Dirsch, A.-C. Lucquin, Solutions for the treatment of highly sour gases, in: *Gas*, 2012, pp. 1-14.
- [102] J. Castel, D. Gadelle, P. Hagyard, M. Ould-Bamba, LNG and GTL drive 50 years of technology evolution in the gas industry, in: *Hydrocarbon Processing*, July 2012.
- [103] A. Chapoy, Phase behaviour in water/hydrocarbon mixtures involved in gas production systems, in, *Ecole Des Mines De Paris*, France, 2004.
- [104] *Ocean Acidification: A National Strategy to Meet the Challenges of a Changing Ocean*, National Research Council, The National Academies Press, Washington, DC, 2010.
- [105] Chapter 8. Microscale Gas Chemistry: Hydrogen Sulfide Information, in, Web Page of Creighton University, [http://mattson.creighton.edu/H2S/H2S\\_Info.html](http://mattson.creighton.edu/H2S/H2S_Info.html).
- [106] B.D. Bhide, A. Voskericyan, S.A. Stern, Hybrid processes for the removal of acid gases from natural gas, *Journal of Membrane Science*, 140 (1998) 27-49.
- [107] M.M. Ghiasi, A.H. Mohammadi, Development of intelligent models for determination of required monoethanolamine (MEA) circulation rate in amine plants, *Journal of Separation Science*, Under Review.
- [108] R.N. Maddox, *Gas and Liquid Sweetening*, Campbell Petroleum Series, Norman, Oklahoma, 1994.
- [109] F.S. Manning, R.E. Thompson, *Oilfield Processing of Petroleum: Natural gas*, PennWell Books, 1991.
- [110] P. Oyarzún, F. Arancibia, C. Canales, G.E. Aroca, Biofiltration of high concentration of hydrogen sulphide using *Thiobacillus thioparus*, *Process Biochemistry*, 39 (2003) 165-170.
- [111] A.K. Datta, P.K. Sen, Optimization of membrane unit for removing carbon dioxide from natural gas, *Journal of Membrane Science*, 283 (2006) 291-300.
- [112] M. Mirfendereski, M. Sadrzadeh, T. Mohammadi, Effect of synthesis parameters on single gas permeation through T-type zeolite membranes, *International Journal of Greenhouse Gas Control*, 2 (2008) 531-538.
- [113] P. Shao, M.M. Dal-Cin, M.D. Guiver, A. Kumar, Simulation of membrane-based CO<sub>2</sub> capture in a coal-fired power plant, *Journal of Membrane Science*, 427 (2013) 451-459.
- [114] J. Albo, P. Luis, A. Irabien, Carbon Dioxide Capture from Flue Gases Using a Cross-Flow Membrane Contactor and the Ionic Liquid 1-Ethyl-3-methylimidazolium Ethylsulfate, *Industrial & Engineering Chemistry Research*, 49 (2010) 11045-11051.

- [115] A.H. Younger, Natural Gas Processing Principles and Technology-Part I, University of Calgary, Calgary, Alberta, 2004.
- [116] S. Mokhatab, W.A. Poe, J.G. Speight, Handbook of Natural Gas Transmission and Processing, Gulf Professional Publishing, USA, 2006.
- [117] R.W. Baker, K. Lokhandwala, Natural Gas Processing with Membranes: An Overview, Industrial & Engineering Chemistry Research, 47 (2008) 2109-2121.
- [118] B. Gue, A. Ghalambor, Natural Gas Engineering Handbook, Gulf Professional Publishing, USA, 2005.
- [119] GPSA, 12th ed., Gas Processors Suppliers Association, USA, 2004.
- [120] D.B. Bennion, F.B. Thomas, B.E. Schulmeister, D. Imer, E. Shtepani, L. Becker, The Phase Behavior of Acid Disposal Gases and the Potential Adverse Impact on Injection or Disposal Operations, in: Canadian International Petroleum Conference, Petroleum Society of Canada, Calgary, Alberta, 2002.
- [121] D.B. Bennion, F.B. Thomas, B.E. Schulmeister, D. Imer, E. Shtepani, L. Becker, The Phase Behaviour of Acid Disposal Gases and the Potential Adverse Impact on Injection or Disposal Operations, Journal of Canadian Petroleum Technology, 43 (2004).
- [122] M. Pooladi-Darvish, H. Hong, R. Stocker, B. Bennion, S. Theys, S. Bachu, Chromatographic Partitioning of H<sub>2</sub>S and CO<sub>2</sub> in Acid Gas Disposal, in: Canadian International Petroleum Conference, Petroleum Society of Canada, Calgary, Alberta, 2008.
- [123] J.J. Carroll, P.J. Griffin, S.F. Alkafeef, Review and Outlook of Subsurface Acid Gas Disposal, in: SPE Middle East Oil and Gas Show and Conference, Society of Petroleum Engineers, Bahrain, Bahrain, 2009.
- [124] K.T. Ho, J. McMullen, P. Boyle, O. Rojek, M. Forgo, T. Beatty, H.L. Longworth, Subsurface Acid Gas Disposal Scheme in Wayne-Rosedale, Alberta, in: SPE Health, Safety and Environment in Oil and Gas Exploration and Production Conference, 1996 Copyright 1996, Society of Petroleum Engineers, Inc., New Orleans, Louisiana, 1996.
- [125] R.A. Wall, D.A. Kenefake, Acid Gas Injection Facilities for Gas Disposal at the Shute Creek Treating Facility, in: International Petroleum Technology Conference, International Petroleum Technology Conference, Doha, Qatar, 2005.
- [126] M. Zirrahi, R. Azin, H. Hassanzadeh, M. Moshfeghian, Prediction of water content of sour and acid gases, Fluid Phase Equilibria, 299 (2010) 171-179.
- [127] M. Javaheri, K. Jessen, Integration of counter-current relative permeability in the simulation of CO<sub>2</sub> injection into saline aquifers, International Journal of Greenhouse Gas Control, 5 (2011) 1272-1283.
- [128] X. Wang, M. Economides, Advanced Natural Gas Engineering, Gulf Publishing Company, Houston, Texas, 2009.
- [129] G. Astarita, D.W. Savage, A. Bisio, Gas treating with chemical solvents, John Wiley, New York, 1983.
- [130] A. Kohl, R. Nielsen, Gas Purification, Gulf Publishing Company, Gulf Publishing Company, 1997.
- [131] W. Echt, Hybrid Systems: Combining Technologies Leads to More Efficient Gas Conditioning, in: Laurance Reid Gas Conditioning Conference, Norman, Oklahoma, 2002, pp. 1-18.
- [132] L. Peters, A. Hussain, M. Follmann, T. Melin, M.B. Hägg, CO<sub>2</sub> removal from natural gas by employing amine absorption and membrane technology—A technical and economical analysis, Chemical Engineering Journal, 172 (2011) 952-960.



- [133] R.L. McKee, M.K. Changela, G.J. Reading, CO<sub>2</sub> removal: membrane plus amine, *Hydrocarbon Processing*, 70 (1991) 63-65.
- [134] M.T. Ho, Techno-economic modelling of CO<sub>2</sub> capture systems for Australian industrial sources, in: *School of Chemical Sciences and Engineering, The University of New South Wales Sydney, Australia*, 2007.
- [135] M. Golombok, R. Schoonebeek, Purification of Natural Gas by forming H<sub>2</sub>S Hydrates, *Energy Technology*, 1 (2013) 457-462.
- [136] T.E. Rufford, S. Smart, G.C.Y. Watson, B.F. Graham, J. Boxall, J.C. Diniz da Costa, E.F. May, The removal of CO<sub>2</sub> and N<sub>2</sub> from natural gas: A review of conventional and emerging process technologies, *Journal of Petroleum Science and Engineering*, 94–95 (2012) 123-154.
- [137] P.J. Herslund, K. Thomsen, J. Abildskov, N. von Solms, Phase equilibrium modeling of gas hydrate systems for CO<sub>2</sub> capture, *The Journal of Chemical Thermodynamics*, 48 (2012) 13-27.
- [138] M. Ricaurte, J.-P. Torré, D. Broseta, J. Diaz, C. Dicharry, CO<sub>2</sub> removal from a CO<sub>2</sub>-CH<sub>4</sub> mixture by hydrate formation: evaluation of additives and operation conditions, in: *Proceedings of the 7th International Conference on Gas Hydrates, Edinburgh, Scotland, United Kingdom*, 2011.
- [139] N. Azmi, M. Hilmi, K.M. Sabil, Removal of high CO<sub>2</sub> content in natural gas by formation of gas hydrates as a potential solution for CO<sub>2</sub> gas emission, in: *International Conference on Environment 2010, Penang, Malaysia*, 2010.
- [140] J. Liu, S. Fan, X. Lang, Y. Wang, CO<sub>2</sub> removal from natural gas by hydrate formation, in: *Second International Conference on Mechanic Automation and Control Engineering (MACE)*, Hohhot, 2011.
- [141] [http://www.esru.strath.ac.uk/EandE/Web\\_sites/02-03/carbon\\_sequestration/Carbon%20Sequestration-426.htm](http://www.esru.strath.ac.uk/EandE/Web_sites/02-03/carbon_sequestration/Carbon%20Sequestration-426.htm), in.
- [142] B. Burr, L. Lyddon, A Comparison of Physical Solvents for Acid Gas Removal, in: *87th Annual GPA Convention, Grapevine, Texas*, 2008.
- [143] <http://www.jmcatalysts.com/ptd/site.asp?siteid=498&pageid=832>, in.
- [144] <http://www.offshore-technology.com/projects/natuna/>.
- [145] J.C.M. Pires, F.G. Martins, M.C.M. Alvim-Ferraz, M. Simões, Recent developments on carbon capture and storage: An overview, *Chemical Engineering Research and Design*, 89 (2011) 1446-1460.
- [146] P.S. Northrop, J.A. Valencia, The CFZ<sup>TM</sup> process: A cryogenic method for handling high-CO<sub>2</sub> and H<sub>2</sub>S gas reserves and facilitating geosequestration of CO<sub>2</sub> and acid gases, *Energy Procedia*, 1 (2009) 171-177.
- [147] H. Strathmann, Membrane separation processes, *Journal of Membrane Science*, 9 (1981) 121-189.
- [148] S. Alexander Stern, Polymers for gas separations: the next decade, *Journal of Membrane Science*, 94 (1994) 1-65.
- [149] S.L. Matson, J. Lopez, J.A. Quinn, Separation of gases with synthetic membranes, *Chemical Engineering Science*, 38 (1983) 503-524.
- [150] R.E. Kesting, A.K. Fritzsche, *Polymeric gas separation membranes*, Wiley, 1993.
- [151] Y. Yampolskii, *Polymeric Gas Separation Membranes*, *Macromolecules*, 45 (2012) 3298-3311.
- [152] H.K. Lonsdale, The growth of membrane technology, *Journal of Membrane Science*, 10 (1982) 81-181.
- [153] S. Sridhar, B. Smitha, T.M. Aminabhavi, Separation of Carbon Dioxide from Natural Gas Mixtures through Polymeric Membranes—A Review, *Separation & Purification Reviews*, 36 (2007) 113-174.

- [154] R.W. Baker, *Membrane Technology and Applications*, 2nd ed., John Wiley & Sons Ltd, UK, 2004.
- [155] J.G. Speight, *Gas processing: environmental aspects and methods*, Butterworth-Heinemann, 1993.
- [156] N. Korens, D.R. Simbeck, D.J. Wilhelm, *Process Screening Analysis of Alternative Gas Treating and Sulfur Removal for Gasification*, in, Revised Final Report, U.S. Department of Energy by SFA Pacific, Inc., 2002.
- [157] M. Rameshni, *State-of-the-art in gas treating*, in, Worley Parsons CA, USA, 2000.
- [158] S. Mudhasakul, H.-m. Ku, P.L. Douglas, A simulation model of a CO<sub>2</sub> absorption process with methyldiethanolamine solvent and piperazine as an activator, *International Journal of Greenhouse Gas Control*, 15 (2013) 134-141.
- [159] M. Safari, A. Ghanizadeh, M.M. Montazer-Rahmati, Optimization of membrane-based CO<sub>2</sub>-removal from natural gas using simple models considering both pressure and temperature effects, *International Journal of Greenhouse Gas Control*, 3 (2009) 3-10.
- [160] J.K. Adewole, A.L. Ahmad, S. Ismail, C.P. Leo, Current challenges in membrane separation of CO<sub>2</sub> from natural gas: A review, *International Journal of Greenhouse Gas Control*, 17 (2013) 46-65.
- [161] S. Kumar, J.H. Cho, I. Moon, Ionic liquid-amine blends and CO<sub>2</sub>BOLs: Prospective solvents for natural gas sweetening and CO<sub>2</sub> capture technology—A review, *International Journal of Greenhouse Gas Control*, 20 (2014) 87-116.
- [162] G.T. Rochelle, Amine scrubbing for CO<sub>2</sub> capture, *Science*, 325 (2009) 1652-1654.
- [163] E.B. Rinker, S.S. Ashour, O.C. Sandall, Absorption of Carbon Dioxide into Aqueous Blends of Diethanolamine and Methyldiethanolamine, *Industrial & Engineering Chemistry Research*, 39 (2000) 4346-4356.
- [164] A.B. Rao, E.S. Rubin, A Technical, Economic, and Environmental Assessment of Amine-Based CO<sub>2</sub> Capture Technology for Power Plant Greenhouse Gas Control, *Environmental Science & Technology*, 36 (2002) 4467-4475.
- [165] M.W. Arshad, H.F. Svendsen, P.L. Fosbøl, N. von Solms, K. Thomsen, Equilibrium Total Pressure and CO<sub>2</sub> Solubility in Binary and Ternary Aqueous Solutions of 2-(Diethylamino)ethanol (DEEA) and 3-(Methylamino)propylamine (MAPA), *Journal of Chemical & Engineering Data*, 59 (2014) 764-774.
- [166] F. Bougie, M.C. Iliuta, CO<sub>2</sub> Absorption in Aqueous Piperazine Solutions: Experimental Study and Modeling, *Journal of Chemical & Engineering Data*, 56 (2011) 1547-1554.
- [167] N. Daneshvar, M.T. Zaafarani Moattar, M. Abedinzadegan Abdi, S. Aber, Carbon dioxide equilibrium absorption in the multi-component systems of CO<sub>2</sub> + TIPA + MEA + H<sub>2</sub>O, CO<sub>2</sub> + TIPA + Pz + H<sub>2</sub>O and CO<sub>2</sub> + TIPA + H<sub>2</sub>O at low CO<sub>2</sub> partial pressures: experimental solubility data, corrosion study and modeling with artificial neural network, *Separation and Purification Technology*, 37 (2004) 135-147.
- [168] S.K. Dash, A.N. Samanta, S.S. Bandyopadhyay, Experimental and theoretical investigation of solubility of carbon dioxide in concentrated aqueous solution of 2-amino-2-methyl-1-propanol and piperazine, *The Journal of Chemical Thermodynamics*, 51 (2012) 120-125.
- [169] S.-H. Wu, A.R. Caparanga, R.B. Leron, M.-H. Li, Vapor pressures of aqueous blended-amine solutions containing (TEA/AMP/MDEA) + (DEA/MEA/PZ) at temperatures (303.15–343.15) K, *Experimental Thermal and Fluid Science*, 48 (2013) 1-7.
- [170] W.-J. Choi, J.-B. Seo, S.-Y. Jang, J.-H. Jung, K.-J. Oh, Removal characteristics of CO<sub>2</sub> using aqueous MEA/AMP solutions in the absorption and regeneration process, *Journal of Environmental Sciences*, 21 (2009) 907-913.

- [171] B.P. Mandal, M. Guha, A.K. Biswas, S.S. Bandyopadhyay, Removal of carbon dioxide by absorption in mixed amines: modelling of absorption in aqueous MDEA/MEA and AMP/MEA solutions, *Chemical Engineering Science*, 56 (2001) 6217-6224.
- [172] D.P. Hagewiesche, S.S. Ashour, H.A. Al-Ghawas, O.C. Sandall, Absorption of carbon dioxide into aqueous blends of monoethanolamine and N-methyldiethanolamine, *Chemical Engineering Science*, 50 (1995) 1071-1079.
- [173] C.-H. Liao, M.-H. Li, Kinetics of absorption of carbon dioxide into aqueous solutions of monoethanolamine+N-methyldiethanolamine, *Chemical Engineering Science*, 57 (2002) 4569-4582.
- [174] D. Barth, C. Tondre, G. Lappai, J.J. Delpuech, Kinetic study of carbon dioxide reaction with tertiary amines in aqueous solutions, *The Journal of Physical Chemistry*, 85 (1981) 3660-3667.
- [175] P.V. Danckwerts, The reaction of CO<sub>2</sub> with ethanolamines, *Chemical Engineering Science*, 34 (1979) 443-446.
- [176] D.W. Savage, E.W. Funk, Selective Absorption of H<sub>2</sub>S and CO<sub>2</sub> into Aqueous Solutions of Methyldiethanolamine, in: AIChE meeting, Houston, Texas, 1981.
- [177] G.R. Daviet, R. Sundermann, S.T. Donnelly, J.A. Bullin, Dome's North Carolina Plant Conversion to MDEA, in: Proceedings of Gas Processors Association Convention, New Orleans, LA, 1984.
- [178] J.A. Bullin, J.C. Polasek, S.T. Donnelly, The Use of MDEA and Mixtures of Amines for Bulk CO<sub>2</sub> Removal, in: Proc. of 69th Gas Processors Association Convention, New Orleans, Louisiana, 1984.
- [179] P.V. Danckwerts, *Gas Liquid Reactions*, McGraw Hill, New York, 1970.
- [180] A.E. Cornelissen, Simulation of Absorption of H<sub>2</sub>S and CO<sub>2</sub> into Aqueous Alkanolamines, in, Shell Laboratory, 1982, pp. 3.1-3.15.
- [181] M.S. Shaikh, A.M. Shariff, M.A. Bustam, G. Murshid, Physicochemical properties of aqueous solutions of sodium glycinate in the non-precipitation regime from 298.15 to 343.15 K, *Chinese Journal of Chemical Engineering*, 23 (2015) 536-540.
- [182] M.E. Hamzehie, H. Najibi, Experimental and theoretical study of carbon dioxide solubility in aqueous solution of potassium glycinate blended with piperazine as new absorbents, *Journal of CO<sub>2</sub> Utilization*, 16 (2016) 64-77.
- [183] M. Rabensteiner, G. Kinger, M. Koller, G. Gronald, S. Unterberger, C. Hochenauer, Investigation of the suitability of aqueous sodium glycinate as a solvent for post combustion carbon dioxide capture on the basis of pilot plant studies and screening methods, *International Journal of Greenhouse Gas Control*, 29 (2014) 1-15.
- [184] H.-J. Song, S. Lee, S. Maken, J.-J. Park, J.-W. Park, Solubilities of carbon dioxide in aqueous solutions of sodium glycinate, *Fluid Phase Equilibria*, 246 (2006) 1-5.
- [185] B.K. Mondal, S.S. Bandyopadhyay, A.N. Samanta, VLE of CO<sub>2</sub> in aqueous sodium glycinate solution – New data and modeling using Kent–Eisenberg model, *International Journal of Greenhouse Gas Control* 36 (2015) 153-160.
- [186] S. Lee, H.-J. Song, S. Maken, H.-C. Shin, H.-C. Song, J.-W. Park, Physical Solubility and Diffusivity of N<sub>2</sub>O and CO<sub>2</sub> in Aqueous Sodium Glycinate Solutions, *Journal of Chemical & Engineering Data*, 51 (2006) 504-509.
- [187] R.D. Deshmukh, A.E. Mather, A mathematical model for equilibrium solubility of hydrogen sulfide and carbon dioxide in aqueous alkanolamine solutions, *Chemical Engineering Science*, 36 (1981) 355-362.
- [188] C.-C. Chen, L.B. Evans, A local composition model for the excess Gibbs energy of aqueous electrolyte systems, *AIChE Journal*, 32 (1986) 444-454.

- [189] U.E. Aronu, S. Gondal, E.T. Hessen, T. Haug-Warberg, A. Hartono, K.A. Hoff, H.F. Svendsen, Solubility of CO<sub>2</sub> in 15, 30, 45 and 60 mass% MEA from 40 to 120 °C and model representation using the extended UNIQUAC framework, *Chemical Engineering Science*, 66 (2011) 6393-6406.
- [190] R.L. Kent, B. Elsenberg, Better data for amine treating, *Hydrocarbon Processing*, 55 (1976) 87-90.
- [191] G. Chen, X. Luo, H. Zhang, K. Fu, Z. Liang, W. Rongwong, P. Tontiwachwuthikul, R. Idem, Artificial neural network models for the prediction of CO<sub>2</sub> solubility in aqueous amine solutions, *International Journal of Greenhouse Gas Control*, 39 (2015) 174-184.
- [192] A. Farasat, A. Shokrollahi, M. Arabloo, F. Gharagheizi, A.H. Mohammadi, Toward an intelligent approach for determination of saturation pressure of crude oil, *Fuel Processing Technology*, 115 (2013) 201-214.
- [193] F. Gharagheizi, A. Eslamimanesh, A.H. Mohammadi, D. Richon, Representation/Prediction of Solubilities of Pure Compounds in Water Using Artificial Neural Network–Group Contribution Method, *Journal of Chemical & Engineering Data*, 56 (2011) 720-726.
- [194] A. Eslamimanesh, F. Gharagheizi, A.H. Mohammadi, D. Richon, M. Illbeigi, A. Fazlali, A.A. Forghani, M. Yazdizadeh, Phase Equilibrium Modeling of Structure H Clathrate Hydrates of Methane + Water “Insoluble” Hydrocarbon Promoter Using Group Contribution-Support Vector Machine Technique, *Industrial & Engineering Chemistry Research*, 50 (2011) 12807-12814.
- [195] A. Shokrollahi, M. Arabloo, F. Gharagheizi, A.H. Mohammadi, Intelligent model for prediction of CO<sub>2</sub> – Reservoir oil minimum miscibility pressure, *Fuel*, 112 (2013) 375-384.
- [196] F. Gharagheizi, A. Eslamimanesh, B. Tirandazi, A.H. Mohammadi, D. Richon, Handling a very large data set for determination of surface tension of chemical compounds using Quantitative Structure–Property Relationship strategy, *Chemical Engineering Science*, 66 (2011) 4991-5023.
- [197] D. Himmelblau, Applications of artificial neural networks in chemical engineering, *Korean J. Chem. Eng.*, 17 (2000) 373-392.
- [198] Y.K. Gidh, A. Purwanto, H. Ibrahim, Artificial Neural Network Drilling Parameter Optimization System Improves ROP by Predicting/Managing Bit Wear, in: *SPE Intelligent Energy International*, Society of Petroleum Engineers, Utrecht, The Netherlands, 2012.
- [199] E.-S.A. Osman, M.A. Ayoub, M.A. Aggour, Artificial Neural Network Model for Predicting Bottomhole Flowing Pressure in Vertical Multiphase Flow, in: *SPE Middle East Oil and Gas Show and Conference*, Society of Petroleum Engineers, Kingdom of Bahrain, 2005.
- [200] M. Koolivand Salooki, R. Abedini, H. Adib, H. Koolivand, Design of neural network for manipulating gas refinery sweetening regenerator column outputs, *Separation and Purification Technology*, 82 (2011) 1-9.
- [201] N. Saghatoleslami, M.K. Salooki, N. Mohamadi, Auto-Design of Neural Network–Based GAs for Manipulating the Khangiran Gas Refinery Sweetening Absorption Column Outputs, *Petroleum Science and Technology*, 29 (2011) 1437-1448.
- [202] H. Adib, F. Sharifi, N. Mehranbod, N.M. Kazerooni, M. Koolivand, Support Vector Machine based modeling of an industrial natural gas sweetening plant, *Journal of Natural Gas Science and Engineering*, 14 (2013) 121-131.
- [203] N. Sipöcz, F.A. Tobiesen, M. Assadi, The use of Artificial Neural Network models for CO<sub>2</sub> capture plants, *Applied Energy*, 88 (2011) 2368-2376.
- [204] Q. Zhou, Y. Wu, C.W. Chan, P. Tontiwachwuthikul, From neural network to neuro-fuzzy modeling: Applications to the carbon dioxide capture process, *Energy Procedia*, 4 (2011) 2066-2073.

- [205] Q. Zhou, C.W. Chan, P. Tontiwachwuthikul, R. Idem, D. Gelowitz, Application of neuro-fuzzy modeling technique for operational problem solving in a CO<sub>2</sub> capture process system, *International Journal of Greenhouse Gas Control*, 15 (2013) 32-41.
- [206] Q. Zhou, Y. Wu, C.W. Chan, P. Tontiwachwuthikul, Modeling of the carbon dioxide capture process system using machine intelligence approaches, *Engineering Applications of Artificial Intelligence*, 24 (2011) 673-685.
- [207] Y. Wu, C.W. Chan, Analysis of data for the carbon dioxide capture domain, *Engineering Applications of Artificial Intelligence*, 24 (2011) 154-163.
- [208] A. Shahsavand, F. Derakhshan Fard, F. Sotoudeh, Application of artificial neural networks for simulation of experimental CO<sub>2</sub> absorption data in a packed column, *Journal of Natural Gas Science and Engineering*, 3 (2011) 518-529.
- [209] H. Pahlavanzadeh, S. Nourani, M. Saber, Experimental analysis and modeling of CO<sub>2</sub> solubility in AMP (2-amino-2-methyl-1-propanol) at low CO<sub>2</sub> partial pressure using the models of Deshmukh–Mather and the artificial neural network, *The Journal of Chemical Thermodynamics*, 43 (2011) 1775-1783.
- [210] B. ZareNezhad, A. Aminian, An artificial neural network model for predicting the H<sub>2</sub>S removal performance of piperazine solvents in gas sweetening plants, *Journal of the University of Chemical Technology and Metallurgy*, 47 (2012) 553-558.
- [211] B. ZareNezhad, A. Aminian, A neuro-fuzzy model for accurate prediction of H<sub>2</sub>S solubilities in aqueous solvents employed in water-wash units of gas refining plants, *Journal of the University of Chemical Technology and Metallurgy*, 47 (2012) 546-552.
- [212] D. Bastani, M.E. Hamzehie, F. Davardoost, S. Mazinani, A. Poorbashiri, Prediction of CO<sub>2</sub> loading capacity of chemical absorbents using a multi-layer perceptron neural network, *Fluid Phase Equilibria*, 354 (2013) 6-11.
- [213] R.B. Grigg, D.S. Schechter, State of the Industry in CO<sub>2</sub> Floods, in: *SPE Annual Technical Conference and Exhibition*, Society of Petroleum Engineers, San Antonio, Texas, 1997.
- [214] K. Jessen, A.R. Kovscek, F.M. Orr, Increasing CO<sub>2</sub> storage in oil recovery, *Energy Conversion and Management*, 46 (2005) 293-311.
- [215] H. Yuan, R.T. Johns, Simplified Method for Calculation of Minimum Miscibility Pressure or Enrichment, in: *SPE Annual Technical Conference and Exhibition*, Society of Petroleum Engineers, San Antonio, Texas, 2002, pp. 1-10.
- [216] F.R. Wassmuth, K. Green, L. Hodgins, Conformance Control for Miscible CO Floods in Fractured Carbonates, in: *Canadian International Petroleum Conference*, Petroleum Society of Canada, Calgary, Alberta, 2005.
- [217] E. Manrique, V. Alvarado, *Chemical Enhanced Oil Recovery Handbook: Screening, Formulation, and Implementation*, Elsevier Science, 2016.
- [218] L.W. Holm, V.A. Josendal, Mechanisms of Oil Displacement By Carbon Dioxide, *Journal of Petroleum Technology*, 26 (1994).
- [219] D.J. Graue, E.T. Zana, Study of a Possible CO<sub>2</sub> Flood in Rangely Field, *Journal of Petroleum Technology*, 33 (1981).
- [220] F. Torabi, K. Asghari, Effect of operating pressure, matrix permeability and connate water saturation on performance of CO<sub>2</sub> huff-and-puff process in matrix-fracture experimental model, *Fuel*, 89 (2010) 2985-2990.
- [221] M.F. Al-Ajmi, O.A. Alomair, A.M. Elsharkawy, Planning Miscibility Tests And Gas Injection Projects For Four Major Kuwaiti Reservoirs, in: *Kuwait International Petroleum Conference and Exhibition*, Society of Petroleum Engineers, Kuwait City, Kuwait, 2009.

- [222] S. Chen, H. Li, D. Yang, P. Tontiwachwuthikul, Optimal Parametric Design for Water-Alternating-Gas (WAG) Process in a CO<sub>2</sub>-Miscible Flooding Reservoir, *Journal of Canadian Petroleum Technology*, 49 (2010) 75-82.
- [223] J.L. Shelton, L. Yarborough, Multiple Phase Behavior in Porous Media During CO<sub>2</sub> or Rich-Gas Flooding, *Journal of Petroleum Technology*, 29 (1977) 1171-1178.
- [224] R.M. Dicharry, T.L. Perryman, J.D. Ronquille, Evaluation and Design of a CO<sub>2</sub> Miscible Flood Project-SACROC Unit, Kelly-Snyder Field, *Journal of Petroleum Technology*, 25 (1973).
- [225] F. Torabi, A. Qazvini Firouz, A. Kavousi, K. Asghari, Comparative evaluation of immiscible, near miscible and miscible CO<sub>2</sub> huff-n-puff to enhance oil recovery from a single matrix-fracture system (experimental and simulation studies), *Fuel*, 93 (2012) 443-453.
- [226] F.I. Stalkup, Carbon Dioxide Miscible Flooding: Past, Present, And Outlook for the Future, *Journal of Petroleum Technology*, 30 (1978) 1102-1112.
- [227] A.M. Elsharkawy, F.H. Poettmann, R.L. Christiansen, Measuring CO<sub>2</sub> Minimum Miscibility Pressures: Slim-Tube or Rising-Bubble Method?, *Energy & Fuels*, 10 (1996) 443-449.
- [228] F.B. Thomas, X.L. Zhou, D.B. Bennion, D.W. Bennion, A Comparative Study of RBA, P-x, Multicontact And Slim Tube Results, *Journal of Canadian Petroleum Technology*, 33 (1994) 17-26.
- [229] R.L. Christiansen, H.K. Haines, Rapid Measurement of Minimum Miscibility Pressure With the Rising-Bubble Apparatus, *SPE Reservoir Engineering*, 2 (1987) 523-527.
- [230] D. Zhou, F.M. Orr, Jr., An Analysis of Rising Bubble Experiments to Determine Minimum Miscibility Pressures, in: *SPE Annual Technical Conference and Exhibition*, Society of Petroleum Engineers, Dallas, Texas, 1995.
- [231] D.N. Rao, A new technique of vanishing interfacial tension for miscibility determination, *Fluid Phase Equilibria*, 139 (1997) 311-324.
- [232] S.C. Ayirala, D.N. Rao, Comparative Evaluation of a New MMP Determination Technique, in: *SPE/DOE Symposium on Improved Oil Recovery*, Society of Petroleum Engineers, Tulsa, Oklahoma, 2006.
- [233] K.A. Rahmatabadi, Advances in Calculation of Minimum Miscibility Pressure, in: *Petroleum & Geosystems Engineering Department*, The University of Texas at Austin, Texas, USA, 2011.
- [234] A. Abedini, N. Mosavat, F. Torabi, Determination of Minimum Miscibility Pressure of Crude Oil-CO<sub>2</sub> System by Oil Swelling/Extraction Test, *Energy Technology*, 2 (2014) 431-439.
- [235] K. Jessen, M.L. Michelsen, E.H. Stenby, Global approach for calculation of minimum miscibility pressure, *Fluid Phase Equilibria*, 153 (1998) 251-263.
- [236] Y. Wang, F.M. Orr Jr, Analytical calculation of minimum miscibility pressure, *Fluid Phase Equilibria*, 139 (1997) 101-124.
- [237] R.B. Alston, G.P. Kokolis, C.F. James, CO<sub>2</sub> Minimum Miscibility Pressure: A Correlation for Impure CO<sub>2</sub> Streams and Live Oil Systems, *Society of Petroleum Engineers Journal*, 25 (1985).
- [238] M.K. Emera, H.K. Sarma, Use of genetic algorithm to estimate CO<sub>2</sub>-oil minimum miscibility pressure—a key parameter in design of CO<sub>2</sub> miscible flood, *Journal of Petroleum Science and Engineering*, 46 (2005) 37-52.
- [239] H.M. Sebastian, R.S. Wenger, T.A. Renner, Correlation of Minimum Miscibility Pressure for Impure CO<sub>2</sub> Streams, *Journal of Petroleum Technology*, 37 (1985).
- [240] W.F. Yellig, R.S. Metcalfe, Determination and Prediction of CO<sub>2</sub> Minimum Miscibility Pressures, *Journal of Petroleum Technology*, 32 (1980) 160-168.

- [241] H. Li, J. Qin, D. Yang, An Improved CO<sub>2</sub>–Oil Minimum Miscibility Pressure Correlation for Live and Dead Crude Oils, *Industrial & Engineering Chemistry Research*, 51 (2012) 3516-3523.
- [242] M.K. Valluri, S. Mishra, J. Schuetter, An improved correlation to estimate the minimum miscibility pressure of CO<sub>2</sub> in crude oils for carbon capture, utilization, and storage projects, *Journal of Petroleum Science and Engineering*, 158 (2017) 408-415.
- [243] A. Tatar, A. Shokrollahi, M. Mesbah, S. Rashid, M. Arabloo, A. Bahadori, Implementing Radial Basis Function Networks for modeling CO<sub>2</sub>-reservoir oil minimum miscibility pressure, *Journal of Natural Gas Science and Engineering*, 15 (2013) 82-92.
- [244] A. Kamari, M. Arabloo, A. Shokrollahi, F. Gharagheizi, A.H. Mohammadi, Rapid method to estimate the minimum miscibility pressure (MMP) in live reservoir oil systems during CO<sub>2</sub> flooding, *Fuel*, 153 (2015) 310-319.
- [245] A. Karkevandi-Talkhooncheh, S. Hajirezaie, A. Hemmati-Sarapardeh, M.M. Husein, K. Karan, M. Sharifi, Application of adaptive neuro fuzzy interface system optimized with evolutionary algorithms for modeling CO<sub>2</sub>-crude oil minimum miscibility pressure, *Fuel*, 205 (2017) 34-45.
- [246] M.M. Ghiasi, A. Bahadori, S. Zendehboudi, Estimation of the water content of natural gas dried by solid calcium chloride dehydrator units, *Fuel*, 117, Part A (2014) 33-42.
- [247] M.M. Ghiasi, A. Bahadori, S. Zendehboudi, A. Jamili, S. Rezaei-Gomari, Novel methods predict equilibrium vapor methanol content during gas hydrate inhibition, *Journal of Natural Gas Science and Engineering*, 15 (2013) 69-75.
- [248] M.M. Ghiasi, M.A. Ghayyem, Application of Artificial Neural Network (ANN) in Prediction of Hydrate Formation Temperature, *Energy Sources, Part A: Recovery, Utilization, and Environmental Effects*, (In Press).
- [249] K. Levenberg, A method for the solution of certain non-linear problems in least squares, *Quarterly of Applied Mathematics*, 2 (1944) 164-168.
- [250] D.W. Marquardt, An algorithm for the least-squares estimation of nonlinear parameters, *SIAM Journal on Applied Mathematics*, 11 (1963) 431-441.
- [251] M.M. Ghiasi, Initial estimation of hydrate formation temperature of sweet natural gases based on new empirical correlation, *Journal of Natural Gas Chemistry*, 21 (2012) 508–512.
- [252] V. Vapnik, *The nature of statistical learning theory*, Springer-Verlag, New York, 1995.
- [253] V.N. Vapnik, An overview of statistical learning theory, *IEEE Transactions on Neural Networks*, 10 (1999) 988-999.
- [254] C. Cortes, V. Vapnik, Support-vector networks, *Mach Learn*, 20 (1995) 273-297.
- [255] J.-T. Jeng, Hybrid approach of selecting hyper-parameters of support vector machine for regression, *IEEE Transactions on Systems, Man, and Cybernetics, Part B: Cybernetics*, 36 (2006) 699-709.
- [256] W.Y.N. Wing, A. Dorado, D.S. Yeung, W. Pedrycz, E. Izquierdo, Image classification with the use of radial basis function neural networks and the minimization of the localized generalization error, *Pattern Recognition*, 40 (2007) 19-32.
- [257] H.H. Tsai, D.W. Sun, Color image watermark extraction based on support vector machines, *Information Sciences*, 177 (2007) 550-569.
- [258] J. Acevedo-Rodríguez, S. Maldonado-Bascón, S. Lafuente-Arroyo, P. Siegmann, F. López-Ferreras, Computational load reduction in decision functions using support vector machines, *Signal Processing*, 89 (2009) 2066-2071.
- [259] V. Ceperic, G. Gielen, A. Baric, Recurrent sparse support vector regression machines trained by active learning in the time-domain, *Expert Systems with Applications*, 39 (2012) 10933-10942.

- [260] Z. Huang, H. Chen, C.-J. Hsu, W.-H. Chen, S. Wu, Credit rating analysis with support vector machines and neural networks: a market comparative study, *Decision Support Systems*, 37 (2004) 543-558.
- [261] H. Li, Y. Liang, Q. Xu, Support vector machines and its applications in chemistry, *Chemometrics and Intelligent Laboratory Systems*, 95 (2009) 188-198.
- [262] R. Stoean, C. Stoean, Modeling medical decision making by support vector machines, explaining by rules of evolutionary algorithms with feature selection, *Expert Systems with Applications*, 40 (2013) 2677-2686.
- [263] A. Subasi, M. Ismail Gursoy, EEG signal classification using PCA, ICA, LDA and support vector machines, *Expert Systems with Applications*, 37 (2010) 8659-8666.
- [264] J. Terzic, C.R. Nagarajah, M. Alamgir, Fluid level measurement in dynamic environments using a single ultrasonic sensor and Support Vector Machine (SVM), *Sensors and Actuators A: Physical*, 161 (2010) 278-287.
- [265] V. Cherkassky, F. Mulier, *Learning from Data - Concepts, Theory and Method*, John Wiley & Sons, New York, 1998.
- [266] J.A.K. Suykens, J. Vandewalle, Least Squares Support Vector Machine Classifiers, *Neural Processing Letters*, 9 (1999) 293-300.
- [267] N. Cristianini, J. Shawe-Taylor, *An Introduction to Support Vector Machines and Other Kernel-based Learning Methods*, Cambridge University Press, 2000.
- [268] B. Schölkopf, C.J.C. Burges, A.J. Smola, *Advances in Kernel Methods: Support Vector Learning*, Philomel Books, 1999.
- [269] B.S. Ikonf, A.J. Smola, *Learning With Kernels: Support Vector Machines, Regularization, Optimization and Beyond*, "The" MIT Press, 2002.
- [270] J.A.K. Suykens, T.V. Gestel, J.D. Brabanter, B.D. Moor, J. Vandewalle, *Least Squares Support Vector Machines*, World Scientific Pub. Co., Singapor, 2002.
- [271] S. Xavier-de-Souza, J.A.K. Suykens, J. Vandewalle, D. Bolle, Coupled Simulated Annealing, *Systems, Man, and Cybernetics, Part B: Cybernetics*, IEEE Transactions on, 40 (2010) 320-335.
- [272] J.S.R. Jang, ANFIS: adaptive-network-based fuzzy inference system, *Systems, Man and Cybernetics*, IEEE Transactions on, 23 (1993) 665-685.
- [273] Z.-H. Zhou, *Ensemble Methods: Foundations and Algorithms*, Chapman & Hall/CRC, 2012.
- [274] Y. Freund, R.E. Schapire, A Decision-Theoretic Generalization of On-Line Learning and an Application to Boosting, *Journal of Computer and System Sciences*, 55 (1997) 119-139.
- [275] H. Drucker, Improving Regressors using Boosting Techniques, in: 97 Proceedings of the Fourteenth International Conference on Machine Learning, Morgan Kaufmann Publishers Inc., San Francisco, CA, USA, 1997, pp. 107-115.
- [276] H. Saghafi, M.M. Ghiasi, A.H. Mohammadi, CO<sub>2</sub> capture with aqueous solution of sodium glycinate: Modeling using an ensemble method, *International Journal of Greenhouse Gas Control*, 62 (2017) 23-30.
- [277] M.M. Ghiasi, A.H. Mohammadi, Application of decision tree learning in modelling CO<sub>2</sub> equilibrium absorption in ionic liquids, *Journal of Molecular Liquids*, 242 (2017) 594-605.
- [278] G.R. Schneider, J. Farrar, *Nucleation and Growth of Ice Crystals*, U.S. Department of the Interior, USA, 1968.
- [279] O.S. Rouher, A.J. Barduhn, Hydrates of iso- and normal butane and their mixtures, *Desalination*, 6 (1969) 57-73.



- [280] S.D. Larson, Phase Studies of the Two-Component Carbon Dioxide-Water System, Involving: the Carbon Dioxide Hydrate, in, University of Illinois, USA, 1955.
- [281] S.L. Miller, W.D. Smythe, Carbon Dioxide Clathrate in the Martian Ice Cap, *Science*, 170 (1970) 531-533.
- [282] J.G. Vlahakis, H.-S. Chen, S.M. S., A.J. Barduhn, The Growth Rate of Ice Crystals: Properties of Carbon dioxide Hydrate, A Review of Properties of 51 Gas Hydrates, in, Prepared for US Department of the Interior, USA, 1972.
- [283] F.T. Selleck, L.T. Carmichael, B.H. Sage, Phase Behavior in the Hydrogen Sulfide-Water System, *Industrial & Engineering Chemistry*, 44 (1952) 2219-2226.
- [284] J.J. Carroll, A.E. Mather, Phase equilibrium in the system water-hydrogen sulphide: Hydrate-forming conditions, *The Canadian Journal of Chemical Engineering*, 69 (1991) 1206-1212.
- [285] A.v. Cleeff, G.A.M. Diepen, Gas hydrates of nitrogen and oxygen, *Recueil des Travaux Chimiques des Pays-Bas*, 79 (1960) 582-586.
- [286] D.R. Marshall, S. Saito, R. Kobayashi, Hydrates at high pressures: Part I. Methane-water, argon-water, and nitrogen-water systems, *AIChE Journal*, 10 (1964) 202-205.
- [287] E. Kamari, M. Oyarhossein, Experimental determination of hydrate phase equilibrium curve for an Iranian sour gas condensate sample, *Journal of Natural Gas Science and Engineering*, 9 (2012) 11-15.
- [288] P.V. Hemmingsen, R. Burgass, K.S. Pedersen, K. Kinnari, H. Sørensen, Hydrate temperature depression of MEG solutions at concentrations up to 60 wt%. Experimental data and simulation results, *Fluid Phase Equilibria*, 307 (2011) 175-179.
- [289] B.-J. Wu, D.B. Robinson, H.-J. Ng, Three- and four-phase hydrate forming conditions in methane + isobutane + water, *The Journal of Chemical Thermodynamics*, 8 (1976) 461-469.
- [290] J.P. Schroeter, R. Kobayashi, M.A. Hildebrand, Hydrate decomposition conditions in the system hydrogen sulfide-methane-propane, *Industrial & Engineering Chemistry Fundamentals*, 22 (1983) 361-364.
- [291] W.I. Wilcox, D.B. Carson, D.L. Katz, Natural Gas Hydrates, *Industrial & Engineering Chemistry*, 33 (1941) 662-665.
- [292] D.-H. Mei, J. Liao, J.-T. Yang, T.-M. Guo, Experimental and Modeling Studies on the Hydrate Formation of a Methane + Nitrogen Gas Mixture in the Presence of Aqueous Electrolyte Solutions, *Industrial & Engineering Chemistry Research*, 35 (1996) 4342-4347.
- [293] S.G. Paranjpe, S.L. Patil, V.A. Kamath, S.P. Godbole, Hydrate Equilibria for Binary and Ternary Mixtures of Methane, Propane, Isobutane, and n-Butane: Effect of Salinity, in: Paper SPE 16871, 379, *Proc. 62nd SPE Annual Conf.*, Dallas, TX, 1987.
- [294] H. Haghighi, A. Chapoy, R. Burgess, B. Tohidi, Experimental and thermodynamic modelling of systems containing water and ethylene glycol: Application to flow assurance and gas processing, *Fluid Phase Equilibria*, 276 (2009) 24-30.
- [295] H. Haghighi, A. Chapoy, R. Burgess, S. Mazloum, B. Tohidi, Phase equilibria for petroleum reservoir fluids containing water and aqueous methanol solutions: Experimental measurements and modelling using the CPA equation of state, *Fluid Phase Equilibria*, 278 (2009) 109-116.
- [296] H. Haghighi, A. Chapoy, B. Tohidi, Methane and Water Phase Equilibria in the Presence of Single and Mixed Electrolyte Solutions Using the Cubic-Plus-Association Equation of State, *Oil & Gas Science and Technology*, 64 (2009) 141-154.
- [297] H. Haghighi, R. Burgess, A. Chapoy, B. Tohidi, Hydrate dissociation conditions at high pressure: experimental equilibrium data and thermodynamic modeling, in: *Proceedings of the 6th International Conference on Gas Hydrates*, Vancouver, British Columbia, Canada, 2008.

- [298] A.H. Mohammadi, D. Richon, Phase equilibria of clathrate hydrates of carbon disulfide + nitrogen or carbon dioxide + water system, *Chemical Engineering Science*, 91 (2013) 146-150.
- [299] A.H. Mohammadi, D. Richon, Methane hydrate phase equilibrium in the presence of salt (NaCl, KCl, or CaCl<sub>2</sub>)&#xa0;+&#xa0;ethylene glycol or salt (NaCl, KCl, or CaCl<sub>2</sub>)&#xa0;+&#xa0;methanol aqueous solution: Experimental determination of dissociation condition, *The Journal of Chemical Thermodynamics*, 41 (2009) 1374-1377.
- [300] A.H. Mohammadi, D. Richon, Gas Hydrate Phase Equilibrium in the Presence of Ethylene Glycol or Methanol Aqueous Solution, *Industrial & Engineering Chemistry Research*, 49 (2010) 8865-8869.
- [301] A.H. Mohammadi, D. Richon, Gas Hydrate Phase Equilibrium in Methane + Ethylene Glycol, Diethylene Glycol, or Triethylene Glycol + Water System, *Journal of Chemical & Engineering Data*, 56 (2011) 4544-4548.
- [302] A.H. Mohammadi, D. Richon, Phase equilibria of hydrogen sulfide and carbon dioxide simple hydrates in the presence of methanol, (methanol&#xa0;+&#xa0;NaCl) and (ethylene glycol&#xa0;+&#xa0;NaCl) aqueous solutions, *The Journal of Chemical Thermodynamics*, 44 (2012) 26-30.
- [303] A.H. Mohammadi, W. Afzal, D. Richon, Gas hydrates of methane, ethane, propane, and carbon dioxide in the presence of single NaCl, KCl, and CaCl<sub>2</sub> aqueous solutions: Experimental measurements and predictions of dissociation conditions, *The Journal of Chemical Thermodynamics*, 40 (2008) 1693-1697.
- [304] A.H. Mohammadi, I. Kraouti, D. Richon, Methane hydrate phase equilibrium in the presence of NaBr, KBr, CaBr<sub>2</sub>, K<sub>2</sub>CO<sub>3</sub>, and MgCl<sub>2</sub> aqueous solutions: Experimental measurements and predictions of dissociation conditions, *The Journal of Chemical Thermodynamics*, 41 (2009) 779-782.
- [305] A.H. Mohammadi, R. Anderson, B. Tohidi, Carbon monoxide clathrate hydrates: Equilibrium data and thermodynamic modeling, *AIChE Journal*, 51 (2005) 2825-2833.
- [306] J. Nixdorf, L.R. Oellrich, Experimental determination of hydrate equilibrium conditions for pure gases, binary and ternary mixtures and natural gases, *Fluid Phase Equilibria*, 139 (1997) 325-333.
- [307] R. Masoudi, B. Tohidi, A. Danesh, A.C. Todd, R. Anderson, R.W. Burgass, J. Yang, Measurement and prediction of gas hydrate and hydrated salt equilibria in aqueous ethylene glycol and electrolyte solutions, *Chemical Engineering Science*, 60 (2005) 4213-4224.
- [308] M.D. Jager, E.D. Sloan, The effect of pressure on methane hydration in pure water and sodium chloride solutions, *Fluid Phase Equilibria*, 185 (2001) 89-99.
- [309] M.D. Jager, C.J. Peters, E.D. Sloan, Experimental determination of methane hydrate stability in methanol and electrolyte solutions, *Fluid Phase Equilibria*, 193 (2002) 17-28.
- [310] T. Maekawa, Equilibrium conditions for gas hydrates of methane and ethane mixtures in pure water and sodium chloride solution, *Geochemical Journal*, 35 (2001) 59-66.
- [311] T. Maekawa, Equilibrium conditions for clathrate hydrates formed from methane and aqueous propanol solutions, *Fluid Phase Equilibria*, 267 (2008) 1-5.
- [312] H.O. McLeod, J.M. Campbell, Natural Gas Hydrates at Pressures to 10,000 psia, *Journal of Petroleum Technology*, 222 (1961) 590-594.
- [313] V.K. Verma, Gas Hydrates from Limid Hydrocarbon-Water Systems, in, University of Michigan, Ann Arbor, MI, 1974.
- [314] V.K. Verma, J.H. Hand, D.L. Katz, Gas Hydrates from Liquid Hydrocarbons, Methane-Propane- Water System, in: *AIChE -VTG Joint Meetin*, Munich, 1974.

- [315] J.L. De Roo, C.J. Peters, R.N. Lichtenthaler, G.A.M. Diepen, Occurrence of methane hydrate in saturated and unsaturated solutions of sodium chloride and water in dependence of temperature and pressure, *AIChE Journal*, 29 (1983) 651-657.
- [316] J.L. Thakore, G.D. Holder, Solid vapor azeotropes in hydrate-forming systems, *Industrial & Engineering Chemistry Research*, 26 (1987) 462-469.
- [317] S. Adisasmito, R.J. Frank, E.D. Sloan, Hydrates of carbon dioxide and methane mixtures, *Journal of Chemical & Engineering Data*, 36 (1991) 68-71.
- [318] S. Adisasmito, E.D. Sloan, Hydrates of hydrocarbon gases containing carbon dioxide, *Journal of Chemical & Engineering Data*, 37 (1992) 343-349.
- [319] M. Ghavipour, M. Ghavipour, M. Chitsazan, S.H. Najibi, S.S. Ghidary, Experimental study of natural gas hydrates and a novel use of neural network to predict hydrate formation conditions, *Chemical Engineering Research and Design*, 91 (2013) 264-273.
- [320] K.Y. Song, R. Kobayashi, Final hydrate stability conditions of a methane and propane mixture in the presence of pure water and aqueous solutions of methanol and ethylene glycol, *Fluid Phase Equilibria*, 47 (1989) 295-308.
- [321] P.G. Lafond, K.A. Olcott, E. Dendy Sloan, C.A. Koh, A.K. Sum, Measurements of methane hydrate equilibrium in systems inhibited with NaCl and methanol, *The Journal of Chemical Thermodynamics*, 48 (2012) 1-6.
- [322] H.-J. Ng, D.B. Robinson, Hydrate formation in systems containing methane, ethane, propane, carbon dioxide or hydrogen sulfide in the presence of methanol, *Fluid Phase Equilibria*, 21 (1985) 145-155.
- [323] H.J. Ng, D.B. Robinson, The Influence of Methanol on Hydrate Formation at Low Temperatures, in: *Gas Processors Association Research Report*, USA, 1984.
- [324] H.-J. Ng, D.B. Robinson, New Developments in the Measurement and Prediction of Hydrate Formation for Processing Needs, *Annals of the New York Academy of Sciences*, 715 (1994) 450-462.
- [325] H.-J. Ng, D.B. Robinson, The role of n-butane in hydrate formation, *AIChE Journal*, 22 (1976) 656-661.
- [326] H.J. Ng, D.B. Robinson, Equilibrium Phase Composition and Hydrating Conditions in Systems Containing Methanol, Light Hydrocarbons, Carbon Dioxide, and Hydrogen Sulfide, in, *Gas Processors Association Research Report No. 66*, 1983.
- [327] H.J. Ng, C.-J. Chen, D.B. Robinson, Influence of High Concentrations of Methanol on Hydrate Formation and the Distribution of Glycol in Liquid-Liquid Mixtures, in, *Gas Processors Association Research Report No. 106*, 1987.
- [328] H.J. Ng, C.-J. Chen, D.B. Robinson, Hydrate Formation and Equilibrium Phase Compositions in the Presence of Methanol: Selected Systems Containing Hydrogen Sulfide, Carbon Dioxide, Ethane or Methane, in, *Gas Processors Association Research Report 87*, 1985.
- [329] D.B. Robinson, H.J. Ng, Hydrate Formation And Inhibition In Gas Or Gas Condensate Streams, *Journal of Canadian Petroleum Technology*, 25 (1986).
- [330] D.B. Robinson, B.R. Mehta, Hydrates In the PropaneCarbon Dioxide- Water System, *Journal of Canadian Petroleum Technology*, 10 (1971).
- [331] J. Jhaveri, D.B. Robinson, Hydrates in the methane-nitrogen system, *The Canadian Journal of Chemical Engineering*, 43 (1965) 75-78.
- [332] S.-P. Kang, M.-K. Chun, H. Lee, Phase equilibria of methane and carbon dioxide hydrates in the aqueous MgCl<sub>2</sub> solutions, *Fluid Phase Equilibria*, 147 (1998) 229-238.
- [333] A. Chapoy, B. Tohidi, Hydrates in high MEG concentration systems, in: *Proceedings of the 7th International Conference on Gas Hydrates*, Edinburgh, Scotland, United Kingdom, 2011.

- [334] B. Tohidi, R.W. Burgass, A. Danesh, A.C. Todd, Hydrate Inhibition Effect of Produced Water: Part 1-Ethane and Propane Simple Gas Hydrates, in: Offshore European Conference, SPE, Aberdeen, 1993.
- [335] B. Tohidi, A. Danesh, R.W. Burgass, A.C. Todd, Hydrates Formed in Unprocessed Wellstreams, in: SPE Annual Technical Conference and Exhibition, 1994 Copyright 1994, Society of Petroleum Engineers, Inc., New Orleans, Louisiana, 1994.
- [336] S.M.H. Nasab, M.V. Sefti, A.A. Izadpanah, Measurement of equilibrium data and estimation of methane hydrate conditions in the presence of thermodynamic mixed-inhibitors in: Proceedings of the 7th International Conference on Gas Hydrates, Edinburgh, Scotland, United Kingdom, 2011.
- [337] Z. Atik, C. Windmeier, L.R. Oellrich, Experimental Gas Hydrate Dissociation Pressures for Pure Methane in Aqueous Solutions of  $\text{MgCl}_2$  and  $\text{CaCl}_2$  and for a (Methane + Ethane) Gas Mixture in an Aqueous Solution of ( $\text{NaCl} + \text{MgCl}_2$ ), Journal of Chemical & Engineering Data, 51 (2006) 1862-1867.
- [338] M.J. Ross, L.S. Toczylkin, Hydrate dissociation pressures for methane or ethane in the presence of aqueous solutions of triethylene glycol, Journal of Chemical & Engineering Data, 37 (1992) 488-491.
- [339] P.D. Dholabhai, P. Englezos, N. Kalogerakis, P.R. Bishnoi, Equilibrium conditions for methane hydrate formation in aqueous mixed electrolyte solutions, The Canadian Journal of Chemical Engineering, 69 (1991) 800-805.
- [340] P.D. Dholabhai, N. Kalogerakis, P.R. Bishnoi, Equilibrium conditions for carbon dioxide hydrate formation in aqueous electrolyte solutions, Journal of Chemical & Engineering Data, 38 (1993) 650-654.
- [341] P.D. Dholabhai, P.R. Bishnoi, Hydrate equilibrium conditions in aqueous electrolyte solutions: mixtures of methane and carbon dioxide, Journal of Chemical & Engineering Data, 39 (1994) 191-194.
- [342] P.R. Bishnoi, P.D. Dholabhai, Equilibrium conditions for hydrate formation for a ternary mixture of methane, propane and carbon dioxide, and a natural gas mixture in the presence of electrolytes and methanol, Fluid Phase Equilibria, 158-160 (1999) 821-827.
- [343] C.F. Ma, G.J. Chen, F. Wang, C.Y. Sun, T.M. Guo, Hydrate formation of ( $\text{CH}_4 + \text{C}_2\text{H}_6$ ) and ( $\text{CH}_4 + \text{C}_3\text{H}_8$ ) gas mixtures, Fluid Phase Equilibria, 191 (2001) 41-47.
- [344] O.L. Roberts, E.R. Brownscombe, L.S. Howe, Constitution diagrams and composition of methane and ethane hydrates, Oil & Gas Journal, 39 (1940) 37-43.
- [345] W.M. Deaton, E.M. Frost, Gas hydrates and their relation to the operation of natural-gas pipe lines, Printed by the American Gas Association, USA, 1946.
- [346] H.H. Reamer, F.T. Selleck, B.H. Sage, Some Properties of Mixed Paraffinic and Olefinic Hydrates, Journal of Petroleum Technology, 4 (1952) 197-202.
- [347] T.J. Galloway, W. Ruska, P.S. Chapplear, R. Kobayashi, Experimental Measurement of Hydrate Numbers for Methane and Ethane and Comparison with Theoretical Values, Industrial & Engineering Chemistry Fundamentals, 9 (1970) 237-243.
- [348] B.J. Falabella, A Study of Natural Gas Hydrates, in, University of Massachusetts, USA, 1975.
- [349] G.D. Holder, G.C. Grigoriou, Hydrate dissociation pressures of (methane + ethane + water) existence of a locus of minimum pressures, The Journal of Chemical Thermodynamics, 12 (1980) 1093-1104.
- [350] G.D. Holder, J.H. Hand, Multiple-phase equilibria in hydrates from methane, ethane, propane and water mixtures, AIChE Journal, 28 (1982) 440-447.

- [351] S.P. Godbole, Dissociation Pressures of Propane and i-Butane Hydrates Below the Ice Point, in, University of Pittsburgh, USA, 1981.
- [352] V.T. John, G.D. Holder, Hydrates of methane + butane below the ice point, Journal of Chemical & Engineering Data, 27 (1982) 18-21.
- [353] D. Avlonitis, Multiphase Equilibria in Oil-Water Hydrate Forming System, in, Heriot-Watt University, Edinburgh, Scotlan, 1988.
- [354] B. Miller, E.R. Strong, Hydrate Storage of Natural Gas, American Gas Association Monthly, 28 (1946) 63-67.
- [355] G.D. Holder, S.P. Godbole, Measurement and prediction of dissociation pressures of isobutane and propane hydrates below the ice point, AIChE Journal, 28 (1982) 930-934.
- [356] H. Kubota, K. Shimizu, Y. Tanaka, T. Makita, THERMODYNAMIC PROPERTIES OF R13 (CCIF<sub>3</sub>), R23 (CHF<sub>3</sub>), R152a (C<sub>2</sub>H<sub>4</sub>F<sub>2</sub>), AND PROPANE HYDRATES FOR DESALINATION OF SEA WATER, Journal of Chemical Engineering of Japan, 17 (1984) 423-429.
- [357] R. Kobayashi, H.J. Withrow, G.B.B. Williams, D.L. Katz, Gas hydrate formation with brine and ethanol solution, in: Proc. Conf. NGAA, 1951, pp. 27-31.
- [358] S.L. Patil, Measurements of Multiphase Gas Hydrates Phase Equilibria: Effect of Inhibitors and Heavier Hydrocarbon Components, in, University of Alaska, USA, 1987.
- [359] P. Englezos, Y.T. Ngan, Incipient equilibrium data for propane hydrate formation in aqueous solutions of sodium chloride, potassium chloride and calcium chloride, Journal of Chemical & Engineering Data, 38 (1993) 250-253.
- [360] E. Breland, P. Englezos, Equilibrium Hydrate Formation Data for Carbon Dioxide in Aqueous Glycerol Solutions, Journal of Chemical & Engineering Data, 41 (1996) 11-13.
- [361] Z. Long, X. Zhou, D. Liang, D. Li, Experimental Study of Methane Hydrate Equilibria in [EMIM]-NO<sub>3</sub> Aqueous Solutions, Journal of Chemical & Engineering Data, 60 (2015) 2728-2732.
- [362] Z. Long, Y. He, X. Zhou, D. Li, D. Liang, Phase behavior of methane hydrate in the presence of imidazolium ionic liquids and their mixtures, Fluid Phase Equilibria, 439 (2017) 1-8.
- [363] K.M. Sabil, O. Nashed, B. Lal, L. Ismail, A. Japper-Jaafar, Experimental investigation on the dissociation conditions of methane hydrate in the presence of imidazolium-based ionic liquids, The Journal of Chemical Thermodynamics, 84 (2015) 7-13.
- [364] C.-K. Chu, P.-C. Chen, Y.-P. Chen, S.-T. Lin, L.-J. Chen, Inhibition effect of 1-ethyl-3-methylimidazolium chloride on methane hydrate equilibrium, The Journal of Chemical Thermodynamics, 91 (2015) 141-145.
- [365] A.R. Richard, H. Adidharma, The performance of ionic liquids and their mixtures in inhibiting methane hydrate formation, Chemical Engineering Science, 87 (2013) 270-276.
- [366] X.-S. Li, Y.-J. Liu, Z.-Y. Zeng, Z.-Y. Chen, G. Li, H.-J. Wu, Equilibrium Hydrate Formation Conditions for the Mixtures of Methane + Ionic Liquids + Water, Journal of Chemical & Engineering Data, 56 (2011) 119-123.
- [367] C. Xiao, N. Wibisono, H. Adidharma, Dialkylimidazolium halide ionic liquids as dual function inhibitors for methane hydrate, Chemical Engineering Science, 65 (2010) 3080-3087.
- [368] Z. Long, X. Zhou, X. Shen, D. Li, D. Liang, Phase Equilibria and Dissociation Enthalpies of Methane Hydrate in Imidazolium Ionic Liquid Aqueous Solutions, Industrial & Engineering Chemistry Research, 54 (2015) 11701-11708.
- [369] J.-H. Cha, C. Ha, S.-P. Kang, J.W. Kang, K.-S. Kim, Thermodynamic inhibition of CO<sub>2</sub> hydrate in the presence of morpholinium and piperidinium ionic liquids, Fluid Phase Equilibria, 413 (2016) 75-79.

- [370] J.W. Mason, B.F. Dodge, Equilibrium absorption of carbon dioxide by solutions of the ethanolamines, *Trans. AIChE*, 32 (1936) 27-47.
- [371] J.I. Lee, F.D. Otto, A.E. Mather, Equilibrium between carbon dioxide and aqueous monoethanolamine solutions, *Journal of Applied Chemistry and Biotechnology*, 26 (1976) 541-549.
- [372] J.I. Lee, F.D. Otto, A.E. Mather, Solubility of hydrogen sulfide in aqueous diethanolamine solutions at high pressures, *Journal of Chemical & Engineering Data*, 18 (1973) 71-73.
- [373] J.-Y. Park, S.J. Yoon, H. Lee, J.-H. Yoon, J.-G. Shim, J.K. Lee, B.-Y. Min, H.-M. Eum, M.C. Kang, Solubility of carbon dioxide in aqueous solutions of 2-amino-2-ethyl-1,3-propanediol, *Fluid Phase Equilibria*, 202 (2002) 359-366.
- [374] S.H. Park, K.B. Lee, J.C. Hyun, S.H. Kim, Correlation and Prediction of the Solubility of Carbon Dioxide in Aqueous Alkanolamine and Mixed Alkanolamine Solutions, *Industrial & Engineering Chemistry Research*, 41 (2002) 1658-1665.
- [375] K.P. Shen, M.H. Li, Solubility of carbon dioxide in aqueous mixtures of monoethanolamine with methyldiethanolamine, *Journal of Chemical & Engineering Data*, 37 (1992) 96-100.
- [376] F.Y. Jou, F.D. Otto, A.E. Mather, Equilibria of H<sub>2</sub>S and CO<sub>2</sub> in triethanolamine solutions, *The Canadian Journal of Chemical Engineering*, 63 (1985) 122-125.
- [377] S. Ma'mun, R. Nilsen, H.F. Svendsen, O. Juliussen, Solubility of Carbon Dioxide in 30 mass % Monoethanolamine and 50 mass % Methyldiethanolamine Solutions, *Journal of Chemical & Engineering Data*, 50 (2005) 630-634.
- [378] F. Porcheron, A. Gibert, P. Mougin, A. Wender, High Throughput Screening of CO<sub>2</sub> Solubility in Aqueous Monoamine Solutions, *Environmental Science & Technology*, 45 (2011) 2486-2492.
- [379] I.S. Jane, M.-H. Li, Solubilities of Mixtures of Carbon Dioxide and Hydrogen Sulfide in Water + Diethanolamine + 2-Amino-2-methyl-1-propanol, *Journal of Chemical & Engineering Data*, 42 (1997) 98-105.
- [380] J. Gabrielsen, M.L. Michelsen, E.H. Stenby, G.M. Kontogeorgis, A Model for Estimating CO<sub>2</sub> Solubility in Aqueous Alkanolamines, *Industrial & Engineering Chemistry Research*, 44 (2005) 3348-3354.
- [381] M.Z. Haji-Sulaiman, M.K. Aroua, A. Benamor, Analysis of Equilibrium Data of CO<sub>2</sub> in Aqueous Solutions of Diethanolamine (DEA), Methyldiethanolamine (MDEA) and Their Mixtures Using the Modified Kent Eisenberg Model, *Chemical Engineering Research and Design*, 76 (1998) 961-968.
- [382] G. Vallée, P. Mougin, S. Jullian, W. Fürst, Representation of CO<sub>2</sub> and H<sub>2</sub>S Absorption by Aqueous Solutions of Diethanolamine Using an Electrolyte Equation of State, *Industrial & Engineering Chemistry Research*, 38 (1999) 3473-3480.
- [383] P.-Y. Chung, A.N. Soriano, R.B. Leron, M.-H. Li, Equilibrium solubility of carbon dioxide in the amine solvent system of (triethanolamine+&#xa0;+&#xa0;piperazine&#xa0;+&#xa0;water), *The Journal of Chemical Thermodynamics*, 42 (2010) 802-807.
- [384] M. Ramdin, T.Z. Olasagasti, T.J.H. Vlught, T.W. de Loos, High pressure solubility of CO<sub>2</sub> in non-fluorinated phosphonium-based ionic liquids, *The Journal of Supercritical Fluids*, 82 (2013) 41-49.
- [385] A. Yokozeki, M.B. Shiflett, C.P. Junk, L.M. Grieco, T. Foo, Physical and Chemical Absorptions of Carbon Dioxide in Room-Temperature Ionic Liquids, *The Journal of Physical Chemistry B*, 112 (2008) 16654-16663.
- [386] M.F. Costa Gomes, Low-Pressure Solubility and Thermodynamics of Solvation of Carbon Dioxide, Ethane, and Hydrogen in 1-Hexyl-3-methylimidazolium

Bis(trifluoromethylsulfonyl)amide between Temperatures of 283 K and 343 K, *Journal of Chemical & Engineering Data*, 52 (2007) 472-475.

[387] Y.S. Kim, W.Y. Choi, J.H. Jang, K.P. Yoo, C.S. Lee, Solubility measurement and prediction of carbon dioxide in ionic liquids, *Fluid Phase Equilibria*, 228–229 (2005) 439-445.

[388] Y.S. Kim, J.H. Jang, B.D. Lim, J.W. Kang, C.S. Lee, Solubility of mixed gases containing carbon dioxide in ionic liquids: Measurements and predictions, *Fluid Phase Equilibria*, 256 (2007) 70-74.

[389] J. Kumelan, Á. Pérez-Salado Kamps, D. Tuma, G. Maurer, Solubility of CO<sub>2</sub> in the ionic liquid [hmim][Tf<sub>2</sub>N], *The Journal of Chemical Thermodynamics*, 38 (2006) 1396-1401.

[390] S. Raeissi, L. Florusse, C.J. Peters, Scott–van Konynenburg phase diagram of carbon dioxide + alkylimidazolium-based ionic liquids, *The Journal of Supercritical Fluids*, 55 (2010) 825-832.

[391] W. Ren, B. Sensenich, A.M. Scurto, High-pressure phase equilibria of {carbon dioxide (CO<sub>2</sub>) + n-alkyl-imidazolium bis(trifluoromethylsulfonyl)amide} ionic liquids, *The Journal of Chemical Thermodynamics*, 42 (2010) 305-311.

[392] A.M. Schilderman, S. Raeissi, C.J. Peters, Solubility of carbon dioxide in the ionic liquid 1-ethyl-3-methylimidazolium bis(trifluoromethylsulfonyl)imide, *Fluid Phase Equilibria*, 260 (2007) 19-22.

[393] M.B. Shiflett, A. Yokozeki, Solubility of CO<sub>2</sub> in Room Temperature Ionic Liquid [hmim][Tf<sub>2</sub>N], *The Journal of Physical Chemistry B*, 111 (2007) 2070-2074.

[394] J.-H. Yim, J.S. Lim, CO<sub>2</sub> solubility measurement in 1-hexyl-3-methylimidazolium ([HMIM]) cation based ionic liquids, *Fluid Phase Equilibria*, 352 (2013) 67-74.

[395] W. Afzal, X. Liu, J.M. Prausnitz, Solubilities of some gases in four imidazolium-based ionic liquids, *The Journal of Chemical Thermodynamics*, 63 (2013) 88-94.

[396] P. Husson-Borg, V. Majer, M.F. Costa Gomes, Solubilities of Oxygen and Carbon Dioxide in Butyl Methyl Imidazolium Tetrafluoroborate as a Function of Temperature and at Pressures Close to Atmospheric Pressure, *Journal of Chemical & Engineering Data*, 48 (2003) 480-485.

[397] J. Jacquemin, M.F. Costa Gomes, P. Husson, V. Majer, Solubility of carbon dioxide, ethane, methane, oxygen, nitrogen, hydrogen, argon, and carbon monoxide in 1-butyl-3-methylimidazolium tetrafluoroborate between temperatures 283 K and 343 K and at pressures close to atmospheric, *The Journal of Chemical Thermodynamics*, 38 (2006) 490-502.

[398] M.C. Kroon, A. Shariati, M. Costantini, J. van Spronsen, G.-J. Witkamp, R.A. Sheldon, C.J. Peters, High-Pressure Phase Behavior of Systems with Ionic Liquids: Part V. The Binary System Carbon Dioxide + 1-Butyl-3-methylimidazolium Tetrafluoroborate, *Journal of Chemical & Engineering Data*, 50 (2005) 173-176.

[399] A.-L. Revelli, F. Mutelet, J.-N. Jaubert, High Carbon Dioxide Solubilities in Imidazolium-Based Ionic Liquids and in Poly(ethylene glycol) Dimethyl Ether, *The Journal of Physical Chemistry B*, 114 (2010) 12908-12913.

[400] M.B. Shiflett, A. Yokozeki, Solubilities and Diffusivities of Carbon Dioxide in Ionic Liquids: [bmim][PF<sub>6</sub>] and [bmim][BF<sub>4</sub>], *Industrial & Engineering Chemistry Research*, 44 (2005) 4453-4464.

[401] J. Jacquemin, P. Husson, V. Majer, M.F. Costa Gomes, Influence of the Cation on the Solubility of CO<sub>2</sub> and H<sub>2</sub> in Ionic Liquids Based on the Bis(trifluoromethylsulfonyl)imide Anion, *J Solution Chem*, 36 (2007) 967-979.

[402] P.J. Carvalho, V.H. Álvarez, I.M. Marrucho, M. Aznar, J.A.P. Coutinho, High pressure phase behavior of carbon dioxide in 1-butyl-3-methylimidazolium bis(trifluoromethylsulfonyl)imide and 1-butyl-3-methylimidazolium dicyanamide ionic liquids, *The Journal of Supercritical Fluids*, 50 (2009) 105-111.

- [403] F. Karadas, B. Köz, J. Jacquemin, E. Deniz, D. Rooney, J. Thompson, C.T. Yavuz, M. Khraisheh, S. Aparicio, M. Atihan, High pressure CO<sub>2</sub> absorption studies on imidazolium-based ionic liquids: Experimental and simulation approaches, *Fluid Phase Equilibria*, 351 (2013) 74-86.
- [404] B.-C. Lee, S.L. Outcalt, Solubilities of Gases in the Ionic Liquid 1-n-Butyl-3-methylimidazolium Bis(trifluoromethylsulfonyl)imide, *Journal of Chemical & Engineering Data*, 51 (2006) 892-897.
- [405] M.S. Manic, A.J. Queimada, E.A. Macedo, V. Najdanovic-Visak, High-pressure solubilities of carbon dioxide in ionic liquids based on bis(trifluoromethylsulfonyl)imide and chloride, *The Journal of Supercritical Fluids*, 65 (2012) 1-10.
- [406] D.-J. Oh, B.-C. Lee, High-pressure phase behavior of carbon dioxide in ionic liquid 1-butyl-3-methylimidazolium bis(trifluoromethylsulfonyl)imide, *Korean J. Chem. Eng.*, 23 (2006) 800-805.
- [407] S. Raeissi, C.J. Peters, Carbon Dioxide Solubility in the Homologous 1-Alkyl-3-methylimidazolium Bis(trifluoromethylsulfonyl)imide Family, *Journal of Chemical & Engineering Data*, 54 (2009) 382-386.
- [408] E.-K. Shin, B.-C. Lee, J.S. Lim, High-pressure solubilities of carbon dioxide in ionic liquids: 1-Alkyl-3-methylimidazolium bis(trifluoromethylsulfonyl)imide, *The Journal of Supercritical Fluids*, 45 (2008) 282-292.
- [409] S. Zhang, X. Yuan, Y. Chen, X. Zhang, Solubilities of CO<sub>2</sub> in 1-Butyl-3-methylimidazolium Hexafluorophosphate and 1,1,3,3-Tetramethylguanidium Lactate at Elevated Pressures, *Journal of Chemical & Engineering Data*, 50 (2005) 1582-1585.
- [410] L.A. Blanchard, Z. Gu, J.F. Brennecke, High-Pressure Phase Behavior of Ionic Liquid/CO<sub>2</sub> Systems, *The Journal of Physical Chemistry B*, 105 (2001) 2437-2444.
- [411] J. Jacquemin, P. Husson, V. Majer, M.F.C. Gomes, Low-pressure solubilities and thermodynamics of solvation of eight gases in 1-butyl-3-methylimidazolium hexafluorophosphate, *Fluid Phase Equilibria*, 240 (2006) 87-95.
- [412] J.E. Kim, J.S. Lim, J.W. Kang, Measurement and correlation of solubility of carbon dioxide in 1-alkyl-3-methylimidazolium hexafluorophosphate ionic liquids, *Fluid Phase Equilibria*, 306 (2011) 251-255.
- [413] J. Kumelan, Á. Pérez-Salado Kamps, D. Tuma, G. Maurer, Solubility of CO<sub>2</sub> in the Ionic Liquids [bmim][CH<sub>3</sub>SO<sub>4</sub>] and [bmim][PF<sub>6</sub>], *Journal of Chemical & Engineering Data*, 51 (2006) 1802-1807.
- [414] Á. Pérez-Salado Kamps, D. Tuma, J. Xia, G. Maurer, Solubility of CO<sub>2</sub> in the Ionic Liquid [bmim][PF<sub>6</sub>], *Journal of Chemical & Engineering Data*, 48 (2003) 746-749.
- [415] A. Shariati, K. Gutkowski, C.J. Peters, Comparison of the phase behavior of some selected binary systems with ionic liquids, *AIChE Journal*, 51 (2005) 1532-1540.
- [416] M.B. Shiflett, A. Yokozeki, Solubility and diffusivity of hydrofluorocarbons in room-temperature ionic liquids, *AIChE Journal*, 52 (2006) 1205-1219.
- [417] P.J. Carvalho, V.H. Álvarez, B. Schröder, A.M. Gil, I.M. Marrucho, M. Aznar, L.M.N.B.F. Santos, J.A.P. Coutinho, Specific Solvation Interactions of CO<sub>2</sub> on Acetate and Trifluoroacetate Imidazolium Based Ionic Liquids at High Pressures, *The Journal of Physical Chemistry B*, 113 (2009) 6803-6812.
- [418] M.B. Shiflett, D.J. Kasprzak, C.P. Junk, A. Yokozeki, Phase behavior of {carbon dioxide + [bmim][Ac]} mixtures, *The Journal of Chemical Thermodynamics*, 40 (2008) 25-31.
- [419] P.J. Carvalho, V.H. Álvarez, I.M. Marrucho, M. Aznar, J.A.P. Coutinho, High carbon dioxide solubilities in trihexyltetradecylphosphonium-based ionic liquids, *The Journal of Supercritical Fluids*, 52 (2010) 258-265.



- [420] M. Costantini, V.A. Toussaint, A. Shariati, C.J. Peters, I. Kikic, High-Pressure Phase Behavior of Systems with Ionic Liquids: Part IV. Binary System Carbon Dioxide + 1-Hexyl-3-methylimidazolium Tetrafluoroborate, *Journal of Chemical & Engineering Data*, 50 (2005) 52-55.
- [421] S. Mattedi, P.J. Carvalho, J.A.P. Coutinho, V.H. Alvarez, M. Iglesias, High pressure CO<sub>2</sub> solubility in N-methyl-2-hydroxyethylammonium protic ionic liquids, *The Journal of Supercritical Fluids*, 56 (2011) 224-230.
- [422] H.N. Song, B.-C. Lee, J.S. Lim, Measurement of CO<sub>2</sub> Solubility in Ionic Liquids: [BMP][TfO] and [P14,6,6,6][Tf<sub>2</sub>N] by Measuring Bubble-Point Pressure, *Journal of Chemical & Engineering Data*, 55 (2010) 891-896.
- [423] J.-H. Yim, H.N. Song, B.-C. Lee, J.S. Lim, High-pressure phase behavior of binary mixtures containing ionic liquid [HMP][Tf<sub>2</sub>N], [OMP][Tf<sub>2</sub>N] and carbon dioxide, *Fluid Phase Equilibria*, 308 (2011) 147-152.
- [424] A.H. Jalili, M. Safavi, C. Ghotbi, A. Mehdizadeh, M. Hosseini-Jenab, V. Taghikhani, Solubility of CO<sub>2</sub>, H<sub>2</sub>S, and Their Mixture in the Ionic Liquid 1-Octyl-3-methylimidazolium Bis(trifluoromethyl)sulfonylimide, *The Journal of Physical Chemistry B*, 116 (2012) 2758-2774.
- [425] M.D. Bermejo, T.M. Fieback, Á. Martín, Solubility of gases in 1-alkyl-3-methylimidazolium alkyl sulfate ionic liquids: Experimental determination and modeling, *The Journal of Chemical Thermodynamics*, 58 (2013) 237-244.
- [426] M.B. Shiflett, A. Yokozeki, Phase Behavior of Carbon Dioxide in Ionic Liquids: [emim][Acetate], [emim][Trifluoroacetate], and [emim][Acetate] + [emim][Trifluoroacetate] Mixtures, *Journal of Chemical & Engineering Data*, 54 (2009) 108-114.
- [427] R. Bogel-Lukasik, D. Matkowska, E. Bogel-Lukasik, T. Hofman, Isothermal vapour-liquid equilibria in the binary and ternary systems consisting of an ionic liquid, 1-propanol and CO<sub>2</sub>, *Fluid Phase Equilibria*, 293 (2010) 168-174.
- [428] K.A. Kurnia, F. Harris, C.D. Wilfred, M.I. Abdul Mutalib, T. Murugesan, Thermodynamic properties of CO<sub>2</sub> absorption in hydroxyl ammonium ionic liquids at pressures of (100–1600) kPa, *The Journal of Chemical Thermodynamics*, 41 (2009) 1069-1073.
- [429] X. Yuan, S. Zhang, J. Liu, X. Lu, Solubilities of CO<sub>2</sub> in hydroxyl ammonium ionic liquids at elevated pressures, *Fluid Phase Equilibria*, 257 (2007) 195-200.
- [430] A. Tagiuri, K.Z. Sumon, A. Henni, Solubility of carbon dioxide in three [Tf<sub>2</sub>N] ionic liquids, *Fluid Phase Equilibria*, 380 (2014) 39-47.
- [431] A.N. Soriano, B.T. Doma, M.-H. Li, Solubility of Carbon Dioxide in 1-Ethyl-3-methylimidazolium Tetrafluoroborate, *Journal of Chemical & Engineering Data*, 53 (2008) 2550-2555.
- [432] A. Shariati, C.J. Peters, High-pressure phase behavior of systems with ionic liquids: Part III. The binary system carbon dioxide + 1-hexyl-3-methylimidazolium hexafluorophosphate, *The Journal of Supercritical Fluids*, 30 (2004) 139-144.
- [433] M. Shokouhi, M. Adibi, A.H. Jalili, M. Hosseini-Jenab, A. Mehdizadeh, Solubility and Diffusion of H<sub>2</sub>S and CO<sub>2</sub> in the Ionic Liquid 1-(2-Hydroxyethyl)-3-methylimidazolium Tetrafluoroborate, *Journal of Chemical & Engineering Data*, 55 (2010) 1663-1668.
- [434] M. Safavi, C. Ghotbi, V. Taghikhani, A.H. Jalili, A. Mehdizadeh, Study of the solubility of CO<sub>2</sub>, H<sub>2</sub>S and their mixture in the ionic liquid 1-octyl-3-methylimidazolium hexafluorophosphate: Experimental and modelling, *The Journal of Chemical Thermodynamics*, 65 (2013) 220-232.
- [435] E.-K. Shin, B.-C. Lee, High-Pressure Phase Behavior of Carbon Dioxide with Ionic Liquids: 1-Alkyl-3-methylimidazolium Trifluoromethanesulfonate, *Journal of Chemical & Engineering Data*, 53 (2008) 2728-2734.

- [436] J.E. Kim, H.J. Kim, J.S. Lim, Solubility of CO<sub>2</sub> in ionic liquids containing cyanide anions: [c2mim][SCN], [c2mim][N(CN)<sub>2</sub>], [c2mim][C(CN)<sub>3</sub>], *Fluid Phase Equilibria*, 367 (2014) 151-158.
- [437] S.A. Kim, J.-H. Yim, J.S. Lim, High-pressure phase behavior of binary mixtures containing methylpyrrolidinium derivative ionic liquids and carbon dioxide, *Fluid Phase Equilibria*, 332 (2012) 28-34.
- [438] K.I. Gutkowski, A. Shariati, C.J. Peters, High-pressure phase behavior of the binary ionic liquid system 1-octyl-3-methylimidazolium tetrafluoroborate + carbon dioxide, *The Journal of Supercritical Fluids*, 39 (2006) 187-191.
- [439] A. Shariati, C.J. Peters, High-pressure phase behavior of systems with ionic liquids: II. The binary system carbon dioxide+1-ethyl-3-methylimidazolium hexafluorophosphate, *The Journal of Supercritical Fluids*, 29 (2004) 43-48.
- [440] S.O. Nwosu, J.C. Schleicher, A.M. Scurto, High-pressure phase equilibria for the synthesis of ionic liquids in compressed CO<sub>2</sub> for 1-hexyl-3-methylimidazolium bromide with 1-bromohexane and 1-methylimidazole, *The Journal of Supercritical Fluids*, 51 (2009) 1-9.
- [441] M. Zoubeik, A. Henni, Experimental and thermodynamic study of CO<sub>2</sub> solubility in promising [TF<sub>2</sub>N and DCN] ionic liquids, *Fluid Phase Equilibria*, 376 (2014) 22-30.
- [442] S. Jang, D.-W. Cho, T. Im, H. Kim, High-pressure phase behavior of CO<sub>2</sub> + 1-butyl-3-methylimidazolium chloride system, *Fluid Phase Equilibria*, 299 (2010) 216-221.
- [443] S. Bishnoi, G.T. Rochelle, Absorption of carbon dioxide into aqueous piperazine: reaction kinetics, mass transfer and solubility, *Chemical Engineering Science*, 55 (2000) 5531-5543.
- [444] P.W.J. Derks, H.B.S. Dijkstra, J.A. Hogendoorn, G.F. Versteeg, Solubility of carbon dioxide in aqueous piperazine solutions, *AIChE Journal*, 51 (2005) 2311-2327.
- [445] Á.P.-S. Kamps, J. Xia, G. Maurer, Solubility of CO<sub>2</sub> in (H<sub>2</sub>O+piperazine) and in (H<sub>2</sub>O+MDEA+piperazine), *AIChE Journal*, 49 (2003) 2662-2670.
- [446] T. Nguyen, M. Hilliard, G.T. Rochelle, Amine volatility in CO<sub>2</sub> capture, *International Journal of Greenhouse Gas Control*, 4 (2010) 707-715.
- [447] J.J. Rathmell, F.I. Stalkup, R.C. Hassinger, A Laboratory Investigation of Miscible Displacement by Carbon Dioxide, in: *Fall meeting of the society of petroleum engineers of AIME, Society of Petroleum Engineers, New Orleans, Louisiana, 1971.*
- [448] E.M.E.-M. Shokir, CO<sub>2</sub>-oil minimum miscibility pressure model for impure and pure CO<sub>2</sub> streams, *Journal of Petroleum Science and Engineering*, 58 (2007) 173-185.
- [449] B.E. Eakin, F.J. Mitch, Measurement and Correlation of Miscibility Pressures of Reservoir Oils, in: *SPE Annual Technical Conference and Exhibition, Society of Petroleum Engineers, Houston, Texas, 1988.*
- [450] R.A. Harmon, R.B. Grigg, Vapor-Density Measurement for Estimating Minimum Miscibility Pressure(includes associated papers 19118 and 19500 ), *SPE Reservoir Engineering*, 3 (1988).
- [451] H.A. Jacobson, Acid Gases And Their Contribution to Miscibility, *Journal of Canadian Petroleum Technology*, 11 (1972).
- [452] R.S. Metcalfe, Effects of Impurities on Minimum Miscibility Pressures and Minimum Enrichment Levels for CO<sub>2</sub> and Rich-Gas Displacements, *Society of Petroleum Engineers Journal*, 22 (1982).
- [453] G.C. Thakur, C.J. Lin, Y.R. Patel, CO<sub>2</sub> Minitest, Little Knife Field, ND: A Case History, in: *SPE Enhanced Oil Recovery Symposium, Society of Petroleum Engineers, Oklahoma, 1984.*
- [454] R.B.C. Gharbi, A.M. Elsharkawy, Neural Network Model for Estimating the PVT Properties of Middle East Crude Oils, *SPE Reservoir Evaluation & Engineering*, 2 (1999).

- [455] M. Dong, S. Huang, S.B. Dyer, F.M. Mourits, A comparison of CO<sub>2</sub> minimum miscibility pressure determinations for Weyburn crude oil, *Journal of Petroleum Science and Engineering*, 31 (2001) 13-22.
- [456] J. Bon, M.K. Emera, H.K. Sarma, An Experimental Study and Genetic Algorithm (GA) Correlation to Explore the Effect of nC<sub>5</sub> on Impure CO<sub>2</sub> Minimum Miscibility Pressure (MMP), in: *SPE Asia Pacific Oil & Gas Conference and Exhibition*, Society of Petroleum Engineers, Adelaide, Australia, 2006.
- [457] H. Saghafi, M.M. Ghiasi, A.H. Mohammadi, Analyzing the experimental data of CO<sub>2</sub> equilibrium absorption in the aqueous solution of DEA+MDEA with Random Forest and Leverage method, *International Journal of Greenhouse Gas Control*, 63 (2017) 329-337.
- [458] M.M. Ghiasi, Y. Noorollahi, A. Aslani, CO<sub>2</sub> hydrate: Modeling of incipient stability conditions and dissociation enthalpy, *Petroleum Science and Technology*, 36 (2018) 259-265.
- [459] J.O. Valderrama, P.A. Robles, Critical Properties, Normal Boiling Temperatures, and Acentric Factors of Fifty Ionic Liquids, *Industrial & Engineering Chemistry Research*, 46 (2007) 1338-1344.
- [460] A. Baghban, A.H. Mohammadi, M.S. Taleghani, Rigorous modeling of CO<sub>2</sub> equilibrium absorption in ionic liquids, *International Journal of Greenhouse Gas Control*, 58 (2017) 19-41.
- [461] J.W. Mason, B.F. Dodge, Equilibrium absorption of carbon dioxide by solutions of the ethanolamines *Trans AICHE*, 32 (1936) 27-47.
- [462] J.A. Heist, T.S. Barron, *Freeze Crystallization Processes: Efficiency by Flexibility*, in, Energy Systems Laboratory, Texas A&M University USA, 1983.
- [463] J.B. Phillips, H. Nguyen, V.T. John, Protein Recovery from Reversed Micellar Solutions through Contact with a Pressurized Gas Phase, *Biotechnology Progress*, 7 (1991) 43-48.
- [464] Y.A. Purwanto, S. Oshita, Y. Seo, Y. Kawagoe, Concentration of liquid foods by the use of gas hydrate, *Journal of Food Engineering*, 47 (2001) 133-138.
- [465] S. Li, F. Qi, K. Du, Y. Shen, D. Liu, L. Fan, An energy-efficient juice concentration technology by ethylene hydrate formation, *Separation and Purification Technology*, 173 (2017) 80-85.
- [466] C.P. Huang, O. Fennema, W.D. Powrie, Gas hydrates in aqueous-organic systems, *Cryobiology*, 2 (1966) 240-245.
- [467] C.P. Huang, O. Fennema, W.D. Powrie, Gas hydrates in aqueous-organic systems, *Cryobiology*, 2 (1965) 109-115.
- [468] M.-K. Chun, H. Lee, Phase equilibria of R22 (CHClF<sub>2</sub>) hydrate system in the presence of sucrose, glucose and lactic acid, *Fluid Phase Equilibria*, 150–151 (1998) 361-370.
- [469] M.-K. Chun, H. Lee, Phase Equilibria of Carbon Dioxide Hydrate System in the Presence of Sucrose, Glucose, and Fructose, *Journal of Chemical & Engineering Data*, 44 (1999) 1081-1084.
- [470] A. Smith, S. Babaei, A.H. Mohammadi, P. Naidoo, D. Ramjugernath, Clathrate hydrate dissociation conditions for refrigerant + sucrose aqueous solution: Experimental measurement and thermodynamic modelling, *Fluid Phase Equilibria*, 413 (2016) 99-109.
- [471] J. Javanmardi, M. Moshfeghian, R.N. Maddox, Simple Method for Predicting Gas-Hydrate-Forming Conditions in Aqueous Mixed-Electrolyte Solutions, *Energy & Fuels*, 12 (1998) 219-222.
- [472] Y. Jin, M. Kida, Y. Konno, J. Nagao, Clathrate Hydrate Equilibrium in Methane–Water Systems with the Addition of Monosaccharide and Sugar Alcohol, *Journal of Chemical & Engineering Data*, 62 (2017) 440-444.

- [473] A.S. Carbone, Inhibition Effects of Glucose on Clathrate Hydrate (H-Lw-V) Equilibrium, in: Department of Chemical Engineering, McGill University, Montreal, Quebec, Canada, 2011.
- [474] D.B. Robinson, B.R. Metha, Hydrates In the PropaneCarbon Dioxide- Water System, *Journal of Canadian Petroleum Technology*, 10 (1971).
- [475] P. Englezos, S. Hall, Phase equilibrium data on carbon dioxide hydrate in the presence of electrolytes, water soluble polymers and montmorillonite, *The Canadian Journal of Chemical Engineering*, 72 (1994) 887-893.
- [476] P.D. Dholabhai, J.S. Parent, P.R. Bishnoi, Carbon Dioxide Hydrate Equilibrium Conditions in Aqueous Solutions Containing Electrolytes and Methanol Using a New Apparatus, *Industrial & Engineering Chemistry Research*, 35 (1996) 819-823.
- [477] P.D. Dholabhai, J. Scott Parent, P. Raj Bishnoi, Equilibrium conditions for hydrate formation from binary mixtures of methane and carbon dioxide in the presence of electrolytes, methanol and ethylene glycol, *Fluid Phase Equilibria*, 141 (1997) 235-246.
- [478] S.-S. Fan, T.-M. Guo, Hydrate Formation of CO<sub>2</sub>-Rich Binary and Quaternary Gas Mixtures in Aqueous Sodium Chloride Solutions, *Journal of Chemical & Engineering Data*, 44 (1999) 829-832.
- [479] M.M. Mooijer-van den Heuvel, R. Witteman, C.J. Peters, Phase behaviour of gas hydrates of carbon dioxide in the presence of tetrahydropyran, cyclobutanone, cyclohexane and methylcyclohexane, *Fluid Phase Equilibria*, 182 (2001) 97-110.
- [480] J.-w. Lee, M.-K. Chun, K.-M. Lee, Y.-J. Kim, H. Lee, Phase equilibria and kinetic behavior of co<sub>2</sub> hydrate in electrolyte and porous media solutions: application to ocean sequestration of CO<sub>2</sub>, *Korean J. Chem. Eng.*, 19 (2002) 673-678.
- [481] V. Belandria, A.H. Mohammadi, D. Richon, Phase equilibria of clathrate hydrates of methane + carbon dioxide: New experimental data and predictions, *Fluid Phase Equilibria*, 296 (2010) 60-65.
- [482] S. Li, S. Fan, J. Wang, X. Lang, Y. Wang, Semiclathrate Hydrate Phase Equilibria for CO<sub>2</sub> in the Presence of Tetra-n-butyl Ammonium Halide (Bromide, Chloride, or Fluoride), *Journal of Chemical & Engineering Data*, 55 (2010) 3212-3215.
- [483] Y. Matsui, Y. Ogura, H. Miyauchi, T. Makino, T. Sugahara, K. Ohgaki, Isothermal Phase Equilibria for Binary Hydrate Systems of Carbon Dioxide + Ethane and Carbon Dioxide + Tetrafluoromethane, *Journal of Chemical & Engineering Data*, 55 (2010) 3297-3301.
- [484] T. Maekawa, Equilibrium conditions of clathrate hydrates formed from carbon dioxide and aqueous acetone solutions, *Fluid Phase Equilibria*, 303 (2011) 76-79.
- [485] T. Maekawa, Equilibrium conditions for clathrate hydrates formed from carbon dioxide or ethane in the presence of aqueous solutions of 1,4-dioxane and 1,3-dioxolane, *Fluid Phase Equilibria*, 384 (2014) 95-99.
- [486] L. Zha, D.-Q. Liang, D.-L. Li, Phase equilibria of CO<sub>2</sub> hydrate in NaCl–MgCl<sub>2</sub> aqueous solutions, *The Journal of Chemical Thermodynamics*, 55 (2012) 110-114.
- [487] Y.-J. Lee, T. Kawamura, Y. Yamamoto, J.-H. Yoon, Phase Equilibrium Studies of Tetrahydrofuran (THF) + CH<sub>4</sub>, THF + CO<sub>2</sub>, CH<sub>4</sub> + CO<sub>2</sub>, and THF + CO<sub>2</sub> + CH<sub>4</sub> Hydrates, *Journal of Chemical & Engineering Data*, 57 (2012) 3543-3548.
- [488] S. Suzuki, K. Yasuda, Y. Katsuta, Y. Matsumoto, S. Hashimoto, T. Sugahara, K. Ohgaki, Isothermal Phase Equilibria for the CO<sub>2</sub> + 1,1,1,2-Tetrafluoroethane and CO<sub>2</sub> + 1,1-Difluoroethane Mixed-Gas Hydrate Systems, *Journal of Chemical & Engineering Data*, 58 (2013) 780-784.

- [489] A. Djavidnia, A.A. Izadpanah, M.V. Sefti, F. Varaminian, The Equilibrium Data and Thermodynamic Modeling of Hydrate Formation for CO<sub>2</sub> and Mixtures of CO<sub>2</sub> and CH<sub>4</sub> in the Presence of Methanol, *Petroleum Science and Technology*, 31 (2013) 2013-2021.
- [490] Z.-C. Xu, D.-Q. Liang, Equilibrium Data of (tert-Butylamine + CO<sub>2</sub>) and (tert-Butylamine + N<sub>2</sub>) Clathrate Hydrates, *Journal of Chemical & Engineering Data*, 59 (2014) 476-480.
- [491] X.-D. Shen, Z. Long, L.-l. Shi, D.-Q. Liang, Phase Equilibria of CO<sub>2</sub> Hydrate in the Aqueous Solutions of N-Butyl-N-methylpyrrolidinium Bromide, *Journal of Chemical & Engineering Data*, 60 (2015) 3392-3396.
- [492] Y. Nema, R. Ohmura, I. Senaha, K. Yasuda, Quadruple point determination in carbon dioxide hydrate forming system, *Fluid Phase Equilibria*, (2016).
- [493] J.-H. Cha, S.-P. Kang, S. Han, J.W. Kang, K.-S. Kim, Phase equilibria of CH<sub>4</sub> and CO<sub>2</sub> hydrates formed from aqueous solutions of glutaric acid and malonic acid, *Fluid Phase Equilibria*, 413 (2016) 71-74.
- [494] P. Ilani-Kashkouli, A.H. Mohammadi, P. Naidoo, D. Ramjugernath, Hydrate phase equilibria for CO<sub>2</sub>, CH<sub>4</sub>, or N<sub>2</sub> + tetrabutylphosphonium bromide (TBPB) aqueous solution, *Fluid Phase Equilibria*, 411 (2016) 88-92.
- [495] M. Mohammadi, A. Haghtalab, Z. Fakhroueian, Experimental study and thermodynamic modeling of CO<sub>2</sub> gas hydrate formation in presence of zinc oxide nanoparticles, *The Journal of Chemical Thermodynamics*, 96 (2016) 24-33.
- [496] Y.-s. Yu, S.-d. Zhou, X.-s. Li, S.-l. Wang, Effect of graphite nanoparticles on CO<sub>2</sub> hydrate phase equilibrium, *Fluid Phase Equilibria*, 414 (2016) 23-28.
- [497] M. Wang, Z.-G. Sun, C.-H. Li, A.-J. Zhang, J. Li, C.-M. Li, H.-F. Huang, Equilibrium Hydrate Dissociation Conditions of CO<sub>2</sub> + HCFC141b or Cyclopentane, *Journal of Chemical & Engineering Data*, 61 (2016) 3250-3253.
- [498] J. Bai, L. Zhang, J. Li, T.-b. Liang, C. Chang, S.-q. Fang, X.-l. Han, D. Liang, Phase Equilibria of CO<sub>2</sub> Hydrate Formation in Glucoamylase Aqueous Solutions, *Journal of Chemical & Engineering Data*, 61 (2016) 891-895.
- [499] D. Sun, J. Ripmeester, P. Englezos, Phase Equilibria for the CO<sub>2</sub>/CH<sub>4</sub>/N<sub>2</sub>/H<sub>2</sub>O System in the Hydrate Region under Conditions Relevant to Storage of CO<sub>2</sub> in Depleted Natural Gas Reservoirs, *Journal of Chemical & Engineering Data*, 61 (2016) 4061-4067.
- [500] M.S. Khan, B. Lal, B. Partoon, L.K. Keong, A.B. Bustam, N.B. Mellon, Experimental Evaluation of a Novel Thermodynamic Inhibitor for CH<sub>4</sub> and CO<sub>2</sub> Hydrates, *Procedia Engineering*, 148 (2016) 932-940.
- [501] M. Wang, Z.-G. Sun, X.-H. Qiu, M.-G. Zhu, C.-H. Li, A.-J. Zhang, J. Li, C.-M. Li, H.-F. Huang, Hydrate Dissociation Equilibrium Conditions for Carbon Dioxide + Tetrahydrofuran, *Journal of Chemical & Engineering Data*, 62 (2017) 812-815.
- [502] J.D. Hoffman, *Numerical methods for engineers and scientists*, 2nd ed., Marcel Dekker, Inc., USA, 2001.
- [503] M.M. Ghiasi, A. Bahadori, A new correlation for accurate estimation of natural gases water content, *Petroleum & Coal*, 56 (2014) 582-594.
- [504] M. Margules, Über die Zusammensetzung der gesättigten Dämpfe von Mischungen, *Sitzungsberichte der Kaiserliche Akademie der Wissenschaften Wien Mathematisch-Naturwissenschaftliche Klasse*, 104 (1895) 1243-1278.
- [505] N.A. Gokcen, Gibbs-duhem-margules laws, *Journal of Phase Equilibria*, 17 (1996) 50-51.
- [506] R. Clausius, Ueber die bewegende Kraft der Wärme und die Gesetze, welche sich daraus für die Wärmelehre selbst ableiten lassen, *Annalen der Physik*, 155 (1850) 500-524.

- [507] M.C. Clapeyron, Mémoire sur la puissance motrice de la chaleur, *Journal de l'École polytechnique*, 23 (1834) 153-190.
- [508] A.T. Bozzo, C. Hsiao-Sheng, J.R. Kass, A.J. Barduhn, The properties of the hydrates of chlorine and carbon dioxide, *Desalination*, 16 (1975) 303-320.
- [509] J.-H. Yoon, Y. Yamamoto, T. Komai, H. Haneda, T. Kawamura, Rigorous Approach to the Prediction of the Heat of Dissociation of Gas Hydrates, *Industrial & Engineering Chemistry Research*, 42 (2003) 1111-1114.
- [510] S.P. Kang, H. Lee, B.J. Ryu, Enthalpies of dissociation of clathrate hydrates of carbon dioxide, nitrogen, (carbon dioxide + nitrogen), and (carbon dioxide + nitrogen + tetrahydrofuran), *The Journal of Chemical Thermodynamics*, 33 (2001) 513-521.
- [511] T. Uchida, A. Takagi, J. Kawabata, S. Mae, T. Hondoh, Raman spectroscopic analyses of the growth process of CO<sub>2</sub> hydrates, *Energy Conversion and Management*, 36 (1995) 547-550.
- [512] G.K. Anderson, Enthalpy of dissociation and hydration number of carbon dioxide hydrate from the Clapeyron equation, *Journal of Chemical Thermodynamics*, 35 (2003) 1171-1183.
- [513] S. Li, Y. Shen, D. Liu, W. Li, Experimental study of concentration of tomato juice by CO<sub>2</sub> hydrate formation, *Chemical Industry and Chemical Engineering Quarterly*, 21 (2015) 441-446.
- [514] S. Li, Y. Shen, D. Liu, L. Fan, Z. Tan, Concentrating orange juice through CO<sub>2</sub> clathrate hydrate technology, *Chemical Engineering Research and Design*, 93 (2015) 773-778.

## Appendix A

### Phase Equilibria of Methane and Carbon Dioxide Hydrates in Sugar Aqueous Solutions: Modeling Using a Semi-Theoretical Framework

#### 1. Introduction

In the realm of food processing and engineering, several studies have been done investigating the application of gas hydrate technology as an alternative to the conventional processes. For example, Heist and Barron [462] reported that using the gas hydrate technology results in a reduction in energy consumption for separation of aqueous solutions through evaporation by 70-90%. Phillips et al. [463] proposed a method for protein recovery from solutions of reversed micellar using the hydrate formation. Purwanto et al. [464] studied the concentration of coffee solutions by the use of xenon hydrate. Li et al. [465] proposed the use of ethane hydrate for concentrating orange juice. The use of bromomethane ( $\text{CH}_3\text{Br}$ ) and trichlorofluoromethane ( $\text{CCl}_3\text{F}$ ) hydrates for concentration of the aqueous solutions of carbohydrates, lipids, and proteins are studied by Huang et al. [466, 467]. Chun and Lee [468] studied the equilibrium conditions of hydrate of chlorodifluoromethane ( $\text{CHClF}_2$ ), also known as R22, in glucose, sucrose, and lactic acid solutions. In another work, Chun and Lee [469] investigated the possibility of concentration of glucose, sucrose, and fructose aqueous solutions by means of carbon dioxide hydrate. Further works on the subject of utilization of hydrates in the food industry have been reviewed by Smith et al. [470].

In continuation of our previous study on the semi-theoretical modeling of a gas hydrate phase equilibria in the presence of an inhibitor containing aqueous solution, we present here a new model for carbon dioxide hydrate incipient stability conditions in aqueous solutions of glucose, sucrose, or fructose that is on the basis of the previously proposed thermodynamic-based framework. This study also introduces an extension of the published model for methane hydrate with the aim of representing/predicting the methane hydrate formation/dissociation conditions in glucose, xylose, and xylitol aqueous solutions. Molecular formula and structure of the aforesaid sugars are given in **Table A.1**. Furthermore, the inhibition effects of tomato and orange juices on the phase equilibrium of carbon dioxide hydrate are investigated.

## 2. Modeling framework for CH<sub>4</sub> hydrate

As described in the original work [35], Eq. (A.1) represents the Clausius-Clapeyron equation. This equation can be employed for calculations related to the solid-gas phase changes like gas hydrate formation/dissociation.

$$\frac{d(\ln(P))}{dT_0} = \frac{\Delta H}{ZRT_0^2} \dots\dots\dots (A.1)$$

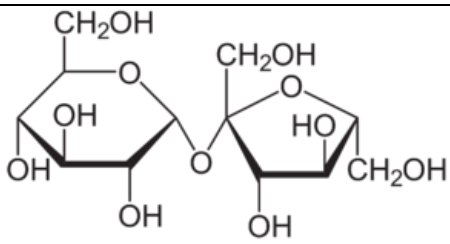
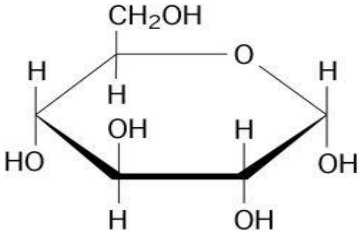
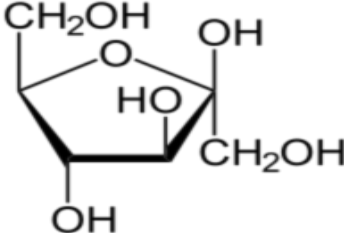
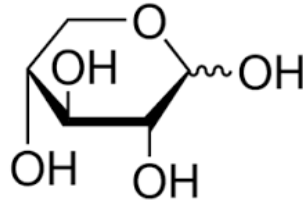
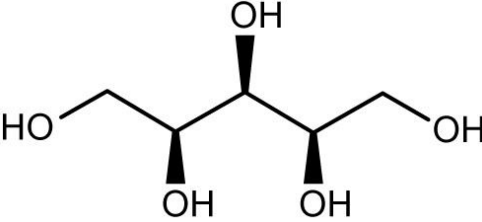
where  $P$  is the pressure of the system;  $T_0$  denotes the incipient hydrate formation/dissociation temperature (HFDT) in pure water;  $Z$  is the compressibility factor; and  $R$  is the gas constant.

In the case of methane hydrate in pure water, the following expression has been proposed by Ghiasi and Mohammadi [35] to represent the left side of Eq. (A.1):

$$\frac{d(\ln(P))}{dT_0} = \frac{64341.4059}{T_0^2} - \frac{15726211.6348}{T_0^3} \dots\dots\dots (A.2)$$



**Table A.1:** Information about the investigated sugars

Name	Formula	Structure
Sucrose	$C_{12}H_{22}O_{11}$	
Glucose	$C_6H_{12}O_6$	
Fructose	$C_6H_{12}O_6$	
Xylose	$C_5H_{10}O_5$	
Xylitol	$C_5H_{12}O_5$	

According to the works by Maddox et al. [80] and Javanmardi et al. [471], the effect of a thermodynamic inhibitor on the formation/dissociation temperature of the natural gas hydrate can be described as follows:

$$\ln(a_w) = \frac{\Delta H}{NR} \left( \frac{1}{T_0} - \frac{1}{T} \right) \dots\dots\dots (A.3)$$

in which  $T$  is the HFDT in the presence of aqueous solution of an inhibitor;  $\Delta H$  and  $N$  denote the hydrate formation/dissociation enthalpy and the number of water molecules in the hydrate; and  $a_w$  is the water activity. From thermodynamics we know that:

$$\ln(a_w) = \ln(x_w \cdot \gamma_w) = \ln(x_w) + \ln(\gamma_w) \dots\dots\dots (A.4)$$

where  $\gamma_w$  indicates the water activity coefficient and  $x_w$  is mole fraction of the water. Eq. (A.5) gives the relationship between the mole fractions of water and inhibitor,  $x_{in}$ .

$$x_w = 1 - x_{in} \dots\dots\dots (A.5)$$

The following equation is the two-suffix Margules activity model that can be used to estimate the value of the water activity coefficient:

$$\ln(\gamma_w) = \frac{A}{RT} x_{in} \dots\dots\dots (A.6)$$

where  $A$  is constant. In the original work [35], the values of  $A$  are obtained for aqueous solutions of NaCl, KCl, CaCl<sub>2</sub>, MgCl<sub>2</sub>, 1-propanol, 2-propanol, methanol, ethylene glycol, diethylene glycol, and triethylene glycol.

By combining the aforementioned equations, the following semi-theoretical formula has been developed by Ghiasi and Mohammadi [35] to predict/represent the methane HFDT in the presence of an inhibitor:

$$T_{CH_4} = \frac{Z \times R \times \left( 11189.8097 - \frac{2734993.3278}{T_0} \right) + A \times x_{in}^2}{Z \times R \times \left( \frac{11189.8097}{T_0} - \frac{2734993.3278}{T_0^2} \right) - R \times \ln(1 - x_{in})} \dots\dots\dots (A.7)$$

With the objective of finding the Margules coefficient for methane hydrate systems including CH<sub>4</sub>+xylose+water, CH<sub>4</sub>+xylitol+water, and CH<sub>4</sub>+glucose+water, the experimental phase equilibrium data have been collected from literature [472, 473]. The operating ranges of temperature, pressure, and concentration of the aforementioned additives in the aqueous phase of the system are tabulated in **Table A.2**. Similar to the original work [35], the following correlation is used to predict the formation/dissociation temperature of the methane hydrate in pure water:

$$T_0 = c_0 + c_1 \ln(P) + c_2 \ln(P)^2 + c_3 \ln(P)^3 + c_4 \ln(P)^4 \dots\dots\dots (A.8)$$

in which  $c_i$  denote the coefficients. The values of the constants of Eq. (A.8) are given elsewhere [35]. The compressibility factors are calculated using the Peng-Robinson equation of state [35, 76].

**Table A.2:** Details regarding the gathered data for methane hydrate in sugar aqueous solutions

System	Reference	Range		
		$T, K$	$P, kPa$	$C_{Sugar}^a$ , mole fraction
CH <sub>4</sub> +xylose+water	[472]	273.51-282.09	3024-6849	0.000627-0.029130

CH <sub>4</sub> +xylitol+water	[472]	273.56-282.51	3021-7093	0.002980-0.029350
CH <sub>4</sub> +dextrose+water	[473]	275.23-281.25	3430-7770	0.010989-0.041095

<sup>a</sup>  $C_{Sugar}$  denotes the concentration of sugar in the aqueous phase

**Table A.3** gives the tuned values of the Margules coefficient for the methane hydrate in the studied sugar aqueous solutions. These values are obtained using the Levenberg-Marquardt optimization algorithm [249-251].

**Table A.3:** Obtained Margules coefficient for methane hydrate in various sugar aqueous solutions at investigated data

System	A value
CH <sub>4</sub> +xylose+water	-10.943
CH <sub>4</sub> +xylitol+water	-6.332
CH <sub>4</sub> +glucose+water	-7.497

### 3. Extension of the framework to CO<sub>2</sub> hydrate

#### *a. Hydrate system of CO<sub>2</sub>+water*

To employ the proposed semi-theoretical approach for prediction of the incipient formation/dissociation temperature of carbon dioxide hydrate in aqueous solution of an inhibitor, the value of the CO<sub>2</sub> HFDT in pure water must be known in advance. In this section we begin to

develop a new empirical tool that can be used for estimation of CO<sub>2</sub> HFDT in pure water. The required data points for empirical model development are the reported experimental three phase L-H-V data of carbon dioxide hydrate in pure water [49, 280, 282, 305, 317, 340, 345, 369, 474-501]. The gathered experimental data, as graphically shown in **Fig. A.1**, cover the temperatures between 273.10 and 283.32 K as well as pressures from 1200 to 4509 kPa.

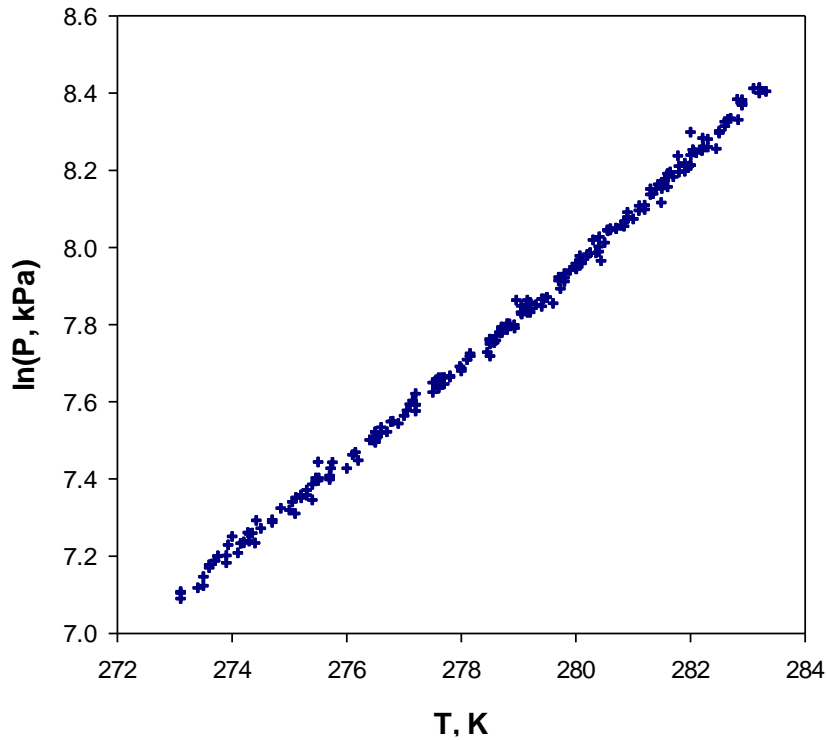


**Fig. A.1:** L-H-V equilibrium data of CO<sub>2</sub> hydrate formation/dissociation conditions in pure water [49, 280, 282, 305, 317, 340, 345, 369, 474-501]

Among the available functions for performing the curve fitting process like trigonometric functions, exponential functions, and polynomials [502], the most employed approximants are polynomials [247, 503]. This work employs a sixth order polynomial for correlating the CO<sub>2</sub> HFDT as a function of the pressure:

$$T_0 = \sum_{i=0}^6 (a_i \times \ln(P)^i) \dots\dots\dots (A.9)$$

where  $a_i$  are the constants. The tuned values of  $a_i$  are given in **Table A.4**.

**Table A.4:** Tuned coefficients used in Eq. (A.9) to predict the CO<sub>2</sub> HFDT in pure water

Constant	Value
$a_0$	1122488.1373938
$a_1$	-863823.979374808
$a_2$	276909.848564922
$a_3$	-47319.2580289076
$a_4$	4546.2447364678
$a_5$	-232.8407071043
$a_6$	4.9664295624

*b. Hydrate system of CO<sub>2</sub>+sugar+water*

In the previous work [35], a general model, as defined by Eq. (A.10), was developed to represent/predict the formation/dissociation temperature of a gas hydrate in the presence aqueous inhibitor solution. This semi-theoretical model has been developed utilizing thermodynamic approaches including two-suffix Margules activity model [504, 505], Clausius-Clapeyron equation [506, 507], and a thermodynamic model for expressing the inhibitor effect on the gas hydrate temperature [80, 471].

$$T = \frac{ZRf_1(T_0)T_0^2 + ANx_{in}^2}{ZRf_1(T_0)T_0 - RN \ln(1 - x_{in})} \dots\dots\dots (A.10)$$

in which  $f_1(T_0)$  is a function. From the original work [35], recall that this function was defined to be:

$$\frac{d(\ln(P))}{dT_0} = f_1(T_0) \dots\dots\dots (A.11)$$

Indeed, Eq. (A.11) says that sketching the three phase equilibrium pressure-temperature data of a gas hydrate in pure water on  $\ln(P)$  versus  $T_0$  plane will contribute to obtain a mathematical expression for the Clausius-Clapeyron equation.

In order to extend the general model to CO<sub>2</sub> hydrate systems, first, an appropriate expression must be find for  $f_1(T_0)$ . Using a third order inverse polynomial and the gathered experimental data for three phase L-H-V equilibrium of carbon dioxide hydrate in pure water,  $\ln(P)$  was correlated as a function of  $T_0$  of carbon dioxide hydrate:

$$\ln(P) = \sum_{i=0}^3 \frac{b_i}{T_0^i} \dots\dots\dots (A.12)$$

where  $b_i$  are the constants. The tuned values of  $b_i$  are given in **Table A.5**. Doing so, we find:

$$\frac{d(\ln(P))}{dT_0} = \frac{-b_1}{T_0^2} + \frac{-2b_2}{T_0^3} + \frac{-3b_3}{T_0^4} \dots\dots\dots (A.13)$$

Reported values of hydration number for CO<sub>2</sub> hydrate are different [280, 282, 508-511]. Theoretically, since the carbon dioxide hydrate is a Type I hydrate, its hydration number can vary between 5.75 and 7.67. Over the temperatures between 272 and 283 K, Anderson [512] found that

the CO<sub>2</sub> hydrate hydration number varies between 6.6 and 5.6 values. In this study it is assumed that  $N = 6.1$ .

**Table A.5:** Tuned coefficients used in Eq. (A.12) to predict the CO<sub>2</sub> HFDP in pure water

Constant	Value
$b_0$	3946.22
$b_1$	-3215797.19
$b_2$	877505741.52
$b_3$	-80035942233.19

In conclusion, we have the following formula for predicting/representing the HFDT of system of CO<sub>2</sub>+inhibitor+water:

$$T_{CO_2} = \frac{Z \times f_1' + (A/R) \times x_{in}^2}{Z \times f_2' - \ln(1 - x_{in})} \dots\dots\dots (A.14)$$

where

$$f_1' = 527,179.867199 - \frac{287,706,800.499507}{T_0} + \frac{39,361,938,803.207557}{T_0^2} \dots\dots\dots (A.15)$$

$$f_2' = \frac{527,179.867199}{T_0} - \frac{287,706,800.499507}{T_0^2} + \frac{39,361,938,803.207557}{T_0^3} \dots\dots\dots (A.16)$$

In order to tune the values of Margules coefficient for carbon dioxide hydrate, the experimental data of Smith et al. [470], Chun and Lee [469], and Carbone [473] for CO<sub>2</sub>+sucrose+water, CO<sub>2</sub>+glucose +water, and CO<sub>2</sub>+fructose+water systems have been gathered. Information about the collected database is given in **Table A.6**.



**Table A.6:** Details regarding the gathered data for CO<sub>2</sub> hydrate in sugar aqueous solutions

System	Reference	Range		
		$T, K$	$P, kPa$	$C_{Sugar}^a$ , mole fraction
CO <sub>2</sub> +sucrose+water	[469, 470]	274.0-281.9	1630-4617	0.05843-0.08764
CO <sub>2</sub> +fructose+water	[469]	273.6-280.6	1800-4240	0.11101-0.16652
CO <sub>2</sub> +glucose+water	[469, 473]	274.0-281.7	1580-4360	0.05551-0.16652

<sup>a</sup>  $C_{Sugar}$  denotes the concentration of sugar in the aqueous phase

As demonstrated in **Fig. A.2**, the reported data by Chun and Lee [469], and Carbone [473] for CO<sub>2</sub>+glucose +water do not follow a unique trend. On the other hand, **Fig. A.3** illustrates that the reported data by Chun and Lee [469] are in agreement with the data of Smith et al. [470], for CO<sub>2</sub> hydrate in 20 wt% sucrose aqueous solution. It seems that the experimental data of Carbone [473] are probably doubtful. As a result, only the data of Chun and Lee [469] and Smith et al. [470], have been employed for fitting the  $A$  values. **Table A.7** gives the obtained  $A$  values for the investigated CO<sub>2</sub> hydrate systems. The values of this parameter are optimized using the Levenberg-Marquardt algorithm [249-251]. Like the methane hydrate systems, the compressibility factor for the hydrate systems of carbon dioxide are calculated using the Peng-Robinson equation of state [35, 76].

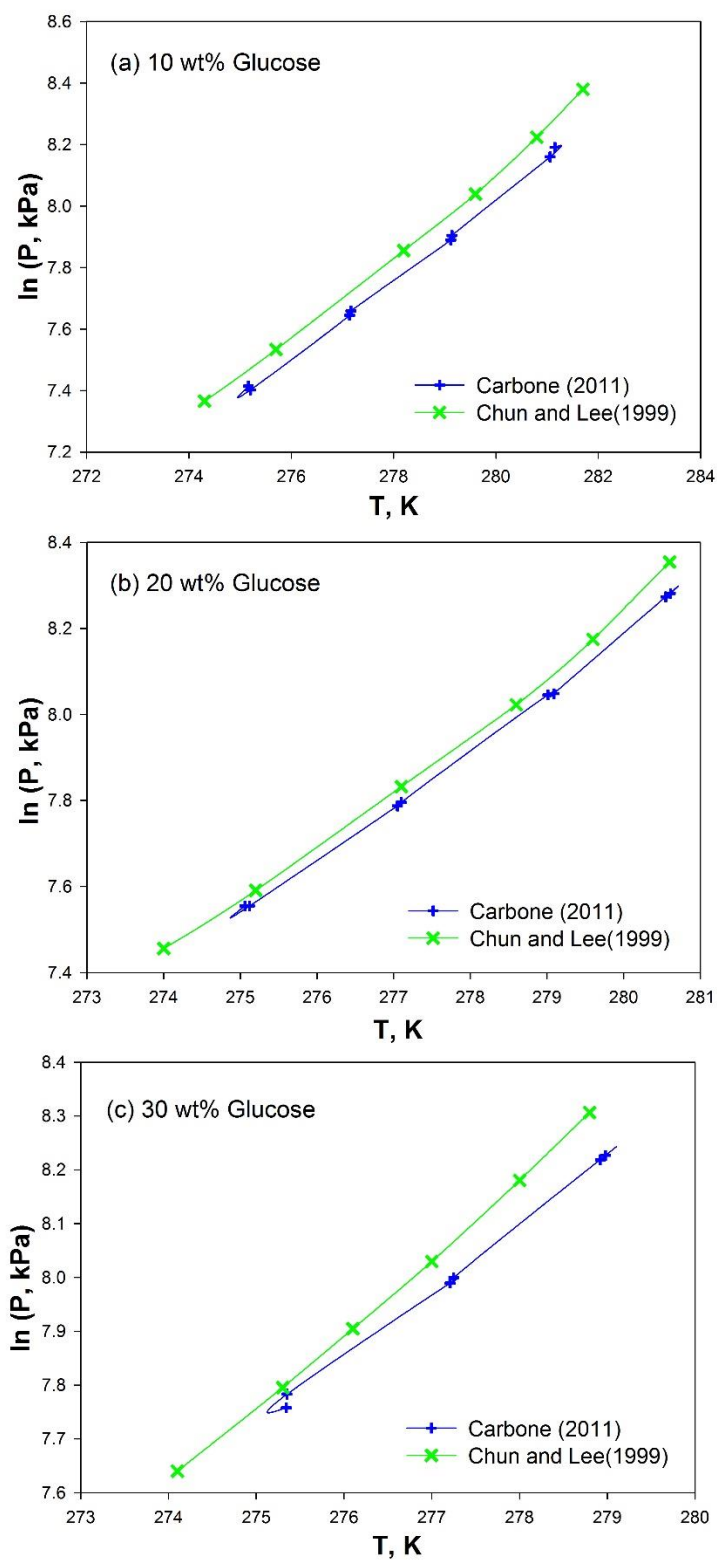


**Fig. A.2:** Comparing the experimental data of Carbone [473] and Chun and Lee [469] for hydrate system of  $\text{CO}_2$ +glucose+water

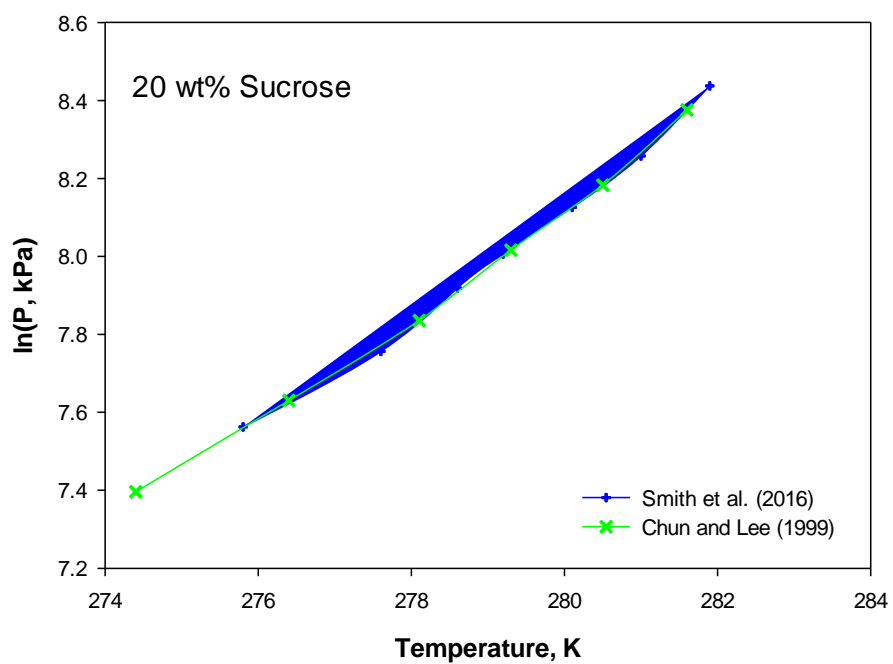


**Fig. A.3:** Comparing the experimental data of Smith et al. [470] and Chun and Lee [469] for hydrate system of CO<sub>2</sub>+glucose+water

**Table A.7:** Obtained Margules coefficient for CO<sub>2</sub> hydrate in various sugar aqueous solutions at investigated data

System	A value
CO <sub>2</sub> +sucrose+water	-50980
CO <sub>2</sub> +fructose+water	-21070
CO <sub>2</sub> +glucose+water	-26940

#### 4. CO<sub>2</sub>+Orange/Tomato Juice hydrate system

The purpose of this section is investigating the phase equilibrium of carbon dioxide hydrate in the presence of tomato or orange juice. To this end, Eq. (A.3) is utilized in order to calculate the water activities. The presented empirical model of Anderson [512], as defined by Eq. (A.17), is employed to estimate the enthalpy of carbon dioxide hydrate dissociation.

$$\Delta H = (62.9 - 0.53(T - 273.15)) \times 1000 \quad \dots\dots\dots$$

(A.17)

in which  $\Delta H$  is in  $J/mol$ .

The employed experimental data are the reported data by Li et al. [513, 514]. **Table A.8** summarizes the composition of the juices for the gathered database.

**Table A.8:** Contents of tomato/orange juice in the gathered experimental data

Solution	Content				
	Reducing sugar, (g/100g)	Total acid, (g/kg)	Vitamin C, (mg/100g)	Soluble solid	Water
Orange juice	4.42	6.08	49.96	10.5%	87.7%
Tomato juice	2.51	3.31	16.85	5.5%	94.2%

#### 5. Results and discussion

##### a. CH<sub>4</sub>+Sugar+Water hydrate systems

**Fig. A.4** shows the outputs of the proposed semi-theoretical methodology with the optimized  $A$  values for hydrate systems of  $\text{CH}_4$ +Xylose+Water,  $\text{CH}_4$ +Xylitol+Water, and  $\text{CH}_4$ +Glucose+Water versus the corresponding experimental values. As can be seen from **Fig. A.4**, there are excellent agreements between the predictions of the proposed model and the target values. The values of the coefficient of determination ( $R^2$ ) of the developed model for the studied systems of methane hydrate are higher than 0.98 indicating the perfect fit of the regression line to the data.

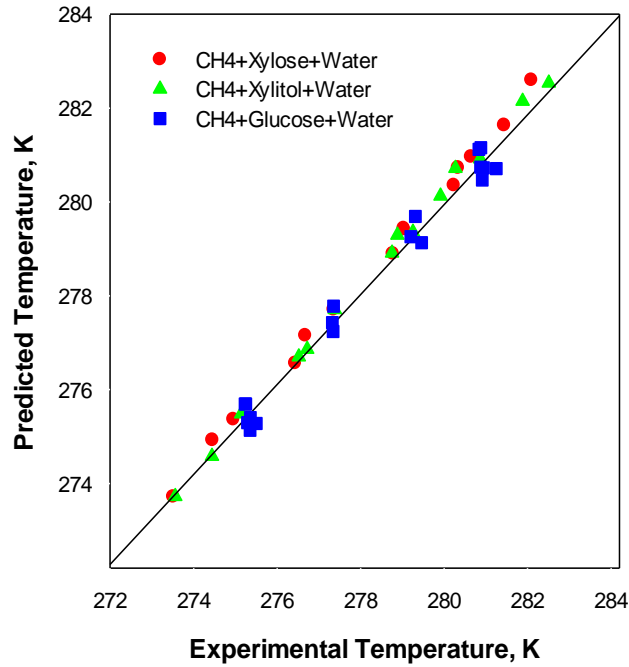


**Fig. A.4:** Cross plot of the predicted vs. experimental methane HFDT in sugar solutions

For all the aforementioned methane hydrate systems, the absolute deviations vary between 0.01 and 0.54  $K$ . In another word, for all the gathered data, the maximum deviation of the experimental target values from the values predicted by the proposed method do not exceeds than 0.54  $K$ . **Table A.9** gives the values of statistical parameters consisting of  $R^2$ , average absolute

deviation (AAD), and average absolute relative deviation percent (AARD%) to give evidence on the accuracy of the semi-theoretical approach. According to the error analysis results tabulated in **Table A.9**, the proposed thermodynamic-based framework can be successfully employed for representing the incipient stability conditions of methane hydrate in the presence of aqueous solutions of different sugars.

**Table A.9:** Error analysis results for the semi-theoretical method to predict/represent CO<sub>2</sub> HFDT equilibrium in sugar aqueous solutions

System	Parameter		
	R <sup>2</sup>	AAD, <i>K</i>	AARD%
CH <sub>4</sub> +Xylose+Water	0.9973	0.33	0.12
CH <sub>4</sub> +Xylitol+Water	0.9976	0.22	0.08
CH <sub>4</sub> +Glucose+Water	0.9826	0.27	0.02

For xylose solution of concentration 1.316 mol%, **Fig. A.5(a)** shows the models' outputs in comparison with the experimental data of Jin et al. [472]. In **Fig. A.5(b)**, the predicted methane HFDTs in 0.298 mol% xylitol solution with the extended model have been graphically compared to the reported data by Jin et al. [472]. Similarly, **Fig. A.5(c)** demonstrates both the model's estimations and the experimental data of Carbone [473] for the glucose concentration in aqueous phase at 2.439 mol%. As the figures display, the experimental targets are magnificently regenerated by the model.

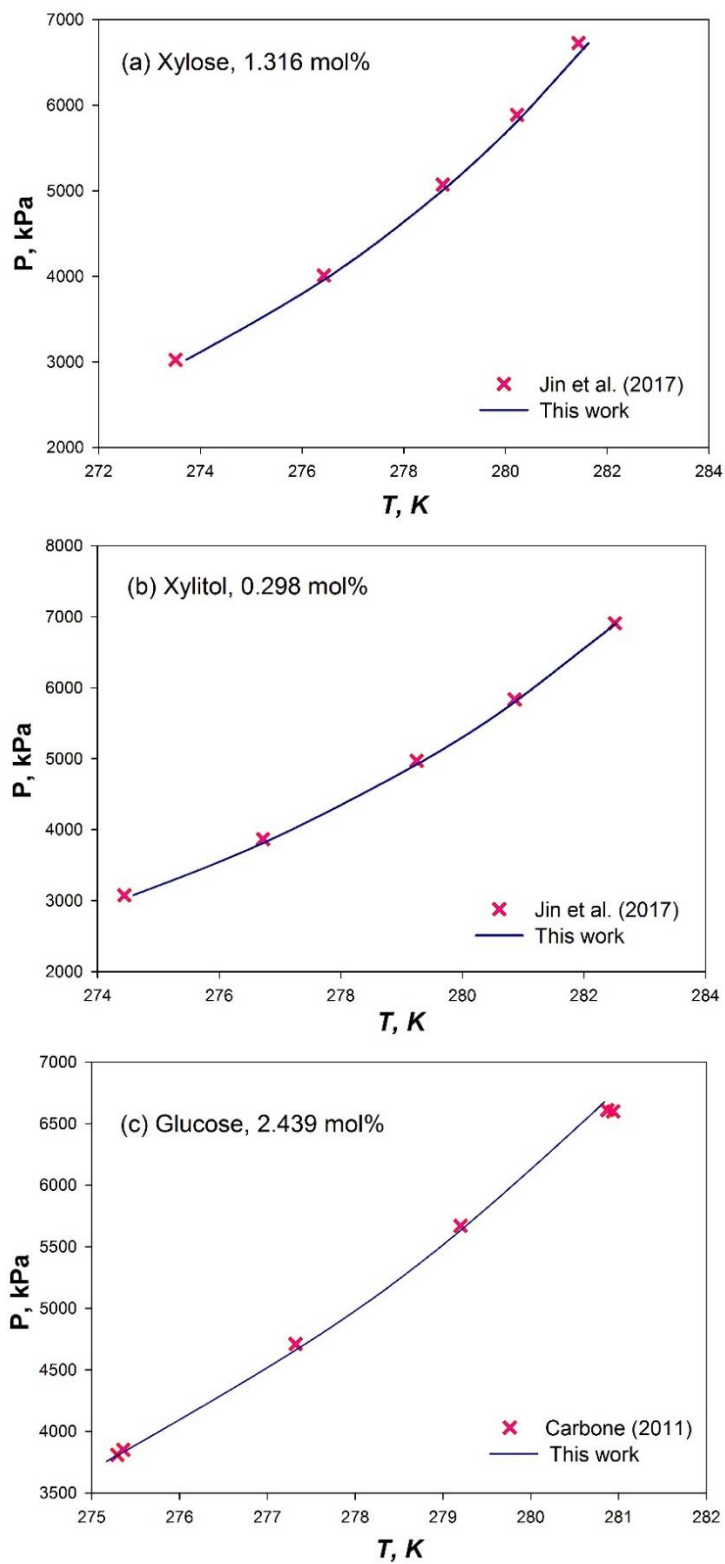


**Fig. A.5:** Comparison of the model outputs with experimental data [472, 473] for  $\text{CH}_4$ +Sugar+Water hydrate systems

*b. CO<sub>2</sub>+Water hydrate system*

Relative deviations (in percent) of the predicted carbon dioxide HFDT in pure water by the developed empirical model (Eq. (9)) from the corresponding experimental values have been shown in **Fig. A.6**. As depicted in **Fig. A.6**, the majority of the data points are located around the zero line. Furthermore, the maximum relative deviation of the new empirical tool is lower than 0.16. In terms of absolute deviation, the maximum error of the model is no more than 0.44 K. In a respective order, the overall  $R^2$ , AAD, and AARD% values for Eq. (9) are 0.9983, 0.08 K, and 0.03 which illustrate the accuracy of the presented model. The goodness of fit of the new model can be observed from **Fig. A.7** that depicts the predictions of the model versus the experimental CO<sub>2</sub> HFDT in pure water.

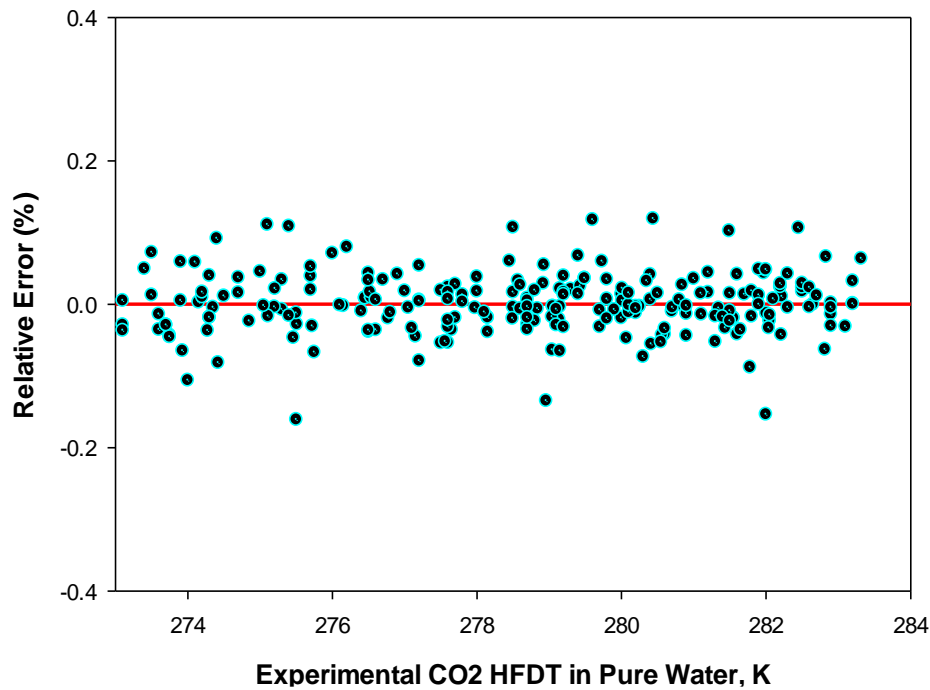


**Fig. A.6:** Relative deviations of the estimated carbon dioxide HFDT in pure water by the new empirical correlation from the experimental data



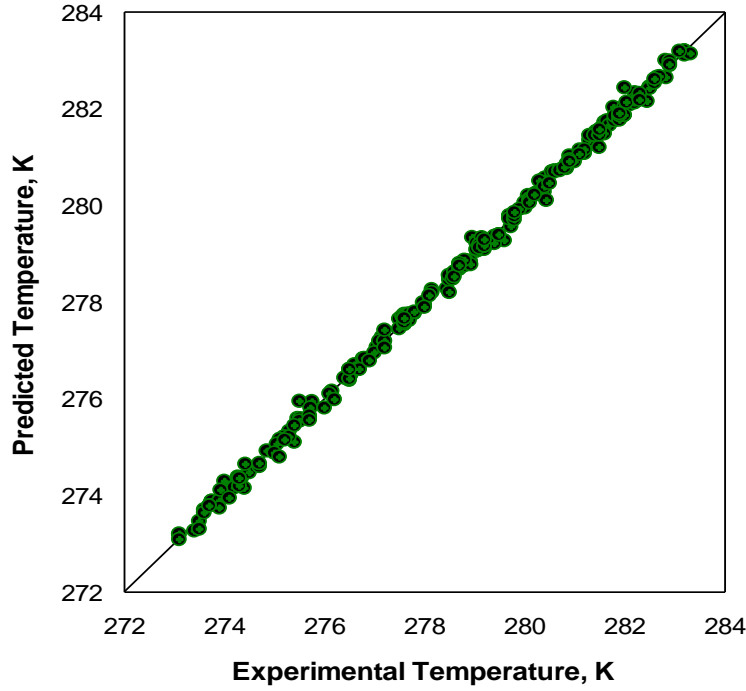


**Fig. A.7:** Cross plot of the predicted vs. experimental carbon dioxide HFDT in pure water

*c. CO<sub>2</sub>+Sugar+Water hydrate systems*

In **Fig. A.8**, the predicted values of CO<sub>2</sub> HFDT in aqueous solutions of glucose, fructose, and sucrose by the presented semi-theoretical model (Eq. (14)) are plotted against the corresponding target values. For the developed model, **Fig. A.8** shows is a heavy concentration of data points around the  $Y=X$  line (  $45^\circ$  line). This means a strong relationship between the outcomes of Eq. (14) and corresponding experimental values for hydrate systems of CO<sub>2</sub>+sucrose+water, CO<sub>2</sub>+glucose+water, and CO<sub>2</sub>+fructose+water.

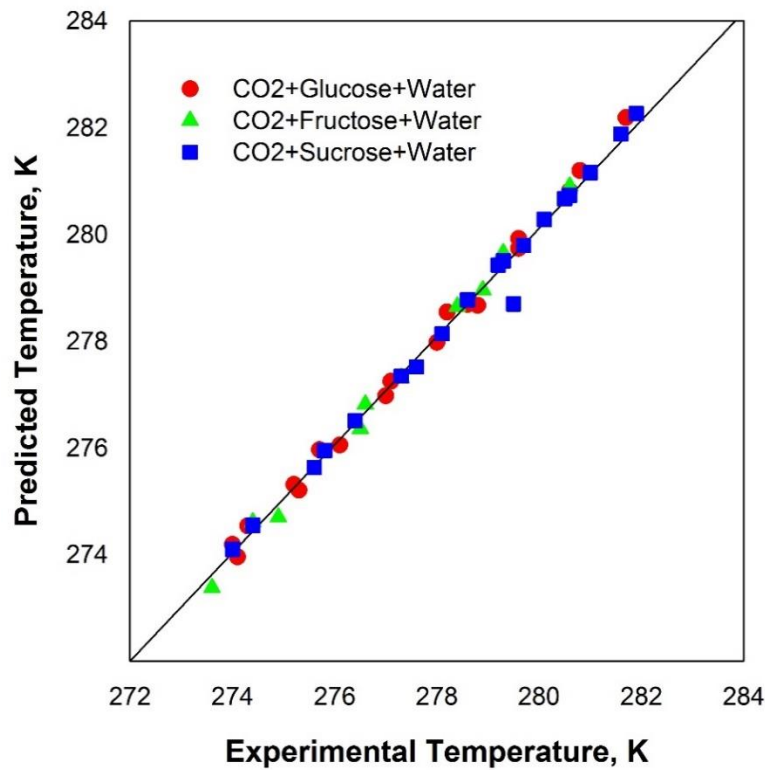


**Fig. A.8:** Cross plot of the predicted vs. experimental carbon dioxide HFDT in sugar solutions

**Table A.10** gives the error analysis results for the developed method to predict/represent the equilibrium temperature at which carbon dioxide hydrate forms/dissociates in the presence of various sugar aqueous solutions. The obtained values for the statistical parameters indicate that the proposed methodology produce consistently accurate predictions across the investigated ranges of temperature, pressure, and concentration of sugar in the aqueous phase. For all conditions, the proposed method showed the maximum absolute deviation to be less than 0.5 *K*.

**Table A.10:** Error analysis results for the semi-theoretical method to predict/represent CO<sub>2</sub> HFDT equilibrium in sugar aqueous solutions

System	Parameter		
	R <sup>2</sup>	AAD, <i>K</i>	AARD%
CO <sub>2</sub> +Sucrose+Water	0.9958	0.19	0.07
CO <sub>2</sub> +Fructose+Water	0.9958	0.20	0.07
CO <sub>2</sub> +Glucose+Water	0.9846	0.20	0.07

The experimentally determined formation/dissociation conditions of carbon dioxide hydrate in sucrose solution of concentration 1.2987 mol%, reported by Smith et al. [470], are compared to the results of the new model in **Fig. 9(a)**. **Fig. 9(b,c)** compares the obtained results of the thermodynamic-based model with the reported data by Chun and Lee [469] for CO<sub>2</sub>+glucose (2.439 mol%)+water, and CO<sub>2</sub>+fructose (4.1094 mol%)+water hydrate systems, respectively.

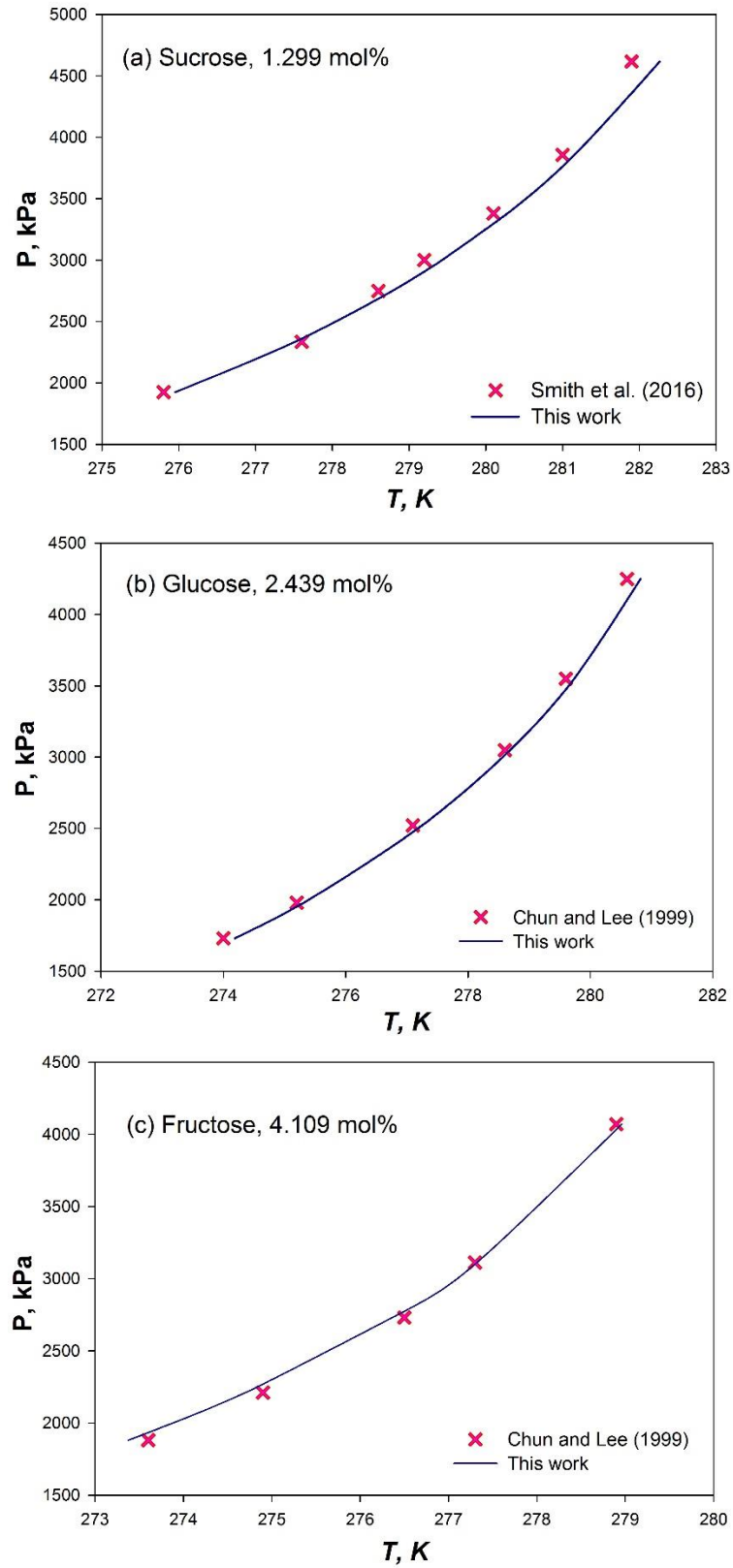


**Fig. A.9:** Comparison of the model outputs with experimental data [469, 470] for  $\text{CO}_2$ +Sugar+Water hydrate systems

*d. CO<sub>2</sub>+Orange/Tomato Juice hydrate systems*

Employing Eq. (A.3) and (A.17), the values of water activities for carbon dioxide hydrate in the presence of tomato or orange juice were calculated. **Table A.11** gives the experimental data of CO<sub>2</sub>+Orange/Tomato Juice hydrate systems as well as the corresponding calculated values of water activity. According to **Table A.11**, both the investigated tomato and orange juices are responsible for the decrease in the water activity. Hence, it can be concluded that both the studied juices are inhibitor containing solutions. However, since the obtained water activities are very close to 1, the tomato and orange juices with the specified contents have a weak inhibiting effect on the carbon dioxide hydrate phase equilibria. Furthermore, the studied orange juice is found to exhibit a stronger inhibition as compared to the tomato juice.

**Table A.11:** calculated values of water activity for CO<sub>2</sub>+Orange/Tomato Juice hydrate systems

System	Experimental data		$a_w$
	P, kPa	T, K	
CO <sub>2</sub> +Tomato Juice	2319.75	278.41	0.9995
	2940.80	280.19	0.9990
	3161.29	280.90	1.0016
	3614.62	281.71	0.9997
	4114.47	282.50	0.9988
CO <sub>2</sub> +Orange Juice	2370.59	278.30	0.9953
	2847.06	279.59	0.9937
	3276.47	280.70	0.9949
	3935.29	281.80	0.9930
	4388.24	282.80	0.9970

The tuned values for the water activity are used for prediction of the CO<sub>2</sub> hydrate formation/dissociation conditions in the defined juices across the operating ranges of the data. The obtained model which is on the basis of Eq. (A.3) and (A.17) is as follows:

$$\frac{1}{T} = \left( \frac{1}{T_0} \right) + \left( \frac{C}{391.829 - T_0} \right) \dots\dots\dots (A.18)$$

where  $C$  is the constant that is equal to  $2.653 \times 10^{-4}$  and  $1.356 \times 10^{-5}$  for CO<sub>2</sub>+Orange Juice and CO<sub>2</sub>+Tomato Juice hydrate systems, respectively. This parameter can be adjusted again if more data are available.

Employing the new model, the obtained AAD values for the investigated hydrate systems of CO<sub>2</sub>+Orange Juice and CO<sub>2</sub>+Tomato Juice are 0.17 and 0.06  $K$ , respectively. **Fig. A.10** demonstrates the accuracy of the presented model in predicting the CO<sub>2</sub> HFDT in tomato and orange juices.

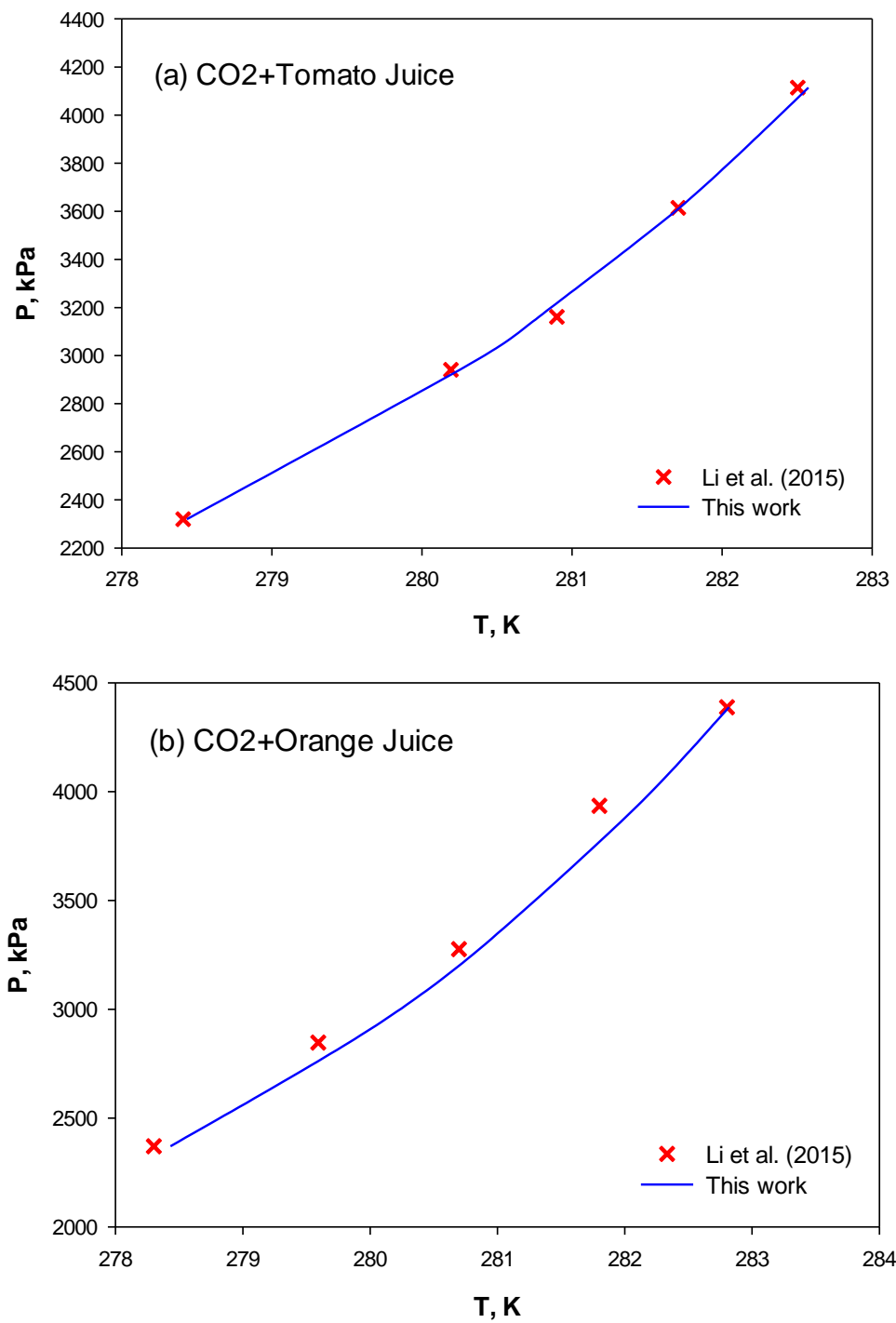


**Fig. A.10:** Comparison of the model outputs with experimental data [513, 514] for CO<sub>2</sub>+Juice hydrate systems

## **Appendix B**

Digraphs of the created CART/AdaBoost-CART models for the studied systems are provided in an electronic file.